Department of Electrical and Computer Engineering

Online Coordinated Charging of Plug-In Electric Vehicles in Smart Grid to Minimize Cost of Generating Energy and Improve Voltage Profile

Amir Sherkat Masoum

Declaration

To the best of my knowledge and belief this thesis contains no material previously published by any other person except where due acknowledgment has been made.

This thesis contains no material which has been accepted for the award of any other degree or diploma in any university.

Signature:

Date: 1/05/2020

STATEMENT OF CONTRIBUTION BY OTHERS

The following people have contributed to the publications of references [55], [56], [57] and [58] related to chapters 4, 5, 6 and 7 (see Appendix B):

- A/Professor Ahmed Abu-Siada: Supervision of research, review of the results and the review and approval of references [55], [56], [57] and [58].
- Professor Syed Islam: Review of the results and the review and approval of references [55], [57] and [58].
- Dr Sara Deilami: Review and approval of references [55], [56] and [57].
- Professor Mohammad Ali Sherkat Masoum: Review and approval of references [55], [56] and [57].

Signature   Date: 1/05/2020
Amir Sherkat Masoum
Ph.D. Candidate

Signature   Date: 11/05/2020
Professor Ahmed Abu-Siada
Ph.D. Candidate Supervisor

Table of Contents

ABSTRACT

Smart Power Grid (SG) is an efficient and intelligent network that improves the operation, efficiency and reliability of electrical power systems through energy sharing, monitoring and management. It promotes rapid developments of renewable distributed generations (DGs), smart metering, grid monitoring, smart loads, and plug-in electric vehicles (PEVs). However, SG technology has made network control and energy trading more complex and is posing significant challenges on design, management, and trading schemes. Moreover, electric utilities are apprehensive of the adverse impacts of overloading and poor power quality on their systems due to high injections of renewable resources and extensive PEV battery charging. This Ph.D. research highlights the negative impacts of random vehicle battery charging on power grid and proposes four practical PEV coordinated battery charging strategies that reduce network and generation costs by integrating renewable energy resources and real-time pricing while considering utility constraints and consumer concerns.

The main contributions of this Ph.D. thesis are:

1) A centralized online maximum sensitivities selection (MSS)-based coordinated battery charging (OL-MSSCC) algorithm for PEVs in smart power grids with the consideration of wind distributed generations (WDGs) [55]. This approach is an expansion to the real-time smart load management (RT-SLM) algorithm of [63].

2) A centralized online fuzzified coordinated battery charging (OL-FCC) strategy/algorithm for PEVs in SG networks with the consideration of WDGs [56].

3) A centralized delayed (overnight) MSS-based coordinated battery charging (DL-MSSCC) strategy/algorithm for PEVs in SG networks with WDGs [57].

4) A centralized combined online fuzzy and delayed MSS-based coordinated battery charging (OL-F/DL-MSSCC) algorithm for PEVs in SG networks with the considerations of wind and solar (rooftop) DGs [58].

The uncoordinated (random) vehicle battery charging and the above four proposed PEV coordinated battery charging algorithms are programed in MATLAB software and tested on an assembled 449-bus SG network with PEVs, WDGs, rooftop PVs, and their performances are compared without and with renewable energy resources.

The main conclusions of this Ph.D. thesis are:

✓ The four proposed PEV coordinated battery charging algorithms can effectively schedule vehicle battery charging without and with renewable DGs and reduce the costs associate with generation and losses whilst maintaining bus voltage regulations/deviations and network maximum demand limits/levels within designated acceptable bounds.

✓ The advantage and main difference of the recommended OL-MSSCC compared to the RT-SLM algorithm of [63] is the addition of WDGs to further reduce the cost and the possibility of overloading the lines and distribution transforms due to the high injections of PEVs predominantly in the hours of peak residential loads.

✓ The contribution of proposed the OL-FCC compared with the OL-MSSCC is the application of the fuzzy reasoning for additional reduction of grid costs for high injection PEV scenarios.

✓ The advantage of proposed DL-MSSCC over OL-MSSCC and OL-FCC is cheap overnight charging with lower grid costs, but it may cause dissatisfactions for the high-priority consumers.

✓ Finally, the proposed OL-F/DL-MSSCC algorithm offers the advantages of OL-MSSCC, OL-FCC and DL-MSSCC while resolving most of their limitations. It reduces the total network cost by considering short term market energy prices and directly leveraging the accessible renewable (wind and solar) generations for vehicle battery charging. It will also maintain the bus voltages and the upper demand levels within the acceptable limits based on maximum sensitivity selections and/or fuzzy reasoning. In addition, OL-F/DL-MSSC improves customer satisfaction by offering: i) three consumer (high, medium and low) priority options, ii) three battery charging (fast online evening, online daytime and cheap overnight) options, iii) three battery charging time (red, blue and green) zones and, iv) the ability to charge at high, medium or low tariff rates.

ABBREVIATIONS

BEV	Battery electric vehicle (also called plug-in electric vehicle; PEV)
CS	Charging station
DCFC	Direct current fast charging
DSM	Demand side management
DG	Distributed generation
ES	Energy storage
EV	Electric vehicles
EVSE	Electric vehicle supply equipment
G2V	Grid-to-vehicle charging
HANs	Home area networks
ICE	Internal combustion engine
ICT	Information and communications technology
IEA	International Energy Agency
ISO	Independent System Operator
LDV	Light-duty vehicle
LSEV	Low-speed electric vehicle
MSS	Maximum sensitivities selection
OL-FCC	online fuzzy coordinated battery charging
OL-MSSCC	Online MSS coordinated battery charging
OL-SLMCA	online smart load management coordination algorithm
PEV	Plug-in EV
PHEV	Plug-in hybrid EV
PV	photovoltaic

RDG   Renewable DG

SG   Smart power grid

SGT   Smart grid technology

V2G   Vehicle-to-grid charging

WDG   Wind Distributed generation

SYMBOLS

$D_{t,max}$	Maximum demand at time t with no PEVs
$D_{t,total}$	total demand at time t
$D_{t,max,overnight}$	Estimated $D_{t,max}$ for delayed (overnight) PEV battery charging
E_{PEV}	Energy to charge one EV
$F_{cost-loss}$	Cost associated with system losses
$F_{cost-gen}$	Cost associated with generation
F_{cost}	Total costs
$F(V) = \Delta S_k$	Mismatch apparent power at bus k (in VA)
$F_{Scheduled}(V)$, $F_{Calculated}(V)$	Scheduled and calculated apparent power at bus k (in VA)
$I_{Bus} = [I]$	Bus current vector
J	Jacobian matrix
K_E	Cost for one megawatt hour of losses
$K_{\Delta t,G}$	Cost for one megawatt hour of generation at *delta t*
MSS_i	bus i sensitivity to EV charging
N_{PEV}	Gross number of EVs in PEV-Queue Table
$P_{k(Scheduled)}$, $P_{k(Calculated)}$	Scheduled and calculated active power at bus k (in W)
$P_{t,k}^{load}$	Total load power at bus k at time t
$P_{t,j}^{PEV}$	PEV battery charging power at bus j at time t
$P_{t,m}^{WDG}$	Wind DG power generation at bus m at specific time t
$P_{t,loss}$	Power losses (total) at time t

$Q_{k(Scheduled)}$, $QP_{k(Calculated)}$	Scheduled and calculated reactive power at bus k (in Var)
$R_{k,k+1}$, $y_{k,k+1}$	Line resistance and reactance between buses k and $k+1$
$S_{k(Scheduled)}$, $S_{k(Calculated)}$	Scheduled and calculated apperent power at bus k (in VA)
$V_{Bus} = [V]$	Bus voltage vector
V_k	Voltage at bus k
V_{rated}	Rated voltage at all buses
Δt	Time interval Δt = 5 minutes
t_{delay}	Starting time for delayed/overnight PEV battery charging
t_{end}	Ending time for delayed/overnight PEV battery charging
T_{delay}	Period of delayed/overnight PEV battery charging
W_D	Weighting factor for maximum demand membership function
W_L	Weighting factor system loss membership functions
W_V	Weighting factor for voltage deviation membership function
Y_{Bus}	Admittance matrix
ΔP_k	Mismatch active power at bus k (in W)
ΔS_k	Mismatch apparent power at bus k (in VA)
ΔQ_k	Mismatch reactive power at bus k (in Vars)
Δt	Time interval Δt = 5 minutes
ΔV_k	Voltage deviation at bus k
ΔV_{max}	Maximum voltage deviation at bus k
μ_D	Fuzzy membership function for maximum demand
μ_{loss}	Fuzzy membership function for loss

$\mu_{\Delta V_k}$	Fuzzy membership function for voltage deviation
$\mu_{PEV,j}$,	Combine fuzzy membership function for PEVat bus j
$S_{PEV,j}$	and its crisp (defuzzify) value
α	The α-cut value used for defuzzifiation

CHAPTER ONE: INTRODUCTION

1.1. Motivations of the Ph.D. Thesis

The innovating smart power grid (SG) technology is broadly considered as an efficient and intelligent power network [1-42]. It improves the operation, efficiency and reliability of power grid through intellectual energy management by promoting rapid developments of renewable distributed generations (DGs), smart metering, grid monitoring, smart loads and plug-in electric vehicles (PEVs) [43-124]. However, SG technology has made network control and energy trading more complex and is posing significant challenges on design, management, and trading schemes. These new challenges are mainly due to the development of new features such as the introduction of intermittent renewable energy resources, diverse energy storage systems and smart appliances as well as the integration of plug-in electric vehicles (PEVs) with grid-to-vehicle (G2V), vehicle-to-grid (V2G) and vehicle-to-vehicle (V2V) modes of operation [5-6].

The main reasons to support the development of SG technology are its new features, green resources and modular structure that can be easily expended by adding new renewable microgrids (MGs). Some benefits and features associated with the smart power grid technology can be as follows [1-9]:

1) ***More Efficient Network with Lower Cost and Improved Security-*** SG can offer more transmission of electricity with faster network restoration after disturbances and faults as well as lower operation, management and maintenance costs for utilities, and eventually cheaper costs for the consumers. The reduced network peak demand will also help to achieve lower electricity rates.

2) ***Distributed Architecture with Sophisticated Communication Backbone-*** SGs can be modeled as grouped architecture consisting of interactive networked (clustered)

renewable MGs [7-9]. The open communication backbone of SG provides fast linkages among the elements of MGs and enables them to participate in the decision making that delivers value to both the utility and consumers. However, controlling the load and generation variations of each MG together with its interconnections with the remaining MGs requires complicated energy management programs [1].

3) ***Increased Integration of Diverse Renewable Energy Resources-*** Large-scale integrations of heterogeneous renewable distributed generations (RDGs) such as solar, wind and hydroelectric power resources will have great positive impacts on power grid operation, our health and lifestyles [1].

4) ***Integration of Distributed Energy Storage:*** With the present technology, the utilization of most energy storages is relatively costly but required to mitigate the variability and intermittency of RDGs [1]. On the positive side, energy storage systems can be smartly used to shift consumers' energy consumption to off-peak load periods and/or overlap them with the peak output times of RDGs.

5) ***Widespread Assimilation of Plug-In/Hybrid Electric Vehicles:*** The bidirectional energy flow between PEVs and SG can help to balance demand and generation in local areas and/or MGs. This can be done using different operation modes of the PEVs including grid-to-vehicle (G2V), vehicle-to-grid (V2G) and vehicle-to-vehicle (V2V). Moreover, since PEVs travel amongst different areas of SG, their energy transportation from one place to another can be smartly used to improve the energy reliability among different MGs [1].

Therefore, considering the above-mentioned benefits and features of SG technology, this Ph.D. thesis intends to explore the negative impacts of uncoordinated PEV battery charging and propose new vehicle coordinated battery charging strategies that consider

both the utility and consumer concerns. The research is performed in two stages:

➢ ***Stage 1 (Literature Reviews)-*** Chapters 2 and 3 present the summarized results of literature reviews on SG technology and coordinated battery charging of PEVs.

➢ ***Stage 2 (Thesis Contributions)-*** Chapters 4 to 7 present four new PEV coordinated battery charging algorithms that are programed in MATLAB and tested on a 449-bus SG network and their performances are compared without and with RDGs.

The research on coordinated PEV battery charging are classified into centralized, decentralized and hierarchical strategies [45]-[48]. Charging can be done separately for each PEV, cooperatively for groups of PEVs or centrally for all PEVs. The main limitations of the existing research are (see chapter three for more details):

a) With centralized coordination schemes, the PEV owners miss the privilege of directly controlling their own vehicle charging. In addition, there are scalability and single point of failure challenges at the ISO level [46]-[47], [62]-[68].

b) The decentralized coordination algorithms cannot guarantee global optimal or near-optimal scheduling solutions. In addition, they usually require large communication overheads [47].

c) Most coordinated PEV charging strategies rely on predicted or forecasted information on the status of EVs, power grid, and renewable energy resources [62], [74], [90], [93]. Most research are targeting either online ([63], [80], [87], [94]) or offline ([62], [90], [93]) battery charging without looking into options for hybrid online-offline coordination strategies

1.2. Objectives of the Ph.D. Thesis

The main objectives of this research are:

▪ Exploring the impacts of random EV charging on the SG operation including network

cost, network losses, transformer loadings, generation demand and bus voltages within charging horizon of 24 hours.

- Improving the performance of SG networks with EV charging activities by including vehicle battery charging time zones, consumers' preferences, and variable energy costs in the formulating of the PEV centralized coordinated battery charging problem.

- Proposing and implementing new PEV battery charging coordination strategies with lower losses, less costs and improved customer satisfaction.

- Programing of the proposed PEV battery charging schemes (in MATLAB), evaluating and comparing their performances on a sample SG network.

- Investigating the impacts of distributed wind and solar generations on the performance and end costs of the proposed PEV battery charging schemes.

1.3. Contributions of the Ph.D. Thesis

After presetting literature reviews on smart power grid and plug-in electric charging technologies, this Ph.D. research proposes, implements, and compares the following four new strategies for centralized coordinated charging of PEV batteries:

1) *The first contribution* is a new centralized online MSS-based coordinated battery charging (OL-MSSCC) algorithm for PEVs in smart power grids with WDGs [55]. This approach is an expansion to the real-time smart load management algorithm of references [63] with the addition of WDGs to further reduce the possibility of overloading the lines and distribution transforms due to the high injections of PEVs particularly in peak hours.

2) *The second contribution* is a new centralized online fuzzy coordinated battery charging (OL-FCC) algorithm for PEVs in SG networks with the consideration of WDGs [56].

3) ***The third contribution*** is a new centralized delayed maximum sensitivity selection-based coordinated battery charging (DL-MSSCC) algorithm/strategy for PEVs in SG networks with WDGs [57].

4) ***The fourth contribution*** is a new centralized combined online fuzzy-based (fuzzified) and delayed maximum sensitivity selection-based coordinated battery charging (OL-F/DL-MSSCC) algorithm/strategy for PEVs in SG networks with the consideration of wind and solar (rooftop) DGs [58].

The uncoordinated (random) vehicle charging and the above four proposed PEV coordinated battery charging algorithms are programed in MATLAB and tested on an assembled 449-bus smart power grid network that contains PEVs, WDGs and rooftop PVs. In addition, their performances are compared without and with renewable energy resources.

1.4. Outline of the Ph.D. Thesis

This thesis is arranged in two parts including literatures (Chapters 2-3) and contributions (Chapters 4-7) followed by the conclusions.

- ***Chapter 2 (Literature Review on Smart Power Grids)*** provides an overview of smart power grid technology with a focus on demand side management and smart power grid infrastructure, as well as future research directions in these areas.

- ***Chapter 3 (Literature Review on Coordinated Battery Charging Tactics for Electric Vehicle)*** presents a survey on the integration of uncoordinated and coordinated battery charging of PEVs and their effects on smart power grids/networks. Chapter 3 also presents classification, properties, and objective functions of PEV charge coordination approaches followed by some anticipated upcoming research avenues.

- ***Chapter 4 (Online MSS-Based Coordinated Battery Charging of PEVs in Smart***

Power Grids Considering Wind Distributed Generations) proposes a new centralized online MSS-based coordinated battery charging (OL-MSSCC) algorithm for PEVs in SGs with WDGs which was published by the author during his Ph.D. studies in [55].

- ***Chapter 5 (Online Fuzzy Coordinated Battery Charging of PEVs in Smart Power Grids with the consideration of Wind Distributed Generations)*** proposes a new centralized online fuzzy (fuzzified) coordinated battery charging (OL-FCC) strategy/algorithm for PEVs in SG networks with WDGs which was published by the author during his Ph.D. studies in [56].

- ***Chapter 6 (Delayed MSS-Based Coordinated Battery charging of PEVs in Smart Power Grid)*** proposes a new centralized delayed maximum sensitivity-based coordinated battery charging (DL-MSSCC) strategy/algorithm for electric vehicles in SG networks which was published by the author during his Ph.D. studies in [57].

- ***Chapter 7 (Combined Online Fuzzy and Delayed MSS Coordinated Battery Charging of PEVs in Smart Power Grids with Wind and Solar Distributed Generations)*** proposes a new centralized joint online fuzzy-based (fuzzified) and delayed maximum sensitivity-based coordinated battery charging (OL-F/DL-MSSCC) strategy/algorithm for PEVs in SGs considering wind and solar (rooftop) distributed generations which was published by the author during his Ph.D. studies in [58].

- ***Chapter 8 (Thesis Summary and Contributions)*** gives the outline, contributions, and conclusions of the thesis in addition to some recommended forthcoming research areas.

CHAPTER TWO: LITERATURE REVIEW ON SMART POWER GRIDS

Chapter 3 gives a literature survey on recent publications on smart power grid technology (SGT). It includes concept and motivations of smart power grid (SG), structure of SG, and the concept of demand response in SG as well as possible future research directions [1-42].

The rising rate of world electricity demand, rapid climate changes and alarming global warming are encouraging more government authorities, industry and power utilities as well as consumers to get actively involved in the transformation from the conventional central-based power grids that mainly rely on fossil energy sources to the emerging distributed-based smart power grids with renewable energy resources. The main fossil sources are oil, coal and natural gas. The main renewable energy resources include solar, wind, water/hydroelectric, geothermal, bioenergy, ocean, nuclear, hydrogen and fuel cells.

This chapter is organized as follows:

- Section 2.1 presents the concept and motivations of smart power grid.

- Section 2.2 reviews the smart power grid infrastructure.

- Section 2.3 reviews the concept of demand response in smart power grid.

- Section 2.4 discusses future research directions in smart power grid technology.

2.1. Concept and Motivations of Smart Power Grid

The majority of the existing conventional power grids are large and old interconnected infrastructures used to deliver electricity from a few large generators to detached end users located away from the generation centres. Although, there have been notable innovations in the information, communication and real-time control frontiers over the

last few decades; unfortunately, the heritage of power grid has not kept pace with such technology invention [2].

The idea of smart power grids is simple but requires a conceptual shift in power delivery from a centralized system with a few large generation systems and distanced loads to a decentralized network with widely distributed renewable generations (DGs) that are located near load centres [4]. An established SG is fully automated with advanced communication and monitoring systems that support two-way real-time flow of electricity and information to enable near-instantaneous balance of supply and demand at the device level as depicted in Fig. 2.1.
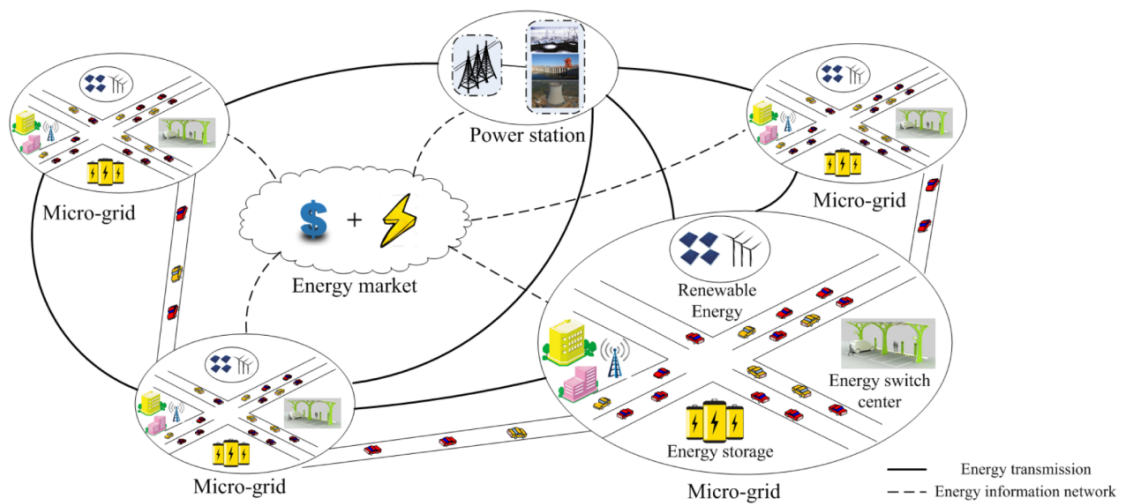
Fig. 2.1. The architecture and new features of SG [1].

Consequently, smart power grids are [4]:

- ✓ **Green–** They can accommodate large injections of renewable energy resources.

- ✓ **Intelligent-** They perform real-time power flow calculations, operate autonomously, quickly detect and respond to overloads, faults and emergency condition.

- ✓ **Efficient-** They meet the increased consumer demand without adding infrastructure, use DG technology to reduce line losses and do require long transmission lines.

✓ *Accommodating-* They recognize all types of green energy and integrate new technologies such as smart loads, PEVs, charging stations, small/medium DGs without and with energy storage systems [10-11].

✓ *Motivating-* They provide end users with opportunities to tailor energy consumption/ generation based on their own priorities, preferences, budget and equipment.

✓ *Resilient*– They are more resistant to natural catastrophes and attacks due to their decentralized nature nested within the SG security protocols.

Smart power grids are expected to be the future generation of electric power networks that will eventually upgrade its generation, transmission, distribution, and consumption sectors. The main idea of SG is to use information and communications technology (ICT) to improve the awareness, efficiency, sustainability, reliability and security of the network by automatically gathering and quickly acting on the recorded online smart meter data [2]. The main components and smart features of SG are renewable distributed energy resources (DERs), advanced metering infrastructure, distributed energy storage systems and the formation of microgrids (MGs) that can operate in grid-connected and/or islanded modes [1-11]. In addition, SG facilitates the integration of incoming PEVs with vehicle-to-grid (V2G), grid-to-vehicle (G2V) and vehicle-to-vehicle modes of operation (Chapter 3, Sec. 3.5). Fig. 2.2 presents an illustration of SG architecture. The physical part of SG consists of the generation, transmission, distribution, and consumption sectors while the cyber part consists of WANs, neighbourhood area networks/field area networks (NANs/FANs), and home area networks/business area networks/industrial area networks (HANs/BANs/IANs) [2].
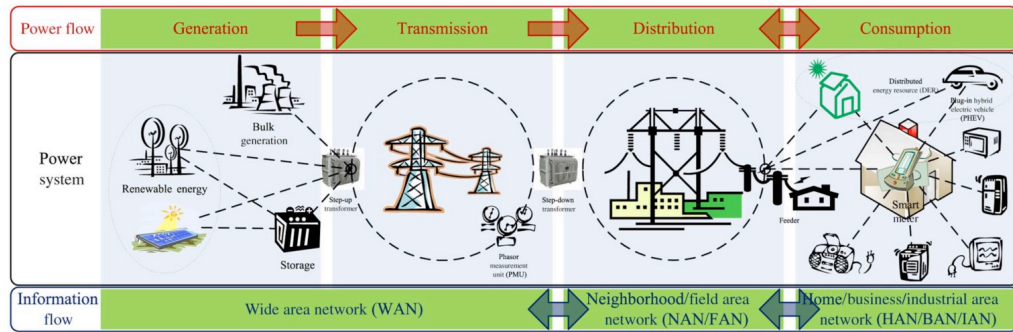
Fig. 2.2. The infrastructure of SG with physical and cyber parts [2].

2.2. Smart Power Grid Infrastructure

SG infrastructure can be classified into three systems including smart energy, information and communication systems [1-6].

2.2.1. Smart Energy System

The energy system of smart power grid relies on two-directional energy flow to perform generation and delivery as well as the consumption of electricity. The smart energy system of SG can be divided into the following four parts [2].

1) **Smart Power Generation-** Unlike the traditional power grids that are built with large fossil-based centralized power generation (e.g., oil, coal and natural gas), the smart power generation takes advantage of the two-way energy/information flows capability of SG to produce electricity from the pollution-free renewable resources (e.g., solar, wind, water/hydroelectric, geothermal, bioenergy, ocean, nuclear, hydrogen and fuel cells) [1-6]. The future smart power generations are expected to be small-scale (3 kW to 10,000 kW) DGs mostly consisting of many rooftop PVs and single wind turbines within the residential sectors as well as a few mini solar small wind farms within the residential parts of SG [4]. The ability of consumers to import (purchase), export (sell) and control their small-scale generators will soon change the traditional terminology of designing large central-based power grids.

2) **Smart Transmission Grid-** The SG transmission is an integrated system with three

interactive components [1-6]. a) Smart high-voltage substations with autonomization, control and coordination technologies that can respond rapidly to improve operator safety [4]. b) Smart control centers with innovative analytical features to monitor, visualize, analysis and evaluate data/information [4]. c) Smart transmission networks with the capability to enhance the security, reliability, and quality of transferred electric power by employing new technologies in computing, signal processing, materials, electronics, sensing and communication [4].

3) *Smart Distribution Grid-* Unlike the conventional distribution networks, the distribution sector of SG ingrates both AC and DC power dispatching and distribution as well accommodation of DGs to control reactive power flow and improve the quality of service to consumers at lowers costs [1-6]. This will require bidirectional power flow control and energy storage facilities that make the distribution system more complicated [4].

4) *Microgrid-* A unique feature of the SG that distinguishes its operation from the conventional power grid is the option for the formation microgrids (MGs) that can operate either in grid-connected or islanding modes (Fig. 2.3) [1-6]. Another interesting point about the SG is that a number of MGs can be joined and operate together to form the so-called networked (also called clustered) MGs [7-9]. In the grid-connected mode, the power generations of the MG can either be exported (sold) to the SG (also called macrogrid), or they can be used to feed the local MG loads. In the islanding, all MG power generations are used locally. Furthermore, a MG can satisfy the requirements of consumers and/or the critical loads. Fig. 2.3 shows the typical architectures of MG which is connected to the main smart power grid (also called macrogrid). Three layers support the MG [4]. The top layer performs smart

information flow as discussed in Section 2.2.2. The layer in the middle performs the required electricity flow in the smart communication flow as discussed in Section 2.2.3. The physical structure of the MG (shown in the lower layer) consists of one wireless access point, four renewable DGs (two wind and two solar generators) and four buildings [4].
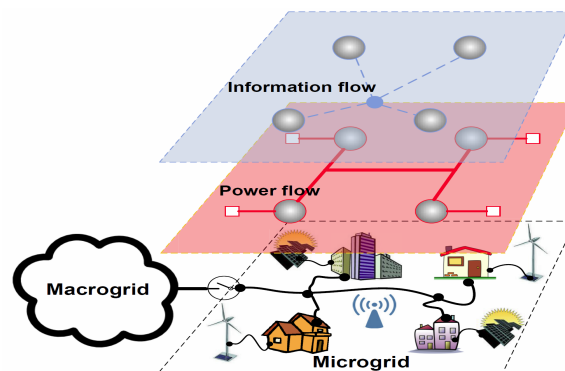
Fig. 2.3. The architectures of Microgrid (MG) [4].

2.2.2. Smart Power Grid Information System

This information system relies on smart metering and smart monitoring to perform management of information within the framework of the SG [1-6]. This is done by observing, analyzing, optimizing, and controlling the flow of information through the network. In fact, the smart information system addresses many the issues related to the distributed automation such as the interoperability and the scalability of exchanged data and its integration with the smart power grid's systems, devices, and applications [4].

An important issue associated with the smart information system is "Information Metering and Measurement". It includes the collection of information from smart sensors, smarter meters, and phasor measurement units (PMUs) as well as utilizing the recorded information for grid status monitoring, appliance control and user billing. The subject studies in the smart information system can be classified in the following two areas [4]:

1) **Smart Metering-** In SGs use an automatic metering infrastructure (AMI) which is a technology built within the automatic meter reading (AMR) systems [4].

2) *Smart Monitoring and Measurement-* The monitoring and measurements are mainly performed using sensors and PMUs. The sensor technology is already embedded in power grid for different purposes such as real-time conditions assessment, real-time monitoring, short-circuit and fault detections [4].

Another important issue associated with the smart information system is "Information Management" which is done to make good use of the information collected from smart metering, sensors and PMUs. The subject studies in the information management are in the areas of modeling, analyzing, optimizing and integration of the data and information.

2.2.3. Smart Power Grid Communication System

The main responsibility of smart communication system is transmitting the information between devices and systems. It comprises of wireless, wired and end-to-end communication management [4].

The Wireless Communication Technology has low installation cost and fast deployment, which makes it suitable for remote applications. There are a number of wireless technologies suitable for SGs such as cellular, satellite and microwave optical communications as well as wireless mesh network [4].

The Wired Communication Technology may be used in SG networks in addition to the wireless communication. There are two types of wired communication including fiber-optic and powerline communications (PLC). Fiber-optic communication is suitable for high-voltage high-speed communication networks due its inherent electromagnetic and radio interference immunity, but has high installment cost of optical fibers. The deployment cost of PLC is comparable to the wireless technology since it is being currently used by many power networks for load control and remote metering and [4].

2.3. Demand Response in Smart Power Grid

Demand response (DR) is a distinct characteristic of SG, which is the rescheduling of consumers' energy consumptions to decrease the operating cost of expensive generators, and defer future capacity addition [1-11]. In general, DR can be classified into three categories as demonstrated in Fig. 2.4 [2]:

- **Peak shaving (clipping)** is decreasing the peak energy consumption to prevent network, substation, transformer and line overloading. Peak shaving may result in customer dissatisfaction since the utility is cutting of their demands.

- **Valley filling** is to promoting off-peak energy consumption with the aid of energy storage. This can be done using rechargeable battery energy storage systems, hybrid electric vehicles (HEVs) and/or plug-in electric vehicles (PEVs).

- **Load shifting** is the process of shifting the energy demand from peak-load hours to off-peak periods without reducing the daily total energy consumption of the consumers. This approach is a combination of the valley filling and peak shaving that considers customer satisfaction.

| (a) | (b) | (c) |
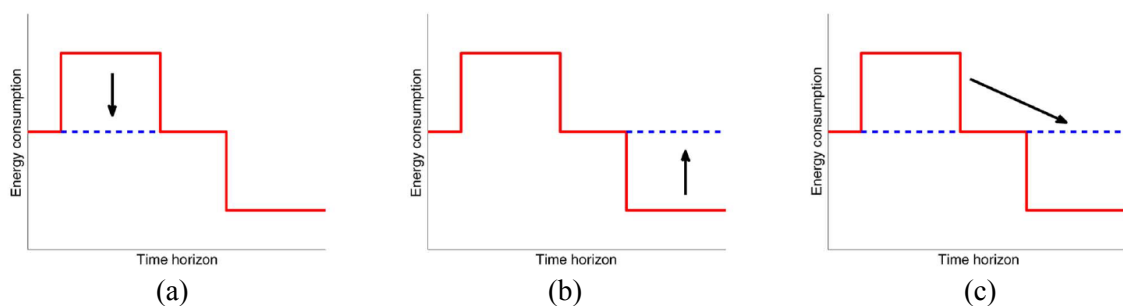
Fig. 2.4. Demand response (DR) functions; (a) peak shaving/clipping, (b) valley filling, (c) load shifting which is a combinations of valley filling and peak shaving [2].

2.3.1. Demand Response Communication Architectures

The DR mechanism involves the interaction between the supply side and the demand side of SG using bidirectional power and information flows as demonstrated in Fig. 2.5(a). The two main drivers of implementing DR into SG are intelligent metering and

bidirectional communications [2]. DR programs are mainly implemented using three types of communication architecture as shown in Fig. 2.5(b). These networks have different sizes, different locations and use a variety of communication standards and technologies.

The first type of DR communication architecture (Fig. 2.5(b)) is the wide area network (WANs) [2]. This architecture uses fiber optics, microwave transmission, and/or cellular networks to facilitate communications between generation, transmission, and meter data management system (MDMS). The second type of DR communication architecture (Fig. 2.5(b)) is the neighbourhood area networks/field area networks (NANs/FANs). This architecture is used for distribution system and MGs to support communications among their substations and field electrical devices. NANs/FANs connect several smart meters to data aggregate unit (DAU) using WiFi, WiMax, and/or cellular networks (such as general packet radio service (GPRS), 3G, and long-term evolution (LTE)) [2]. The third type of DR communication architecture (Fig. 2.5(b)) is the home area networks/business area networks/industrial area networks (HANs/BANs/IANs). This architecture is used to connect smart appliances in industrial plants, commercial buildings and residential units to the SG through ZigBee, WiFi, and/or PLC technologies [2].

(a)

(b)
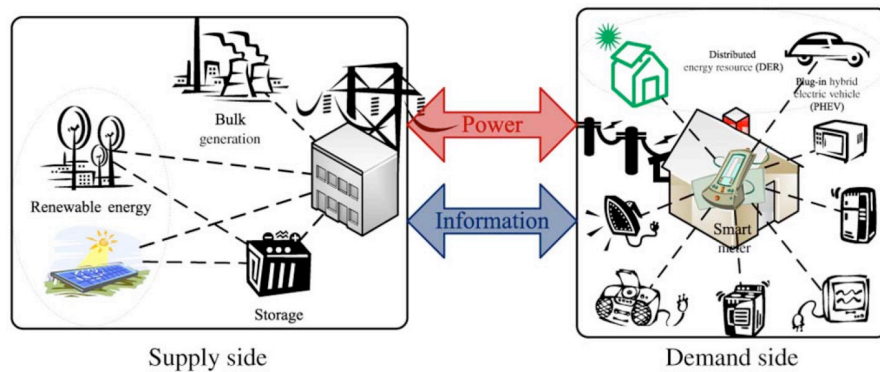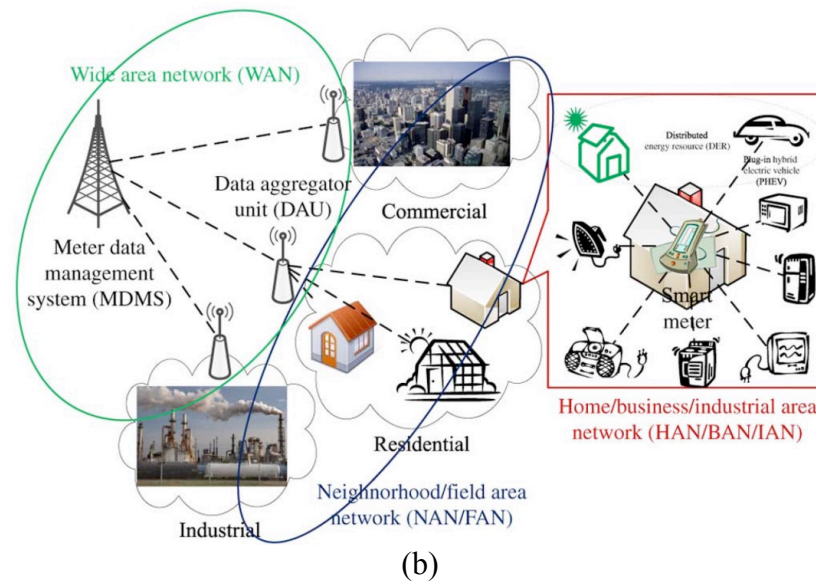
Fig. 2.5. (a) Smart demand response mechanism with two-way flows of power and information between the supply and demand, (b) DR communication architectures with three types of networks based on various communication standards and technologies [2].

2.3.2. Demand Response Programs

Demand response (DR) programs are the means or tariffs that utilities use to encourage customers to modify (reschedule) their conventional patterns of energy usage and try to postpone some loads to off-peak hours. DR can be divided into two main categories of incentive-based programs and price-based programs [2].

a) Incentive-based DR Program

Incentive-based DR programs are based on the idea of paying the users that participate in DR by reducing their demands during peak load times or system contingencies (e.g., the unexpected loss or failure of a part and/or an equipment such as transmission line, feeder, transformer, and generator). They offer incentive payments to the participating users. The main types of incentive-based DR programs are [2]:

1) *Direct Load Control (DLC)-* is based on the idea of reducing user loads at peak hours. Therefore, the utility needs to have remote access to shut down or control the cycle of certain user loads such as water heater, air conditioner and electric vehicle

30

charging. DLC is a well-stablished approach. In fact, some utilities have been offering DLC options to their residential and commercial customers [2].

2) ***Interruptible/Curtailable Load-*** is based on the idea of cutting down some portion of the user interruptible and/or curtailable loads. This is done if system reliability is at risk. The participating users receive some incentive discounts on their electricity bills [2].

3) ***Demand Bidding and Buyback-*** is designed for participations of larger users (e.g., over 1MW) to restrict some of their usage at a specific times during peak demand or system contingencies [2]. Small users can also participate through third agents.

4) ***Emergency Demand Reduction-*** is also intended for participations of larger users who are willing to quickly reduce their loads within very short notice during emergency conditions and accidents when grid is out of reserve [2].

b) Price-based DR programs

Price-based DR programs are alternatives to the incentive-based programs and use smart pricing strategies. They provide different electricity prices within the 24 hours with higher rates during the peak load periods [2]. Consequently, most consumers will reduce their electricity demands/consumptions at peak hours. As shown in Fig. 2.6, there are various time-based pricing tariffs. The main pricing strategies used in price-based DR programs are [2]:

1) ***Time-of-use (ToU)-*** pricing strategy charges users with different electricity prices depending on the time of the day or season of the year. Time periods are usually longer than an hour. Fig. 2.6(a) shows a typical three-level ToU pricing with three different tariffs for the on-peak, mid-peak and off-peak time periods. Obviously, the electricity price is much higher for the on-peak time block compare to the mid-peak

and off-peak time periods [2]. The ToU time blocks and the corresponding tariffs must be carefully designed to persuade consumers to shift their loads over the designated (daily, weekly, annual) time horizon.

2) ***Critical peak pricing (CPP)-*** strategy is the same as ToU pricing with the exception that periods that the grid reliability is at risk, a higher pre-specified higher rate is used instead of the peak price to reduce consumers' demand [2]. Note that CPP is only implemented for limited numbers of hours or limited number of days per year.

3) ***Dynamic or Real-Time Pricing (RTP)-*** strategy is implemented to have various electricity prices at different time intervals (e.g., 15 minutes or one hour) of a day. RTP is typically released on an hour-ahead or day-ahead (DAP) basis is considered to be one of the most economic pricing regimes [2].

4) ***Inclining Block Rate (IBR)-*** is the same as ToU with the exceptions that: i) the tariff has two-level rate structures with lower and higher blocks, ii) the pay rate per kWh increases as a consumer uses more electricity beyond a certain threshold [2]. Therefore, users can pay less dollars per kWh by consuming less electricity. IBR is designed to incentivize users in order to limit their hourly/daily/monthly energy consumptions and indirectly spread their loads to off-peak periods of a day. This will reduce the peak-to-average ratio (PAR) demand of the grid. Utilities have been adapting IBR since 1980s.
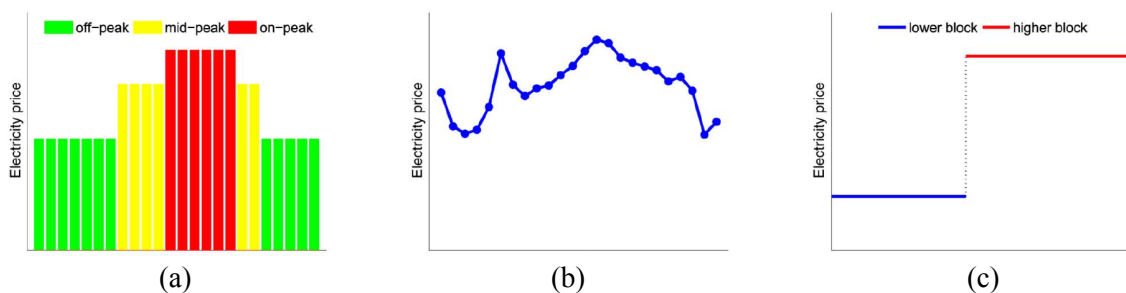
Fig. 2.6. Illustration of time-based pricing tariffs: (a) Time-of-use (ToU) pricing, (b) Real-time pricing (RTP), (c) Inclining block rate (IBR) [2].

2.3.3. Demand Response Modelling and Formulation Approaches

DR programs are typically implemented in the residential sectors of SG with limited recent applications to the commercial and industrial sections [2]. The reason is that residential consumers are more sensitive to the electricity price since they have more appliances that can be easily controlled, deferred and interrupted such as washers, variable-speed air conditioners, dryers, dishwashers, swimming pool pumps and plug-in electric vehicles [12]. This section discusses the modelling and formulation of DR problem followed by possible solution approaches.

A. Demand Response Models

DR is based on the collaboration between the utility and the consumer. Therefore, the behaviors of both sides need to be mathematically modeled which is done using the following function models [2]:

- *Utility Function Model* is used to model the behaviors of different users. To do this, the levels of users satisfaction are expressed in terms of their consumptions. Any type of utility function can be utilized as long as it has the following two properties [13]:

  ✓ Users can accomplish more tasks and gain more as they consume more power until reaching their chosen amounts of energy consumption.

  ✓ Marginal benefits to the users are decreasing such that their obtained comforts are gradually saturated when users' consumptions reach the chosen levels.

- *Cost Function Model* is used to model the utility expense for generating and delivering the electricity. This can be any increasing and strictly convex cost function as long as it satisfies two following two properties [14]:

  ✓ Energy cost increases when the total load increases.

  ✓ The utility marginal expense is increasing.

B. Demand Response Problem Formulation

33

Considering the above-mentioned utility and cost functions, DR is mathematically formulated as the following problems [2]:

1) **Utility Maximization** that is from the social viewpoint, the grid wants to increase the individual user comfort while decreasing the utility expenditures [2].

2) **Cost Minimization** that is from the utility's perspective, it is desirable to reduce the cost of generating and delivering electricity [14-15].

3) **Price Prediction** which is required to perform RTP if the utility broadcasts electricity rates only hour ahead bases.

4) **Renewable Energy** which is required to include the uncertain and irregular behavior of renewable resources such as solar irradiation and wind speed into the bulk generation [16].

5) **Energy Storage** is taking advantage of the of energy storage systems such as rechargeable batteries, HEVs and PEVs [10-12].

C. Demand Response Solution Approaches

DR can be formulated as an optimization problem, and solved using various approaches such as [2]:

1) **Convex Optimization-** with convex objective and constraint functions [12].

2) **Game Theory-** which is the study of selfish and rational individuals and/or a model of interactive decision-making processes [14].

3) **Dynamic Programming-** that decomposes the complex DR problem into a sequence of simple subproblems that cab be quickly solved [17].

4) **Stochastic Programming-** which deals with uncertain optimization problems by taking advantage of the associated known/estimated probability distributions [18-19].

5) ***Artificial Intelligence (AI) Optimization-*** which is based on simulating human behavior through computation by designing computer systems that are able to execute tasks which require human intelligence. DR programing can be formulated and solved using compuational intelligence AI methods that include; i) artificial neual network, ii) fuzzy logic, iii) evolutionary computation such as particle swarm optimization (PSO) and ant colony optimization (ACO) algorithms [20-22].

2.4. New Research in Smart Power Grid Technology

Some possible future research directions related to smart power grid technology are:

- ***New Genrations of Smart Mircogrid (MG) and Community Grids-*** which is a group of interconnected loads and DGs (mainly renewable resources) that can operate either in isolated or gird-connected modes. The future research directions may be in optimal design, control, managenet and real-time and operation of AC, DC and hybrid AC/DC micor gides [5], [23-24].

- ***Networked MGs-*** which is an interconnected system of MGs that takes advantage of various complementary power sources and effectively coordinates the energy sharing and/or trading among the MGs and the SG to improve the stability, reliability, and energy efficiency of the system. Future reaserch directions in networked MGs can be on coordination and energy exchange among the interconnected MGs, distributed energy management schemes, correlation of renewable power generation, and reactive power exchange among MGs [7-9], [25-26].

- ***Optimal Operation of SG and Management of Energy Storage-*** With the increasing applications of intermittent renewable DGs, controllable loads such as smart appliances, and time-depending portable loads such as PEV loads, the structure of SGs are becoming more time-dependent, stochastic and geographically distributed.

Therefore, power management and control of the smart power grid is becoming very challenging since its operation conditions can change very rapidly. Future research direction can be on real-time distributed control of SG, robust SG network models and advanced energy storage systems for improving the economy, flexibility and security of SGs and MGs [2], [10-11], [27-32].

- *Advanced Metering, Information and Communication Infrastructures-* SG integrates advanced metering infrastructure (AMI), sensing and control, as well as information and communication technology (ICT). AMIs are responsible for the collection and anlyses of the data recorded by smart meters, as well as controlling, monitoring, and managing multiple domains of the power grid. ICTs bring significant innovations to generation, transmission, delivery, consumption and storage of electricity. Future research areas my be on scalable AMI architecture, advanced defensive mechanisms against threats and attacks, privacy and security of users, application of AMI in smart cities [33-36].

Power Quality, Resilience, Security and Internet of Things (IoT)- The increasing injection of renewable generation and extensive applications of switching devices in SGs and MGs is deteriorating the quality of power. On the other hand, the extensive adoption of the Internet of Things (IoT) technologies is increasing the possibilities attacks and intrusion on network. Future research directions can be in new smart power electronics-based distributed generations, energy storages, and modern loads to control power quality. In addition, the safety, stability, resilience and security of SG and MGs can be improved using effective methods such as energy storage, big data, cloud computing, internet of things (IoT), artificial intelligence, and cyber physical systems [37-42].

The smart grid technology can be used to meet environmental targets by accommodating demand response, renewable DGs, storage capabilities and high penetration of PEVs including all-electric and plug-in hybrid electric vehicles. However, connection of PEVs can have serious impacts on the existing and future smart grids such as overloading of

lines and transformers, increasing network losses, and causing poor power quality. Chapter three highlights negative impacts of random PEVs charging activities followed by a through literature review on the recent PEV charging coordination strategies and research gaps.

CHAPTER THREE: LITERATURE REVIEW ON COORDINATED BATTERY CHARGING STRATEGIES FOR ELECTRIC VEHICLES

Chapter 3 provides a literature review on recent coordination approaches for centralized charging of plug-in electric vehicles (PEVs). It starts with an introduction to EV technology with emphasis on their markets, charging types, advantages, limitations and effects of uncoordinated PEV battery charging on smart power grids [43-60] followed by literature reviews on the classification, properties and objectives of PEV battery charging coordination [61-109]. It will also present anticipated future research directions for the coordinated battery charging of PEVs. Some materials of this chapter were published by the author during his Ph.D. studies in references [53]-[54].

This chapter is organized as follows:

- Section 3.1 discusses the present and future markets of electric vehicles as well as their benefits and drawbacks.

- Section 3.2 presents EV charging levels, types and characteristics.

- Section 3.3 discusses the effects of uncoordinated PEV battery charging on power grid.

- Section 3.4 gives a classification of PEV battery charging coordination schemes.

- Section 3.5 presents the properties of PEV coordinated battery charging schemes.

- Section 3.6 presents the objective functions of PEV battery charging schedule optimization.

- Section 3.7 discusses future research in battery charging coordination of PEVs.

3.1. Electric Vehicles

There are two main types of EVs. The plug-in hybrid electric vehicle (PHEV) with both internal combustion engine (ICE) and electric engine, and the plug-in electric vehicle

38

(PEV) that only relies on electric engines [43]-[44]:

1) PHEVs are suitable for people who mostly travel short distances. They can travel on electric power alone for 10-15 miles and then switch the vehicle operation mode to the usual gasoline engine to extend their travel range. These drivers will still need to visit gas stations but not as often as when they were using the conventional ICT vehicles.

2) PEVs (also called battery electric vehicles; BEVs) are more efficient with lower maintenance costs since they use fewer components than both PHEVs and the conventional ICE vehicles. The new models of PEVs have extended driving range and only need daily charging from 110-volt outlets without requiring the purchasing/installation of 240-volt chargers.

Currently, most EV owners (over 80%) prefer home charging. This can cause power grid overloading predominantly in the evening customer peak load hours when many drivers come home and plug-in their EV [43]-[44]. One way to resolve this issue, as proposed in this Ph.D. thesis, is to coordinate the EV charging activities and try to move them to off-peak load hours. Another approach that is the vision of most utilities is to promote public charging at EV charging stations. This can be done by providing fast AC and ultra-fast DC charging (UFC) facilities/stations that can recharge a vehicle at a speed comparable to traditional fuel stations (e.g., in few minutes). However, EV charging stations with UFC technology will pose extraordinary challenges to the existing power networks particularly during peak traffic hours due to their large power density and impulsive load characteristics [43]-[44].

Planning the locations and ratings (electric capacities) of charging stations (with fast and UFC technology) is critical to prevent their negative impacts on power network such as grid asset depreciation, poor power quality and network instabilities [45].

3.1.1. Present Global EV Market

The upgrading of conventional transportation network (with ICE technology) to the emerging electric vehicle network (that relies on the EV technology) has been rapidly growing since the launch of "Nissan Leaf" and "GE Chevrolet Volts" in December 2011 [43]-[44]. Figures 3.1 and 3.2 show the global passenger EV stock from 2013 to 2018. Surprisingly, the global grow rate of EV technology, sales and stocks have been significantly increasing [43]-[44]:

✓ In 2018, the global EV fleet was 5.1 million which is over 2 million higher than year 2017. As with the previous years, the global EV market in 2018 was led by China with 2.3 million (e.g., 45% of the total global 5.1 million) followed by Europe (1.2 million) and U.S. (1.1 million). In 2018, there were over 460,000 vehicles on the world's roads, almost 100,000 more than year 2017. Figures 3.1-3.2 shows the global EV sales and the corresponding market shares of different countries from year 2013 to year 2018.

✓ In 2018, there were over 5.2 million light-duty vehicles (LDVs) chargers worldwide. These chargers comprise mostly of level 1 level and 2 slow chargers (Tables 3.1) at residential homes and workplaces as well as 540,000 publicly accessible chargers and 157,000 fast chargers for buses [44].

✓ In 2018, there were over 5 million low-speed electric vehicles (LSEVs) worldwide. These vehicles are all located in China. LSEVs are not subject to restricted registration regulations since they are significantly smaller than regular EVs [44].

✓ In 2018, there were also over 300 million electric two/three-wheelers worldwide which are mostly located in China.
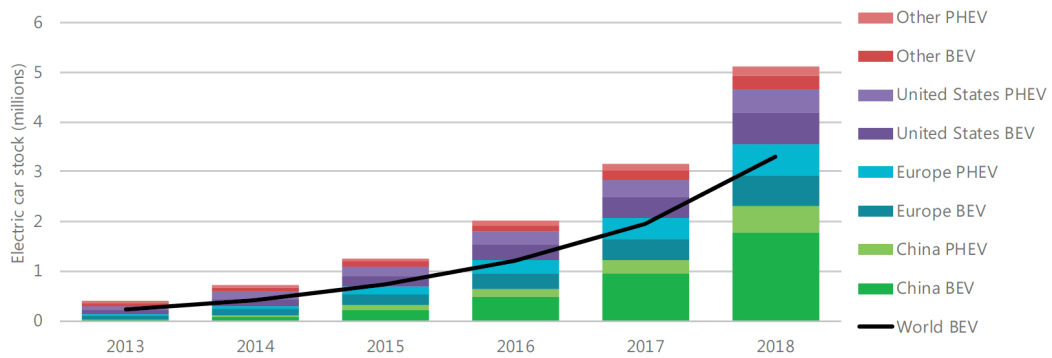
Fig. 3.1. The global passenger EV stock from 2013 to 2018 in the top-three electric vehicle initiative countries including the plug-in hybrid electric vehicles PHEVs and the battery electric vehicles BEVs (also called plug-in electric vehicles PEVs) indicating there were 5.1 million passenger EVs worldwide in 2018 (45% in China) [44].
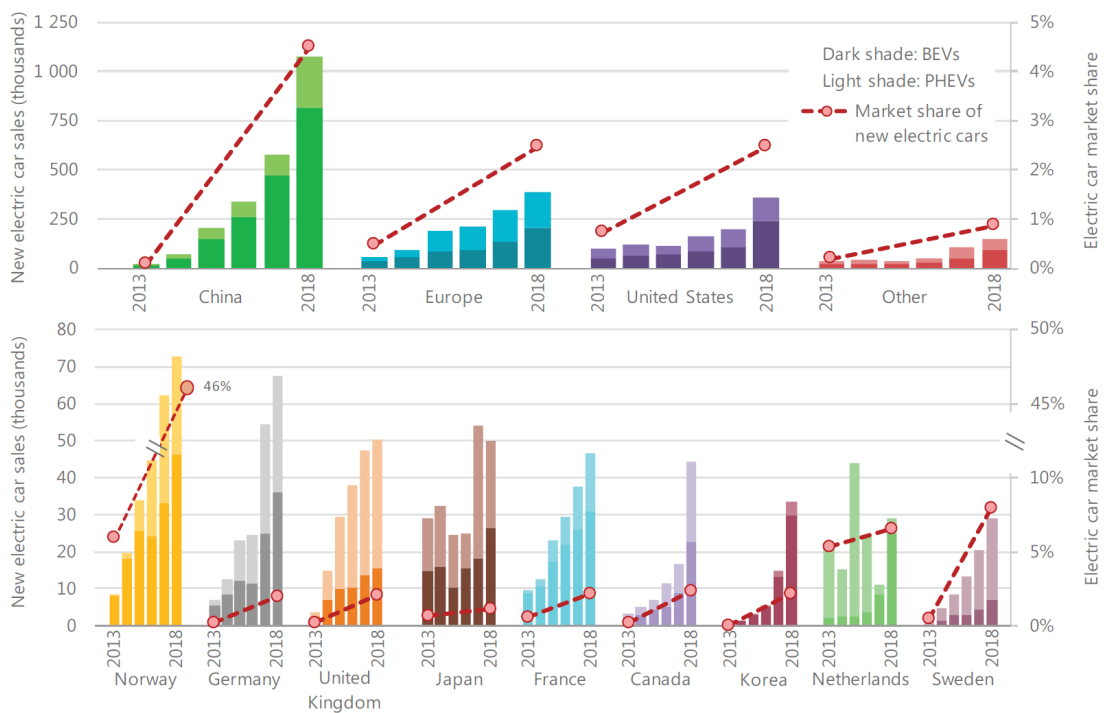
Fig. 3.2. The global EV numbers and EV sales from year 2013 to year 2018 showing market shares of different countries [44].

3.1.2. Projected Future Global EV Market

The International Energy Agency (IEA) along with the Clean Energy Ministerial and the Eclectic Vehicles Initiative have used the following two scenarios to explore and estimate the future development of EVs by the year 2030 [44]:

A. The New Policies Scenario

This scenario aims to illustrate future impacts of the announced policy ambitions on the future development of PEVs. The summarized outcomes of this study are shown in Figure 3.3 [44]:

✓ In general, policies will have significant impacts on the development of EVs.

✓ In 2030, the global EV sales will extent the 23 million mark and the global EV stock will exceed 130 million vehicles (not including two-wheelers and three-wheelers).

✓ In 2030, the demand for oil products will be cut by about 2.5 million barrels per day.

B. The EV30@30 Scenario

This scenario considers the EV initiative's campaign to reach a 30% EV market share by the year 2030. This percentage includes all car types with the exception of the two-wheelers. The summarized results of this study are also shown in Figure 3.2 [44]:

✓ In 2030, the global EV sales will be almost doubled. It will reach the tempting mark of 43 million while the global stock will also be almost doubled reaching 250 million.

✓ In 2030, the three countries with leading EV market shares are China (57%), Europe (26%) and Japan (21%).

✓ In 2030, the demand for oil products will be cut by about 4.3 million barrels per day, which is much higher than the 2.5 million barrels per day reported by the first IEA scenario. This is expected since the anticipated future (year 2030) number of EVs

reported by this scenario (e.g., 43 million) is 87% larger than the 23 million mark resulting from the new policies scenario.

C. The Country-Specified EV Injection Target

A number of countries have set roadmaps and target injection levels for the employment of EVs. The country-specified EV (not including PHEVs) injection targets for a few countries are listed as follows [43], [44], [50], [59]:

1) United States: 10% EV injection by year 2025.

2) China: 20% EV injection by year 2025.

3) Norway: 100% EV injection by year 2025.

4) Netherlands: 100% EV injection by year 2035.

5) United Kingdom: 100% EV injection by year 2040.

6) Japan: 20-30% EV injection by year 2030.

7) Australia: The opposition government in 2019 proposed an EV injection target of 50% by 2030. The government analysis in 2019 also forecasted 50% by 2035.
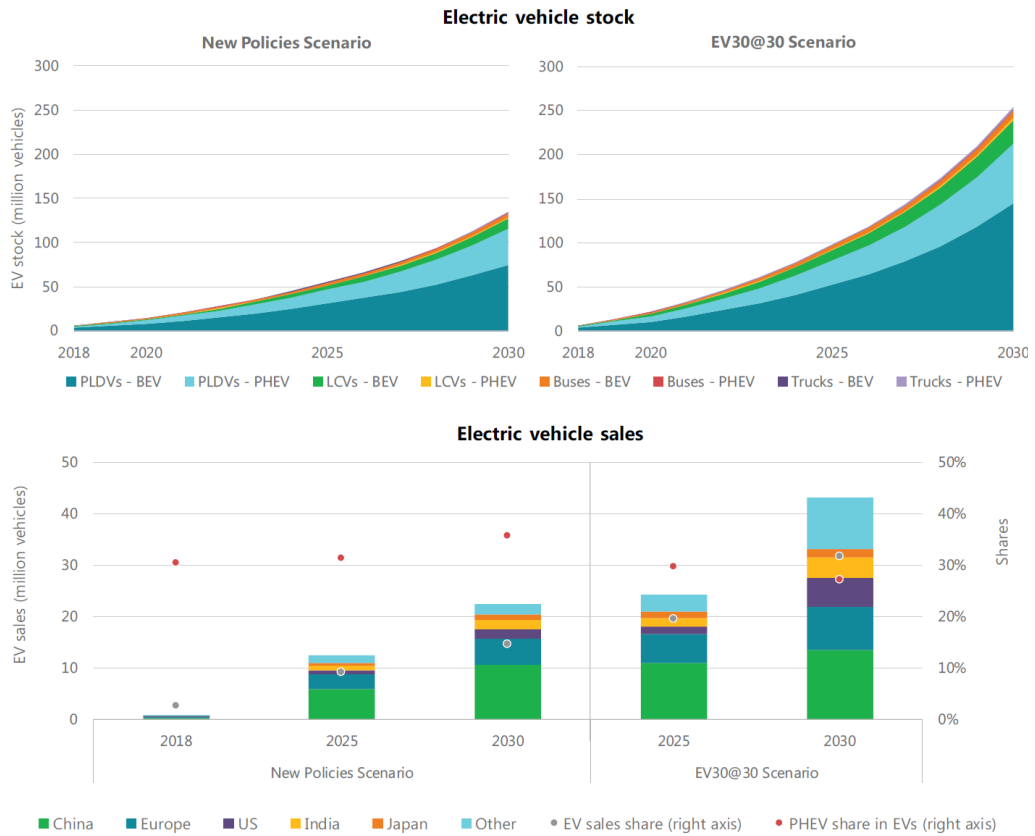
Fig. 3.3. The future global EV stock and EV sales by scenario for years 2018-2030 [44].

3.1.3. Benefits and Drawbacks of EVs

The sell market of EVs and their integrations into power grids have been noticeably growing in recent years [45], [50]. This is due to the many benefits that EVs can offer to both the consumers and the environment. Unfortunately, there are also issues and problems associated with uncoordinated (random) EV charging.

A. Main Benefits of EVs

The main reason for the increasing uptake of EVs is the awareness of our societies to the detrimental environmental impacts of combustion engine vehicles such as Co2 and greenhouse gas emissions as well as other harmful toxins that threaten our health. Many automobile manufacturers are now building new generations of EVs that come in different classes, sizes, models and prices.

Battery operated EVs (also called PEVs) have many advantages over their combustion counterparts including [45]:

✓ EVs have less maintenance cost (e.g., no oil changes), less wear outs (e.g., fewer moving parts), smoother, more quiet (inside and outside), faster (e.g., higher torque power).

✓ EVs provide options for convenient home charging with discount rates during off-peak load hours. The consumers have the choice of cheap overnight charging.

B. Main Drawbacks of EVs

In the present market and present battery technology, there are two main issues preventing the widespread use of EVs [45]:

1) **The EV Range Anxiety-** Fortunately, this issue is being quickly resolves. Many car manufacturers have been tackling and resolving this issue by taking advantage of the advancements in battery technology and electric regenerative systems. Many governments are helping to resolve the second issue by offering significant rebates and tax credits for purchasing EVs.

2) **The EV Price-** In today's market, the EV prices are not competitive with the conventional ICE automobiles. However, this issue is expected to be eventually resolved as the prices of most rechargeable batteries are sharply dropping. In the meantime and until we reach a state that EV purchase prices are as low as the ICE vehicles, the law makers and governments are trying to resolve this issue by offering significant rebates and tax credits for purchasing and driving EVs. At present, there EV incentives and tax credits in China, United States, Australia, Japan and many European countries.

B. Possible Solutions to EV Drawbacks

There are a few solution approaches to overcome the obstacles associated with EV deployment including [44]:

➢ Cost saving in rechargeable battery manufacturing.

➢ Cost reduction in EV manufacturing.

➢ Cost reduction by adapting battery sizes to travel needs. For example, we can reduce/avoid costs due to oversizing of batteries by matching the range of vehicles to the driver travel habit. This is already considered in the most designs of electric buses.

3.2. EV Charging Levels, Types and Characteristics

In accordance with the EV and battery changer standards, there are there AC levels and three DC levels for charging the batteries of electric vehicles as listed in Table 3.1 [43], [44,[49], [50], [60]. Some references also mention an ultra-fast DC level, which is not yet standardised [50]. Note that the high voltage, power and kWh of level 3 for both AC and DC charger are not yet finalized [49].

- The AC Level 1 EV charger can be plugged-in to a standard household outlet of 120 V_{AC} with current rating of 15 A or 20 A. The charging time of 15A is twice as long as the 20 A. This charger can draw from 1.44 kW to 1.92 kW of power [60]. The AC Level 1 can typically add around 2-5 miles (3.25-8.1 km) of EV driving range per hour of charging time [46].

- The AC Level 2 EV charger is typically designed both private and public facilities. It can be used for private installation with single-phase 240 V_{AC} and current-handling capacity of 40 A as well as public installation with three-phase 400 V_{AC} and current-handling capacity of 80 A [60]. The AC Level 2 can typically add around 10-20 miles (16.1-32.2 km) of EV driving range per hour of charging time [46].

- DC fast charging is typically used in public charging stations. It can add around 60-80 miles (97-128 km) of EV driving range to per 20-30 minutes of charging time [46].

- Wireless charging based on wireless power transfer techniques have also been considered for EV applications. The present limitations are low efficiency and high cost due to the inherent large air gap between the EV and the wireless charger [46].

A. Impacts of EV Charged Type on Power Transformer Loading

In selecting the EV charger type, we need to consider its loading impacts on the power transformers. According to reference [49]:

- Low injections of EV loads will not have major impacts on transformers.

- However, EV loading over 30% may overload the transformer beyond its rated limits, may result in hot spot winding temperature and loss of life.

- Level-1 EV charger has minor impacts on the loading of transformers.

- Level-2 EV charger may cause transformers failure due to extreme temperature rise.

- To avoid transformer overloading and failures, coordinated EV charging instead of random charging is recommended.

B. EV Charging Systems

There are different types of EV charging systems [60]:

- *Conductive EV Charging-* This is the usual EV charging method. It transfers power through direct contact. It uses a conductor to connect the EV charger to the outlet at home, office, parking lot or charging station. Conductive charging is simple and very efficient and can be designed to AC, DC, on-board and off-board.

- *Inductive EV Charging-* This is also called wireless charging. It uses the concept of induction and electromagnetic field to transfer electricity to the EV battery without using any conductor. It is very convenient but has low efficiency that has prevented its

widespread applications. High quality commercial inductive charger can have efficiencies of up to 85% [60].

- ▪ *Battery Swapping-* In this charging method, the drivers swap their empty battery with charged batteries at battery swapping stations. It is not convenient but has advantages such as low cost of battery management, long battery lives and low time consuming. Battery swapping can also avoid EV loading during peak hours and money.

Table 3.1 Standard EV charging levels [43], [44], [49], [50], [60].

Charger Level	EV Charger Type (Voltage/Current Rates)	Maximum Power (kW)	Battery Size (kWh)	Charging Time (h)	Charger Location	Typical Use
AC Level 1	120 V_{AC}-15 A (12 A**) 120 V_{AC}-20 A (16 A**)	1.44 1.92	24 (19.2**)	10-13	On-board 1-phase	Home, office
AC Level 2	240 V_{AC}-40 A (32 A**) 400 V_{AC}-80 A (64 A**)	7.7 25.6	24 (19.2**)	1-3	On-board 1or 3-phase	Private, public
AC Level 3 Fast	480 V_{AC}-up to 80 A	>22 (to be determined)	To be determined	To be determined	To be determined	To be determined
DC Level 1	208 V_{DC}-80 A (64 A**) 600 V_{DC}-80 A (64 A**)	13.3 38.4	24 (19.2**)	0.5-1.44	Off-board DC	Public, commercial
DC Level 2	208 V_{DC}-200A (160 A**) 600 V_{DC}-200A (160 A**)	33.3 96	24 (19.2**)	0.2-0.6	Off-board DC	Public, commercial
DC Level 3 Fast*	208 V_{DC}-400A (320 A**) 600 V_{DC}-400A (320 A**)	To be determined	To be determined	< 0.2	Off-board DC	Public, commercial
Wireless charging	To be determined	To be determined	To be determined	To be determined	Off-board AC	Private, commercial

*) Also called direct current fast charging (DCFC) or ultra-fast DC charging. The high voltage, power and kWh of level 3 for both AC and DC charger are not yet finalized [49].
**) The useable/available current/energy.

3.3. Impacts of Random Electric Vehicle Charging on Power Network

The extend of EV impacts on power network and the severity of their charging demand depend highly on their injection, battery sizes, locations, random plug-in and plug-out times as well as the charging technology (Table 3.1) such as charging level, voltage, current and power [43]. The majority of EV charging is in the residential sectors (e.g., at homes and building complexes connected to residential feeders) and commercial areas (e.g., at office, parking lots and charging stations connected to low-voltage distribution networks). EVs are sizable, portable and random loads [43]. Hence, we need to have clear

understandings of EVs technology, charging patterns and traffic paths (e.g., usage patterns) for their integration, control, and coordination within the power grids.

3.3.1. Effects of Random EV Battery Charging on Smart Power Grids

Main effects of random/uncoordinated battery charging of EVs on the electricity network may be summarized as follows [43]-[50], [53]-[54]:

- The extra EV demand should not cause an issue in the future power networks. The IEA studies indicate that the additional EV energy demands are sizable but manageable loads. It is estimated that the global EV loads will only be about 1.5% of the total electricity demand by year 2030.

- At the generation level, the high demand and scarce capacity of EVs could increase the electricity prices.

- At the transmission level, the stress on the system particularly during peak load periods could require more reserve capacity and extra system services such as frequency control.

- At the distribution level, the high EV demand could overload lines and power transformers as well as voltage drops particularly towards the end of the feeders.

3.3.2. Mitigation Potential Negative Impacts of EV Charging

There are many options to control and mitigate the negative impacts of EV charging. A few potential solution approaches are summarized below [43]-[49], [52]-[54], [53]-[58], [60]:

- ➢ *Option 1- Installing of custom-designed EVSEs* at locations and with technologies that reduce negative impacts of EV charging on power grid. This can be done by the installation of charging infrastructures (e.g., charging points) in areas where the projected EV impact is low and the daily utilisation is high. Good candidate locations for charging points are near high population residential, business and commercial areas

with higher power capacity tariffs during off peak hours. This is being effectively practiced in the Netherlands with the charging points tied to residential areas where EV owners have high demands for parking permits [43].

➢ ***Option 2- Incentivising EV owners to maximise self-consumption*** through the utilization of renewable generation resources such as rooftop PVs without/with energy storage systems [43], [55], [58].

➢ ***Option 3- Controlling EV charging*** through centralized and distributed (also called decentralized) coordination strategies. This thesis proposes and implements four centralized PEV coordination algorithms in Chapters 4-7 [46], [47], [57]-[60].

➢ ***Option 4- Scaling up charging infrastructures to follow EV uptake*** through careful planning to bring economic advantages and grid stability. This can be done through gradual upgrading and deployment of EVSE as shown in Fig. 3.4. The three set-up phases of EVSE deployment are: i) dedicating one charging point for each EV, ii) performing load balancing over charging points and, iii) performing load balancing over buildings [43], [60].

➢ ***Option 5- Defining interoperability standards*** among EVs, CSs and SG network. Interoperability is the exchange of power and information among the stakeholders at the electricity network and ICT interface levels, respectively. Common standards and interoperability regulations are required to guarantee compatibility, efficient communication, and accurate flow of information at the network level (e.g., grid generations, operating conditions, loading and capacities) and user level (e.g., EV information such as its location, battery condition, G2V charging and V2G discharging requests) [43].

As the EV injection progressively increases in smart power grids, the above-mentioned options should be individually or concurrently implemented to offer cost saving to the EV and infrastructure owners as well as utilities, operators and distribution grids.
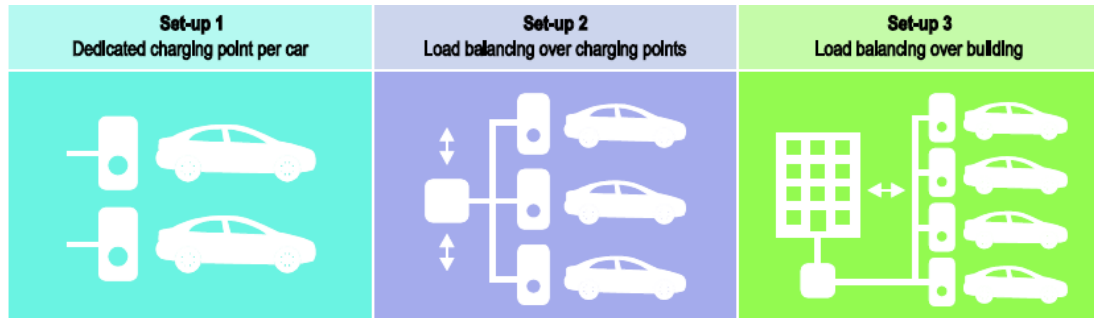
Fig. 3.4. Scaling up charging infrastructures to follow growth of EV uptake [43].

3.4. Classification of PEV Battery Charging Coordination Schemes

Despite many environmental benefits of PEVs, their anticipated large injections and massive demands can threaten the performance, economy and security of power networks [43]-[44], [61]. Therefore, it is crucial to design and implement proper PEV charge strategies that will not jeopardize network operation and offer cost savings to aggregators and PEV users. The PEV charge coordination control is an optimization problem with a set of constraints. The inputs are parameters, requirements and constraints of the EV chargers, users, aggregators and the network. The objective is typically a cost function and the output is a charging schedule with the starting and ending times being selected by each drivers.

The charging decisions/coordination can be made separately for each vehicle, collectively for groups of vehicles or centrally for all plugged vehicles. There are three main strategies for charging coordination of PEVs [45]-[48]:

1) *Centralized PEV Coordination-* A central aggregator (e.g., the independent system operator; ISO) makes the charging decisions as illustrated in Fig. 3.5(a).

2) ***Decentralized PEV Coordination-*** Individual PEVs make their own charging

decisions as shown in Figs. 3.5(b)-(c).

3) ***Hierarchical PEV Coordination-*** The aggregators and PEVs are arranged in tree

formations to make the charging decisions as demonstrated in Figs. 3.5(d)-(h).

The second (decentralized) and third (hierarchical) charging approaches are also called

distributed PEV coordination [47].

3.4.1. Centralized PEV Battery Charging Coordination

A centralized coordination architecture is used to allow the direct aggregator (or ISO) to

control the charging activities of all PEVs as shown in Fig. 3.5(a). In the literature, there

is a significant number of proposed centralized PEV battery charging coordination

algorithms such as [55]-[58], [62]-[68].

The centralized PEV scheduling can be implemented based on the following steps [63]:

1) The direct ISO continuously collects updated information of the SG (e.g., network

parameters, constraints and operating conditions) and the vehicles (e.g., plug-in times,

locations, and battery state of charge) as well as drivers' requirements and requests.

This is done through the SG communication system in real-time or using an online

approach.

2) The EV owners send charging request signals to ISO upon random plug-in of their

vehicles. The EV chargers automatically transmit the request signals.

3) At each time interval Δt, ISO solves the PEV battery charging coordination

optimization problem, generates a charge schedule and sends it to all vehicles.

4) All PEV battery chargers will follow the central schedule to complete their charging

process.

5) A vehicle can stop charging at any time and send back a charging termination signal

to ISO.

The centralized PEV battery charging coordination algorithms have two essential benefits

for the are ISO and the power utilities [46]-[47], [53]-[58], [62]-[68]:

✓ Their ability to generate near-optimal solutions since the central aggregator (ISO) has

access to the information of all vehicles and the entire network.

✓ They can easily consider various global network states and constraints (such as maximum generations, loadings, demands and voltage violations) within the optimization process.

Nevertheless, there are some disadvantages associated the centralized PEV battery charging coordination schemes [46]-[47], [53]-[58], [62]-[68]:

☒ The PEV owners do not have direct control of their own vehicle charging, but can submit their requests to the direct aggregator. From the users' point of view, this is the main disadvantage of the centralize PEV coordination strategy. Furthermore, the consumers may have concern about the privacy of their PEV information transmitted through the SG communication network.

☒ Scalability is a key challenge in the application of centralized PEV coordination algorithms to real life networks. This can become as issue particularly when the size of the optimization problem increases due to the large number/injection of PEVs and/or long scheduling time horizon. Furthermore, the widespread communicates of PEVs with ISO may lead to practical complications such as communication bandwidth limitations and costly expansions of communication infrastructure..

☒ A single point of failure at the ISO level (e.g., failure to solve optimal PEV scheduling problem) could potentially collapse the entire system.

3.4.2. Decentralized PEV Battery Charging Coordination

In decentralized PEV battery charging coordination strategies, each user acts as an independent aggregator who solves its own PEV battery charging problem as shown in Figs. 3.5(b-c). In the literature, there are many proposed decentralized PEV battery charging coordination algorithms such as [14], [69]-[79].

The main benefit of decentralized PEV battery charging coordination algorithms is [47]:

✓ They are highly scalable which makes them very practical for many field implementations associated with large networks due to low computational complexity.

✓ They are more resilient to network failures since their controllers are usually designed to withstand centralized communication failures.

However, there are some disadvantages related the decentralized PEV battery charging coordination schemes [47]:

☒ They cannot always capture the global optimal or near-optimal scheduling solution since the PEVs do not have to access to the complete network information.

☒ They have large communication overheads since PEVs need to continuously communicate their locally generated scheduling information with the other vehicles within the network.

The implementation of decentralized PEV coordination depend on the structure of GS communication network. There are two decentralized PEV coordination designs; DT1 and DT2, as shown in Figs. 3.5(b-c) [47]:

➢ **Decentralized DT1 Design-** In this design, each PEV keeps trying to locally compute and adjust its own charging schedule by communicating with the other vehicles until a global equilibrium is achieved. This will require EVs to continuously communicate their scheduling information with each other that can result in large communication overheads. Decentralized DT1 is proposed/used in references [14], [69]-[70].

➢ **Decentralized DT2 Design-** An indirect aggregator is introduced to reduce the communication overhead. The indirect aggregator gathers certain network information and broadcasts certain scheduling signals to all PEVs. Therefore, there is no need for large-scale communication infrastructures. Decentralized DT2 is proposed/used in references [71]-[79].

(a) Centralized   b) Decentralized (DT1)   c) Decentralized (DT2)

d) Hierarchical (HT1)   e) Hierarchical (HT2)   f) Hierarchical (HT3)

g) Hierarchical (HT4)   h) Hierarchical (HT5)
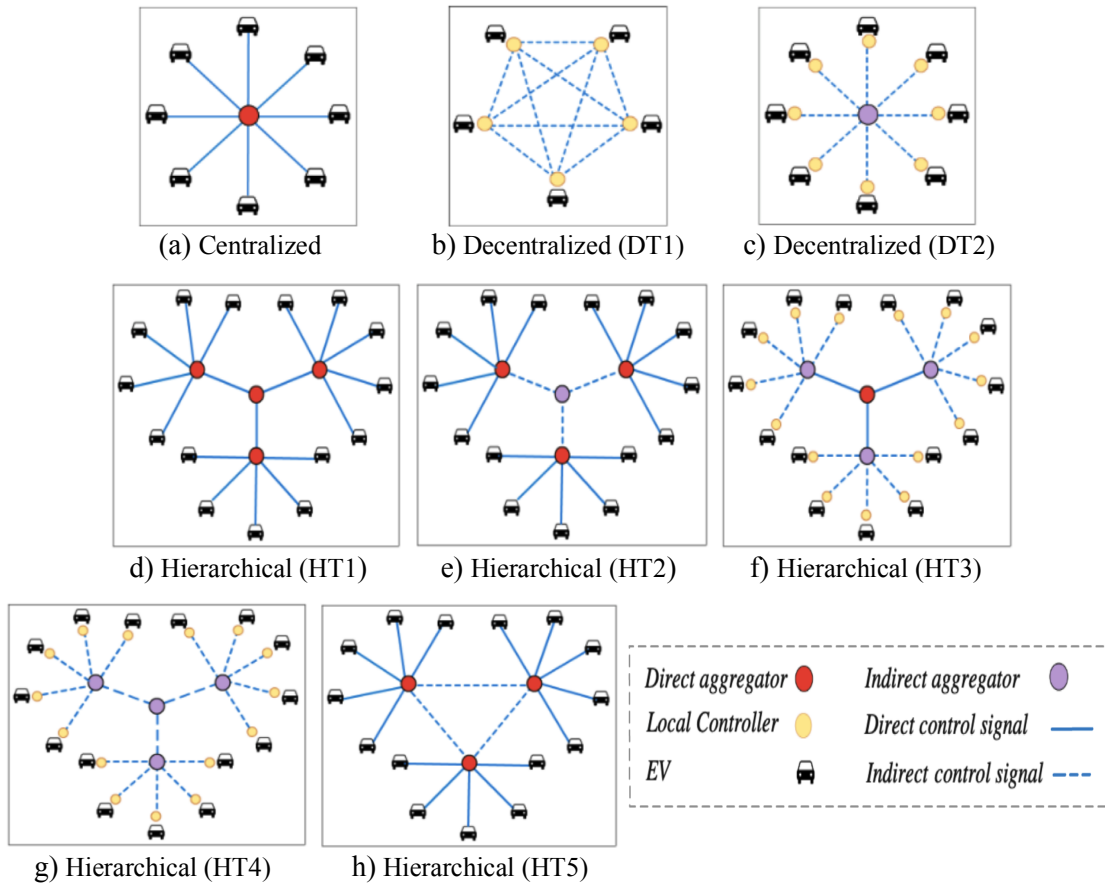
Fig. 3.5. PEV battery charging coordination types; (a) Centralized (C), (b-c) Decentralized types DT1 and DT2, (d-h) Hierarchical types HT1 to HT5 [47].

3.4.3. Hierarchical PEV Battery Charging Coordination

In this approach is based on hybrid combinations of the centralized and decentralized PEV battery charging coordination algorithms. An aggregator is allowed to directly or indirectly supervise the charging activities of a group of vehicles by broadcasting charge profiles' information to the PEVs as shown in Figs. 3.5 (d-h). This will ultimately reduce the requirement for computationally powerful tools and software.

The main benefits of hierarchical PEV battery charging coordination algorithms comes from their tree formation structures [47]:

✓ They balance the benefits of centralized and decentralized PEV coordination tactics by engaging different hierarchical tree architecture

✓ Unlike the centralized and decentralized PEV coordination strategizes, they do not require global and network-wide communications.

However, there are some disadvantages related the hierarchical PEV battery charging coordination schemes [47]:

☒ As with the centralized and decentralized PEV coordination algorithms, the hierarchical structures of Figs. 3.5(d-g) are vulnerable to single points of failure.

☒ The structure of Fig. 3.5(h) resolves the single points of failure issue; however, if one of the aggregators falls, then all PEVs supervised by that particular aggregator will be uncontrolled.

In the literature, five hierarchical architectures have been proposed. The first four structures (depicted in Figs. 3(d-g)) feature three tiers: a central aggregator on the top tier, sub-aggregators in the middle tier, and EVs at the lower tier. The five proposed hierarchical tree architecture are summarized as follows:

➢ *Hierarchical Type HT1-* This architecture (Fig. 3.5(d)) consists of an ISO (central aggregator) that is directly supervising a collection (in this case three) of sub-aggregators. Each sub-aggregator solves its charging coordination problem and decides on its own PEVs. Hierarchical HT1 is proposed/used in references [80]-[82].

➢ *Hierarchical Type HT2-* In this architecture (Fig. 3.5(e)), the ISO (central aggregator) indirectly supervising each sub-aggregator by transmitting computational overheads. Each sub-aggregator uses the information to solve its own optimization problem and

genrate the charge schedules of the PEVs in its group. Hierarchical HT2 is proposed/used in references [83]-[86].

➢ *Hierarchical Type HT3-* In this architecture (Fig. 3.5(f)), the ISO (central aggregator) calculates a collective charging plan for all sub-aggregators. Then, each sub-aggregator indirectly controls a group of PEVs by broadcasting signals, transferring the computational overhead of calculating charge schedules to the EVs. Note that this architecture preserves the decentralized behavior of PEVs. Hierarchical HT3 is proposed/used in references [87]-[88].

➢ *Hierarchical Type HT4-* In this architecture (Fig. 3.5(g)), all the aggregators (e.g., ISO and all sub-aggregators) and PEVs coordinate via indirect control signals. Note that this architecture also preserves the decentralized behavior of PEVs. As with the centralized and decentralized strategies, architecture HT1-HT4 are also vulnerable to single points of failure (e.g., if ISO collapses then all the sub-aggregators and PEVs will be unsupervised/uncontrolled). Hierarchical HT4 is used in reference [89].

➢ *Hierarchical Type HT5-* The last architecture (Fig. 3.5h) consists of a number of indirect aggregators and is intended to resolve the vulnerability of designs HT1-HT4 to single points of failure. This is done by inclusion of a communication network across all indirect aggregators. Note that if one of the links between two indirect aggregators fails, there is still an alternative communication path to prevent overall failure. The unresolved limitation of HT5 is that if one of the aggregators collapses, EVs connected to that particular aggregator will remain uncontrolled. Hierarchical HT5 is proposed/used in references [90]-[92].

Table 3.2 summarizes the main advantages and limitations of different EV charging coordination strategies discussed in this chapter.

Table 3.2 Summary of respective advantages and limitations of different EV charging coordination techniques.

Design	Main Advantages	Main Limitations
Centralized EV Charging Coordination (Fig. 3.5(a) [47])		
Online MSS-based coordination for peak shaving considering charging stations [62]	▪Near-optimal solutions. ▪Easy consideration of global network states and constraints. ▪[55] and [56] also include wind DGs. ▪[57] provides more grid savings by delaying the EV charging process. ▪[62] performs peak shaving considering charging at both home and charging stations. ▪[64] considers some mobility aspects of EVs.	▪PEV owners do not have direct control of their EV charging. ▪Scalability challenges. ▪Single point of failure. ▪[57] has the disadvantage of delaying EV charging.
Online MSS sensitivity-based coordination [63]		
Mobility-aware and static PEV battery charging to minimize system losses [64]		
Load scheduling and dispatch for PEV aggregators [67]		
Optimal PEV coordination by controlling rate of charging to maximize total power to EVs [68]		
Delayed (offline) MSS-based coordination [57]		
Online MSS sensitivity-based coordination considering wind DGs [55]		
Online Fuzzy and MSS-based coordination considering wind DGs [56]		
Combined online and delayed MSS-based coordination [58]		
Decentralized/Distributed EV Charging Coordination (Figs. 3.5(b-c) [47])		
Design DT1: Optimal distributed charging rate control of PEVs for demand management [69]	▪Highly scalable with low computational complexity. ▪More resilient since they can withstand centralized communication failures.	▪Cannot always capture global optimal or near-optimal scheduling solution. ▪ Have large communication overheads (for DT1 design).
Design DT1: Distributed cost-optimal charging control of PEVs for demand management [70]		
Design DT2: Decentralized charging of PEVS with distribution feeder overload control [71]		
Design DT2: Distributed control of PEV charging based on energy demand forecast [74]		
Design DT2: Optimal demand-side management for PEVs [75], [76]		

Design DT2: Enabling reliability-differentiated service in residential networks with EVs based on a hierarchical game approach [72]		
Design DT2: Optimal day-ahead charging scheduling of EVs based on an aggregative game model [78]		
Design DT2: Coordinated PEV charging in unbalanced residential networks [79]		
Hierarchical EV Charging Coordination (Figs. 3.5(d-h) [47])		
Design HT1: Coordination of PEVs across multiple aggregators [80]	▪Balance benefits of centralized and decentralized tactics by engaging different hierarchical tree architecture. ▪Do not require global and network-wide communications ▪HT3 preserves the decentralized behavior of PEVs.	▪HT1-HT4 are vulnerable to single point of failure. ▪HT5 resolves the failure issue, but if one aggregator falls, then all PEVs supervised by this aggregator will fall.
Design HT1: Coordination of EV charging stations for active power compensation [81]		
Design HT1: Hierarchical coordinated dispatch of PEVs [82]		
Design HT2: Economics of EV charging based on game theory [83]		
Design HT2: Coordinated control of PEVs in multifamily houses [84]		
Design HT2: Coordinated charging of EVs for congestion prevention in distribution grids [85]		
Design HT2: A stochastic game approach for PEV charging station operation [86]		
Design HT3: A scalable approach for demand side management of PEVs [87]		
Design HT3: Charge control of large populations of EVs [88]		
Design HT4: Decentralized PEV charging selection in power systems [89]		
Design HT5: Game-theoretic EV charging management resilient to non-ideal user behavior [90]		
Design HT5: Distributed power profile tracking for heterogeneous charging of EVs [91]		
Design HT5: Charge scheduling of PEVs using inter-aggregator collaboration [92]		

3.5. Properties of PEV Coordinated Battery Charging Schemes

This section introduces some common properties of PEV charge coordination schemes.

3.5.1. Unidirectional (G2V) Versus Bidirectional (G2V and V2G) Power Flow

In general, electric vehicles can be designed to operate in grid-to-vehicle or vehicle-to-grid modes which are also known as G2V and V2G modes, respectively. The G2V design assumes unidirectional power flow in the network from the grid to the vehicle when the PEV is charging [46], [47], [62], [63], [89], [117]. On the order hand, the concept of V2G is based on bidirectional power flow where the PEV battery can operate in both charging and discharging conditions [104], [113], [114], [115], [116]. Clearly, the vehicle's battery cannot be simultaneously charging and discharging [46], [47]. Currently, most manufactured EVs are designed for V2G operation. However, with minor modifications to their battery chargers they can also operate in V2G mode using the existing network infrastructure and charging station facilities. The advantage of V2G design is that the PEV owners can earn incentives from the utility by discharging their vehicles during peak load hours. Reference [49] provide an extensive literature review on V2G challenges and applications. This thesis only considers and discusses V2G mode of operation.

3.5.2. Offline Open-Loop versus Online Closed-Loop PEV Coordination

In the offline PEV coordination algorithms, the charging schedule is calculated one-time using open-loop control based on the predicted (forecasted) network operation conditions. The offline algorithms assume ISO, aggregators and sub-aggregators have perfect network and PEV parameter (e.g., their plug-in times) knowledge in advance, which is not true in most real-life applications. References [57], [62], [90] and [93] propose/use offline coordination. On the other hand, the online strategies use recursive closed-loop feedback measurements to calculate/optimize the PEV battery charging schedule multiple

times. Hence, they can handle uncertainties such as the mobility of PEVs. References [55], [56], [58], [63], [80], [87] and [94] propose/use online coordination.

3.5.3. Variable Rate versus Discrete Rate PEV Battery Charging

The charging and discharging of PEV batteries can be performed with [47]:

- Variable charge rates that can take an infinite number of values between zero and the maximum battery charge rate [83], 91], [95] (Fig. 3.6(a)).

- Fix charge rate that is set to the maximum battery charge rate [96] (Fig. 3.6(b)).

- Discrete charge rates that is performed in an interrupted manner [89] (Figs. 3.6(c)).

Most of the published PEV literature assumes variable battery charge rates for G2V and V2G operations. However, fix and discrete charge rates are more common for practical applications since charger is simple, cheaper and more efficient [118]. In the cases of discrete rate charging, the charger rate is restricted by the maximum charging power of the battery. The main applications of variable rate chargers are in engagements of PEVs in demand side management of SG as discussed in Chapter 2 (Section 2.3).
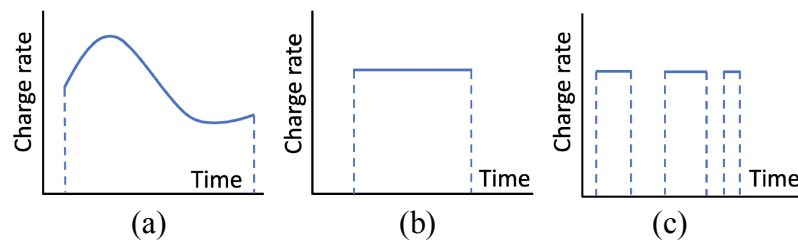
Fig. 3.6. PEV battery charging rate options; (a) Variable rate, (b) Fix rate, (c) Discrete rate [47].

3.5.4. Static versus Mobility-Aware PEV Battery Charging Coordination

Since PEV users are moving within the traffic network, they may need to charge their vehicles at different locations during the day. Considering PEV movements, there are two types of charge scheduling:

- *Mobility-aware PEV battery charging coordination* that takes into consideration the mobility aspects of the vehicles such as their locations (home, office, private or public

charging station), arrival (plug-in) times, their departure (plug-out) times, trip history (route information, average speed), and unplanned departures.

- ▪ **Static PEV battery charging coordination** that ignores the mobility and temporal properties of vehicles by treating them as stationary loads.

Mobility-aware model are more realistic but also more complicated since spatial temporal behaviour of vehicles requires a more complex problem formulation.

Mobility-aware and static PEV charge scheduling have been studied in the literature. Static PEV battery charging has been assumed in most publications such as [66], [64], [67] and [68]. Some mobility behaviour of the PEVs have been assumed in references [62], [63], [65], [74], [92], [94], [114], [116], [119], [120], [121] and [122]. For example:

- ✓ Reference [92] presents a mobility-aware PEV charge schedule model based on the hierarchical HT5 architecture (Fig. 3.5(h)). There is a set of aggregators that are collaborating to control a set of charging stations and schedule PEVs that are subscribed to the stations. This model allows the PEVs to move between aggregators and select their preferred charting station.

- ✓ Reference [74] is a decentralized online charging scheme based on DT2 architecture (Fig. 3.5(c)) that aims to minimize the mean square error between the reference point and the real-time aggregate load. In this model, data related to non-PEV load and PEV mobility are used offline to estimate the reference operating point.

3.5.5. Pricing Strategies

A promising approach to indirectly mange residential loads including PEVs is the so-called smart pricing. Flat rate pricing refers to the simple approach of considering a fixed fee for energy regardless of the time and duration of the consumption. Smart pricing refers to an approach where the users are encouraged to manage their own loads by reducing their energy consumption (such their PEV battery charging) during peak load periods. There are different ways to implement smart pricing such as:

➢ Time-of-use (TOU)- The electricity price is different during peak, shoulder and off-peak periods. This will offer incentives to encourage customers to try to move their EV charging loads (e.g., PEV battery charging) to off peak hours. A possible issue may be the formation of new charging (rebound) peaks [47].

➢ Real-time pricing (RTP)- The price of electricity varies and is higher during peak loads periods in the evenings, hot summer days and cold winter days. There are two possible issues with RTP: i) it may become confusing for the users to manually respond to the changing prices, and ii) it may cause load synchronization (e.g., a large portion of load is shifted from peak load hours to off peak hours without significant reduction in the average peak load) [14].

➢ Critical-peak pricing (CPP)- The customers are offered lower rates during non-critical hours and non-critical days but higher rates during critical hours [123].

3.6. Objective Functions of PEV Battery Charging Schedule Optimization

In the literature, PEV battery charging coordination problem is mostly expressed as a constrained optimization problem [46]-[47]. The decision variables are typically charge rates and charge durations. The selected constraints intend to combine the requirements of grid operator (ISO), PEV users, direct and indirect aggregators (Fig. 3.5). Various forms of objective functions have been proposed and implemented. For the centralized

PEV coordination of Fig. 3.5(a), the large-scale optimization problem is solved directly [46]. For the hierarchical PEV coordination of Figs. 3.5(d-h), the centralized optimization problem is divided into a set of small-scale sub-problems to reduce the computational burden [47]. In general, the objective functions of the optimization problem can be classified in two broad categories [46]-[47]:

✓ Objective functions considering grid operation aspects.

✓ Objective functions considering grid cost aspects.

3.6.1. Objective Functions Considering Operation Aspects

The objective function of the PEV battery charging coordination can be formulated to consider operation aspects of the power grid. The formulation can be done from the perspectives of the grid operator (ISO), the aggregators or the PEV users.

A. Operation Aspects from Grid Operator's Perspective

From the viewpoint of grid operator (ISO), the PEV charge coordination objectives should incorporate the operation aspects of grid.

1) *Load Regulation-* Much of the literature focuses on flattening the PEV and non-PEV load curves and filling the overnight load valley to prevent line and transformer overloading. For example, PEV coordinated battery charging considering load regulation is performed in references [74], [76], [93], [95], [96].

2) *Load Regulation with Voltage regulation and/or Overload Control-* The literature also emphases on performing load regulation while properly maintaining node voltage levels and/or feeder transformer limits with designated values. For example, PEV coordinated battery charging considering load regulation are performed: i) with overload constraints in references [71], [75], [80], [84], [85], [97] and [98], ii) with voltage regulation constraints in reference [99], and iii) with both voltage and overload constraints in references [62], [73] and [100].

3) ***Maximizing Operational Efficiency-*** Another important ISO concern is the balancing generation and demand to improve operational efficiency. This is done in references [63] and [101].

B. Operation Aspects from Aggregators' Perspective

If good incentives are offered, the aggregators and PEV users will most likely want to participate in proving ancillary services. There are many publications investigating PEV participations in ancillary services such as voltage control ([62]), frequency regulation ([66], [102]) and spinning reserve [103] as well as active and reactive power compensation [81].

C. Operation Aspects from PEV Users' Perspective

From the viewpoint of the PEV users, the coordination objectives should also consider their participations in improving operation aspects of the grid.

1) ***PEV User Provision of Ancillary Services-*** There is significant publications on the PEV user involvement (without any aggregators) in ancillary services such as [104] and [105].

2) ***Maximizing PEV User Convenience-*** Most PEV users would like to attain a high level of convenience in their vehicle charging process. For example, they may require fast charging during early evening hours or would like to have their vehicles fully (partially) charge by certain time. For example, inclusions of some of these factors in the PEV charge coordination schedule are examined in references [89] and [91].

3) ***Minimizing Battery Losses and Degradation-*** From the perspective of PEV users, other factors to include in the objective function are battery losses, health and degradation. These concerns are investigated in references [69], [70], [72], [76], [82] and [94].

4) **Charing Fairness-** Most heuristic PEV battery charging coordination algorithms consider/ensure some type of fairness norms such as "first come first serve", "earliest deadline first" and "shortest job first". Impacts of some of these factors on the PEV battery charging schedule are investigated in references [73] and [106].

3.6.2. Objective Functions Considering Cost Aspects

Another option for the formulation of the objective function is to consider the cost aspects from the perspectives of grid operator, aggregators or the PEV users.

A. Cost Aspects from Grid Operator's Perspective

From the perspective of ISO, the cost aspects of grid should be included in the objective function. This can be done by considering: a) reducing the power generation required for PEV battery charging as investigated in references [82], [88], [100] and [107] and/or b) maximize the grid operator revenue as performed in references [83] and [108].

B. Cost Aspects from Aggregators' Perspective

From the viewpoints of the aggregators who are profit-seeking individuals purchasing energy at wholesale prices, their cost aspects should be considered in the PEV charge schedules. This can be done by; a) maximizing the aggregators profit as performed in references [80], [84], [98], [109], [110] and [111] and/or minimizing the cost of power supply as done in references [86] and [87].

C. Cost Aspects from PEV Users' Perspective

Some PEV users may be willing to adjust their charge/discharging periods according to their impact on the real-time electricity price. The formulation of objective function can be defined to minimize the PEV battery charging cost as demonstrated in references [14], [83], [85], [86], [90], [94], [97], [101], [107] and [109].

3.7. Future Research in Battery Charging Coordination of PEVs

Some possible future research directions and innovative areas related to PEV battery charging coordination are:

- Development of more public and private PEV battery charging stations and facilities [61].

- More research on PEV battery charging coordination strategies that integrate both mobility-awareness and network-awareness [47].

- More research on distributed charging schemes with multiple objectives considering both the operational and cost aspects [47].

- Development more practical PEV charge control schemes involving realistic and accurate battery models [47].

- More research on improving the security and privacy of the PEV charge/discharge coordination algorithms [46].

- More research on the impacts of PEV mobility and the influence of dynamic user choices on the charge scheduling [46].

- More investments on enhancing abttery technology and reducing battery charging time to make PEVs more attractive and more flexibale [61].

- Optimal placemnet and sizing of charging stations considering both the traficc and power networks [60].

CHAPTER FOUR: ONLINE MSS-BASED COORDINATED BATTERY CHARGING OF PEVS IN SMART POWER GRIDS CONSIDERING WIND DISTRIBUTED GENERATIONS

The integration of renewable energy resources such as photovoltaic (PV) and wind distributed generations (WDGs) within the EV networks is one of the key technologies in the future smart power grid systems. The first contribution of the Ph.D. thesis is a centralized online MSS-based coordinated battery charging (OL-MSSCC) algorithm for PEVs in smart power grids with WDGs which was published by the author during his Ph.D. studies in reference [55]. The proposed OL-MSSCC algorithm operates on real-time (online) bases (e.g., performing the PEV coordination every 5 minutes) using the grid, PEVs and WDGs information transmitted by the smart meters. The approach is an extension to the real-time smart load management (RT-SLM) algorithm of ([63], [51], [52], [124]) with the addition of WDGs to reduce the possibility of overloading the lines and distribution transforms due to the high injections of PEVs particularly for the duration of the peak load.

This chapter is organized as follows:

- Section 4.1 reviews the ideas of centralized online and offline PEV battery charging coordination.

- Section 4.2 presents the power flow formulation based on the concept of zero mismatch power and summaries the iterative Newton-Raphson load flow solution.

- Section 4.3 introduces the concepts and formulation of the proposed OL-MSSCC algorithm for coordinated battery charging of PEVs in smart power grids.

- Section 4.4 implements the OL-MSSCC algorithm by modify the RT-SLM

algorithm of [63] to include WDGs.

- Section 4.5 introduces the IEEE-based 449-bus smart power grid test system that is used to perform the simulations of Chapters 4-7.

- Section 4.6 investigates the performance of the proposed OL-MSSCC algorithm by performing detailed simulations for coordination of PEVs in the 449-bus smart power grid network without and with WDGs.

- This chapter ends with the conclusions in Section 4.7.

4.1. Centralized Online and Offline Battery Charging Coordination of PEVs

As mentioned in the previous chapters, PEV battery charging coordination are classified into centralized ([55]-[58], [62]-[68]), decentralized ([14], [69]-[79]) and hierarchical ([80]-[92]) schemes. The centralized PEV battery charging coordination approaches can be executed through online, offline, or hybrid online-offline algorithms (Fig. 4.1) [45]:

- ***Online PEV battery charging coordination algorithms*** rely on real-time (online) information on SG operation, PEVs status and renewable generation output powers. The main challenges are related to the complexity, computer storage requirements, computing time and speed of these online algorithms particularly at high injections of PEVs in large power networks. The chief advantage of online PEV coordination compared to the off-line strategies is the real-time consideration of PEVs, DGs and network status as well as the associated constraints within the charging coordination algorithm. Chapters 4 and 5 propose two online PEV battery charging coordination algorithms.

- ***Offline algorithms for PEV coordination*** use forecasted (or estimated) data and for PEV battery charging demands, daily load curves, DG output variations, etc. The main concerns about these algorithms are the availability and accuracy of the estimated data.

68

However, these algorithms are executed offline and don't need to be very fast. Conventionally, offline PEV coordination strategies are easier to implement as they do not directly consider DG, PEV and network status. Chapter 6 proposes an offline (overnight) PEV battery charging coordination algorithm.

- *Hybrid online-offline strategies* combine the online and offline coordination tactics. Chapter 7 proposes a combined online-offline PEV battery charging coordination algorithm.
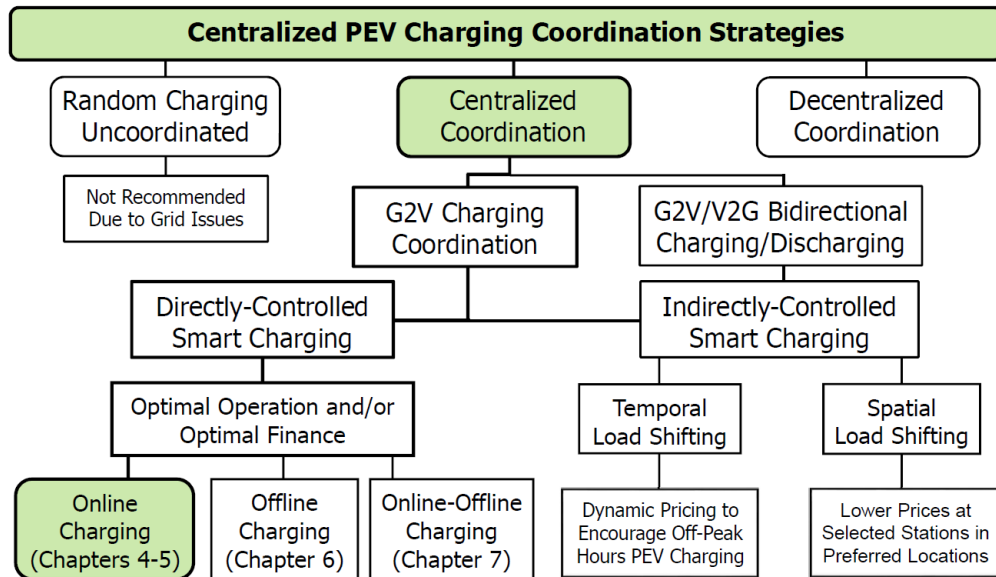
Fig. 4.1. Classification of PEV battery charging schemes (based on Figure 3 of [45]). The proposed OL-MSSCC is an "Online Charging" algorithm within the "Centralized Coordination" strategies.

4.2. Review of Newton-Raphson Power Flow Formulation and Calculations

This section provide a review of power flow formulation and its solution based on the well-known Newton-Raphson iterative method. The materials of this section are based on Chapter 7 of [125].

4.2.1. Bus Types and Bus Mismatch Power

Bus Variables: In power grid modeling and load flow formulation, there are four variables associated with each bus: i) voltage magnitude $|V|$, ii) voltage phase angle θ, iii)

generated/consumed active power *P* and, iv) generated/consumed reactive power *Q*.

Bus Types: There are three important bus types where at each bus, two of the above-mentioned variables are known while the other two must be determined by the load flow solution [125]:

1) PQ Bus (Load Bus)- *P* and *Q* are given, while |*V*| and θ must be computed by the load flow algorithm (Fig. 4.2(a)). These buses are mostly used to model the loads of power networks.

2) PV Bus (Voltage-Controlled Bus)- P and |V| are given, while Q and θ must be computed by the load flow algorithm (Fig. 4.2(b)). These buses are mostly used to model the loads of power networks.

3) Swing Bus (Slack Bus)- |V| and θ are assumed (usually 1 per unit (pu) and zero degree), while the net injected P and the net injected/observed Q and θ are not known and must be computed by the load flow algorithm (Fig. 4.2(c)). This bus is used to provide network losses by: i) producing active power to the system, and ii) producing/absorbing reactive power to/from the system.

| (a) | (b) | (c) |
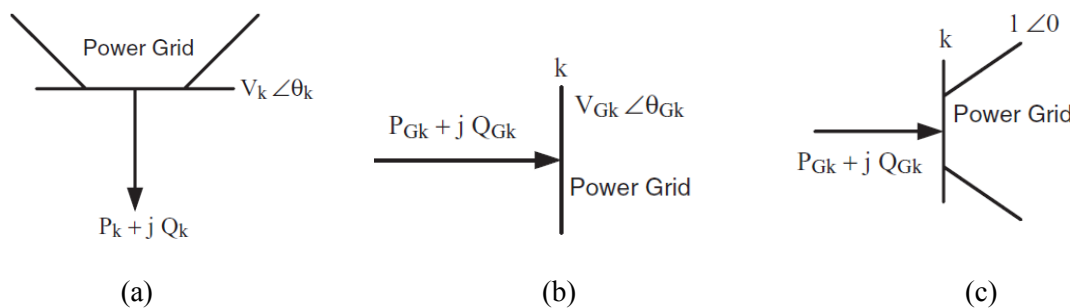
Fig. 4.2. The three important bus types used for load flow modeling and calculations; a) PQ (load) bus, b) PV (voltage-controlled) bus, c) swing (slack) bus [125].

Mismatch Power ($F_k=\Delta S_k=S_{k\text{-}Scheduled} - S_{k\text{-}Calculate}$): At each bus *k,* the mismatch (residual) power $F_k = \Delta S_k$ is defined as the difference between scheduled apparent power $S_{k\text{-}Scheduled}$ (e.g., the sum of all given load and generator power at bus *k*) and calculated apparent

power $S_{k\text{-}Calculate}$ (e.g., the sum of all power through the lines connected to bus k):

$$F_k = \Delta S_k = \Delta P_k + j\Delta Q_k = S_{k(Scheduled)} - S_{k(Calculated)} \tag{4.1}$$

where $\Delta P_k = P_{k(Scheduled)} - P_{k(Calculated)}$ and $\Delta Q_k = Q_{k(Scheduled)} - Q_{k(Calculated)}$

are the mismatch active power and mismatch reactive power at bus k, respectively.

4.2.2. Formulation of Load Flow Problem based on Zero Mismatch Power

In general, any n bus system including the power grid network can be modeled using

Kirchhoff's Current Law (KCL):

$$I_{Bus} = Y_{Bus} \cdot V_{Bus} \tag{4.2}$$

where Y_{Bus} is the "2n×2n" admittance matrix while the "1×2n" and the "2n×1" current

and voltage vectors are defined as:

$$[V] = [V_1, V_2, \cdots\cdots V_n]^t. \tag{4.3}$$

$$[I] = [I_1, I_2, \cdots\cdots I_n]^t. \tag{4.4}$$

Admittance matrix: The admittance matrix can be easily calculated as follows [125].

$$\begin{bmatrix} Y_{11} & Y_{12} & \cdots & Y_{1n} \\ Y_{21} & Y_{22} & \cdots & Y_{2n} \\ \vdots & \vdots & \ddots & \vdots \\ Y_{n1} & Y_{n2} & \cdots & Y_{nn} \end{bmatrix} \tag{4.5}$$

where: $\begin{cases} Y_{ii} = \sum y, & \text{If } i = j \text{ (i.e., summation of all admitances connected to bus } i) \\ Y_{ij} = 0, & \text{If } i \neq j \text{ and bus } i \text{ is not connected to bus } j. \\ Y_{ij} = -y_{ii}, & \text{If } i \neq j \text{ and bus } i \text{ is connected to bus } j \text{ through admittance } y_{ij} \end{cases}$

Unfortunately, Eq. 4.2 cannot be used directly to model a power system since we usually

have neither V_{Bus} nor I_{Bus}, but rather know the power of the loads (P_L and Q_L) and the

power injected by generators plus their voltage magnitudes (P_G and $|V_G|$). Therefore, in

power grid modelling [125]:

✓ The apparent power (Eq. 4.6) is used to formulate the power flow problem.

✓ The concept of zero mismatch power ($Fk = \Delta Sk = Sk\text{-}Scheduled - Sk\text{-}Calculate$) at

all buses (Eqs. 4.7-10) is used to solve the power flow problem.

At each bus (e.g., bus k), the complex apparent power ($Sk = Pk + jQk$) is calculated as the product of voltage vector and the complex conjugate of current vector:

$$S_k = V_k \cdot I_k^*. \tag{4.6}$$

Mismatch Power Vector: Substituting Eq. 4.2 into Eq. 4.6, we get the equation of mismatch power at bus k:

$$F_k = S_k - V_k \sum_{j=1}^n Y_{kj}^* \cdot V_j^* = 0, \quad k = 1, 2, \dots \dots n. \tag{4.7}$$

where $Y_{kj} = G_{kj} + jB_{kj}$, $\theta_{kj} = \theta_k - \theta_j$ is the kj element of the admittance matrix.

Eq. 4.7 can be used to calculate the mismatch power at each bus [125]:

$$F_1 = S_{1(Scheduled)} - S_{1(Calculate)} = S_1 - V_1 \sum_{j=1}^n Y_{1j}^* \cdot V_j^* \rightarrow f_1(V) = 0 \tag{4.8a}$$

$$F_2 = S_{2(Scheduled)} - S_{2(Calculate)} = S_2 - V_2 \sum_{j=1}^n Y_{2j}^* \cdot V_j^* \rightarrow f_2(V) = 0 \tag{4.8b}$$

$$F_n = S_{n(Scheduled)} - S_{n(Calculate)} = S_n - V_n \sum_{j=1}^n Y_{nj}^* \cdot V_j^* \rightarrow f_n(V) = 0 \tag{4.8c}$$

Therefore, the mismatch power vector in matrix form is:

$$F(V) = F_{Scheduled}(V) - F_{Calculated}(V) = \begin{bmatrix} f_1(V) \\ f_2(V) \\ \vdots \\ f_n(V) \end{bmatrix} = 0 \tag{4.9}$$

Taylor Series of Mismatch Power: Expanding row 1 of Eq. 4.9 in a Taylor Series about a guess solution $V^{(0)}$ we get:

$$f_1(V) = f_1(V_1, V_2, \dots V_n) = f_1\left(V_1^{(0)}, V_2^{(0)}, \dots V_n^{(0)}\right) + \frac{\partial f_1}{\partial V_1}\bigg|_{V^{(0)}} \Delta V_1$$

$$+ \frac{\partial f_1}{\partial V_2}\bigg|_{V^{(0)}} \Delta V_2 + \cdots \frac{\partial f_n}{\partial V_n}\bigg|_{V^{(0)}} \Delta V_n + \text{higher ordet terms.} \tag{4.10}$$

If we expand all rows of Eq. 4.9 (similar to Eq. 410) and ignore the higher order terms:

$$\begin{cases} f_1(V) = f_1(V^{(0)}) = \sum_{j=1}^n \frac{\partial f_1}{\partial V_j}\bigg|_{V^{(0)}} \Delta V_j = 0 \\ f_2(V) = f_2(V^{(0)}) = \sum_{j=1}^n \frac{\partial f_2}{\partial V_j}\bigg|_{V^{(0)}} \Delta V_j = 0 \\ f_n(V) = f_n(V^{(0)}) = \sum_{j=1}^n \frac{\partial f_n}{\partial V_j}\bigg|_{V^{(0)}} \Delta V_j = 0 \end{cases} \tag{4.11}$$

Finally, the zero-mismatch power vector equation in matrix format is [125]:

$$F(V^{(0)}) = [J]_{V^{(0)}}[\Delta V] = 0 \tag{4.12}$$

In the above equation, the Jacobian matrix is:

$$J(V) = \begin{bmatrix} \dfrac{\partial f_1}{\partial V_1} & \dfrac{\partial f_1}{\partial V_2} & \cdots & \dfrac{\partial f_1}{\partial V_n} \\[2mm] \dfrac{\partial f_2}{\partial V_1} & \dfrac{\partial f_2}{\partial V_2} & \cdots & \dfrac{\partial f_2}{\partial V_n} \\[2mm] \vdots & \vdots & \ddots & \vdots \\[2mm] \dfrac{\partial f_n}{\partial V_1} & \dfrac{\partial f_n}{\partial V_2} & \cdots & \dfrac{\partial f_n}{\partial V_n} \end{bmatrix}$$ (4.13)

Iterative Power Flow Solution Based on Zero Mismatch Power: In summary, a guess voltage vector $V^{(0)}$ must be iteratively updated/corrected by the voltage correction vector ΔV in order to force the mismatch power $F(V)$ to zero and capture (converge to) the power flow solution:

✓ The voltage correction vector ΔV is:

$$[\Delta V] = -[J]_{V^{(0)}}^{-1} \cdot F(V^{(0)})$$ (4.14)

✓ The updated (corrected) voltage vector is:

$$[V] = [V^{(0)}] + [\Delta V] .$$ (4.15)

4.2.3. Newton-Raphson Power Flow Solution

The power flow formulation of Eqs. 4.1-4.10 is nonlinear because it is written in terms of the complex apparent power S which is the product of "voltage" and "complex conjugate of current" ($S = V \cdot I^*$). Furthermore, we have ignored the higher order terms of the Taylor Series (Eq. 4.10); therefore, the load flow solution (Eqs. 4.12, 4.14-15) is obtained using an iterative procedure. The most popular iterative methods used in power networks are the Newton-Raphson and the Gauss-Seidel [125].

Figure 4.3 presents the overall flow chart of the Newton-Raphson algorithm which is used in this thesis to solve the power grid without and PEV battery charging. The iterative Newton-Raphson power flow solution can be summarized as follows.

Iteration 0 (Make an Initial Guess $V^{(0)}$ for Voltage Vector Solution):

- Step 1- Starts with an initial guess solution for the voltage vector $V^{(0)}$ (Eq. 4.3). The most popular and convenient guess is to set all bus voltage magnitudes to 1.0 per unit with angles of zero degree ($V_k = 1.0$ pu$\angle\, 0^0$, for $k = 1, 2, \ldots, n$).

- Step 2- Calculate admittance matrix Y_{bus} and mismatch power $F(V^{(0)})$ (Eqs. 4.5-4.9).

- Step 3- If mismatch power $F(V^{(0)}) \leq \varepsilon$ stop; otherwise, set $V = V^{(0)}$ and continue.

Iteration i (Calculate Correction Voltage Vector ΔV and Check Convergence):

- *Step 1*- Calculate the Jacobian matrix $J(V)$ (Eq. 4.13).

- *Step 2*- Calculate the correction voltage vector ΔV (Eq. 4.14).

- *Step 3-* Update the solution voltage vector $V = V + \Delta V$ (Eq. 4.15).
- *Step 4-* Calculate the mismatch power vector $F(V)$ (Eq. 4.9).

Check Convergence ($F(V) \leq \varepsilon$ or $\Delta V \leq \varepsilon$):

- *Step 1a (Stop)-* If $F(V) = 0$, stop. In practice, the iterative procedure is stopped when $F(V)$ and/or ΔV are smaller than a tolerance of error ε. For the Newton-Raphson load flow algorithm adapted in this thesis, the tolerance is selected to be $\varepsilon = 1 \times 10^{-5}$ and the iterative procedure is stopped when $|F(V_k)| \leq \varepsilon$ at all buses of the network.
- *Step 1b (Iterate)-* Otherwise ($F(V) > \varepsilon$), set "$i = i + 1$" and repeat "Iteration i".

Iteration 0: Initialization
- Input network, load and generator parameters.
- Guess an initial voltage vector $V^{(0)}$ (Eq.4.3).
- Calculate Y_{bus} (Eq.4.5) and $F(V^{(0)})$ (Eq.4.9)
- If $F(V^{(0)}) \leq \varepsilon$ stop; otherwise, set $V = V^{(0)}$.

Iterations $i = 1$ to N

Iteration i: Power Flow Calculations
- Calculate Jacobian matrix $J(V)$ (Eq.4.13).
- Calculate correction voltage vector ΔV (Eq.4.14).
- Update solution voltage vector $V = V + \Delta V$ (Eq.4.15).
- Calculate mismatch power vector $F(V)$ (Eq.4.9).

$i = i + 1$ No   **Check Convergence** $F(V) \leq \varepsilon = 10^{-6}$?   Yes   Store V & Stop

Fig. 4.3 Flow chart of the Newton-Raphson algorithm for power flow solution

4.3. Concepts and Formulation of OL-MSSCC

According to Fig. 4.1, the proposed OL-MSSCC is classified as an "Online Charging" algorithm within the "Centralized Coordination" strategies. It aims to perform a combination of "Optimal Finance" (by reducing the cost according to Eq. 4.16) and "Optimal Operation" (by controlling bus voltage profiles and preventing overloading of transformers and lines according to Eqs. 4.17-18).

4.3.1. Concepts of OL-MSSCC

The concepts of OL-MSSCC algorithm are similar to those adapted in references [52], [55], [63], [51], [55], [124]:

- ***Problem Formulation of OL-MSSCC (Eqs. 4.16-4.18)-*** The PEV problem

formulation is based on cost minimization and is solved online (e.g., every 5 minutes) based on the updated grid, PEV and WDG information received by the smart meters.

- ***Planning Time Horizon and Time Interval of OL-MSSCC (Fig. 4.4)-*** The scheduling time horizon for PEV coordination is selected to be 24 hours. It starts at 1600h for 24 hours and is divided into 24(60)/5=288 time intervals. Therefore, each time interval is $\Delta t = 5$ minutes.

- ***Independent System Operator (ISO)-*** oversees grid operation and centralized PEV battery charging coordination. Upon random arrival of each PEV: i) a signal is sent to ISO by the PEV charger/controller, ii) ISO implements the OL-MSSCC algorithm and sends a signal to the PEV to start charging, and iii) PEV charger sends a signal back to ISO upon unplugging.

- ***Charging Time Zones of OL-MSSCC (Fig. 4.4)-*** three time zones are defined to factor in variable energy pricing including: i) the PEV charging time between 1800h and 2200h (called the red time zone) is dedicated for high-priority customers paying high tariff, ii) the PEV charging time between 2200h and 0200h (called the blue time zone) is dedicated for medium-priority customers paying medium tariff and iii) the PEV charging time between 0200h and 0800h (called the green time zone) is dedicated for low-priority customers that would like to pay low tariff.

- ***Subscription (High, Medium and Low) Priority Options of OL-MSSCC (Fig. 4.4)-*** are defined to consider customer preferences and enquires: i) high-priority customers who are willing to pay high tariff for quick charging during early evening hours within the red time zone, ii) medium-priority customers who are willing to pay medium tariff for late night charging within the blue time zone, and iii) low-priority customers looking for inexpensive overnight charging within the green time zone.

- *PEV-Queue Table of OL-MSSCC (Table 4.1)-* is established and updated on real-time bases (e.g., every 5 minutes) to keep track of all vehicles' statuses. At the beginning of each time interval $t=\Delta t$, the PEV-Queue Table is resorted to update the order of PEVs according to their subscription priority (red, blue or green) and plugged-in / plug-out times such that the vehicles with highest priority are placed at the top rows of the table while the lower priority vehicles are pushed towards the bottom of the table. If it is not possible to service a high-priority PEV due to a constraint violation (Eqs. 4.17-4.18), the charging will be postponed to the next time interval; however, the EV will be kept at the top rows of the queue up table. This process will be continued until leftover PEV is charged as soon as possible. Therefore, the PEV-Queue Table may contain uncharged vehicles from prior time interval(s) that are waiting to be charged since they were not attended due to voltage and/or demand violations.

- *Random PEV Plug-In Times Replicated by Gaussian Distribution-* The proposed PEV coordination algorithms of this Ph.D. thesis and their simulations are performed for random arrivals (e.g., random plug-in) of PEVs at homes. However, in order to compare simulation results for various coordination strategies and various case studies presented in Chapters 4-7, Gaussian (Normal) distributions of charging loads ([55], [63]) with PEV injections of 16%, 32%, 47% and 63% occurring within red (1800h-2200h), blue (1800h-0100h) and green (1800h-0800h) charging time zones are generated and used in this thesis (Fig. 4.4(b)).

Therefore, the cost/fee of purchasing energy that is required for EV charging will be reduced by: 1) introducing charging zones at different hours that correspond to the utilities intentions to cut generation cost during peak hours of residential loads, 2) allowing the customers (PEV owners) to select their own preferred charging time zones, 3) classify

high-, medium-, and low-priority customers according to the selected charging time zones, 4) designing the proposed OL-MSSCC algorithm to accommodate these preferences at each time interval $t=\Delta t$ while considering the objective cost function (Eq. 4.16) and system constraints (Eqs. 4.17-4.18).

In the literature, there are no standards or classifications for the PEV injection/penetration levels and the PEV charging time zones. The selected very low (16%), low (32%), medium (47%) and high (63%) EV injection levels (Fig. 4.7) as well as the chosen red (1800h-2200h), blue (1800h-0100h) and green (1800h-0800h) PEV changing time zones (Fig. 4.4) are adopted from references [62] and [63] which are well-known papers and have been cited over 370 and 950 times, respectively.
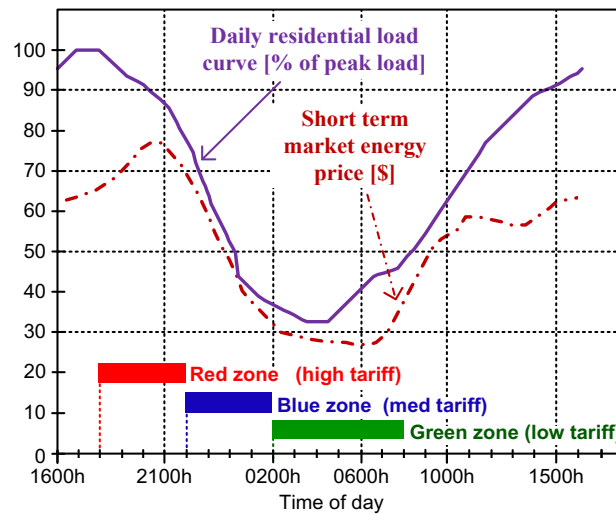
Fig. 4.4(a). PEV charging time zones, price of energy and residential daily load curve (based on Fig. 1a of [55]).

77
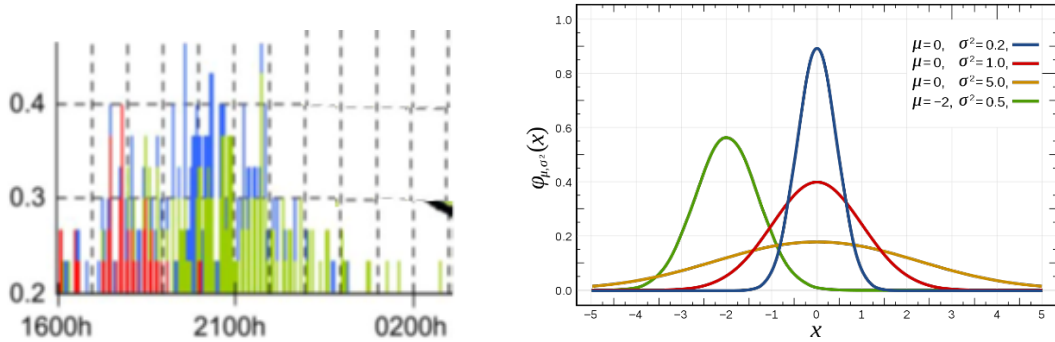
Fig. 4.4(b). The Gaussian (Normal) distribution of vehicle arrivals for PEV injections of 63% [55], [63]. Similar Gaussian distribution charging loads are generated for PEV injections of 16%, 32% and 47% and used to compare simulation results for various coordination strategies and various case studies presented in Chapters 4-7. The red, blue and green colors represent high, medium, and low priority PEVs, respectively.

Table 4.1. An example of the PEV-Queue Table showing the order of PEVs within the three subscription priority options. Within each priority group, the PEVs are sorted according to the MSS vector of Eq. 4.19 and are waiting in the queue to be scheduled for charging by the ISO.

PEV-Queue Table for Online Coordinated Battery Charging (OL-MSSCC) of PEVs			
Sorting Scheme	PEV Type	PEV Number in the Queue	PEV Status
According to MSS Sensitivity Vector (Eq. 4.19)	High Priority to be Charged Early Evening Hours (Red Zone; Fig. 4.4)	$R_{charged,1}$	Charged
		…..	…..
		$R_{charged,max}$	Charged
		$R_{charging,1}$	Charging
		…..	…..
		$R_{charging,max}$	Charging
		$R_{waiting,1}$	Waiting to be scheduled with high priority*
		…..	…..
		$R_{red,max}$	Waiting to be scheduled with high priority*
According to MSS Sensitivity Vector (Eq. 4.19)	Medium Priority to be Charged Late Evening Hours (Blue Zone; Fig. 4.4)	$B_{charged,1}$	Charged
		…..	…..
		$B_{charged,max}$	Charged
		$B_{charging,1}$	Charging
		…..	…..
		$B_{charging,max}$	Charging
		$B_{waiting,1}$	Waiting to be scheduled with medium priority*
		…..	…..
		$B_{blue,max}$	Waiting to be scheduled with medium priority *
According to MSS Sensitivity Vector (Eq. 4.19)	Low Priority to be Charged Overnight (Green Zone: Fig. 4.4)	$G_{charged,1}$	Charged
		…..	…..
		$G_{charged,max}$	Charged
		$G_{charging,1}$	Charging
		…..	…..
		$G_{charging,max}$	Charging
		$G_{waiting,1}$	Waiting to be scheduled with low priority*
		…..	…..
		$G_{green,max}$	Waiting to be scheduled with low priority *

*) Uncharged vehicles from prior time interval(s).

4.3.2. Problem Formulation of OL-MSSCC

The problem formulation of OL-MSSCC is similar to references [51], [52], 62], and [63] with the addition of WDGs injecting active power into the grid. The PEV coordination is formulated as a constrained optimization problem which is solved in real-time (e.g., every 5 minutes) based on the grid status and WDGs information transmitted by smart meters. The objective function of OL-MSSCC is to reduce the overall cost of PEV battery charging plus system energy losses [63]:

$$\min F_{cost} = F_{cost-loss} + F_{cost-gen}$$
$$= \sum_t K_E \cdot P_{t,loss} + \sum_t K_{t,G} \cdot D_{t,total}, \quad t = \Delta t, 2\Delta t, \dots 24 \ hours. \quad (4.16)$$

In above equation, the total losses are $P_{t,loss} = \sum_{k=0}^{n-1} R_{k,k+1} \left(|V_{k=1} - V_k| |y_{k,k+1}| \right)^2$ while the the total costs of losses and generation are represented by $F_{cost-loss}$ and $F_{cost-gen}$, respectively. $D_{t,total}$ is the total demand at time t (see Eqs. 4.18). Δt is the selected time interval which is equal to 5 minutes, K_E is the cost per MWh of system losses which is equal to 50 \$/MWh, [126]-[128] and $K_{t,G}$ is the MWh generation cost at time t (e.g., Fig. 4.4) while n and k represent total number of buses and the bus number, respectively. There are two constraints associated with Eq. 4.16 [52], [63], [124]:

1) **The bus voltage constraint** is included by considering a maximum voltage deviation limit (set by ISO or the utility):

$$\Delta V_k = |V_k - V_{rated}| \ll \Delta V_{max}, \quad \text{for } k = 1, \dots \dots, n. \quad (4.17)$$

where ΔV_k is the per unit (pu) voltage deviation of bus k which is limited to $\Delta V_{max} = 0.1$ pu in this thesis.

2) **A limit for the total maximum system demand** to prevent overloading of transformers and lines from PEV battery charging:

$$D_{t,total} = \sum_k P_{t,k}^{load} + \sum_j P_{t,j}^{PEV} - \sum_m P_{t,m}^{WDG} \ll D_{t,max} \quad \text{for} \begin{cases} k = 1, \dots . n \\ j = 1, \dots j_m \\ m = 1, \dots m_m \end{cases} \quad (4.18)$$

where k, j and m are the counters for load-buses (PQ buses without PEVs), PEV-buses, and WDGs, respectively. The $P_{t,k}^{load}$ and $P_{t,j}^{PEV}$ are the total active load power and total PEV charge demand at bus k at time $t = \Delta t$ while $P_{t,m}^{WDG}$ is the injected wind DG power at bus j at time $t = \Delta t$. $D_{t,max}$ is the highest allowed demand (that may be set based on the highest loading of the distribution transformer) at $t = \Delta t$ that can be set to the maximum demand without any PEVs.

At each time interval $t=\Delta t$, the OL-MSSCC needs to assess the state of the SG with PEV which is necessary for the calculation of the objective function (Eq. 4.16) and checking of constraints (Eqs. 4.17-4.18). This is done by using Newton-Raphson power flow calculations where: i) loads in the residential and distribution sectors are considered as constant power type loads with their P and Q values updated according to their daily load curves (Fig. 4.4), ii) all PEV battery charging loads are treated as constant active power loads and, iii) all WDGs are treated as constant power sources injecting active power to the grid.

4.4. Implementation of OL-MSSCC

The centralized OL-MSSCC algorithm will manage the start times and the order of PEVs battery charging by using the SG communications system that can send and receive signals from/to the independent system operator (ISO) to/from the individual PEV chargers. Consequently, PEV battery charging is centrally controlled by the OL-MSSCC algorithm rather than the PEV owners.

Therefore, based on the PEV owner preferences for charging time zone, the energy prices, load variations over the scheduling/planning time horizon of 24 hour, and the load flow

solutions, the OL-MSSCC algorithm will assign charging schedules to each PEV to improve SG operational performance Eqs. 4.17-4.18 (e.g., bus voltage profiles and transformer loadings) while reducing the cost (Eq. 4.16).

4.4.1. PEV Coordination Based on Maximum Sensitivity Selections

The online PEV battery charging of OL-MSSCC involves loss reduction (first component of Eq. 4.16, $F_{cost-loss}$), voltage magnitude regulation (Eq. 4.17) and maximum demand control (Eq. 4.18) while also considering PEV owner (high-, medium-, low-priorities) preferences and generation cost reduction (second component of Eq. 4.16, $F_{cost-gen}$). This can be achieved through AI optimization methods such as genetic and particle swarm optimization algorithms (GA and PSO). However, while most AI optimizations are accurate, many of them are not computationally suitable for online optimization of large networks that require small time steps (e.g., 5 minutes as selected in this thesis). Therefore, OL-MSSCC utilizes the fast and practical MSS approach adopted in [63] to sort PEV buses within a given priority (high, medium, low) group. Bus sorting is done based on the sensitivity of network losses to PEV battery charging power demand.

The MSS vector is calculated by considering the objective function sensitivities (Eq. 4.16, $F_{cost-gen}$) to the PEV power consumption and location using the following partial derivatives [63]:

$$MSS_{t,j} = \partial P_{t,loss} / \partial P_{t,j}^{PEV} \quad for \ j = 1, ... j_m \quad\quad (4.19)$$

where $MSS_{t,j}$ (the entry number j of the vector at time interval $t=\Delta t$) is the sensitivity of system losses to EV battery charging at bus j at time t, j_m is the total/overall number of PEVs, $P_{t,loss}$ is the total/overall value of SG loss at the time t, and $P_{t,j}^{PEV}$ is the total/overall power consumption of the EV that are connected to bus number j. At each time interval, the partial derivatives of Eq. 4.19 are extracted from the Jacobian (already calculated) matrix J (Eq. 4.13):

$$\begin{bmatrix} \dfrac{\partial P_{loss}}{\partial P} \\[2ex] \dfrac{\partial P_{loss}}{\partial Q} \end{bmatrix} = \begin{bmatrix} \dfrac{\partial P}{\partial \theta} & \dfrac{\partial Q}{\partial \theta} \\[2ex] \dfrac{\partial P}{\partial |V|} & \dfrac{\partial Q}{\partial |V|} \end{bmatrix}^{-1} \begin{bmatrix} \dfrac{\partial P_{loss}}{\partial \theta} \\[2ex] \dfrac{\partial P_{loss}}{\partial |V|} \end{bmatrix} \qquad (4.20)$$

Therefore, determination of the MSS vector (Eq. 4.19) does not require any extra calculations since the Jacobian matrix (Eq. 4.13) is already calculated by the Newton-Raphson load flow.

4.4.2. Updating of MSS Vector and PEV-Queue Table

Since PEV scheduling based on MSS is simple, fast and efficient without requiring complex calculations, it is practical for centralized online charging coordination of PEVs in large networks. It quantifies the objective function sensitivities (system losses) to the PEV charger loads at each time interval $t=\Delta t$. This is done by defining a new bus type (called PEV-bus) in the load flow program and calculating the MSS vector consisting of the system losses sensitivities with respect to active power demand of the PEV-buses. The MSS vector is calculated and is used to update the PEVs order in the PEV-Queue Table based on the following steps:

1) Temporarily activating all PEV-buses with about 5% of their nominal battery charger power ratings.

2) Executing the load flow program and using Jacobian entries to compute the loss sensitivities due to power consumption of each EV (Eq. 4.4), and storing the results in the MSS vector.

3) Using the MSS vector to update the order of PEVs in the PEV-Queue Table. Consequently, OL-MSSCC will first schedule the PEVs that have less impacts on the system losses.

4) Steps 1-3 are repeated at each time interval for each of the descending priority group. The result of steps 1-4 is a PEV-Queue Table.

4.4.3. Inclusion of Wind Distributed Generations in OL-MSSCC

The first contributions of this Ph.D. thesis is the inclusion of WDGs in the centralized

online PEV battery charging coordination (RT-SLM) algorithm of [63].

In the formulation of OL-MSSCC, WDGs are included as negative active power loads.

The WDG characteristics used in this thesis is generated by scaling down

readings/measurements of an existing wind farm; the Walkway wind farm in WA,

Australia on July 7, 2012 (Fig. 4.5). In the later sections of this chapter, the impact of

wind power generation characteristic on the performance of OL-MSSCC will be

scrutinized by shifting the peak out power period. Two of these characteristics are shown

in Fig. 4.5 with the peak power period shifted to early evening hours1800h-2100h (WDG

#1) and early morning hours 2400h-0300h (WDG #2).
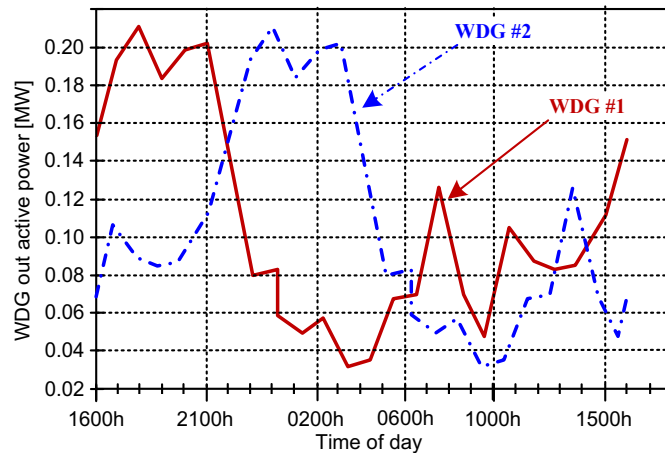
Fig. 4.5. The output power of wind DGs used for the simulations of this thesis which are generated by scaling down the measurements of an existing wind farm; the Walkway wind farm in WA, Australia on July 7, 2012, with the peak output power periods shifted to early evening hours1800h-2100h (WDG #1) and early morning hours 2400h-0300h (WDG #2) (based on Fig. 1(b) of [55]).

4.4.4. The Flow Chart Representation of Proposed OL-MSSCC Considering WDGs

The OL-MSSCC algorithm reduces the cost/expenditure of generating/supplying energy

for EV battery charging (Eq. 4.16) while considering network operation constraints

(Eqs.4.17-4.18). This is done by: 1) prioritizing/ranking PEVs according to the sensitivity/MSS vector of Eq. 4.19, 2) with the consideration of the real-time variations of loads and energy pricing (Fig. 4.4), 3) utilizing the energy generated by WDGs (Fig. 4.5) for EV charging, and 4) considering consumers' preferences by defining charging time zones (Fig. 4.4) that correspond to utilities interest in reducing generation cost during peak load hours.

The flow chart of OL-MSSCC algorithm is shown in Fig. 4.6 [55]. There are four stages associated with each time interval $t = \Delta t = 5$ minutes.

Stage 1 (Updating PEV and WDG Status):

- Step 1.1- Check for random arrival (plug-in) and departure (plug-out) of PEVs.

- Step 1.2- Update PEV-Queue Table 4.1 according to plug-in/out of all EVs.

- Step 1.3- Update status of WDGs according to wind information by smart meters.

- Step 1.4- Update $D_{t,max}$ (Eq. 4.18) based on WDGs output power.

- Step 1.5- Update market energy price based on real-time pricing.

Stage 2 (Online MSS-Based PEV Coordination Scheduling):

- Step 2.1- Run Newton-Raphson load flow of Fig. 4.3.

- Step 2.2- Extract MSS vector (Eq. 4.19) from the Jacobian (already calculated) matrix (Eq. 4.13).

- Step 2.3- Calculate cost function (Eq. 4.16) and network constraints (Eqs. 4.17-18).

- Step 2.4- Sort the PEVs in Table 4.1 in accordance with Eq. 4.19.

- Step 2.5 (Scheduling of eligible PEVs):

  ➢ Step 2.5.1- Temporary charge the PEV at top of PEV-Queue Table 4.1.

  ➢ Step 2.5.2- If $\sum$demands>$D_{t,max}$ then go to Step 2.5.7 (postpone charging of this PEV until next Δt since it causes a damned constraint violation according to Eq. 4.18).

➢ Step 2.5.3- Run Newton-Raphson load flow of Fig. 4.3.

➢ Step 2.5.4- If voltage violation ($|\Delta V| \leq \Delta Vmax$ (Eq. 4.17)) then go to Step 2.5.7 (postpone charging of this PEV until next time interval since it causes a voltage constraint violation according to Eq. 4.17).

➢ Step 2.5.5- Schedule the PEV for charging.

➢ Step 2.5.6- Remove the Scheduled PEV from PEV-Queue Table 4.1.

➢ Step 2.5.7- Go to Step 2.5.1 for scheduling next eligible PEV.

Stage 3 (Updating Daily Load Curve):

▪ Step 3.1- Update the daily load curve by including the scheduled PEVs.

Stage 4 (Go to Next Time Interval Δt and Repeat):

▪ Step 4.1- If $t = 24$ hours, then stop.

▪ Step 4.2- Repeat Stages 1-3 for the next time interval Δt.

Input network, PEV and DG parameters. Initialize variables

Stage 1: Updating — Update Statuses of PEVs and WDGs, Resort PEV-Queue Table

✓ Check for plug-in/plug-out of PEVs.
✓ Update PEV-Queue Table (Table 4.1).
✓ Update statuses of all WDGs based on wind speeds and/or output powers.

✓ Update maximum allowed demand level $D_{t,max}$ (Eq. 4.18) based on the output powers of WDGs.
✓ Update the market energy price.

Stage 4: Repeat for Next Time Interval — Repeat Stages 1-3 for the Next Time Interval ($\Delta t = 5$ Minutes) within the Scheduling Time Horizon of 24 Hours

Stage 2: MSS PEV Charging Coordination — Perform MSS-Based PEV Charging Coordination by Calculating and Checking the Objective Function and Constraints

✓ Run Newton-Raphson load flow (Fig. 4.3 and Eqs. 4.9-4.15).
✓ Calculate cost objective function and constraints (Eqs. 4.16-4.18).
✓ Extract MSS vector (Eq. 4.19) from the Jacobian Matrix (Eq. 4.13).
✓ Sort PEV-Queue Table (Table 4.1) according to the MSS vector.
✓ Keep high-priority (red) PEVs at top of PEV-Queue Table followed by medium-priority (blue) PEVs, and low-priority (green) PEVs.

Temporarily schedule the PEV at top of PEV-Queue Table for charging.

Is $\sum$ demands $\leq D_{t,max}$ (Eq. 4.18)? — no

yes

Run Newton-Raphson load flow (Fig. 4.3 and Eqs. 4.9-4.15).

Is $|\Delta V| \leq \Delta V_{max}$ (Eq. 4.17)? — no → Postpone PEV charging until next Δt.

yes

✓ Permanently schedule PEV for charging.

Select next PEV from PEV-Queue Table.

More PEVs within selected priority group? — no → Postpone PEV charging until next Δt.

yes → **Select next priority group.**

More priority group? — yes

no

Stage 3 — Update Daily Load Curve

Update and save daily load curve, losses, total cost, voltage deviations, transformer and line loadings according to the number of PEVs being charged at this time interval.

Select next time interval Δt.

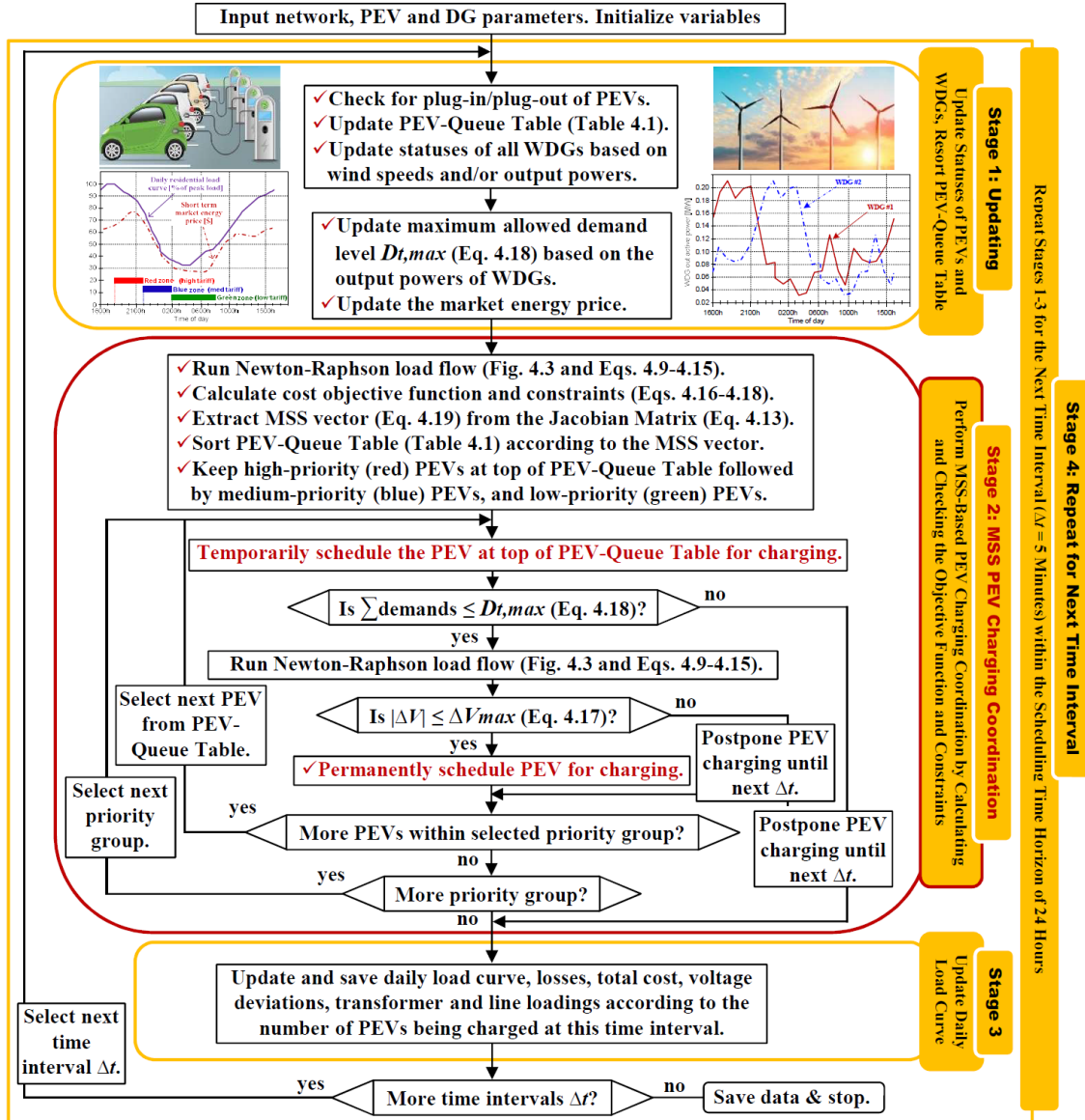More time intervals Δt? — yes / no → Save data & stop.

Fig. 4.6. Flow chart of the proposed OL-MSSCC algorithm (based on Fig. 2 of [55]).

4.5. The 449 Smart Power Grid Distribution System

The 449-bus smart power grid test system of Fig. 4.7 with three WDGs [55] is used to demonstrate the performance of the proposed OL-MSSCC algorithm.

4.5.1. Topology of Smart Power Grid System

The designated system for the simulations and analysis of this Ph.D. thesis is the 449-bus network of Fig. 4.7 [55],[63]. It is based on the IEEE 31 bus 23 kV distribution test system [129] combined with three WDGs and 22 low voltage 415 V residential feeders [55]. Each residential feeder has 19 buses. Simulations are performed for PEVs injection levels of 3/19≈16%, 6/19≈32%, 9/19≈47% and 12/19≈63%.
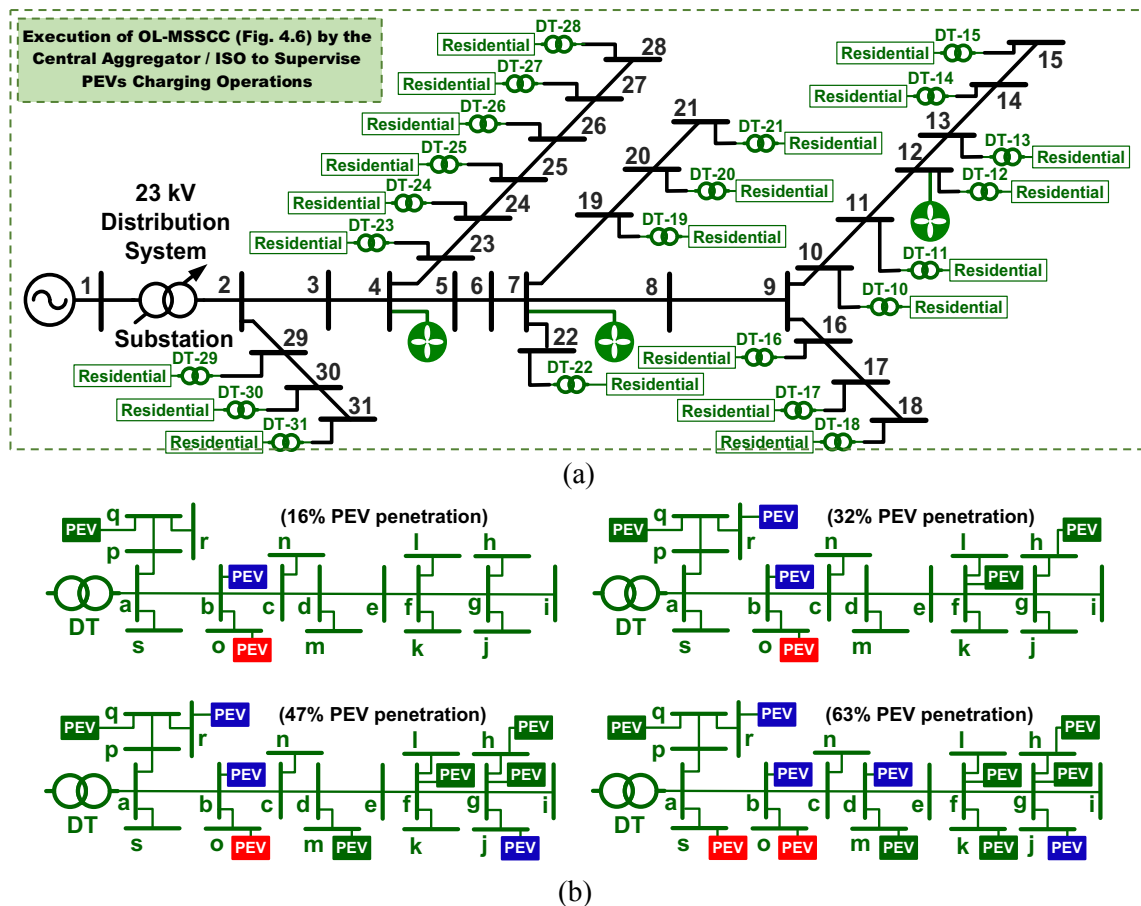

(a)

(b)

Fig. 4.7. The 449-bus smart power grid comprising of the IEEE 31-bus high-voltage 23 kV distribution network [129] joint with three WDGs (at buses 4, 7 and 12) and twenty two low-voltage 415 V residential feeders; (a) system one-line diagram, (b) One of the residential feeders with PEV injections of 3/19≈16%, 6/19≈32%, 9/19≈47% and 12/19≈63% highlighting the high (red color), medium (blue color) and low (green color) priority consumers/PEVs [55], [63].

The PEV, load and line data are presented in Tables 4.2 and 4.3. The selected buses for PEV battery charging and the corresponding assigned priorities and charging time zones are presented in Fig. 4.7(b).

Table 4.2. The PEV parameters and the loads of the 19-bus LV residential feeders and the 31-bus HV distribution system of Fig. 4.7 [55], [63], [124].

Linear and PEV Load (Figs. 4.7a-b)		Power	
Load Type	Load Location	(kW)	(kVAR)
Household PQ loads	Buses a - s (Fig. 4.7(b))	2.0	0.97
PEV charger load	Selected buses (Table 4.4)	4.0	0

Table 4.3a. Parameters of the lines in residential feeders of Fig. 4.7 [55], [63], [124].

Line Between Buses	Resistance of Line R (mΩ)	Reactance of Line X (mΩ)	Line Between Buses	Resistance of Line R (mΩ)	Reactance of Line X (mΩ)
a and b	41.5	14.5	f and l	1360.5	135.7
b and c	42.4	18.9	d and m	140.0	14.0
c and d	44.4	19.8	c and n	776.3	77.4
d and e	36.9	16.5	b and o	597.7	59.6
e and f	52.0	23.2	a and p	142.3	49.6
f and g	52.4	23.4	p and q	83.7	29.2
g and h	0.50	0.20	q and r	312.3	31.1
g and i	200.2	19.9	a and s	16.3	6.2
g and j	173.4	172.9	Reactance of Distribution Transformers DT-10 to DT-31		65.4
f and k	260.7	26.0			

Table 4.3b. Line parameters of 31-bus 23 kV distribution test system of Fig. 4.7 [124].

Line Between Buses	Resistance of Line R (Ω)	Reactance of Line X (Ω)	Line Between Buses	Resistance of Line R (Ω)	Reactance of Line X (Ω)
2 and 3	0.4	6.9	12 and 13	259.7	146.3
2 and 29	52.7	2.8	13 and 14	259.7	146.3
3 and 4	83.9	83.0	14 and 15	163.3	142.0

4 and 5	163.3	142.0	16 and 17	163.3	142.0
4 and 23	163.3	142.0	17 and 18	259.7	146.3
5 and 6	259.7	146.3	19 and 20	163.3	142.0
6 and 7	259.7	146.3	20 and 21	83.9	83.0
7 and 8	259.7	146.3	23 and 24	83.9	83.0
7 and 19	259.7	146.3	24 and 25	163.3	142.0
7 and 22	259.7	146.3	25 and 26	163.3	142.0
8 and 9	259.7	146.3	26 and 27	163.3	142.0
9 and 16	259.7	146.3	27 and 28	259.7	146.3
9 and 10	0.2597	0.1463	29 and 30	52.7	2.8
10 and 11	0.2597	0.1463	30 and 31	259.7	146.3
11 and 12	163.3	142.0			

Table 4.4. Details of charging time zones [55], [63].

19-Bus Feeders (Fig. 4.7(b))	PEV Injection Levels (see Fig. 4.7(b))*			
	16%	32%	47%	63%
bus a				
bus b	■	■	■	■
bus c				
bus d				■
bus e				
bus f		■	■	■
bus g			■	■
bus h		■	■	■
bus i				
bus j			■	■
bus k				■
bus l				
bus m			■	■
bus n				
bus o	■	■	■	■
bus p				
bus q	■	■	■	■
bus r		■	■	■
bus s				■

*) Table entries with white color are buses without any PEVs.

4.5.2. PEV Energy Requirements

The PEV batteries are usually a few tens of kWh. In this thesis, the PEV battery capacities are assumed to be 10 kWh with the justification that small affordable EVs will more likely lead the future market [63]. To prevent premature aging of the battery and optimize its

life, reference [63] chooses DOD of 70% of the rated battery life. This means the PEV battery can deliver 7 kWh. Assuming 88% charger efficiency [130], a single EV battery demands 8 kWh of energy from the smart power grid.

4.5.3. Residential Load Profiles and EV Battery Chargers

In Australia, there are standard 240V single-phase outlets as well as 5A single-phase and 20A three-phase outlets that can supply approximately 2.4kW, 4 kW and 14.4 kW, respectively. References [55] and [63] use a fixed charging power of 4 kW since this is readily available in most Australian residential households without requiring infrastructure reinforcement. These references also use a representative residential load curve based on readings from a distribution transformer in Western Australia to represent the domestic load variations without any PEV battery charging activities for a typical day (Fig. 4.4). The maximum power intake of each resident is 2 kW at 0.9 power factor. In this thesis, the PEV energy requirements, battery size, charger size, and the residential daily load curve of references [55] and [63] are used for the simulations.

4.5.4. Injection and Designated Priorities of PEVs

PEV injection level is specified as the number of buses with PEVs in each residential feeder divided by the total 19 buses. Each household is assigned a maximum of one PEV. Electric vehicles are arbitrarily placed along the LV networks. The PEVs are divided in three groups as demonstrated in Fig. 4.7. Four PEV injection levels with the assigned locations and priorities for of Table 4.4 and Fig. 4.7(b) are simulated:

✓ Very low PEV injection of (3 PEVs) / (19 LV buses) ≈ 16%.

✓ Low PEV injection of (6 PEVs) / (19 LV Buses) ≈ 32%.

✓ Medium PEV injection of (9 PEVs) / (19 LV Buses) ≈ 47%.

✓ High PEV injection of (12 PEVs) / (19 LV Buses) ≈ 63%.

Majority of PEVs owners are subscribed to green and blue time zones to represent a realistic breakdown of priorities ([55], [63]).

4.6. Simulation and Analyses of PEV Coordination with Proposed OL-MSSCC

Simulations and assessments are done for the 449-bus smart power grid network of Fig. 4.7 for both uncoordinated/random and coordinated (using the proposed OL-MSSCC) PEV battery charging situations without/with WDGs. Comprehensive simulations are performed for PEV injections of 16%, 32%, 47% and 63%, as well as various locations/buses, various peak times, and various rates of WDGs. A time interval (Δt) of five minutes is used for all simulations. Table 4.5 shows the simulated scenarios for the smart power grid network of Fig. 4.7. Simulation results are presented in Figs. 8-13 and summarized in Tables 4.6 and 4.7.

The following six cases are simulated ad analysed (Table 4.5):

- *Case A*: Uncoordinated PEV battery charging without WDGs. Simulation results are shown in Fig. 4.8.

- *Case B:* Coordinated PEV battery charging (using proposed OL-MSSCC algorithm) without WDGs. Simulation results are presented in Fig. 4.9.

- *Case C:* Coordinated PEV battery charging (using proposed OL-MSSCC algorithm) with three WDGs (Fig. 4.5; WDG #1) having total peak wind generation of 3×0.2=0.6 MW (corresponding to wind power injection of 3×20%=60%). Simulation results are presented in Fig. 4.10.

- *Case D*: Same as Case C except the wind peak generation time is shifted to 8 pm, 10 pm, and 12 am. Simulation outcomes are presented in Fig. 4.11.

- *Case E:* Same as Case C except wind power injections are adjusted to 5%, 10%, 20%, 30% and 40%. Simulation results are presented in Fig. 4.12.

▪ *Case F*: For the PEV injection of 63%, the impacts of WDG locations on system losses are examined by alternately placing one large WDG of 0.6 MW (corresponding to wind power injection of 60%) at buses 2 to 31 of the 449-bus network (Fig. 4.7). Simulation results are presented in Fig. 4.13.

Table 4.5. Simulated case studies for the online MSS-based OL-MSSCC PEV battery charging coordination of the 449-bus smart power grid network in Fig. 4.7.

Case Study	PEV Coordination	Injection of PEV (%)	Injection of WDG (%)	Locations of WDGs	WDG Peak Time	Results
A	Uncoordinated	16, 32, 47, 63%	0	-	-	Fig. 4.8
B	OL-MSSCC	16, 32, 47, 63%	0	-	-	Fig. 4.9
C	OL-MSSCC	16, 32, 47, 63%	$3 \times 20 = 60\%$	Buses 4, 7, 12	6 pm	Fig. 4.10
D	OL-MSSCC	63%	$3 \times 20 = 60\%$	Buses 4, 7, 12	6 pm, 8 pm, 10 pm,12 am	Fig. 4.11
E	OL-MSSCC	63%	5% to 40%	Buses 4, 7, 12	6 pm	Fig. 4.12
F	OL-MSSCC	63%	$1 \times 60 = 60\%$	Buses 2 to 31	6 pm	Fig. 4.13

4.6.1. Random Charging of PEVs without WDGs (Case A)

The first case study (Case A) investigates the impacts/effects of uncoordinated/arbitrary EV battery charging on the network of Fig. 4.7 by considering random plugging of electric vehicles without any waiting for the centralized coordination. In order to compare simulation results, Gaussian (Normal) distributions of charging loads (Fig. 4.4(b)) with PEV injections of 16%, 32%, 47% and 63% within the three battery charging time zones (Fig. 4.4(a)) are generated and used for the simulations of Cases A-F. According to the simulations results of Figs. 4.8a-c and Table 4.6 (rows 2-6), the following points can be highlighted which are also confirmed in [55] and [63]:

✓ Even at low PEV injections (e.g., 16% corresponding to only two PEVs in each residential feeder of Fig. 4.7), there are some increases in power demand, power generation, voltage deviations, and power losses predominantly during peak load hours as reported in Figs. 4.8a-c and Table 4.6 (row 3).

✓ At high injections of PEVs (e.g., 47% and 63% corresponding to nine and twelve PEVs in each residential feeder of Fig. 4.7), there are significant increases in the overall cost (up to 50% and 59% as reported in column 6 (rows 5-6) of Table 4.6). This is primarily due to the consuming of electricity for PEV battery charging at high prices during the evening hours when most PEVs are being randomly plugged-in (Fig. 4.8(a)) and charged without any coordination.

✓ There could also be issues with substation transformer loadings. For example, transform loading is increased by 0.8 MW, as PEV injection is increased from %16 injection to %64 injection as reported in Table 4.6 (column 7, rows 2 and 6).
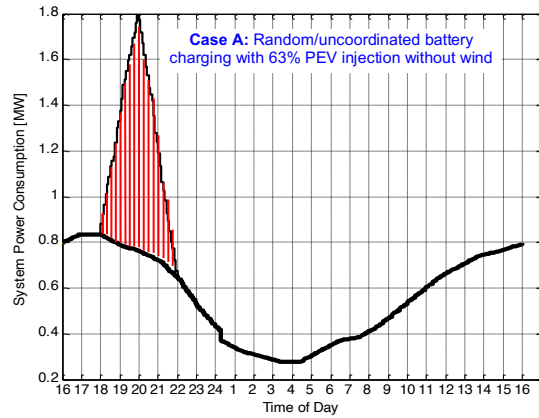
(a)
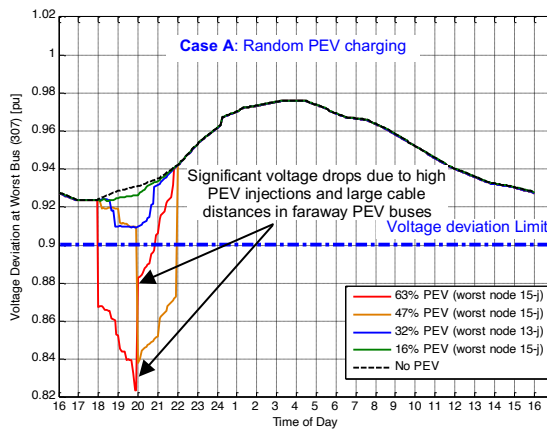
(b)
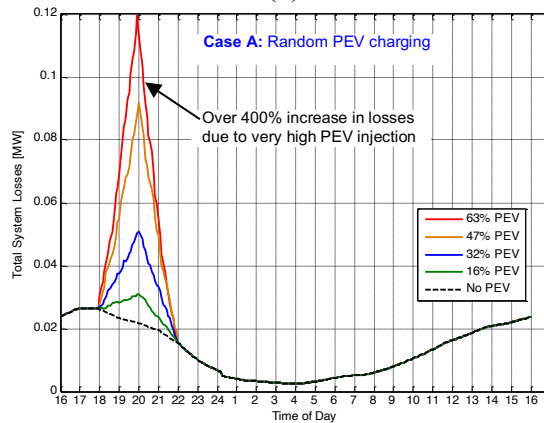
(c)

Fig. 4.8. Simulation results for Case A: Uncoordinated PEV battery charging in Fig. 4.7 without WDGs; (a) System power demand for 63% injection of PEVs, (b)-(c) Voltage deviation at worst bus and total system losses [55].

4.6.2. The OL-MSSCC of PEVs without WDGs (Case B)

The second simulated scenario (Case B) demonstrates the performance of OL-MSSCC algorithm for the coordination of PEVs in Fig. 4.7 without the three WDGs. Simulation results are presented in Fig. 4.9 which are also published by the author in [55]. Note that

the maximum demand level ($D_{t,max}$ in Eq. 4.18) is intentionally reduced after midnight to push the charging load of low-priority PEVs to early morning hours with lower energy prices (Fig. 4.4(a)). Based on the simulations results of Figs. 4.9a-c and Table 4.6 (rows 7-11), the following analysis are made [55]:

✓ There are notable augmentations in system performance with notable reductions in the operational expenses/costs (Fig. 4.9 and Table 4.6, rows 7-11).

✓ Unlike Case A (uncoordinated PEV battery charging), all bus voltages are regulated within the permitted limit of $\Delta V_{max} = 10\%$ (Eq. 4.17) even at high injection levels of 47% and of 63%.

✓ In addition, OL-MSSCC algorithm has effectively managed to control the peak generation, distribution transformer loading and system losses.

4.6.3. The OL-MSSCC of PEVs with WDGs (Case C)

Case C is intended to demonstrate the first contribution of this thesis which is the inclusion of WDGs in the MSS-based coordination of PEVs. Three WDGs with the total peak wind generation of 3×0.2=0.6 MW (corresponding to wind power injection of 3×20%=60%) are positioned at buses 4, 7 and 12 of Fig. 4.7. The wind peak generation time is 6-9 pm (Fig. 4.5; WDG #1). Simulations results are presented in Fig. 4.10 and Table 4.6 (rows 12-16) [55]. Comparison of the PEV battery charging without (Fig. 4.9) and with (Fig. 4.10) wind power generation indicates that WDGs will generally improve the overall system performance and PEV scheduling:

✓ Depending on the speed, duration and peak time of the wind, WDGs can provide opportunities to charge more PEVs beyond the maximum demand level without overloading the substation transformer. This is due to the distributed nature of WDGs acting as local energy generation resources.

✓ Wind power can significantly decrease the burden on the substation transformer reducing its loading. For example, substation transformer loading is declined from 0.85 MW (without WDGS) to 0.75 MW (with WDGS) as reported in Table 4.6 (last column, rows 7-11 and 12-16).

✓ As expected, the addition of wind power has also reduced the generation and total costs. As an example, for 16% PEV injection, the increase in cost has improved from +5.96% to -10.56% (Table 4.6; column 6, rows 8 and 13).

4.6.4. Impacts of Peak Wind Generation Times on OL-MSSCC of PEVs (Case D)

Case C is repeated with the wind peak generation time shifted form 6 pm (Fig. 4.5; WDG #1) to 8 pm (Case D1), 10 pm (Case D2) and 12 am (Case D3). Simulation results are presented in Fig. 4.11 and Table 4.6 (rows 17-31) [55]. These results reveal:

✓ Altering the wind peak DG time within 6 pm to 12 am will not have a major impact on OL-CAA scheduling; however, the overall system performance is improved compared with both Case A (uncoordinated/random PEV battery charging) and Case B (coordinated PEV battery charging with no wind DGs).

✓ The ideal situation is when the peak wind generation time overlaps with the peak PEV battery charging demand (Case C).

4.6.5. Impact of Wind Power Injection on OL-MSSCC of PEVs (Case E)

Five WDG sizes corresponding to the total wind power injections of 5%, 10%, 20%, 30%, and 40% are simulated and the results are summarized in Table 4.7 [55]. For this case study, the PEV injection is 63%. The impacts of wind power injection on the substation transformer loading are shown in Fig. 4.12. According to these results:

✓ There are considerable reductions in transformer loading as the wind power injection is increased (Fig. 4.12).

✓ There are also gorgeous cost reductions as the wind power injection is increased. For example, the total cost for wind power injection of 5% is +10.30% (e.g., 10.30% more than the cost with no PEVs) while this cost drops to -15.4% when the wind power injection is 40% (Table 4.7, column 6; rows 3 and 7).

✓ However, increasing the wind power injection beyond 10% will not have substantial influences on the total system losses (Table 4.7, column 3; rows 5-7).

4.6.6. Impacts of WDG Positions on OL-MSSCC of PEVs (Case F)

To investigate the influences of WDG locations/positions on the OL-MSSCC strategy and system performance, a large WDG of 0.6 MW (corresponding to wind power injection of 60%) is alternately placed on the HW buses 2 to 31 of the 449-bus SG network (Fig. 4.7). The PEV injection is 63% and simulation results are shown in Fig. 4.13. According to the results:

✓ The proposed OL-MSSCC algorithm can successfully coordinated PEV battery charging with substantial improvements compared with uncoordinated Case A and coordinated Case B without WDGs.

✓ However, distributing the wind power resources along the HV network is more advantageous. For example, using three WDGs rated at 3× 0.2 MW distributed along the HW network results in less system losses as compared with installing one WDG rated at 1× 0.6 MW.

✓ The most beneficial areas for the installation of WDGs are located at the ends of HV feeders.

✓ The best buses for the placement of WDGs in the order of preference are: i) buses 10-15, ii) buses 6-8, iii) buses 16-18, iv) buses 20-21, and v) buses 24-28.
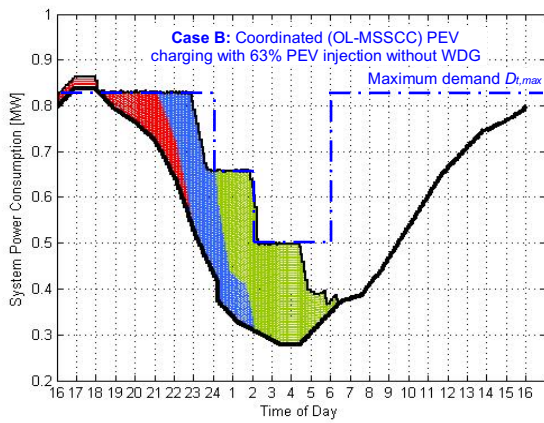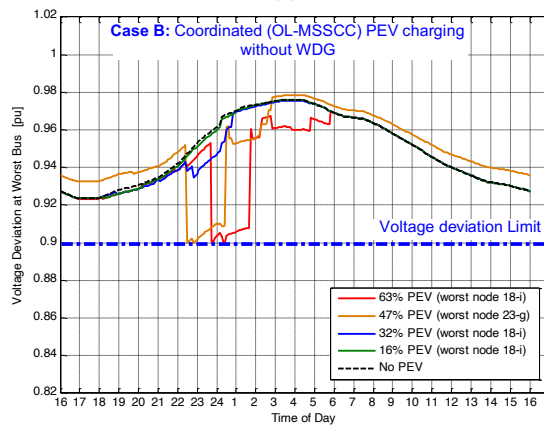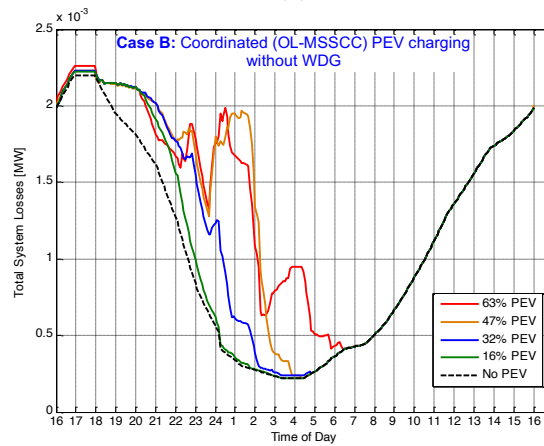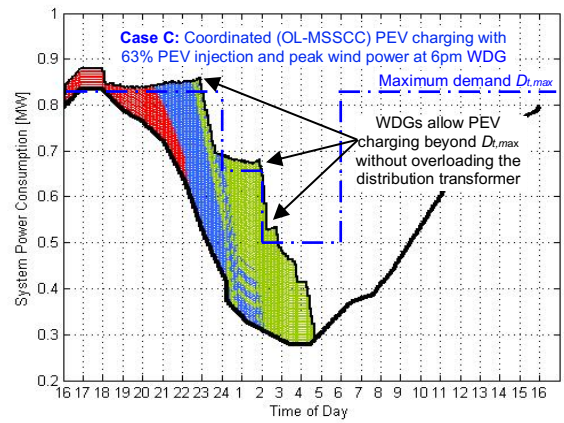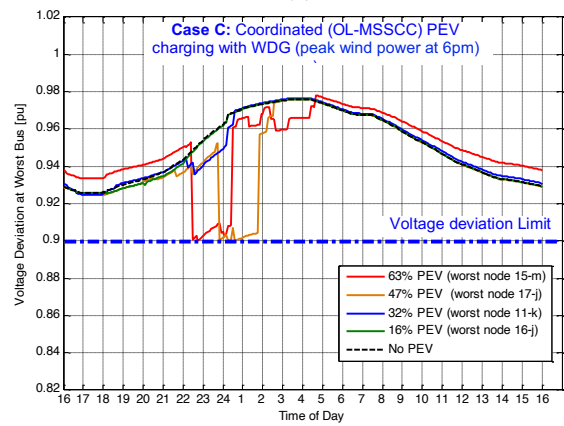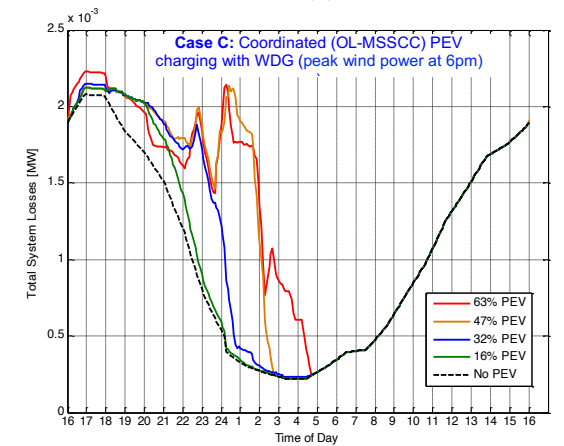
Fig. 4.9. Simulation results for Case B: Coordinated (OL-MSSCC) PEV battery charging in Fig. 4.7 without WDGs; (a) System power demand for 63% injection of PEVs, (b)-(c) Voltage deviation at worst bus and total system losses [55].

Fig. 4.10. Simulation results for Case C: Coordinated (OL-MSSCC) PEV battery charging in Fig. 4.7 with three 0.2 MW WDGs with wind peak generation time at 6pm; (a) System power demand for 63% injection of PEVs, (b)-(c) Voltage deviation at worst bus and total system losses [55].
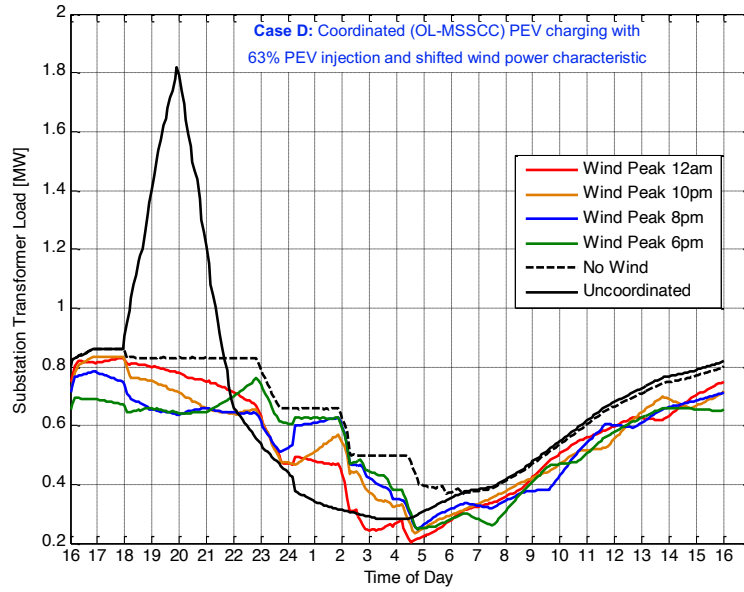
Fig. 4.11. Simulation results for Case D: Coordinated (OL-MSSCC) PEV battery charging in Fig. 4.7 with three 0.2 MW WDGs (total injection of 3×20%=60%) and maximum wind output power at 6, 8, 10 and 12pm; (a) System power demand, (b)-(c) Voltage deviation and total system losses [55].
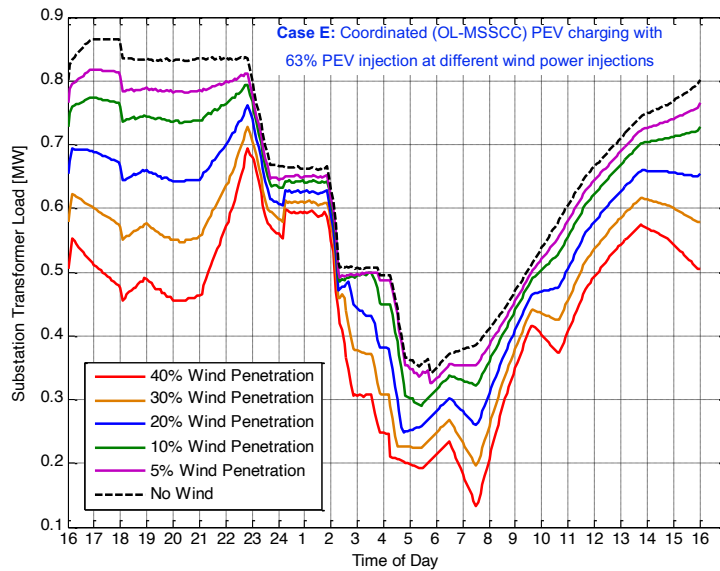
(b)

Fig. 4.12. Simulation results for Case E: Substation transformer loading for coordinated (OL-MSSCC) PEV battery charging in Fig. 4.7 with wind power injections of 5%, 10%, 20%, 30% and 40% (wind peak power generation at 6pm) [55].
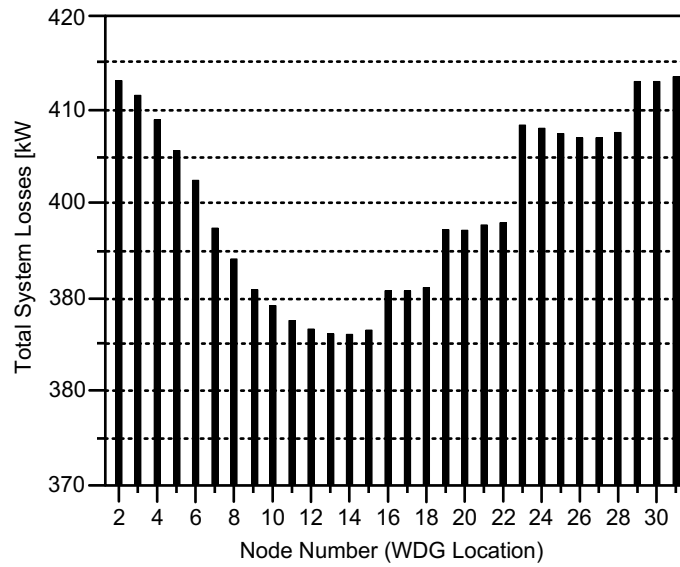
Fig. 4.13. Case F simulations: Impacts of WDG positions/locations on the total network losses of Fig. 4.7 with coordinated (OL-MSSCC) PEV battery charging. For the PEV injection of 63%, one large WDG of 0.6 MW (corresponding to wind power injection of 60%) is alternately placed at HW buses 2 to 31 [55].

Table 4.6. Summary of simulation results for Cases A, B and C showing the performance of proposed OL-MSSCC for the smart power grid network of Fig. 4.7 without and with WDGs. Each WDGs has a maximum output power of 0.2 MW (corresponding to 20% wind power injection) with unity power factor. The time interval (Δt) is 5 minutes [55]. For comparison, the same Gaussian function is used to generate random Gauss PEV distributions and random Gauss PEV plug-in times in all residential feeders. For nominal operation without any PEVs or WDGs, the values for "$|\Delta V|$", "Imax", "Generation Cost" and "Total Cost" are 7.646%, 0.147%, 770.3 \$/day and 786.2 \$/day.

PEV (%)	$\|\Delta V\|$ (%)	Imax (%)	Cost of Generation (\$/day) / (%)*	Total Network Cost (see Eq.4.16) (\$/day) / (%)*	Loading of Substation Transformer (MW)
Case A: Uncoordinated/random PEV battery charging without WDGs; Figs. 4.8a-c						
63	17.60	0.307	958/24.4	1,250/59.0	1.80
47	16.20	0.263	916/18.9	1,180/50.0	1.50
32	9.050	0.218	871/13.07	1,090/38.6	1.30
16	7.690	0.179	829/7.62	1,030/31.0	1.00
Case B: Coordinated (OL-MSSCC) PEV battery charging without WDGs; Figs. 4.9a-c						
63	10.00	0.171	875/13.59	895/13.84	0.86
47	10.00	0.160	858/11.38	878/11.67	0.85
32	7.65	0.159	838/8.79	855/8.75	0.85
16	7.65	0.159	808/4.89	825/4.93	0.85
Case C: Coordinated (OL-MSSCC) Charging with WDGs (Peak Generation at 6pm; Fig. 4.10)						
63	10.00	0.170	761/-1.20	781/-0.63	0.76
47	10.00	0.166	742/-3.67	761/-3.18	0.76
32	7.52	0.172	720/-6.53	737/-6.23	0.75
16	7.46	0.163	687/-10.81	703/-10.56	0.66
Case D1: Coordinated (OL-MSSCC) Charging with WDGs (Peak Generation at 8pm; Fig. 4.11)						
63	10.00	0.172	768/-0.29	787/0.12	0.78
47	10.00	0.166	748/-2.89	767/-2.41	0.75
32	7.59	0.172	726/-5.75	743/-5.47	0.75
16	7.55	0.163	694/-9.90	710/-9.67	0.74
Case D2: Coordinated (OL-MSSCC) Charging with WDGs (Peak Generation at 10pm; Fig. 4.11)						
63	10.00	0.172	773/-0.35	792/0.76	0.84
47	10.00	0.167	752/-2.37	771/-1.90	0.79
32	7.61	0.172	730/-5.23	747/-4.96	0.79
16	7.59	0.172	696/-9.64	712/-9.41	0.79
Case D3: Coordinated (OL-MSSCC) Charging with WDGs (Peak Generation at 12pm; Fig. 4.11)						
63	10	0.172	771/-0.99	791/0.64	0.83
47	9.98	0.189	750/-2.89	769/-2.16	0.81
32	7.72	0.173	726/-6.30	743/-5.47	0.81
16	7.62	0.176	691/-10.29	707/-10.05	0.81

*) Increase or decrease in daily cost (excluding renewable energy cost) in percentage of the nominal cost without any PEVs or WDGs.

Table 4.7. Impact of WDG injection on losses, cost and substation transformer loads of Fig. 4.7 with the proposed OL-MSSCC, PEV injection of 63%, unity WDG power factor and time interval (Δt) of 5 minutes [55]. For nominal operation without any PEVs or WDGs, the values for "$|\Delta V|$", "Imax", "Generation Cost" and "Total Cost" are 7.646%, 0.147%, 770.3 $/day and 786.2 $/day, respectively.

WDG (%)	$|\Delta V|$ (%)	Total Network Power Loss (MW/day)	Cost of Generation ($/day) / (%)*	Total Network Cost (see Eq.4.16) ($/day) / (%)*	Loading of Substation Transformer (MW)
Case E: Coordinated (OL-MSSCC) PEV battery charging with WDG Injections of 5 to 40% (PEV Injection of 63% and Peak Wind Generation at 6 pm; Fig. 4.12)					
40	10.00	0.2025	646/-16.13	665/-15.40	0.69
30	10.00	0.2041	704/-8.60	723/-8.02	0.73
20	10.00	0.2068	761/-1.20	781/-0.63	0.76
10	10.00	0.2101	818/6.19	838/6.61	0.79
5	10.00	0.2112	847/9.99	867/10.3	0.82

*) Increase or decrease in daily cost (excluding renewable energy cost) in percentage of the nominal cost without any PEVs or WDGs.

4.7. Discussions and Conclusions

In this chapter, a centralized online MSS-based coordinated battery charging (OL-MSSCC) algorithm for PEVs in smart power grid networks with WDGs is proposed, formulated, and implemented [55]. The OL-MSSCC is intended for real-time PEV battery charging (e.g., every 5 minutes) and relies on the grid, PEVs and WDGs information that are to be collected by smart meters and transmitted to the ISO who will supervise the central coordination. The approach is like the real-time smart load management (RT-SLM) algorithm of [63] but with the addition of WDGs. To demonstrate the performance of OL-MSSCC, it is implemented on the IEEE 449-bus smart power grid network of Fig. 4.7 without and with WDGs considering high- medium- and low-priority PEVs with injection levels of 16%, 32%, 47% and 63%. The following main conclusions are noted based on the detailed simulations results of Tables 4.6- 4.7 and Figs. 4.8-4.13:

- Uncoordinated vehicle charging can result in substantial escalations in demand, voltage changes/deviations, losses and generation predominantly in the evening peak load hours with large number of PEVs being charged [55], [63].

- The proposed OL-MSSCC algorithm can effectively schedule vehicle battery charging without and with WDGs at all PEV injections [55]. This is done by considering three consumer (high, medium, and low) priorities, three charging time zones (red, blue and green), dynamic energy prices and grid operation constraints within the formulation and implementation of OL-MSSCC.

- The proposed OL-MSSCC algorithm is a potential candidate for online coordination of PEVs in large smart power grid networks since it is quite simple, fast, practical and easy to implement.

- Increasing the injection of wind power generation will substantially reduce system losses, generation cost and transformer loadings. The proposed OL-MSSCC takes advantage of the available renewable wind energy for charging more PEVs. For the smart power grid network of Fig. 4.7, there are significant cost reductions as the wind power injection is increased.

- The best spots for the installation of WDGs are near the residential feeders with high injections of PEVs, at the ends of the HV feeders and close to the charging stations. For the simulated smart power grid network of Fig. 4.7, the best buses for the placement of WDGs in the order of preference are: i) buses 10-15, ii) buses 6-8, iii) buses 16-18, iv) buses 20-21, and v) buses 24-28.

- If possible, moving the wind peak generation periods to early evening hours will enhance the overall network performance. The ultimate situation is when the peak wind DG generation overlaps with the peak PEV battery charging.

CHAPTER FIVE: CENTRALIZED ONLINE FUZZY COORDINATED BATTERY CHARGING OF PEVs IN SMART POWER GRIDS CONSIDERING WIND GENERATION

The second contribution of this Ph.D. thesis is a new centralized online fuzzy coordinated battery charging (OL-FCC) algorithm for PEVs in smart power grid networks with WDGs which was published by the author during his Ph.D. studies in reference [56]. The approach is like the OL-MSSCC of Chapter 4; however, fuzzy reasoning is included to improve the PEV coordination performance and achieve additional reduction in the total grid cost. The proposed OL-FCC algorithm is also solved on real-time bases using the grid, PEVs and WDGs information transmitted by the smart meters. The performances of uncoordinated PEV battery charging, coordinated sensitivity-based charging (OL-MSSCC of Chapter 4 [55]) and the fuzzy-based charging (OL-FCC of this chapter [56]) are compared and their impacts on total cost, gird losses and voltage profiles are investigated by implementing them on the 449-bus network of Fig. 4.7 without and with WDGs. The key advantage/benefit of OL-FCC compared with OL-MSSCC of Chapter 4 is a further cost reduction within the selected scheduling/planning time horizon (e.g., 24 hours).

The proposed fuzzy-based coordination charging algorithm of this chapter has the following advantages compared to the existing EV coordination techniques (discussed in Chapter 3):

✓ The low computational cost and high calculation speed of OL-FCC makes it a good candidate for online PEV coordination in real-life smart grid networks.

✓ The outstanding processing efficiency of OL-FCC makes it possible to perform large-scale PEV coordination using low-cost microcontrollers.

✓ The complex nonlinear EV coordination optimization process is simplified by minimizing the objective function based on the sensitivity of network losses to charging demand.

✓ Simple mathematics, expert knowledge, and fuzzy human reasoning are used to incorporate optimization constraints associated with loss and voltage regulation.

✓ The quality of coordination solution is further improved by incorporating time-dependent maximum demand weighting factors associated with the red, blue, and green time zones designed for high-, medium, and low-priority PEV groups.

This chapter is organized as follows:

- Section 5.1 reviews fuzzy sets, Fuzzification and Defuzzification techniques.

- Section 5.2 presents the formulation and flow chart of the proposed OL-FCC algorithm for PEVs.

- Section 5.3 investigates the performance of the proposed OL-FCC algorithm without WDGs by performing detailed simulations for coordination of PEVs in the 449-bus smart power grid network of Fig. 5.7.

- Section 5.4 investigates the performance of the proposed OL-FCC algorithm with three WDGs in the 449-bus smart power grid network.

- This chapter ends with the conclusions in Section 5.5.

5.1. Fuzzy Sets, Fuzzification and Defuzzification Techniques

In 1975, Professor Lotfi Aliasker Zadeh (L.A. Zadeh) defined a number of new and impacting ideas regarding fuzzy systems that have been extensively used by many researchers both in theory and applications in many fields including Science and

Engineering. Zadeh defined the concept of type-2 fuzzy set along with the associated concepts and mathematical functions [131]-[134]:

✓ The extension principle (EP) that extends the conventional point-valued operations from the crisp mathematical setting to a corresponding fuzzy mathematical setting. This is the essential idea used for fuzzifying the classical mathematical concepts.

✓ The α-cut (also called λ-cut) decomposition theorem that allows the same extension of the EP but in a set-valued manner.

Zadeh's idea is to decompose fuzzy sets (FSs) into a collection of crisp sets related together via the α levels. This decomposition theorem has been extended to fuzzy sets with interval membership grades known either by interval valued fuzzy sets (IVFSs) or interval type-2 fuzzy sets (IT2FSs).

5.1.1. Fuzzy Set

Fuzzy numbers are an extension of real numbers [131]. However, a fuzzy number does not refer to one single value but rather to a set of possible values that have weights (called membership function) between 0 and 1. Fuzzy sets were introduced by Zadeh in 1965 and are somewhat like the classical sets whose elements have degrees of membership [131].

- Let A be a crisp subset of the universe X, it is a function $A : X \rightarrow \{0 , 1\}$ that assigns 1 to elements of the domain that belong to A and 0 otherwise. Let $C(X)$ be the set of all crisp subsets of $X1$. Let A be an interval over X. It is defined by $A = [x^-, x^+]$ where x^-, $x^+ \in X$ and $x^- \leq x^+$.

- In addition, let I(X) be the set of all interval subsets of X. Note that an interval is a special crisp set with $A(x) = 1$, $x^- \leq x \leq x^+]$ and 0 otherwise.

- Let a type-1 fuzzy set T1FS (also called fuzzy set (FS)) A be a subset of X, and defined to be a function $A : X \rightarrow [0 , 1]$. It is a generalization of both crisp sets and intervals. Let **F(X)** be the set of all fuzzy subsets of X.

5.1.2. Fuzzification

Fuzzification is the process of converting a crisp quantity to a fuzzy quantity [134]. This is done since most realistic crisp quantities are in fact are not deterministic at all since they carry considerable uncertainty. If the uncertainty of a quantity is due to imprecision, ambiguity, or vagueness, then the quantity is probably fuzzy and can be represented by a membership function.

For example, in the real world, most hardware such as digital voltmeters provide crisp reading values, but these values are subject to experimental error. Fig. 5.1 shows a possible range of error (e.g., ±1.5%) for a typical voltage reading and the associated triangular membership function that can be used to characterize its imprecision.
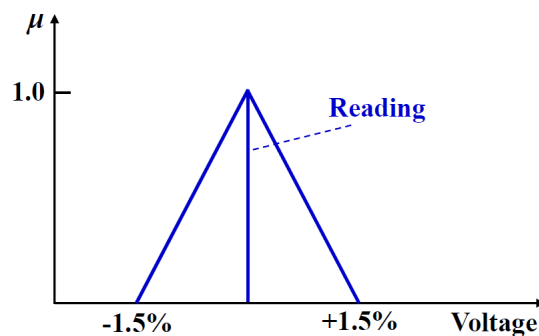
Fig. 5.1. A membership function representing the imprecision associated with a voltmeter measurement (based on Fig. 4.6 of [134]).

5.1.3. Membership Functions

All information contained in a fuzzy set is described by its membership function. For a fuzzy set A, Fig. 5.2 shows the terms used to describe special features of its membership function $\mu(x)$ [134]:

- The core of $\mu(x)$ is the region of universe characterized by full membership in the set A. The core includes those elements x of the universe such that $\mu(x) = 1$.

- The support of $\mu(x)$ is the region of universe characterized by nonzero membership in set A. The support includes those elements x of the universe such that $\mu(x) > 0$.

108

- The boundaries of $\mu(x)$ is the region of universe containing elements that have a nonzero membership but not complete membership. The boundaries include those elements x of the universe such that $0 < \mu(x) < 1$. These elements have some degree of fuzziness, or only partial membership in the fuzzy set A.

There are various types of fuzzy sets (Fig. 5.3) [134]:

- A normal fuzzy set A (Fig. 5.3a) has membership function with at least one element x in the universe whose membership value is unity. Otherwise, the fuzzy set is subnormal (Fig. 5.3b).

- A convex fuzzy set A (Fig. 5.3c) has membership values that are: i) strictly monotonically increasing or, ii) strictly monotonically decreasing or, iii) strictly monotonically increasing then strictly monotonically decreasing with increasing values for elements in the universe. Otherwise, the fuzzy set is nonconvex (Fig. 5.3d).

- Fuzzy membership functions can be continuous or discrete. There are different types (shapes) of fuzzy membership functions such as triangular, trapezoidal, exponential, bell-shaped, sigmoidal, Gaussian, z-shape and s-shape.
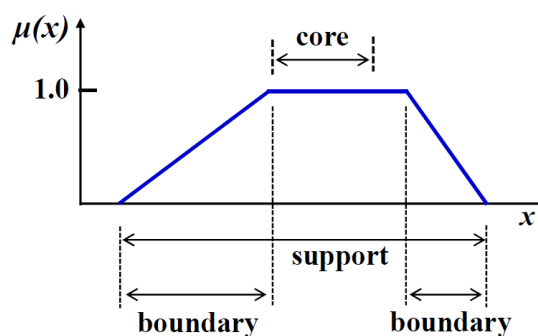
Fig. 5.2. A typical membership function of a fuzzy set showing its core, support, and boundaries (based on Fig. 4.1 of [134]).
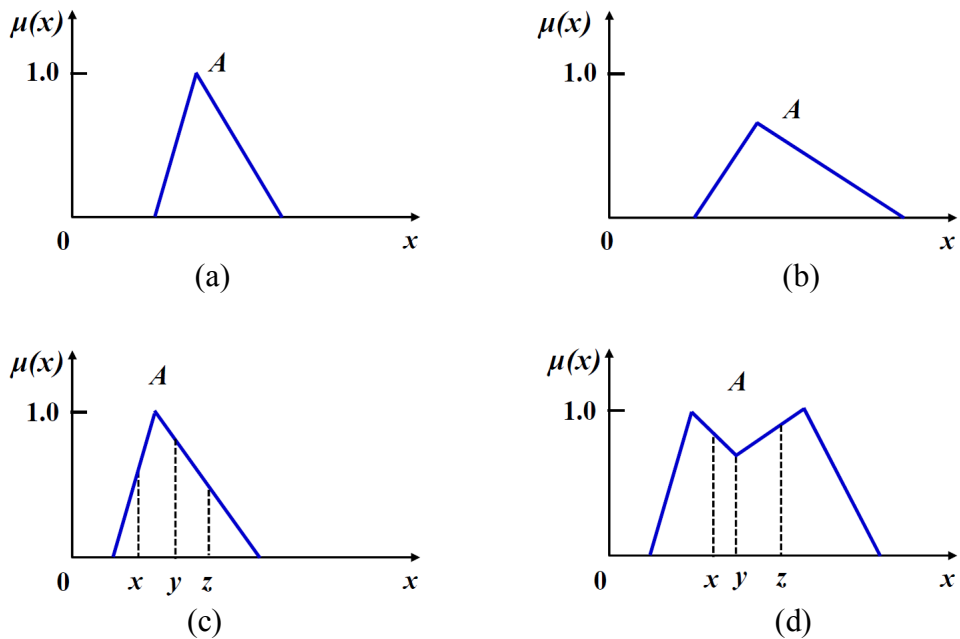
Fig. 5.3. Examples of Fuzzy membership functions; (a) normal, (b) subnormal, (c) convex normal, (d) nonconvex normal (based on Figs. 4.2-4.3 of [134]).

5.1.4. Defuzzification Using Alpha-Cut Method

In many engineering applications such as the PEV coordination problem of this chapter there is a need to "defuzzify" the fuzzy results obtained from a fuzzy system analysis [131], [134]. For example, if we decide to fuzzify the constraints associated with the vehicle battery charging, then the PEV coordination algorithm will require their corresponding crisp values (e.g., defuzzified values) to perform scheduling. Therefore, defuzzification process consists of reducing a fuzzy number to a crisp number, or a fuzzy set to a crisp single-valued quantity, or a fuzzy matrix to a crisp matrix. In order words, defuzzification is the process of deducing the membership degrees into a specific decision or real value. A famous approach for defuzzification of fuzzy sets is the α-cut (also known as λ-cut).

Consider a fuzzy set A and define a crisp set called α-cut set such that [131], [134]:

$$A_\alpha = \{x \mid A(x) \geq \alpha\} \quad \text{where} \quad \alpha \in [0, 1], x \in X. \tag{5.1}$$

Any particular fuzzy set A can be transformed into an infinite number of α-cut sets.

110

For example, consider the discrete fuzzy set shown in Fig. 5.4 that can be defined on the universe $X = \{a, b, c, d, e, f\}$ as follows [134]:

$$A = \left\{\frac{1}{a} + \frac{0.95}{b} + \frac{0.65}{c} + \frac{0.3}{d} + \frac{0.01}{e} + \frac{0}{f}\right\}$$

The above fuzzy set A can be reduced based on Eq. 5.1 into several crisp α-cut sets. For example, we can define α-cut sets for α = 1, 0.95, 0.3, 0+, and 0 as follows [134]:

$$A_1 = \{a\}, A_{0.95} = \{a, b\}, A_{0.3} = \{a, b, c, d\}, A_{0+} = \{a, b, c, d, e\}, A_0 = X.$$
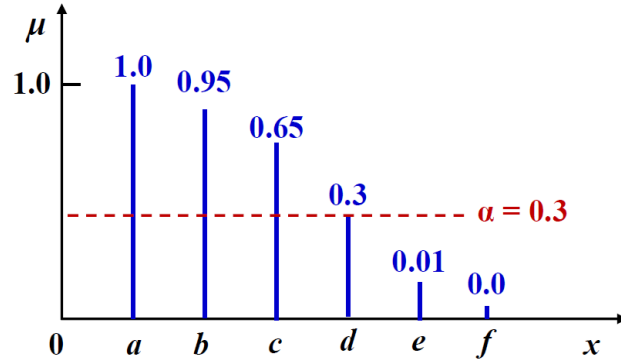
Fig. 5.4. An Example of discrete fuzzy set A (based on Fig. 4.8 of [134]). The horizontal red line visualizes α-cut defuzzification of A for α = 0.3 resulting in $A_{0.3}$ = {a, b, c, d}.

5.2. Formulation of Proposed Online Fuzzy Coordinated Battery Charging (OL-FCC) Algorithm for PEVs to Reduce Total Cost

This chapter leverages the stimulating fuzzy technology to attain additional reduction in total cost of PEV battery charging. Formulations of the objective cost function and the associated constraints are the same as Chapter 4 with the addition of fuzzy reasoning.

5.2.1. Objective Cost Function and Constraints of Proposed OL-FCC

The previously defined formulations of objective cost function (Eq. 4.16), constraints (Eqs. 4.17-4.18) and MSS vector (Eqs. 4.19-4.20) are also used in the proposed OL-FCC. Therefore, the quick and fairly precise MSS-based cost minimization methodology of Chapter 4 ([55], [63]) is also used in the proposed OL-FCC to quantify/measure the sensitivity of objective (network losses) function to PEV battery charging at each time interval $t = \Delta t$. However, a Fuzzy approach is used to incorporate the constraints.

5.2.2. Fuzzification of System Losses and Constraints Using Membership Functions

At each time interval $t = \Delta t$ of OL-FCS, fuzzy reasoning is used to participate the PEV constraints of Eqs. 4.17-4.18 in the coordination process and to pick the most appropriate/suitable vehicles for charging within the high-, medium- and low-priority PEV groups defined in Section 4.3.1 and Fig. 4.4. This is done using the fuzzy/fuzzified membership functions that are shown in Figs. 5.5 (a)-(c). The new ideas are [56]:

a) Fuzzify the sensitivities of losses ($P_{t,loss}$ in Eq. 4.16), voltage deviation (ΔV_k in Eq. 4.17) and maximum demand level ($D_{t,max}$ in Eq. 4.18) for battery/PEV charging at each bus k using the fuzzy/fuzzified membership functions that are presented in Figs. 5.5(a), (b) and (c), respectively. These ideas are formulated in Eqs. 5.2-5.4.

b) To assure full charge of all vehicle batteries by 6am, consider time-dependent weighting factors to adjust $D_{t,max}$ (Fig. 5.5 (d)) for red, blue and green charging time zones. This idea is implemented in Eq. 5.4 and the maximum demand membership function of Fig. 5.5(c).

<u>Fuzzifying Voltage Deviations (ΔV_k)</u>

At each bus (e.g., bus number k), the exponential function of the membership (Eq. 5.2; plotted in Fig. 5.5(a)) is employed to fuzzify the constraints (Eq. 4.17) related to the deviations/changes of voltage magnitude with respect to the vehicle battery charging at the same bus [56]:

$$\mu_{\Delta V_k} = \begin{cases} 1 & \text{if } \Delta V_k \leq \Delta V_0 \\ e^{-(\Delta V_k - \Delta V_0)/T_V} & \text{if } \Delta V_k > \Delta V_0 \end{cases} \quad \text{for } k = 1, \quad n. \qquad (5.2)$$

where T_V is the time constant of the membership function for voltage deviation and the value of $\Delta V_0 = \Delta V_{max}/2$ is elected such that all system buses that have voltage deviations less than ΔV_0 will have get full memberships. In this thesis, $\Delta V_0 = 0.05$ pu. Also, T_V is

chosen to be $T_V = 0.034$; which means $\mu_{\Delta V_k} = 0.23$ for $\Delta V_k = \Delta V_{max} = 0.1$ pu

(Equation 4.17). Therefore, according to Eq. 5.2 and Fig. 5.5(a), OL-FCC algorithm will

assign low membership values to PEV buses with high voltage deviations.

Fuzzifying Total Losses ($P_{t,loss}$)

At each $t = \Delta t$ of OL-FCS, an exponential membership function (Eq. 5.3; plotted in Fig.

5.5(b)) is used to constrain the total power losses (Eq. 4.16) resulting from PEV battery

charging [56]:

$$\mu_{loss} = e^{-P_{t,loss}/T_{loss}} \tag{5.3}$$

where T_{loss} is the time constant of the membership function for loss deviation and should

be adjusted such the system losses at time interval t are less than the rated losses

$P_{loss,rated}$ (e.g., rated losses without any PEV battery charging activities). In this thesis,

$T_{loss}=0.034$; such that $\mu_{loss} = 0.5$ when total losses are equal to the rated losses ($P_{t,loss} =$

$P_{loss,rated}$ without any PEV battery charging; Eq. 4.16). Therefore, according to Eq. 5.3

and Fig. 5.5(b), OL-FCS will assign low membership values to PEV battery charging

situations that results in high system losses.
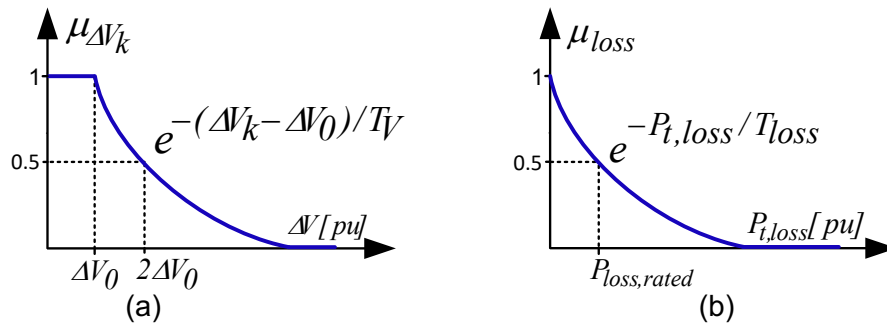
Fig. 5.5(a-b). Fuzzy membership functions for the proposed OL-FCC algorithm; (a) voltage
deviations (Eq. 4.17 and Eq. 5.2), (b) total system losses (Eq. 4.16 and Eq. 5.3) [56].

Fuzzifying Maximum Demand Level ($D_{t,max}$)

At each $t = \Delta t$ of OL-FCS, two exponential membership functions (Fig. 5.5(c)) are used to control the maximum total demand (Eq. 4.18) during PEV battery charging periods [56]:

$$\mu_D = \begin{cases} e^{-\Delta D / T_{D+}} & \text{if } \Delta D = D_{t,total} - W_D D_{t,max} \geq 0 \\ e^{+\Delta D / T_{D-}} & \text{if } \Delta D = D_{t,total} - W_D D_{t,max} < 0 \end{cases} \tag{5.4}$$

where W_D is the maximum demand weight factor, T_{D+} and T_{D-} are the time constants of the membership functions for over-demand and under-demand conditions, respectively. In general, it is desired to: i) set $T_{D+} \ll T_{D-}$ T_{D+} to avoid situations where the total system demands is larger than the designated maximum value of $D_{t,max}$ (Eq. 4.18) and, ii) adjust W_D based on the PEV waiting times recorded in the queue table. In this thesis, the time constant values are selected to be $T_{D+} = 0.0125$ and $T_{D-} = 0.125$ while the three time-dependent characteristics of Fig. 5.5(d) are uses for W_D in the three designated charging time zones. Therefore, according to Eq. 5.4 and Fig. 5.5(c), OL-FCS will assign low membership values to PEV battery charging situations that results in total demands that are either higher or lower than $D_{t,max}$.

Time-Dependent Maximum Demand Weight Factors ($W_D(t)$)

At each time interval $t = \Delta t$ of OL-FCS, three linear time-dependent maximum demand weight factors with steep, moderate and sharp slopes (W_D in Eq. 5.4 and Fig. 5.5(c)) are adopted for the PEV battery charging in the three designated charging time zones as shown in Fig. 5.5(d). The main reason for using time-depending weight factors for the maximum demand membership functions of Fig. 5.5(c) is to design OL-FCC so that on one hand vehicle battery charging are deferred to off-peak hours as frequently as possible (e.g., aiming for the reduction of energy cost) and on the other hand PEVs are charged as

soon as possible (e.g., aiming to assure/improve customer satisfaction by fully charging all/most EV batteries before 0600h) [56].

The next section presents a procedure for the Fuzzy combination of OL-FCC membership functions of Figs. 5.5(a)-(c).
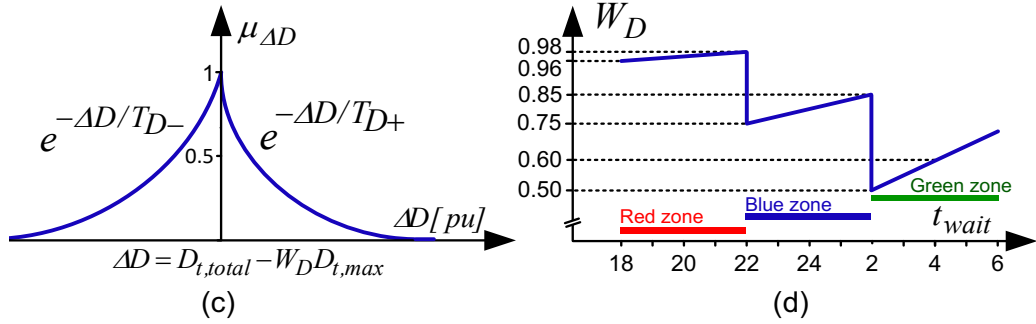
Fig. 5.5(c-d). Fuzzy membership functions for the proposed OL-FCC algorithm; (c) exponential functions to set the maximum demand level (Eq. 4.18 and Eq. 5.3), (d) linear functions to set maximum values of the demand weighting factors (Eq. 5.3 and Fig. 5.5(c)) [56].

5.2.3. Fuzzied Combination of All Membership Functions

To combine the fuzzy membership functions we can use the additive generators or multiplicative generators of a t-norm (also called triangular norm) [135], [136]. For the simulations and analyses of this thesis, an additive t-norm generator is adapted to cluster/combine the selected membership functions for the voltage deviations ΔV_k (Figs. 5.5(a)), system losses $P_{t,max}$ (Figs. 5.5(b)) and maximum demand level $D_{t,max}$ (Figs. 5.5(c)) [56]:

$$\mu_{PEV,j} = W_V \cdot \mu_{\Delta V_k} + W_L \cdot \mu_{loss} + W_D \cdot \mu_{\Delta D} \qquad \text{for} \quad j = 1, \dots, j_m \qquad (5.5)$$

where: i) W_V is the weighting factor for voltage deviation membership function, ii) W_L is the weighting factor for system loss membership function and, iii) W_D is the weighting factor for maximum demand membership function. In this thesis, the selected weighing factors of Eq. 5.5 are $W_V = 0.3$, $W_L = 0.3$ and $W_D = 0.4$.

5.2.4. Defuzzifiation Based on α-Cut Method

To direct OL-FCC toward the permissible constraint region, the α-cut process (Eq. 5.1) is used to defuzzify $\mu_{PEV,j}$ (Eq. 5.5) and to find the its crisp value (e.g., the sensitivity of buses with PEV to the charging demand):

$$S_{PEV,j} = \{X \mid \mu_{PEV,j}(x) \gg \alpha = 0.6\}, \qquad x \in X \quad \text{and} \quad j = 1, \dots, j_m \qquad (5.6)$$

where $S_{PEV,j}$ is the crisp (defuzzified) value of the combined fuzzy membership function value of the jth PEV representing the sensitivity of bus with this PEV to the charging demand. For the simulations and analyses of this thesis, the α-cut level in Eq. 5.6 is selected to be $\alpha = 0.6$.

Therefore, at each time interval Δt, all PEVs with the crisp value of $S_{PEV,j} \geq 0.6$ will be allowed to start charging while the charging of the vehicles with $S_{PEV,j} < 0.6$ will be postponed to the next time interval.

5.2.5. Analyses of Proposed OL-FCC Algorithm

The proposed OL-FCC algorithm monitors all charging events by continually updating the vehicle statistics (e.g., locations and priorities of all vehicles, and the corresponding times for their plug-in/out times) and resorting their orders in the queue table at the beginning of each time interval.

- However, since OL-FCC is online, there are no information on the numbers and plug-in times of the vehicle in the upcoming (next) time intervals. This makes the online PEV battery charging quite complicated.

- Therefore, OL-FCC is designed to use time-dependent maximum demand weighting factors $W_D(t)$. The value and the slop of $W_D(t)$ in the fuzzy membership functions of Eq. 5.4 and Fig. 5.5(c) are deliberately changed with time as shown in Fig. 5.5(d).

- Furthermore, OL-FCS will assign larger W_D values to red zone PEV battery charging (e.g., $W_D = 0.96$ to 0.98) as compared with blue zone (e.g., $W_D = 0.75$ to 0.85) and green zone PEV battery charging (e.g., $W_D = 0.50$ to 0.75).

- Finally, the slop of W_D is increased as Δt approaches early morning hours (Fig. 5.5(d)) to assure (or increase the possibility of) full charge of the vehicle batteries by the designated time of 0600h. That is the positive slope of $W_D(t)$ is very sharp for green zone charging (e.g., (0.75-0.50) / (0600h-0200h) = 0.625) and flattens for blue zone charging (e.g., (0.85-0.75) / (0200h-2200h)= 0.025) and red zone charging (e.g., (0.98-0.96) / (2200h-1800h) = 0.005).

At each $t = \Delta t$, OL-FCC algorithm will use the recorded and/or calculated data to either start charging of a vehicle or defer it to next time interval. The decision will depend on:

1) The vehicle priority group. The high-priority consumers who are willing to pay high-tariff for quick PEV battery charging in the red zone will be attended first, followed by the medium-priority and low-priority consumers.

2) The vehicle ranking/location in the queue table (Eq. 4.19 and Table 4.1).

3) The vehicle combined fuzzy membership value (Eq. 5.5) and its corresponding defuzzified (crisp) value $S_{PEV,j}$ calculated by Eq. 5.6.

Therefore, at each time interval Δt, all PEVs with the crisp value of $S_{PEV,j} \geq \alpha$ will be allowed to start charging while the charging of the vehicles with $S_{PEV,j} < \alpha$ will be postponed to the next time interval. Obviously, the postponing of a PEV battery charging is due to one (or all) of the following anticipated issues (based on the fuzzy reasoning associated with by membership functions; Figs. 5.5):

- ☒ Voltage violation.

- ☒ Maximum demand volition.

- ☒ High system losses due to PEV battery charging.

5.2.6. The OL-FCC Flow Chart

The OL-FCC algorithm of this chapter minimizes/optimizes the cost of energy required for PEV battery charging with the consideration of network operation constraints (Eqs.4.16-4.18). This is done by: i) ranking PEVs considering the MSS sensitivity vector (Eq. 4.19) and the consumers' preferences by defining charging time zones of Fig. 4.4, ii) considering real-time load variations, energy pricing, and WDGs outputs (Fig. 4.4-4.5), iii) continuously recording and resorting vehicle statues in the PEV-Queue Table 4.1, and iv) deciding to start (or defer) vehicle battery charging at each time interval $t = \Delta t$ based on vehicle combined fuzzy membership value (Eq. 5.5) and the corresponding defuzzified crisp value (Eq. 5.6).

The flow chart of OL-FCC is shown in Fig. 5.6 [56]. There are four stages associated with each time interval $t = \Delta t = 5$ minutes. Stages 1, 3 and 4 are like the OL-MSSCC of Chapter 4 (Fig. 4.6).

Stage 1 (Updating PEV, WDG, Energy Price and Maximum Demand):

▪ Step 1.1- Update PEV-Queue Table 4.1 according the random arrival (plug-in) and departure (plug-out) of PEVs.

▪ Step 1.2- Update $D_{t,max}$ (Eq. 4.18) based on WDGs output power according to wind information by smart meters.

▪ Step 1.3- Update market energy price based on real-time pricing of Fig. 4.4.

Stage 2 (Online Fuzzy-Based PEV Coordination Scheduling for Time Interval Δt):

▪ Step 2.1- Run Newton-Raphson load flow (Fig. 4.3), calculate cost objective function with constraints (Eqs. 4.16-18), extract MSS vector from Jacobian matrix (Eqs. 4.13 and 4.19), and sort the queue table according to the MSS values (Eq. 4.19).

- Step 2.2 (Fuzzification)- Fuzzify losses and constraints by constructing fuzzy membership functions of Figs. 5.5(a)-(c) considering the time-dependent maximum demand weighting factor of Fig. 5.5(d).

- Step 2.3 (T-Norm & α-Cut Defuzzification to Select Most Suitable PEVs for Charging)

  - Step 2.3.1- Temporary charge the PEV at top of PEV-Queue Table 4.1.

  - Step 2.3.2- Run Newton-Raphson load flow (Fig. 4.3).

  - Step 2.3.3- Calculate membership function values (Eqs. 5.2-5.4).

  - Step 2.3.4- Combine the membership function values using the additive t-norm approach (Eq. 5.5).

  - Step 2.3.5- Defuzzify the combine membership function value using α-cut to calculate its crisp value S_{PEV} (Eq. 5.6).

Step 2.4 (Check Suitability of PEV for Charging)- For each vehicle check the crisp value of $S_{PEV,j}$ to decide on whether to permanently charge it or defer its charging to the next time interval.

Step 2.5- Repeat Steps 2.1 to 2.4 for all high- medium- and low-priority PEVs.

Stage 3 (Updating Daily Load Curve):

- Step 3.1- Update the daily load curve by including the scheduled PEVs.

Stage 4 (Go to Next Time Interval Δt and Repeat):

- Step 4.1- If $t = 24$ hours, then stop.

- Step 4.2- Otherwise, repeat Stages 1-3 for the next time interval Δt.

The flowchart contains the following text elements:

Input network, PEV and DG parameters. Initialize variables

Stage 1: Updating
Update Statuses of PEVs and WDGs, Resort PEV-Queue Table

- ✓ Check for random plug-in and plug-out of PEVs.
- ✓ Update PEV-Queue Table (Table 4.1).
- ✓ Update statuses of all WDGs based on wind speeds and/or output powers.
- ✓ Update maximum allowed demand level $D_{t,max}$ (Eq. 4.18) based on the output powers of WDGs.
- ✓ Update the market energy price.

Stage 2: Fuzzy PEV Charging Coordination
Calculate Objective Function, Fuzzify Constraints, Use Fuzzy Membership Functions, T-Norm & α-Cut to Select Most Suitable PEVs for Charging

- ✓ Run Newton-Raphson load flow (Fig. 4.3 and Eqs. 4.9-4.15).
- ✓ Calculate cost objective function and constraints (Eqs. 4.16-4.18).
- ✓ Extract MSS vector (Eq. 4.19) from the Jacobian Matrix (Eq. 4.13).
- ✓ Sort PEV-Queue Table (Table 4.1) according to the MSS vector.
- ✓ Keep high-priority (red) PEVs on top of PEV-Queue Table followed by medium-priority (blue) PEVs, and low-priority (green) PEVs.

Fuzzify losses and constraints by constructing membership functions (Figs. 5.5(a)-(d)).

Temporarily schedule the PEV at top of PEV-Queue Table for charging.

- ✓ Run Newton-Raphson load flow (Fig. 4.3 and Eqs. 4.9-4.15).
- ✓ Calculate membership function values (Eqs. 5.2-5.4).
- ✓ Use additive t-norm to combine membership function values (Eq. 5.5).
- ✓ Defuzzify using α-cut (Eq. 5.6) to calculate S_{PEV}.

Is $S_{PEV} \geq \alpha$ (Eq. 5.6)? — no → Postpone PEV charging until next Δt.

yes ↓

✓ **Permanently schedule PEV for charging.**

Select next PEV from PEV-Queue Table.

More PEVs within selected priority group? — yes

Select next priority group. — yes ← More priority group?

no

Stage 3
Update Daily Load Curve

Update and save daily load curve, losses, total cost, voltage deviations, transformer and line loadings according to the PEVs being charged at this time interval.

Select next time interval Δt. — yes ← More time intervals Δt? — no → **Save data & stop.**

Stage 4: Repeat for Next Time Interval
Repeat Stages 1-3 for the Next Time Interval ($\Delta t = 5$ Minutes) within the Scheduling Time Horizon of 24 Hours

Fig. 5.6. Flow chart of the proposed OL-FCC algorithm [56]. The algorithm is based on the load flow solution of Eqs. 4.1-4.15, the MSS PEV battery charging coordination of Eqs. 4.16-4.20 and the Fuzzy reasoning of Eqs. 5.2-5.6.

5.3. Simulation Results of OL-FCC of PEVs without WDGs

The same 449-bus smart power grid test system that is used in Chapter 4 (Fig. 4.7) is also utilized in this chapter (Fig. 5.7) to compare the performance of the proposed OL-FCC [56] with the OL-MSSCC of Chapter 4 [55] without and with the three WDGs. The load, PEV and line parameters are presented in Tables 4.3 to 4.4. The WDG active power characteristics are presented in Fig. 4.5 which is based on the scaled down actual

recordings from the Walkway wind farm in Western Australia on July 7, 2012.

Eight case studies are investigated (Table 5.1; Cases A-H). Simulation results with time interval of $\Delta t = 5$min for PEV injection levels of 16%, 32%, 47% and 63% without and with the three WDGs are presented in Figs. 5.8-5.15 and Tables 5.2-5.3.

(a)

(b)
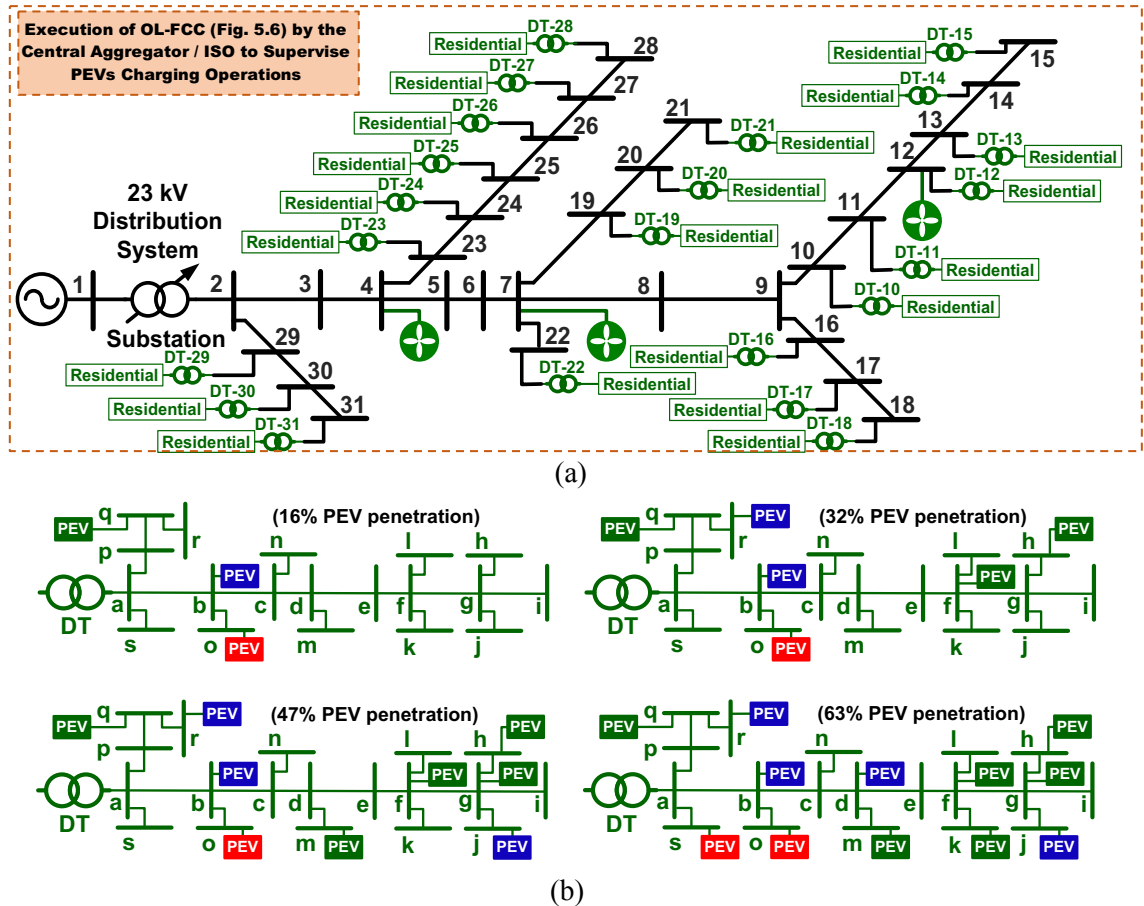
Fig. 5.7 (Same as Fig. 4.7). The 449-bus smart power grid comprising of the IEEE 31-bus high-voltage 23 kV distribution network [129] joint with three WDGs (at buses 4, 7 and 12) and twenty two low-voltage 415 V residential feeders; (a) system one-line diagram, (b) One of the residential feeders with PEV injections of 3/19≈16%, 6/19≈32%, 9/19≈47% and 12/19≈63% highlighting the high (red color), medium (blue color) and low (green color) priority consumers/PEVs [55], [63].

Table 5.1. PEV battery charging scenarios for the online MSS-based (OL-MSSCC) and Fuzzy-based (OL-FCC) PEV coordinated battery charging of the 449-bus SG system in Fig. 5.7 with three WDGs (Fig. 4.5) considering the three designated battery charging time zones, the energy pricing and the residential daily load curve of Fig. 4.4 (based on Table I of [56]).

Case	Battery Charging Coordination Method	Results
A	PEV battery charging without coordination	Fig. 4.8 and Table 5.2
B	PEV battery charging with OL-MSSCC coordination (Fig. 4.6) without WDGs	Fig. 5.8 and Table 5.2
C	PEV battery charging with OL-FCC coordination (Fig. 5.6) without WDGs	Figs. 5.9-5.10 and Table 5.2
D	OL-MSSCC with WDGs (wind power injection $= 3\times5\%=15\%$)	Fig. 5.11(a) and Table 5.2
E	OL-FCC with WDGs (wind DG power injection $= 3\times5\%=15\%$)	Fig. 5.11(b) and Table 5.2
F	OL-FCC: Investigating effects of peak wind generation time	Fig. 5.12
G	OL-FCC: Investigating effects of wind injection level	Fig. 5.13and Table 5.3
H	OL-FCC: Investigating effects of wind location	Fig. 5.14

5.3.1. PEV Battery Charging without Coordination (Case A)

This case study is the same as Case A in Section 4.6.1 (Fig. 4.8 and Tables 4.6). For comparison, simulation results are presented again in Table 5.2 (rows 4-8). As mentioned in Chapter 4, uncoordinated PEV battery charging is very convenient for the consumers as they can start charging their vehicles as soon as it is plugged. However, it can result in significant increases in voltage deviations, power generation, power losses, power demand, and total cost. According to Table 5.2, even for the very low PEV injection of 16%, the total cost is increased by 31% (Table 5.2; row 5, column 6).

5.3.2. PEV Battery Charging with OL-MSSCC Coordination (Case B)

The PEV coordination/management methodology of Chapter 4 is used and the simulation results are summarized in Fig. 5.8 and rows 9-13 of Table 5.2. As expected, and observed in Chapter 4, there are significant improvements compared with the uncoordinated battery charging of Case A. All voltage deviations even at extremely high PEV injection of 63% are within the permitted range of 10%. There are considerable cost savings. For example, the increase in total cost for PEV injections of 47% has dropped from 50.19% (Case A) to 12.44% (Case B).

5.3.3. PEV Battery Charging with OL-FCC Coordination (Case C)

The OL-FCC algorithm of this chapter (Fig. 5.6) is applied to the network of Fig. 5.7 without the WDGs. The results are presented in Figs. 5.9-5.10 and Table 5.2 (rows 14-18). Comparisons of Figs. 4.8 and 5.8-5.10 reveals significant improvements in the network operation and performance compared with both uncoordinated (Case A) and OL-MSSCC coordinated (Case B) PEV battery charging:

✓ As expected, the proposed OL-FCC provides significant improvements compared with uncoordinated battery charging of Case A in terms of maximum demand and voltage regulation and as well as system losses and total cost.

✓ Both coordination methods keep the maximum demand levels and the bus voltage magnitudes within the designated allowable limits at all PEV injection levels.

✓ Unlike the OL-MSSCC algorithm of Chapter 4, the proposed OL-FCC of this Chapter permits small violations of the voltage constraint (according the functions of Fig. 5.5(a)) and small violations of the maximum demand/constraint (based on Fig. 5.5(c)). This is done to allow more PEV battery charging and improve the chances of full charging for all vehicles before 0600h. For example, there are minor voltage violations from 2315h to 2345h for PEV injection of 47% (Fig. 5.9(b)). There are also minor maximum demand violations around 2100h and 2000h as shown in Fig. 5.10(a) and Fig. 5.10(b), respectively.

✓ Unlike OL-MSSCC algorithm that charges the medium-priory (blue) and the low-priority (green) vehicles as soon as possible, the proposed OL-FCC intentionally postpones their services to later hours and charges them with lower energy prices. This is done according to the time-dependent maximum demand weighting factors $W_D(t)$ of Fig. 5.5(d). For example, for the PEV injection of 63%, OL-MSSCC starts charging the medium-priory (blue) and low-priority (green) vehicles at 2100h and 2300h (Fig. 5.8(a)) while OL-FCC postpones their services to 2215h and 0100h (Fig. 5.9(a)), respectively.

✓ As a result of postponing medium- and low-priority PEV battery charging according to the fuzzy membership functions of Fig. 5.5, OL-FCC can decrease the total cost as demonstrated in Table 5.2 (see the cost statistics in the last column). For instance, at PEV injection of 63%, the percentage increase of total cost (Table 5.2, column 6; rows 8, 13 and 18) is improved from 59 percent (for battery charging without coordination)

123

and 15.2 percent (for battery charging with OL-MSSCC coordination) to 12.7 percent (for battery charging with OL-FCC coordination).

Fig. 5.8. Simulation results for Case B: Coordinated (OL-MSSCC) PEV battery charging in Fig. 5.7 without WDGs; (a) System power demand for 63% injection of PEVs, (b)-(c) Voltage deviation at worst bus and total system losses (Tables 5.1 and 5.2) [56].
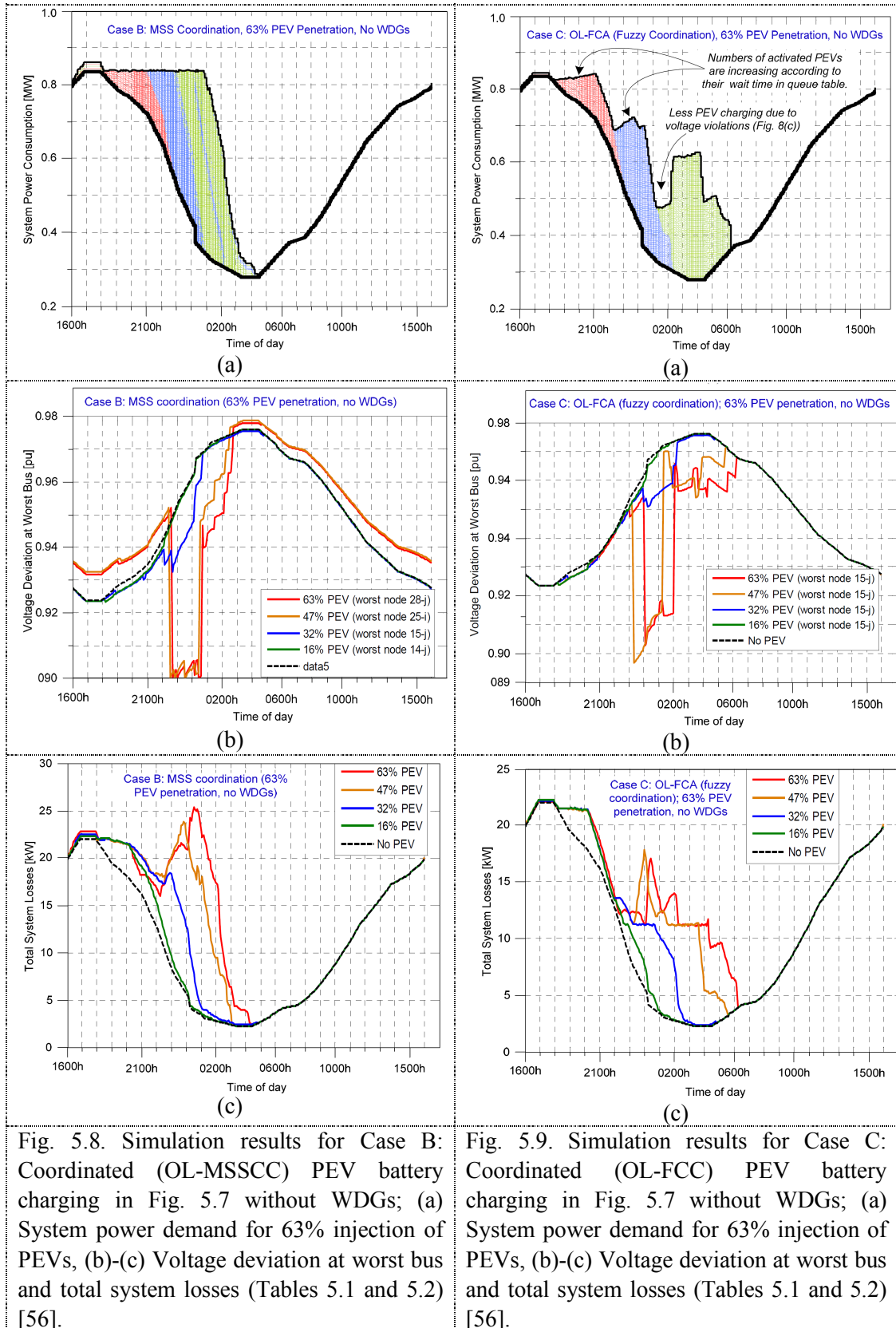
Fig. 5.9. Simulation results for Case C: Coordinated (OL-FCC) PEV battery charging in Fig. 5.7 without WDGs; (a) System power demand for 63% injection of PEVs, (b)-(c) Voltage deviation at worst bus and total system losses (Tables 5.1 and 5.2) [56].
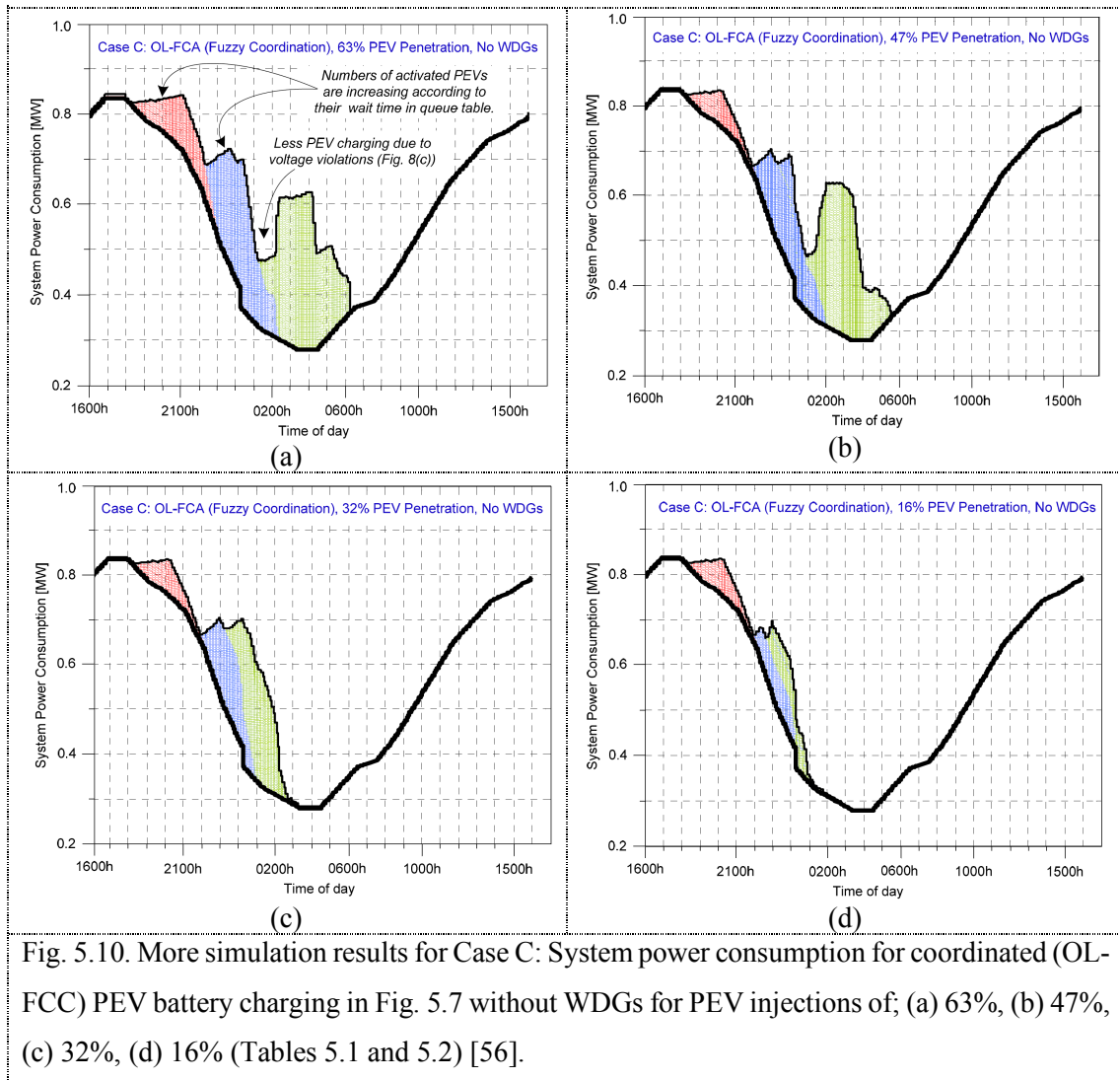
Fig. 5.10. More simulation results for Case C: System power consumption for coordinated (OL-FCC) PEV battery charging in Fig. 5.7 without WDGs for PEV injections of; (a) 63%, (b) 47%, (c) 32%, (d) 16% (Tables 5.1 and 5.2) [56].

5.4. Simulations of PEV Battery Charging with OL-FCC Coordination and WDGs

This section investigates the impacts of WDGs injection levels, locations and peak generation times (Table 5.1, Cases D-H) on the operation of the 449-bus network of Fig. 5.7 with the proposed OL-FCC PEV coordination strategy.

5.4.1. Fuzzy and MSS-Based PEV Charging Coordination with WDGs (Cases D-E)

Both the proposed OL-MSSCC (of Chapter 4) and the proposed OL-FCC (of this chapter) are able to accommodate wind energy by simulating them as PQ buses that inject power into the network. The amount, time and period of the injected power will depend on the wind status which is updated at each time interval of OL-MSSCC and OL-FCC. To

demonstrate the possibility of wind energy resources participations and their pollution-free contributions to PEV battery charging:

1) Three WDGs (with peak output power of 50kW at 6pm, Fig. 4.5) are connected at buses 4, 7 and 12 as shown in Fig. 4.7. This will represent a total wind injection of $3 \times 5\% = 15\%$.

2) Detailed simulation are performed with both OL-MSSCC (proposed in Chapter 4) and OL-FCC (proposed in this Chapter) coordination approaches for 63% PEV injection and the corresponding system power consumptions are plotted in Fig. 5.11(a) and Fig. 5.11(b), respectively. These results are also presented in Table 5.2 (rows 19-28).

Inspection of Table 5.2 (rows 19-28) and comparisons of Fig. 5.11(a) and Fig. 5.11(b) reveals the advantages and limitations of OL-FCC compared with OL-MSSCC:

✓ The presence of WDGs will further improve the overall system performance at all PEV injection levels by the decreasing total cost, lowering losses, and reducing voltage deviations.

✓ The OL-MSSCC strategy makes use of the entire accessible WDG power to charge as many vehicles as possible. This is particularly appreciated during the peak hours of load as well as the late evening hours (Fig. 5.11(a), 1700h-2200h). However, the problem with this easy sensitivity based battery charging approach (e.g., proving charging service to all consumers including the medium-priority (blue) and low-priority (green) vehicles in early evening hours) is the possibility of not being able to provide full service to vehicles with high priority that may be plugged within the next few time intervals.

✓ Consequently, the proposed OL-FCC strategy prefers to use the available WDG power during peak hours to strictly charge the high-priority vehicles as demonstrated in Fig. 5.11(b) for the period of 1700h to 2000h. In this way, OL-FCC will also reduce transform loading and may even prevent its overloading during peak (see Fig. 5.12). This is done through the designed time-dependent maximum demand weighting factors of Fig. 5.5(d). For instance, at PEV injection of 16%, OL-FCC quickly charges all high-priority (red) vehicles as they are being randomly plugged-in within 1630h-2100h while the charging of the medium-priority (blue) and low-priority (green) vehicles are done within 2200h-0200h and 0100h-0600h, respectively (Fig. 5.11(b)).

This is justified since high-priority consumers are seeking quick services and willing to pay high-tariff energy prices.
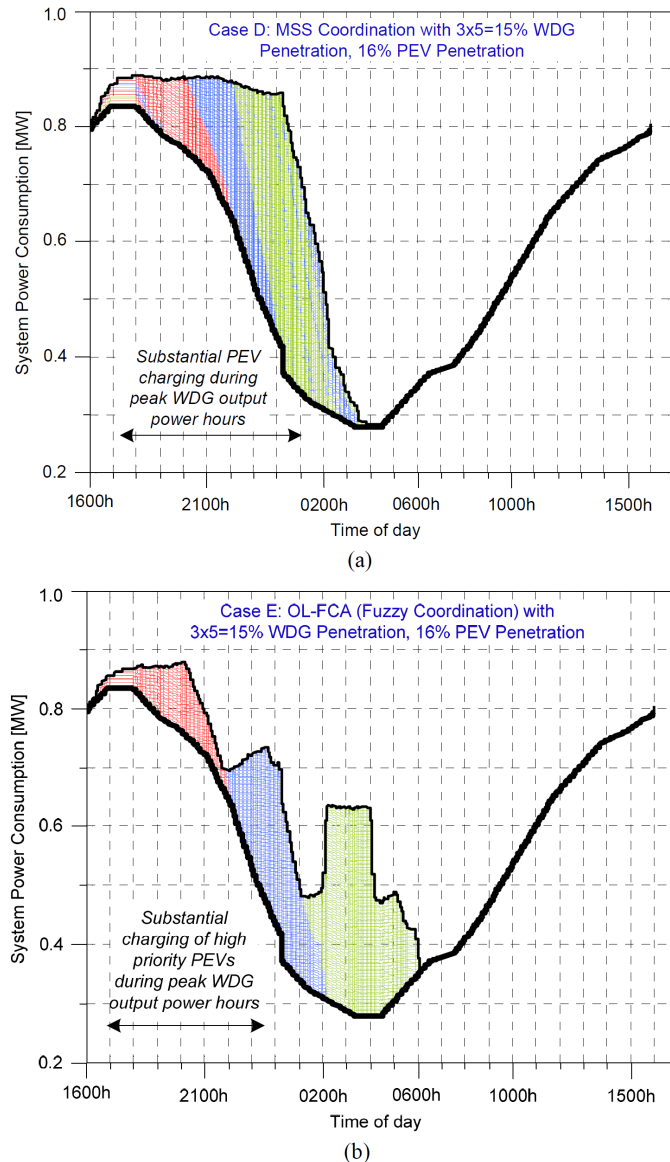
Fig. 5.11. Comparison of simulation results for Cases D-E: System power consumption of Fig. 5.7 with the total WDG injection of 3×5=15%; (a) Case D with the OL-MSSCC coordination of Chapter 4 [55], (b) Case E with the OL-FCC coordination of this Chapter [56].

5.4.2. Effects of Peak Wind Generation Time on OL-FCC (Case F)

WDGs have the potential to decrease total losses and total cost of smart power grid networks as well as the reducing transformer loading. However, the time and duration of wind power generation resources will randomly change within the selected charging planning time horizon of 24 hours. In most practical cases, the peak wind generation times

will not coincide with the peaks of residential and/or PEV-charging loads as illustrated in Figs. 4.4 and 4.5. To explain the impacts of peak wind generation time on the performance of OL-FCC algorithm, we have repeated Case C, but shifted the wind peak generation time from 6pm (1800 h) to i) 8pm (2000 h), ii) 10pm (2200 h) and, iii) 12pm (2400 h). Fig. 5.12 compares these simulations results. As expected, we see more reduction in transformer loading for wind peak times during early evening hours (e.g., 0600-0800h) due to more sustainable PEV battery charging activities.

5.4.3. Effects of Wind Injection Level on OL-FCC (Case G)

The impacts of total WDG injection on the distribution transformer loading are explored and the results are presented in Fig. 5.13. Six scenarios with total wind power injections of 5, 15, 10, 20, 30, and 40 percentages and PEV injection of 63% are investigated. Simulation results with OL-FCC coordination are also summarized in Table 5.3. As expected, there are substantial reductions in system losses, generation cost and particularly transformer loading as the wind injection is increased from 5% to 40%. According to Fig. 5.13:

✓ During the early peak evening hours (1600h-1800h), the distribution transformer loading in reduced from 0.85 MW (without WDGs) to 0.75 MW (with wind injection of 20%), to 0.68 MW (with wind injection of 30%), and to 0.62 MW (with wind injection of 40%). This indicates significant distribution transformer loading reductions of (0.85 - 0.75) / 0.85 = 11.8% (with wind injection of 20%), (0.85 - 0.68) / 0.85 = 20% (with wind injection of 30%), and (0.85 - 0.62) / 0.85 = 27% (with wind injection of 40%).

✓ There are no reduction in transformer loadings 1800h-1900h since the WDG output slightly deceased (Fig. 4.5) and the OL-FCC is starting to slowly charge the high-priority (red) vehicles (see Fig. 5.9(a)).

✓ During the late evening hours around 2100h, the distribution transformer loading in reduced from 0.85 MW (without WDGs) to 0.7 MW (with wind injection of 20%), to 0.63 MW (with wind injection of 30%), and to 0.58 MW (with wind injection of 40%). This indicates significant distribution transformer loading reductions of (0.85 - 0.7) / 0.85 = 17.6% (with wind injection of 20%), (0.85 - 0.63) / 0.85 = 25.9% (with wind injection of 30%), and (0.85 - 0.58) / 0.85 = 31.8% (with wind injection of 40%).

✓ Around 0600h with WDG injection of 40%, there is reverse power flow (the extra wind power is being exported to the main utility grid at bus 1 and the distribution transformer loading is negative (-0.1MW). This fortunate situation is due to high wind injection and no PEV battery charging activities providing the opportunity to the microgrid of Fig. 5.7 to export its extra green power generation to the main utility grid.
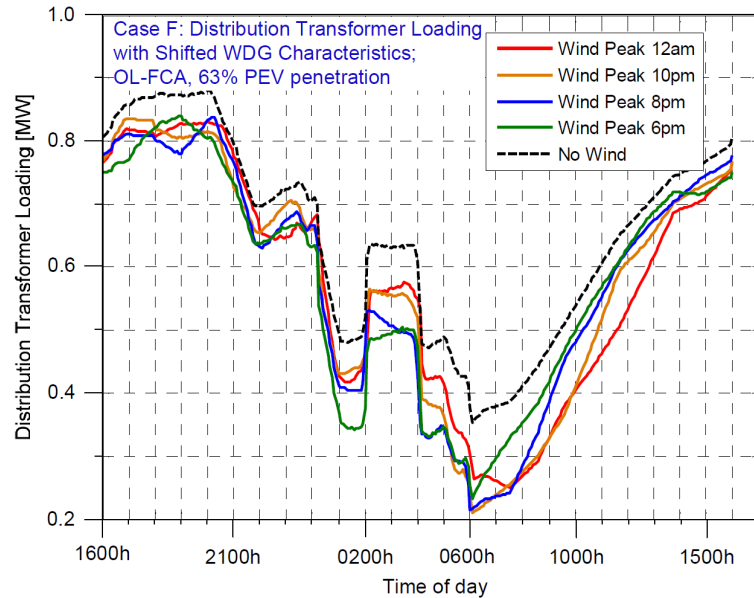

Fig. 5.12. Case F: Effects of peak wind generation on the loading of distribution transformer (OL-FCC battery charging coordination with 63% PEV injection) [56].
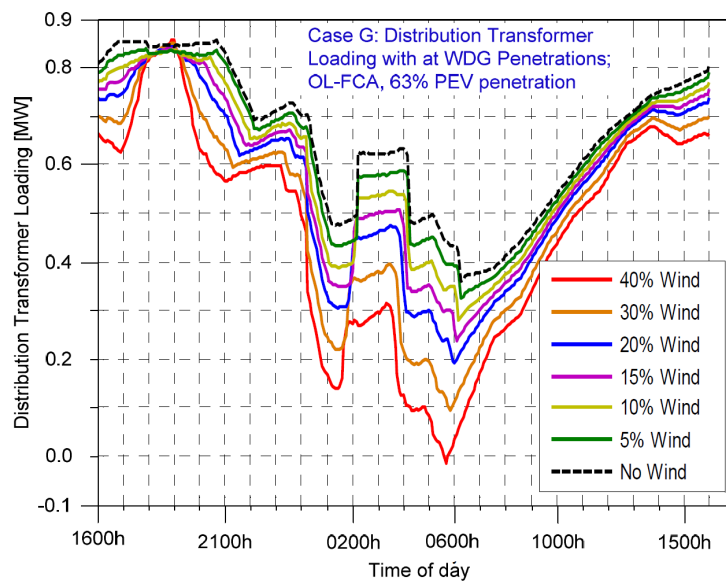
Fig. 5.13. Case G: Effects of wind injection level on the loading of distribution transformer (OL-FCC charging coordination with 63% PEV injection and peak wind generation at 6pm) [56].

129

5.4.4. Effects of Wind Location on OL-FCC (Case H)

To explore the effects of wind location on the operation of Fig. 5.7 with OL-FCC of PEVs, a 21kW WDG unit is sequentially attached at each bus. Fig. 5.14 illustrates the corresponding total system/network losses for the PEV injection of 63%. Bases on the information in Fig. 5.14, the most beneficial areas for the installation of WDGs are at the ends of the HV lines, near residential feeders and close to the charging stations. The best buses for the placement of WDGs in the order of preference are: i) buses 10-15, ii) buses 6-8, iii) buses 16-18, iv) buses 20-21, and v) buses 24-28.
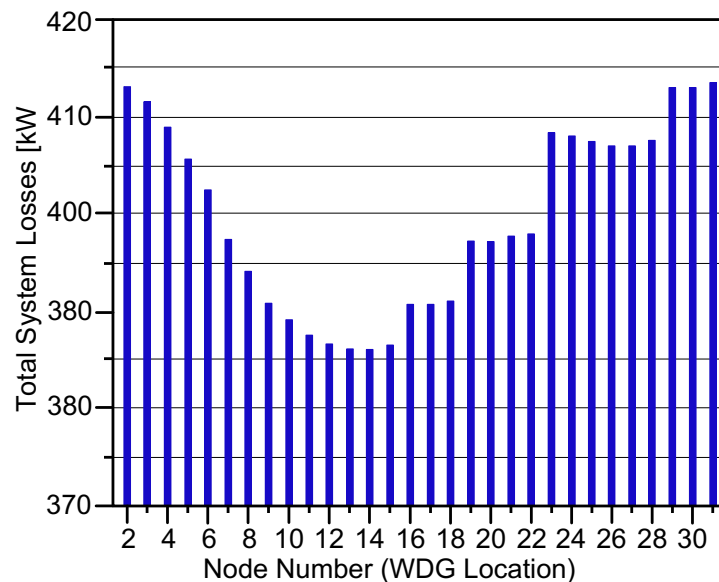

Fig. 5.14. Case G: Effects of wind location on total losses (OL-FCC battery charging coordination with 63% PEV injection and one 21kW wind unit connected at different buses) [56].

Table 5.2. Detailed simulation results for the impact of uncoordinated PEV battery charging and coordinated PEV battery charging (with the OL-MSSCC of Chapter 4 [55] and the proposed OL-FCC of this chapter [56]) on the network of Fig. 5.7 without and with WDGs. For comparison, the same Gaussian function is used to generate Gauss random PEV distributions and Gauss random PEV plug-in times. For nominal operation without any PEVs or WDGs, the values for "|ΔV|", "Imax", "Generation Cost" and "Total Cost" are 7.646%, 0.147%, 770.3 \$/day and 786.2 \$/day, respectively.

PEV (%)	|ΔV| (%)	Imax (%)	Cost of Generation (\$/day) / (%)*	Total Network Cost (see Eq. 4.16) (\$/day) / (%)*
Case A: Uncoordinated PEV without WDGs; Fig. 4.8				
63	17.60	0.307	958/24.4	1,250/59.0
47	16.20	0.263	916/18.9	1,180/50.0
32	9.050	0.218	871/13.07	1,090/38.6
16	7.690	0.179	829/7.62	1,030/31.0
Case B: OL-MSSCC Coordination [55] without WDGs; Fig. 5.8				
63	10.00	0.172	886/15.02	906/15.24
47	10.00	0.163	865/12.29	884/12.44
32	7.66	0.167	841/9.17	858/9.12
16	7.67	0.161	808/4,89	825/4.93
Case C: OL-FCC Coordination [56] without WDGs; Figs. 5.9 and 5.10				
63	9.72	0.159	866/15.02	886/12.70
47	10.32	0.160	842/9.30	861/9.51
32	7.65	0.158	828/7.49	845/7.48
16	7.65	0.159	805/4.50	821/4.42
Case D: OL-MSSCC Coordination with (15% injection) WDGs; Fig. 5.11(a)				
63	10.00	0.182	805/4.5	825/4.93
47	10.00	0.189	782/1.51	801/1.88
32	7.83	0.178	754/-2.11	771/-1.91
16	7.66	0.177	717/-6.91	733/-6.76
Case E: OL-FCC Coordination with WDGs (15% injection); Fig. 5.11(b)				
63	9.78	0.172	778/0.99	797/1.37
47	10.04	0.160	753/-2.22	771/-1.93
32	7.78	0.160	738/-4.19	755/-3.97
16	7.65	0.160	714/-7.30	730/-7.14

*) Increase or decrease in daily cost (excluding renewable energy cost) in percentage of the nominal cost without any PEVs or WDGs.

Table 5.3. Detailed simulation results for Case G: Effects of WDG injection on the network of Fig. 5.7 with 63% PEV injection and OL-FCC battery charging coordination. For nominal operation without any PEVs or WDGs, the values for "|ΔV|", "Imax", "Generation Cost" and "Total Cost" are 7.646%, 0.147%, 770.3 $/day and 786.2 $/day, respectively.

WDG (%)	$\|\Delta V\|$ (%)	Cost of Generation ($/day) / (%)*	Total Network Cost (see Eq. 4.16) ($/day) / (%)*	Total Network Power Loss (MW/day)
40	10.05	639/-17.04	658/-16.3	0.2012
30	9.96	696/-9.64	715/-9.05	0.2031
20	9.87	753/-2.24	772/-1.81	0.2053
15	9.78	781/1.39	801/1.88	0.2065
10	9.74	808/4.89	827/5.19	0.2078
5	9.70	838/8.79	858/9.13	0.2093

*) Increase or decrease in daily cost (excluding renewable energy cost) in percentage of the nominal cost without any PEVs or WDGs.

5.4.5. Power Consumption of OL-FCC without and with WDGs Considering

To further investigate the impacts of WDGs on the outcomes and performance of the proposed OL-FCC algorithm, the power consumptions (daily load curve with PEV coordination) of the 449-bus SG network are plotted and compared for two additional operating conditions with three and two consumer groups without and with WDGs.

A. OL-FCC Power Consumption with Three Consumer Priority Groups and WDGs

The total power consumptions of the 449-bus SG network with the proposed fuzzy-based PEV coordination are plotted and compared in Fig. 5.15 without and with the three WDGs. Three types of consumer groups including high-priority (red), medium-priority (blue) and low-priority (green) customers are considered. Comparisons of the power consumption plots in Fig. 5.15(a),(c),(e),(g) and Fig. 5.15(b),(d),(f),(h) indicates that:

- The presence of WDGs improves the performance of OL-FCC coordination in providing faster services to more PEVs. The level of improvement depends on the times and durations of the peak wind power generations. The improvements are noted at all vehicle injections, particularly for the high PEV injections of 63% and 47%.

- For PEV injection of 63% without WDGs (Fig. 5.15(a)), the charging process does not essentially start until 1830h due to the maximum power demand restriction of 0.83 MW. This will reduce the maximum number of high-priority consumers that can be

132

attended within the red charging time zone. It will also delay the charging of medium-priority and low-priority consumers to early morning hours.

- However, the addition of the three WDGs (Fig. 5.15(b)) provides the opportunity to charge most of the high-priority PEVs during early evening hours around 1800h-2100h without overloading the network. It has also accelerated the service to medium-priority and low-priority consumers.

B. OL-FCC Power Consumption with Two Consumer Priority Groups and WDGs

The pervious scenario is repeated with only high-priority (red) and low-priority (green) customers. The network power consumptions without and with WDGs are plotted and compared in Fig. 5.16. Note that:

- The proposed OL-FCC strategy can successfully perform PEV coordination with any number of consumer groups. All PEVs are fully charged by 0600h for operating conditions with three consumer groups (Fig. 5.15(a),(c),(e),(g)) and two consumer groups (Fig. 5.16(a),(c),(e),(g)).
- The addition of WDGs will further improve the OL-FCC performance (Fig. 5.16(b),(d),(f),(h)). It has provided the opportunity to charge more high-priority PEVs at early evening hours without overloading the network and accelerate the service to the low-priority PEVs.
- The absence of medium-priority group (Fig. 5.16), will not impact the service to the high-priority consumers, but will improve the quality of service to the low-priority PEVs without and with WDGs.

(a) PEV of 63% without WDGs   (b) PEV of 63% with WDGs

(c) PEV of 47% without WDGs   (d) PEV of 47% with WDGs

(e) PEV of 32% without WDGs   (f) PEV of 32% with WDGs

(e) PEV of 16% without WDGs   (f) PEV of 16% with WDGs

Fig. 5.15. The power consumption of the 449-bus SG (Fig. 5.7) with high (red)-, medium (blue)- and low (green)-priority consumers and the proposed OL-FCC strategy for PEV injections of 63%, 47%, 32% and 16% without and with the three WDGs.

134

(a) PEV of 63% without WDGs

(b) PEV of 63% with WDGs

(c) PEV of 47% without WDGs

(d) PEV of 47% with WDGs

(e) PEV of 32% without WDGs

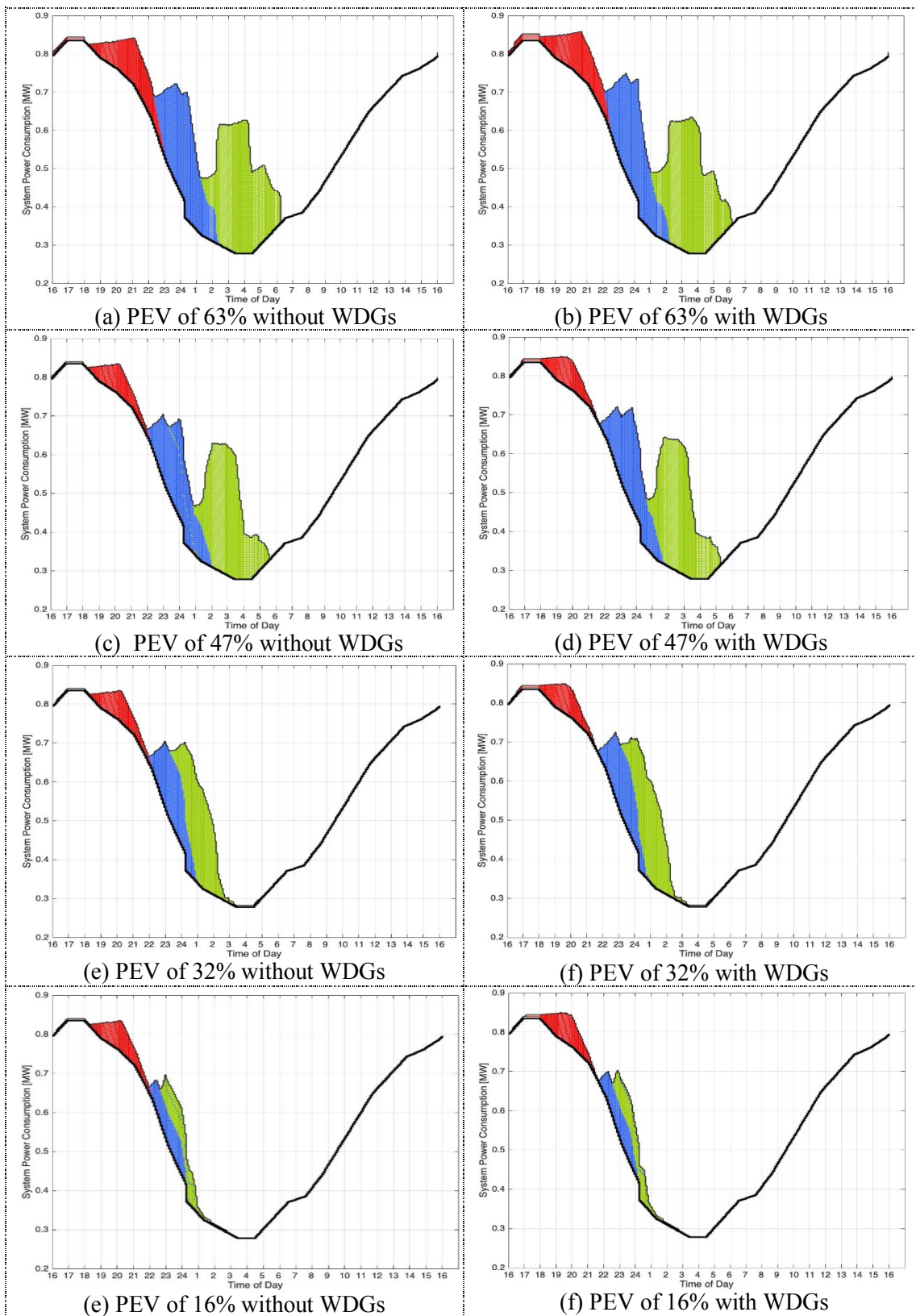(f) PEV of 32% with WDGs

(e) PEV of 16% without WDGs

(f) PEV of 16% with WDGs
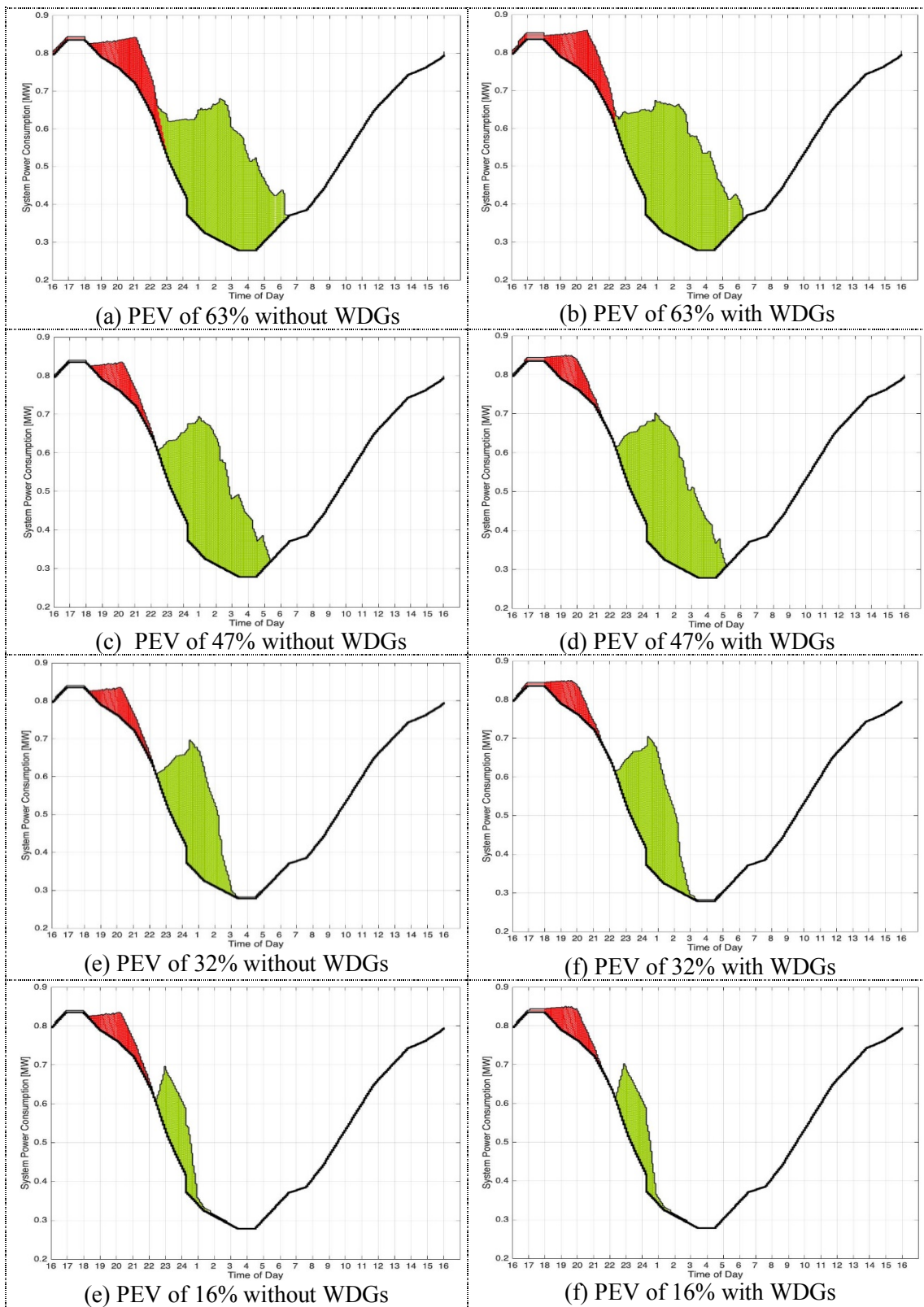
Fig. 5.16. Power consumption of the 449-bus SG (Fig. 5.7) with high (red)- and low (green)-priority consumers and the proposed OL-FCC strategy for PEV injections of 63%, 47%, 32% and 16% without and with the three WDGs.

135

5.5. Conclusion

A practical and fast online fuzzy coordinated battery charging coordination (OL-FCC) strategy for PEVs is proposed and implemented in this chapter which is based on MSS and fuzzy reasoning. The algorithm is implemented and tested on a 449-bus 23 kV smart power grid system with three WDGs and 22 low voltage residential networks that are populated with PEVs. For comparison, the same Gaussian function is used to generate random PEV distributions and random PEV plug-in times. Comprehensive simulations are performed for four levels of PEV injections and three customer priority types. Simulation results of Tables 5.2-5.3 and Figs. 5.9-5.14 indicate the following points, advantages, and capabilities of the proposed OL-FCC algorithm for PEVs in smart power grids:

- As with the OL-MSSCC of Chapter 4, the proposed OL-FCC also considers three customer battery charging time zones which are designed based on the client priorities. It also regulates voltage magnitudes of all buses and limits the network peak demand to enhance the economy and efficiency the network by lowering the costs of energy generation and losses.

- However, compared to the OL-MSSCC of Chapter 4, the proposed OL-FCC of this chapter offers further improvements in terms of total system loss and total cost reduction as it relies on fuzzy reasoning and fuzzy membership functions (Fig. 5.5) to: i) provide quick service to the high-priority consumers and charge their vehicles during early evening hours, ii) intentionally postpone the services to medium-priority and low-priority consumers to reduce the total cost, iii) dynamically adjust the tolerance of maximum demand level by using time-dependent maximum demand weighting factors (Fig. 5.5(d)) and, iv) allow minor violations in voltage deviation and maximum demand constraints.

- Due to its inherent online monitoring and control nature, the proposed OL-FCC does not necessitate any forms of renewable or EV forecast information. All required information are gathered based on the online smart meter readings.

- The coordination strategy of OL-FCC will intrinsically lower the loadings of the network transformers and consequently lowers the risk of equipment failures.

- The main advantage of OL-FCC compared with OL-MSSCC is the applications of fuzzy theory, fuzzy reasoning and fuzzy membership functions to improve the chances of finding a better-quality solution predominantly at high injections of PEVs. However, for a give network, OL-FCC requires the knowledge of experienced engineers to design and develop suitable fuzzy membership functions.

CHAPTER SIX: DELAYED (OVERNIGHT) MSS-BASED COORDINATED BATTERY CHARGING OF PEVS IN SMART POWER GRID

The third contribution of this Ph.D. thesis is a new centralized delayed (overnight) MSS-based coordinated battery charging (DL-MSSCC) algorithm for PEVs in smart power grid networks which was published by the author during his Ph.D. studies in reference [57]. The methodology is like the OL-MSSCC algorithm of chapter 4. But, instead of aiming to charge the vehicles (particularly the high-priority PEVs) as soon as they are being randomly plugged-in, the services for all consumers will be deferred/delayed to early morning hours. Therefore, unlike the OL-MSSCC of Chapter 4 and the ON-FCC of Chapter 5, the proposed DL-MSSCC of this chapter does not offer any priority options to the PEV owners. In this chapter, the concept, formulation and algorithm of DL-MSSCC are introduced and its performance is compared with the online OL-MSSCC of Chapter 4 and the online OL-FCC of Chapter 5 for the 449 SG network of Fig. 6.3.

This chapter is organized as follows:

- Section 6.1 presents the formulation of the proposed DL-MSSCC algorithm for coordinated overnight charging of PEVs.

- Section 6.2 presents the formulation of DL-MSSCC.

- Section 6.3 presents the formulation of DL-MSSCC.

- Section 6.4 investigates the performance of the proposed DL-MSSCC algorithm by performing detailed simulations for coordination of PEVs in the 449-bus smart power grid network of Fig. 6.3.

- This chapter ends with the conclusions in Section 6.5.

6.1. Concepts of Proposed Delayed PEV Coordinated Battery Charging

In contrast to the online OL-MSSCC and OL-FCC EV coordination ideas of the previous chapters that try to charge vehicle batteries as quickly as possible staring with the high-priority consumers, the proposed delayed DL-MSSCC strategy of this chapter aims to take full advantage of the inexpensive electricity prices during the off-peak (early morning) hours. This is done by postponing the PEV battery charging process until a later time after the peak-load hours. The concepts of DL-MSSCC are like those adopted in Chapter 4 for the OL-MSSCC with the following resemblances and differences:

- **PEV Coordination Strategy of DL-MSSCC-** Unlike the online OL-MSSCC coordination algorithm of Chapter 4, the strategy of DL-MSSCC is offline and the PEV battery charging is deliberately pushed to a later time T_{delay} after the peak-load hours.

- **Planning Time Horizon and Time Interval of DL-MSSCC (Fig. 6.1)-** The scheduling time horizon for PEV coordination is selected to be 24 hours which is like the OL-MSSCC of Chapter 4 (Fig. 4.4). It starts at 1600h for 24 hours and is divided into 24(60 minutes) / (5 minutes) =288 time intervals. Therefore, each time interval of DL-MSSCC is Δt = 5 minutes.

- **Independent System Operator (ISO)-** As with the OL-MSSCC of Chapter 4, the ISO oversees grid operation and executes the centralized but delayed (off-line) EV battery charging coordination based on the DL-MSSCC tactic. This is accomplished as follows: i) PEV charger sends a signal to the ISO upon random plugging, ii) ISO updates the PEV-Queue Table, implements the DL-MSSCC algorithm and sends a signal back to the PEV to start charging, and iii) PEV charger sends a signal back to the ISO upon unplugging or full-charge.

- *Charging Time Zone and Subscription Priority Options of DL-MSSCC (Fig. 6.1)-* Unlike the OL-MSSCC and OL-FCC of Chapters 4-5 that consider three designated battery charging time zones and three chosen consumer priorities, the DL-MSSCC of this chapter is designed to charge all vehicles in only one (green) time zone with low tariff without considering any consumer priorities.

- *PEV-Queue Table of DL-MSSCC (Table 6.1)-* As with the OL-MSSCC, the PEV-Queue Table of DL-MSSCC is also filled and updated on real-time bases (e.g., every 5 minutes) to keep track of all vehicles' statuses. At the beginning of each time interval $t=\Delta t$, the newly plugged-in vehicles are added to the end of the PEV-Queue Table without considering any priorities (reordering).

- *Random PEV Plug-In Times Replicated by Gaussian Distribution-* As with the OL-MSSCC and OL-FCC of Chapters 4-5, the random arrival times of PEVs are generated using Gaussian (Normal) distributions ([55], [63]) with PEV injections of 16%, 32%, 47% and 63%.
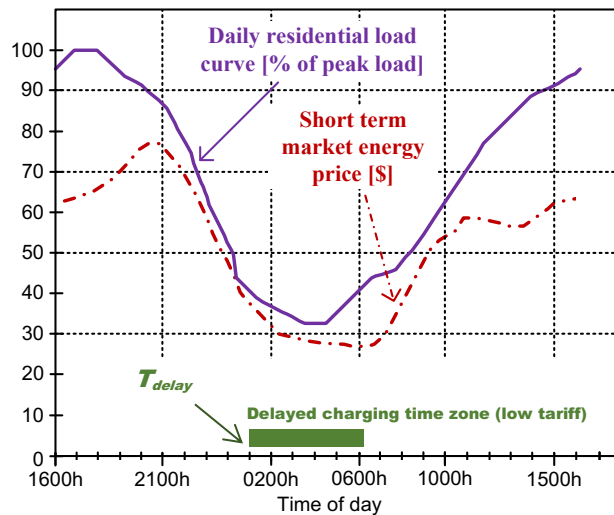

Fig. 6.1. The delayed PEV charging time zone, price of energy and residential daily load curve for the formulation and implementation of the proposed DL-MSSCC algorithm [57].

Table 6.1. An example of the PEV-Queue Table for the DL-MSSCC algorithm showing vehicles waiting to be scheduled for charging. It is similar to Table 4.1 with the exception of allowing for only one charging time zone. The PEVs are added in the table upon random plugging and their order is sorted at each time interval Δt after $t = T_{delay}$ according to the MSS vector of Eq. 4.19.

PEV-Queue Table for Delayed Overnight Coordinated battery charging (DL-MSSCC) of PEVs			
Sorting Scheme	PEV Type	PEV Number in the Queue	PEV Status
According to MSS Sensitivity Vector (Eq. 4.19)	Only one type to be Charged Overnight within the Green Zone of Fig. 6.1	G_1	Charged
		…..	…..
		$G_{charged,max}$	Charged
		$G_{charging,1}$	Charging
		…..	…..
		$G_{charging,max}$	Charging
		$G_{waiting,1}$	Waiting to be scheduled for overnight charging
		…..	…..
		$G_{blue,max}$	Waiting to be scheduled for overnight charging

6.2. Formulation of DL-MSSCC

Formulation of DL-MSSCC is the same as the OL-MSSCC of Chapter 4. Therefore, the previous definitions for the cost objective function (Eq. 4.16), constraints (Eqs. 4.17-4.18) and the sensitivity vector (Eq. 4.19) are also used in the formulation of DL-MSSCC. However, all battery charging activities will begin and terminate at designated times which are not within the peak load periods while the amount of maximum demand for overnight charging ($D_{t,max}$ in Eq. 4.18) is set according to the following estimated value:

$$D_{t,max} = D_{t,max,overnight} = \left(N_{PEV} \times E_{PEV} + E_{load,overnight}\right)/\left(t_{delay} - t_{end}\right) \quad (6.1)$$

In the above equation, t_{delay} and t_{end} are the selected beginning/starting time and terminating/ending time for the overnight EV battery charging, N_{PEV} is the total number of PEVs in the PEV-Queue Table at time $t = t_{delay}$, E_{PEV} is the energy required to charge one PEV, and $E_{load,overnight}$ is the estimated total load energy for the period of delayed charging ($T_{delay} = t_{delay} - t_{end}$) plus the energy required to charge vehicles that are

plugged-in after time $t = t_{delay}$.

For the simulations and analyses of this thesis, the selected values are t_{delay}=2400h, t_{end}=0600h, $T_{delay} = 6$ hours, $E_{load,overnight}$= (0.334 kW/hour)(6 hours)= 2 kW, and E_{PEV}= 8 kW (see Section 4.5.2). For example (Fig. 6.3 and Eq. 6.1):

1) **For the PEV injection of 63%** corresponding to N_{PEV}= (12 PEVs) (22 residential feeders) = 264 PEVs, the estimated value of $D_{t,max}$=$D_{t,max,overnight}$ for delayed/overnight charging is:

$$D_{t,max,overnight} = \frac{(12\ PEVs \times 22\ Feeders) \times 8kW + 0.34MW \times 6}{(1200h - 0600h)} = \frac{[4.152MW]}{6} = 0.692MW.$$

2) **For the PEV injection of 47%** corresponding to N_{PEV}= (9 PEVs) (22 residential feeders) = 198 PEVs, the estimated value of $D_{t,max}$=$D_{t,max,overnight}$ for delayed/overnight charging is:

$$D_{t,max,overnight} = \frac{(9\ PEVs \times 22\ Feeders) \times 8kW + 0.34MW \times 6}{(1200h - 0600h)} = \frac{[3.624MW]}{6} = 0.604MW.$$

3) **For the PEV injection of 32%** corresponding to N_{PEV}= (6 PEVs) (22 residential feeders) = 132 PEVs, the estimated value of $D_{t,max}$=$D_{t,max,overnight}$ for delayed/overnight charging is:

$$D_{t,max,overnight} = \frac{(6\ PEVs \times 22\ Feeders) \times 8kW + 0.34MW \times 6}{(1200h - 0600h)} = \frac{[3.096MW]}{6} = 0.516MW.$$

4) **For the PEV injection of 16%** corresponding to N_{PEV}= (3 PEVs) (22 residential feeders) = 66 PEVs, the estimated value of $D_{t,max}$=$D_{t,max,overnight}$ for delayed/overnight charging is:

$$D_{t,max,overnight} = \frac{(3\ PEVs \times 22\ Feeders) \times 8kW + 0.33MW \times 6}{(1200h - 0600h)} = \frac{[2.568MW]}{6} = 0.428MW.$$

6.3. Flow Chart of Proposed DL-MSSCC

The DL-MSSCC strategy is similar to the OL-MSSCC of Chapter 4 with the following

differences:

- ❖ There are no consumer priority options and there is only one (green) charging time zone.

- ❖ Only the recordings of network information and updating of PEVs status (Table 6.1) are done online while the actual PEV battery charging coordination is delayed until a later time t_{delay} after the peak-load hours.

- ❖ The starting (t_{delay}) and ending (t_{end}) times of coordination are selected by ISO.

- ❖ The maximum demand level for overnight PEV battery charging ($D_{t,max}$ in Eq. 4.18) is estimated using Eq. 6.1.

Fig. 6.2 reveals the overall arrangement of DL-MSSCA which is like the OL-MSSCC of Fig. 4.6 with some modifications required to execute a delayed PEV battery charging tactic. There are four stages associated with each time interval $t = \Delta t = 5$ minutes.

Stage 1- Online Updating of PEV and WDG Status (Fig. 6.2):

- ▪ Step 1.1- Check for random arrival (plug-in) and departure (plug-out) of PEVs.

- ▪ Step 1.2- Update PEV-Queue Table 6.1 according to plug-in and plug-out of PEVs .

- ▪ Step 1.3- Update status of WDGs according to wind information by smart meters.

- ▪ Step 1.5- Update market energy price based on real-time pricing.

- ▪ If $t_{delay} \geq t \geq t_{end}$ go to Stage 3.

Stage 2- Delayed MSS-Based PEV Coordination Scheduling (Fig. 6.2):

- ▪ Step 2.1- Estimate the maximum demand level for delayed overnight PEV battery charging ($D_{t,max}$ in Eq. 4.18) using Eq. 6.1 ($D_{t,max} = D_{t,max,overnight}$).

- ▪ Step 2.2- Run Newton-Raphson load flow of Fig. 4.3.

- ▪ Step 2.3- Excerpt MSS vector (Eq. 4.19) from the Jacobian matrix (Eq. 4.13).

- Step 2.4- Sort the order of EV in the queue table according to the MSS (Eq. 4.19).

- Step 2.5 (Scheduling of Eligible PEVs):

  - Step 2.5.1- Temporary charge the PEV at top of PEV-Queue Table 4.1.

  - Step 2.5.2- If $\sum demands \ll D_{t,max}$, go to Step 2.5.7 (postpone charging this PEV until next Δt since it causes a damned constraint violation according to Eq. 4.18).

  - Step 2.5.3- Run Newton-Raphson load flow of Fig. 4.3.

  - Step 2.5.4- If $|\Delta V| \ll \Delta V_{max}$, go to Step 2.5.7 (postpone charging this PEV until next time interval since it causes a voltage constraint violation based on Eq. 4.17).

  - Step 2.5.5- Schedule the PEV for charging and remove it from PEV-Queue Table 6.1.

  - Step 2.5.7- Go to Step 2.5.1 for scheduling the next eligible PEV.

Stage 3- Updating Daily Load Curve (Fig. 6.2):

- Step 3.1- Update the daily load curve by including the scheduled PEVs.

Stage 4- Go to Next Δt and Repeat (Fig.6.2):

- Step 4.1- If $t = 24$ hours stop; otherwise, repeat Stages 1-3 for the next time interval Δt.

The proposed PEV battery charging coordination algorithms of this Ph.D. thesis including the DL-MSSCC algorithm of this chapter rely on the smart grid communication system for the energy management to make reliable communications between the EV owners and the ISO (central controller or aggregator). As with all centralized PEV coordination schemes, any interruption or loss of communication can have negative impacts on the performance of the proposed algorithms such as:

- Interruptions or loss of communication may cause a single point of failure (SPOF) at the ISO level. A SPOF is referred to a part of the system that, if it fails, will terminate the entire communication system.

- In case of SPOF, the optimal PEV scheduling problem cannot be solved, or the attained solutions will not be accurate due to the lack of PEVs, grid and DGs information. This could potentially collapse the entire EV coordination algorithm.

- Interruptions or loss of communication may also disturb the quality of service to the consumers.

- The severity of disturbance depends on the number and durations of the interruptions. It could cause unexpected delays in charging services for the affected PEVs since their charge requests will not be submitted to ISO on time but postponed to the next time step when the communication system is restored.

The impacts of communication failure on the reliability and expectancy of EV coordination is still an open issue. However, the above-mentioned impacts can be prevented by incorporating backup communication networks and/or alternative communication paths.

The impacts of communication failure and/or interruptions on the performance and resilience of the purposed EV battery charging coordination algorithms are recommended as a potential field for future research work.

The flowchart contains the following text elements:

Top box: Input network, PEV and DG parameters. Select *Tend and Tdelay*. Initialize variables.

Stage 1: Online Updating — Recording PEVs States in PEV-Queue Table and updating statues of WDGs

- ✓ Check for plug-in/plug-out of PEVs.
- ✓ Update PEV-Queue Table (Table 6.1).
- ✓ Update statuses of all WDGs based on wind speeds and/or output powers.
- ✓ Update market energy price (Fig. 6.1).

Tend ≥ t ≥ Tdelay ? — no (no PEV charging) / yes (offline/delayed/overnigh PEV charging)

Stage 2: Dalyed PEV Charging Coordination — Perform MSS-Based PEV Charging Coordination and Checking the Objective Function and Constraints

Estimate $D_{t,max,overnight}$ (Eq. 6.1) for delayed/overnight PEV charging.

- ✓ Run Newton-Raphson load flow (Fig. 4.3 and Eqs. 4.9-4.15).
- ✓ Calculate cost objective function and constraints (Eqs. 4.16-4.18).
- ✓ Extract MSS vector (Eq. 4.19) from the Jacobian Matrix (Eq. 4.13).
- ✓ Sort PEV-Queue Table (Table 6.1) according to the MSS vector.

Temporarily schedule the PEV at top of PEV-Queue Table for charging.

Is $\sum$ demands $\leq D_{t,max} = D_{t,max,overnight}$ (Eq. 4.18)? — no

Run Newton-Raphson load flow (Fig. 4.3 and Eqs. 4.9-4.15).

Is $|\Delta V| \leq \Delta V_{max}$ (Eq. 4.17)? — no

- ✓ Permanently schedule PEV for overnight charging.

Select next PEV from PEV-Queue Table.

Postpone PEV charging until next Δt.

More PEVs in PEV-Queue Table ? — yes / no

Stage 3 — Update Daily Load Curve

Update and save daily load curve, losses, total cost, voltage deviations, transformer and line loadings according to the number of PEVs being charged at this time interval.

Select next time interval Δt.

More time intervals Δt ? — yes / no → Save data & stop.

Stage 4: Repeat for Next Time Interval — Repeat Stages 1-3 for the Next Time Interval (Δt = 5 Minutes) within the Scheduling Time Horizon of 24 Hours
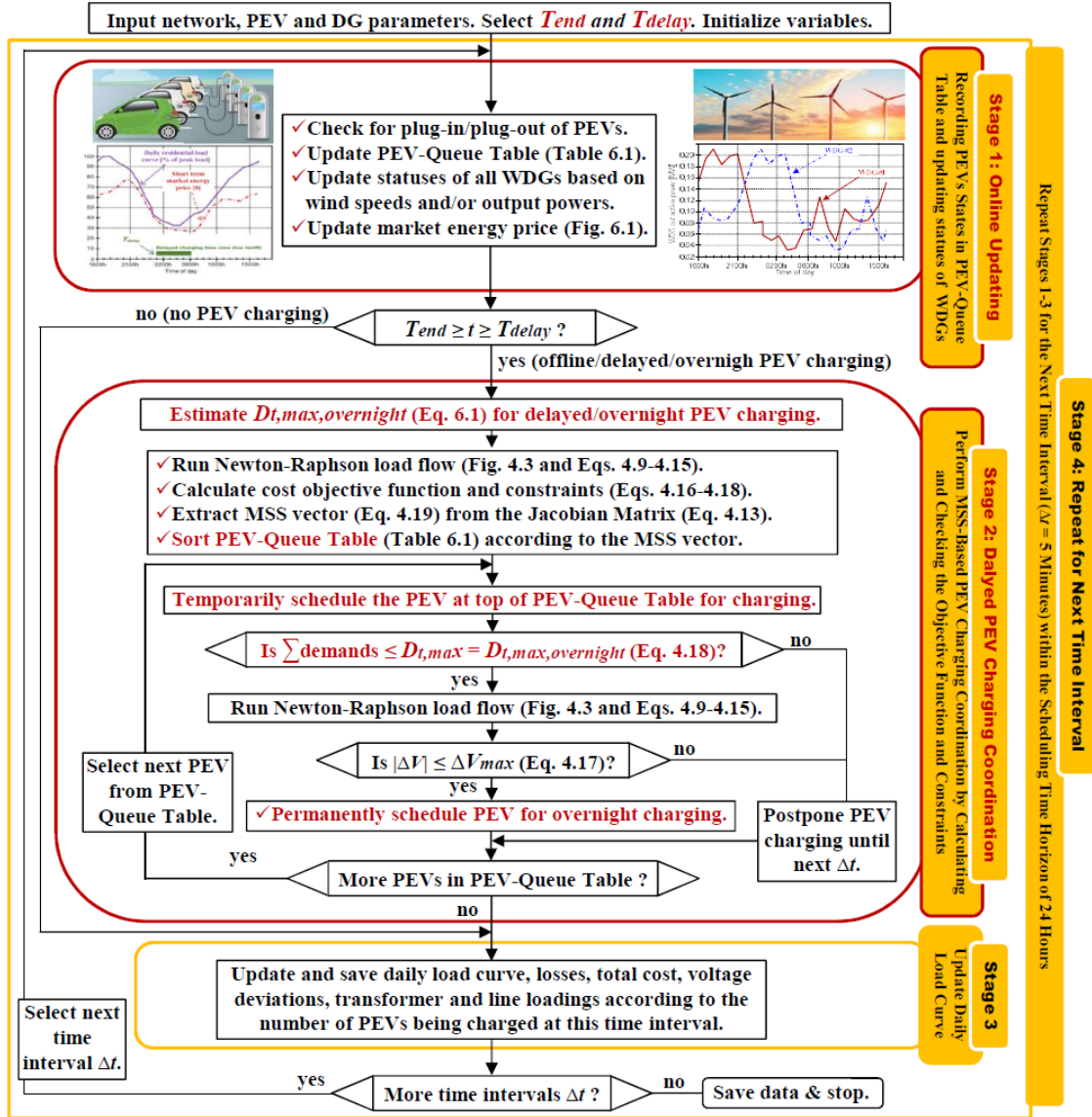
Fig. 6.2. Flow chart of DL-MSSCC for inexpensive overnight PEV battery charging coordination

6.4. Simulation Results for Delayed DL-MSSCC Coordinated battery charging of PEVs

Detailed simulations are performed in this section for the SG test network of Fig. 6.3 (without and with the three WDGs) considering random and coordinated PEV battery charging with the online OL-MSSCC strategy of Chapter 4 and the proposed delayed overnight DL-MSSCC approach of this chapter. Four PEV injection levels are considered with 3, 6, 9 and 12 electric vehicles in each of the 22 residential feeders of Fig. 6.3(a)

which correspond to PEV injections of 3/19≈16%, 6/19≈32%, 9/19≈47% and 12/19≈63%, respectively. Four PEV battery charging scenarios without WDGs (Cases A-C) and with WDGs (Case D) are simulated (Table 6.2). Simulation results with time intervals of five minutes are provided in Figs. 6.4-6.8 and summarized in Table 6.3.
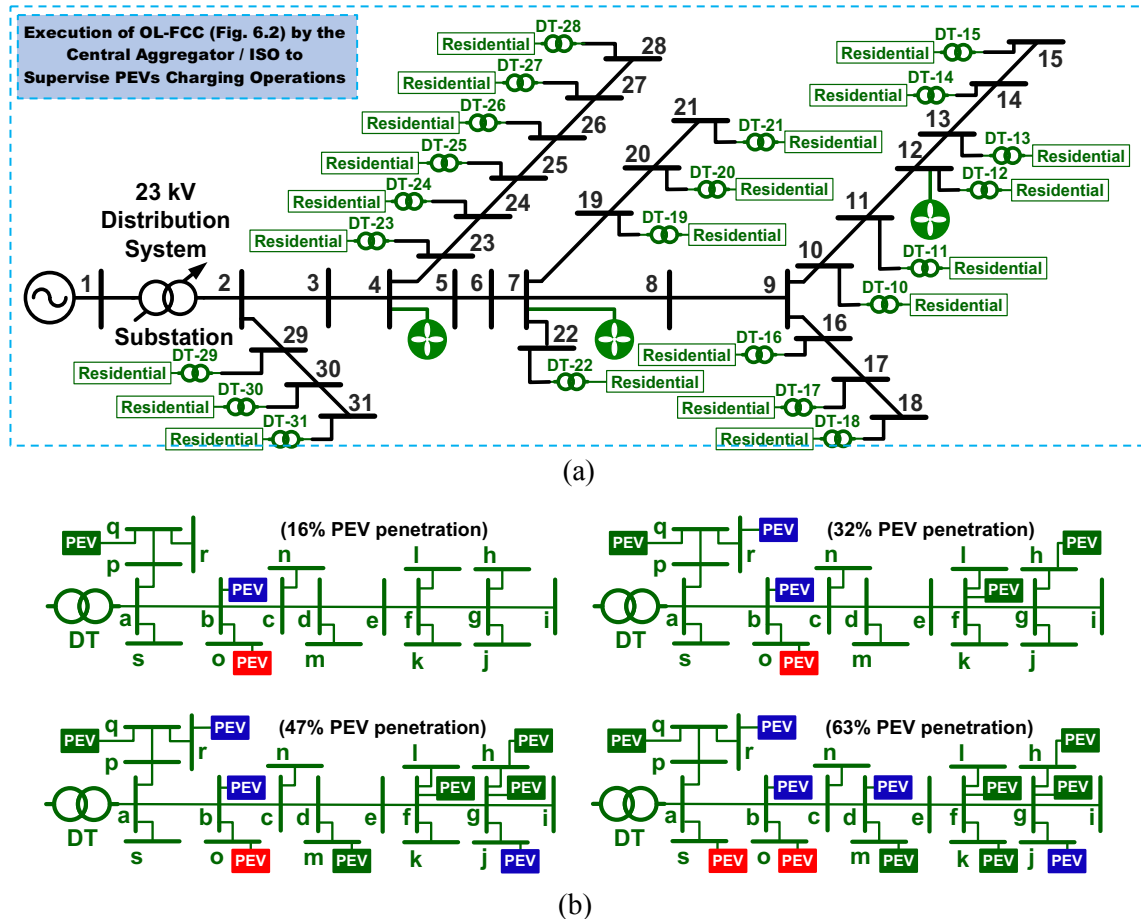

(a)

(b)

Fig. 6.3 (Similar to Figs. 4.7 and 5.7). The 449-bus smart power grid comprising of the IEEE 31-bus high-voltage 23 kV distribution network [129] joint with three WDGs (at buses 4, 7 and 12) and twenty two low-voltage 415 V residential feeders; (a) system one-line diagram, (b) One of the 19-bus residential feeder with PEV injections of 3/19≈16%, 6/19≈32%, 9/19≈47% and 12/19≈63% highlighting the high (red color), medium (blue color) and low (green color) priority consumers/PEVs [55], 57], [63].

Table 6.2. The simulated PEV battery charging cases for uncoordinated, online MSS-based (OL-MSSCC) and delayed MSS-based (DL-MSSCC) PEV coordinated battery charging of 449-bus SG system in Fig. 6.2 considering the designated delayed battery charging time zone, energy pricing, and residential load variations of Fig. 6.1.

Case	Battery Charging Coordination Method	Simulation Results
A	PEV battery charging (no coordination, without WDGs).	Table 6.3, Figs. 6.4(a), 6.5(a), and 6.6(a)
B	PEV battery charging with OL-MSSCC coordination (Fig. 4.6) without WDGs	Table 6.3, Figs. 6.4(b), 6.5(b), and 6.6(b)
C	PEV battery charging with DL-MSSCC (Fig.6.2) without WDGs.	Table 6.3, Figs. 6.4(c), 6.5(c), 6.6(c), 6.7, and 6.8

Table 6.3. Detailed results for uncoordinated, OL-MSSCC (of Chapter 4 [55]), and proposed DL-MSSCC (of this chapter [57]) PEV battery charging in SG of Fig. 6.3 without the three WDGs. For comparison, the same Gaussian function is used to generate random Gauss PEV distributions and random Gauss PEV plug-in times in residential feeders. For nominal operation without any PEVs or WDGs, the values for "$|\Delta V|$", "Imax", "Generation Cost" and "Total Cost" are 7.646%, 0.147%, 770.3 \$/day and 786.2 \$/day.

PEV (%)	$\|\Delta V\|$ (%)	Imax (%)	Cost of Generation (\$/day) / (%)*	Total Network Cost (see Eq. 4.16) (\$/day) / (%)*
Case A: Uncoordinated/Random PEV battery charging; Figs. 6.4(a), 6.5(a), 6.6(a)				
63	17.60	0.307	958/24.4	1,250/59.0
47	16.20	0.263	916/18.9	1,180/50.0
32	9.050	0.218	871/13.07	1,090/38.6
16	7.690	0.179	829/7.62	1,030/31.0
Case B**: Coordinated (OL-MSSCC) PEV battery charging; Figs. 6.4(b), 6.5(b), 6.6(b)				
63	10	0.171	883.52/14.69	903.99/15.00
47	10	0.160	862.78/12.00	882.37/12.23
32	7.65	0.159	839.44/8.97	857.14/9.11
16	7.65	0.159	808.33/4.93	824.84/4.92
Case C: Coordinated (DL-MSSCC) PEV battery charging; Figs. 6.4(c), 6.5(c), 6.6(c), 6.7				
63	9.45	0.147	843.67/9.52	863.33/9.81
47	9.35	0.147	825.53/7.17	844.28/7.39
32	7.65	0.147	806.94/4.75	823.97/4.80
16	7.65	0.147	788.21/2.32	804.4/2.31

*) Increase or decrease in daily cost (excluding renewable energy cost) in percentage of the nominal cost without any PEVs or WDGs.

**) Assuming only low-priority PEV battery charging option.

6.4.1. Random PEV Battery Charging (Case A)

The first simulated scenario is the same as Case A in Chapters 4 and 5. Simulations outcomes are presented here (Table 6.3, rows 4-8) to compare them with the delayed coordinated PEV battery charging of Case C. In this situation, the charging process starts as soon as vehicles are being randomly plugged in during early evening rush hours. As verified in Sections 4.6.1 and 5.3.1, random PEV battery charging results in substantial power demand (Fig. 6.4(a)), voltage deviations (Fig. 6.5(a)) and power losses (Fig. 6.6(a)). Particularly, at high PEV injection levels of 63% and 47%, random charging has noticeably increased the overall network cost by 50.1% and 59%, respectively (see Table 6.3, last column, rows 7-8).

6.4.2. Online MSS-Based OL-MSSCC Coordinated PEV Battery Charging (Case B)

The second simulated scenario is like Case B in Chapters 4 and 5 except for assuming all consumers have selected the low-priority PEV battery charging option and pay low tariff. Since there are no high and medium priority consumers, the OL-MSSCC algorithm of Chapter 5 will start charging the vehicles as quickly as possible. Therefore, some lucky consumers will have fast services during early evening hours while paying inexpensive low tariff. Simulations results are presented in order to compare them with the delayed coordinated PEV battery charging of Case C. Note that the vehicles' information such as their priorities and plug-in times are continuously recorded and stored in the EV queue (Table 6.1). Nevertheless, the orders and times of vehicle charging are determined by the OL-MSSCC algorithm of Chapter 4 based on their plug-in times, their priorities (e.g., only low-priority consumers in this case) and the MSS vector of Eq. 4.19.

As verified in Sections 4.6.2 and 5.3.2, compared to Case A, the online MSS-based coordinated PEV battery charging greatly reduces power demand (Fig. 6.4(b)), improves voltage regulation (Fig. 6.5(b)) and decreases power losses (Fig. 6.6(b)). Detailed

simulation results are provided in Table 6.3 (row numbers 9-13). For instance, at PEV injection of 47%, voltage deviation ΔV is improved from 16.2% (Case A) to 10%, generation cost has dropped from 916 $/day (Case A) to 862.78 $/day and the total cost is reduced from 1180 $/day (Case A) to 882.37 $/day.
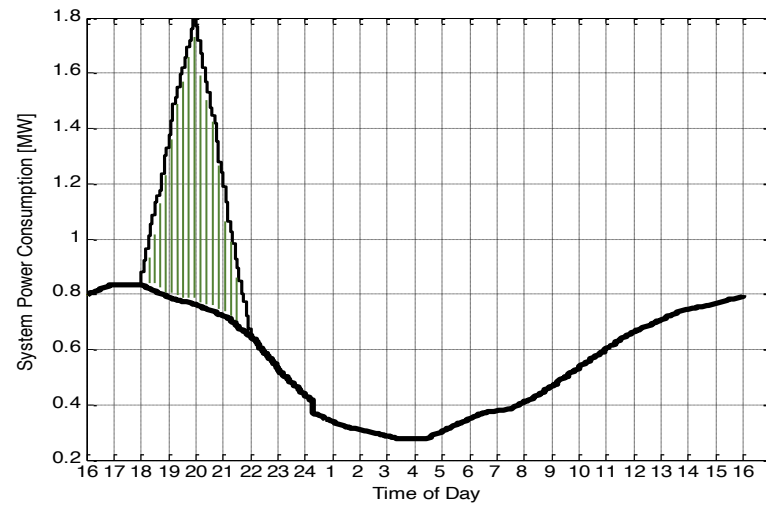
6.4.3. Delayed Coordinated PEV Battery Charging without Wind DGs (Case C)

Performance of the delayed DL-MSSCC (Table 6.3; rows 14-18) is better than both the random charging of Case A (Table 6.3; rows 4-8) and the online OL-MSSCC of Case B (Table 6.3, row numbers 9-13):
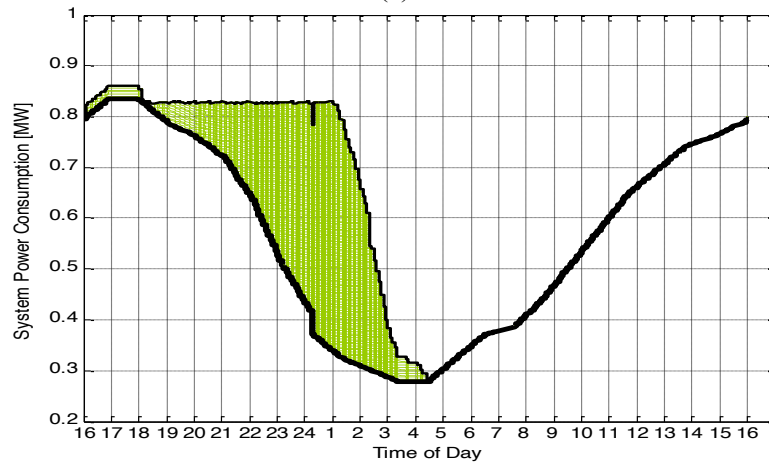
✓ For EV injection of 63%, the increase in total system cost compared with the nominal operation with no PEVs has improved from 59% (Case A) and 15% (Case B) to only 9.8% (Case C) according to Table 6.1 (last column, rows 8, 13 and 18). The generation cost has also significantly improved from 958 $/day and 883.52 $/day (Cases A and B) to 843.67 $/day for Case C (Table 6.1; column 4, rows 8, 13 and 18).

✓ For the EV injection of 47%, the increase in the total cost compared with the nominal situation with no PEVs has improved from 50.1% (Case A) and 12.23% (Case B) to only 7.39% (Case C) according to Table 6.1 (last column, rows 7, 12 and 17). The generation cost has significantly improved from 916 $/day for Case A and 862.78 $/day for Case B to 825.53 $/day for Case C (Table 6.1; rows 7, 12 and 17).

✓ Similar figures are noticed for the PEV injections of 32% and 16%.

The significant improvements associated with the DL-MSSCC coordination are also confirmed by the waveforms of Figs. 6.4-6.6. In all studied cases, there was a markable enhancement in the performance of the system compared to the uncoordinated and OL-MSSCC PEV battery charging. The total system power consumption is limited way below the designated maximum value (Fig. 6.4(c)) and there is a markable reduction in total network losses as shown in Fig. 6.6(c) while voltage magnitude regulations are within the
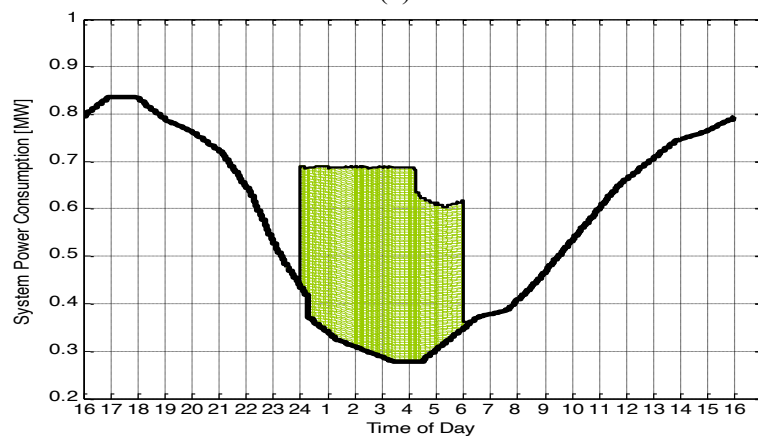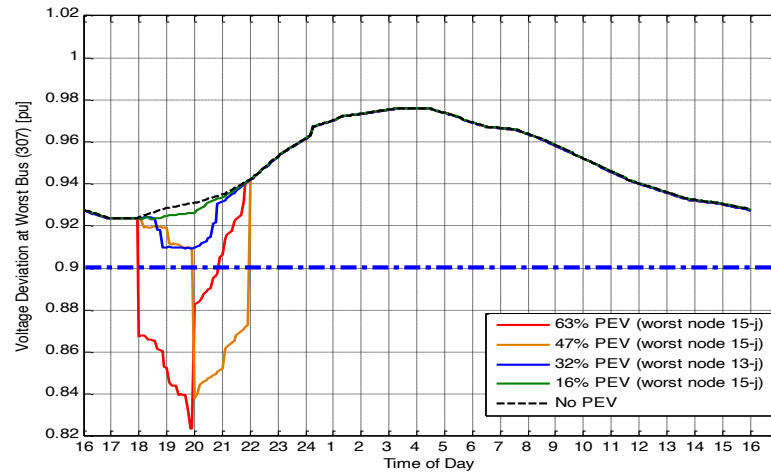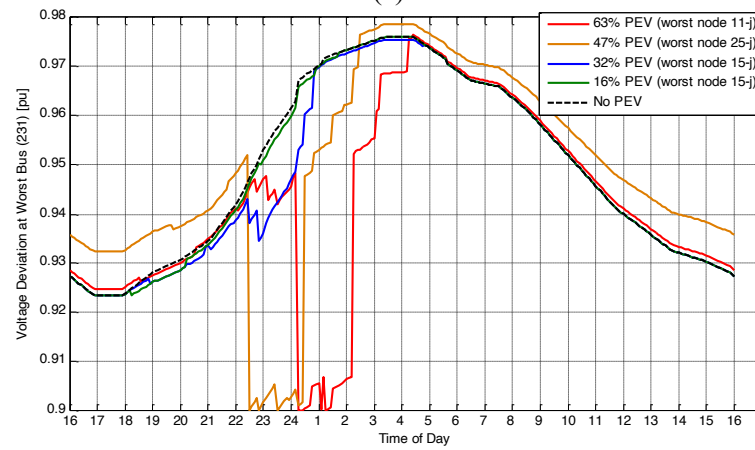
acceptable chosen limit of 10% (Fig. 6.5(c)).

Fig. 6.4. The power intake for the network of Fig. 6.3 with 63% PEV injection; (a) uncoordinated PEV battery charging, b) online OL-MSSCC coordinated PEV battery charging of Chapter 4 (assuming only low-priority PEVs), c) proposed delayed DL-MSSCC coordinated PEV battery charging of this chapter [57].

151
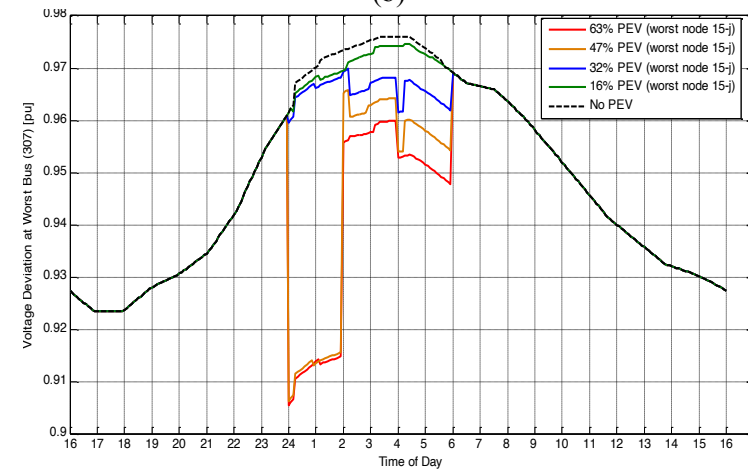
Fig. 6.5. The voltage profile/variation characteristics of worst affected buses for gird of Fig. 6.3 with; (a) uncoordinated EV battery charging, b) online OL-MSSCC coordinated PEV battery charging of Chapter 4 (assuming only low-priority PEVs), c) proposed delayed DL-MSSCC coordinated PEV battery charging of this chapter [57].

(a)

(b)

(c)

Fig. 6.6. The characteristics of total system power losses for network of Fig. 6.3 with; (a) uncoordinated PEV battery charging, b) online OL-MSSCC coordinated PEV battery charging of Chapter 4 (assuming only low-priority PEVs), c) proposed delayed DL-MSSCC coordinated PEV battery charging of this chapter [57].
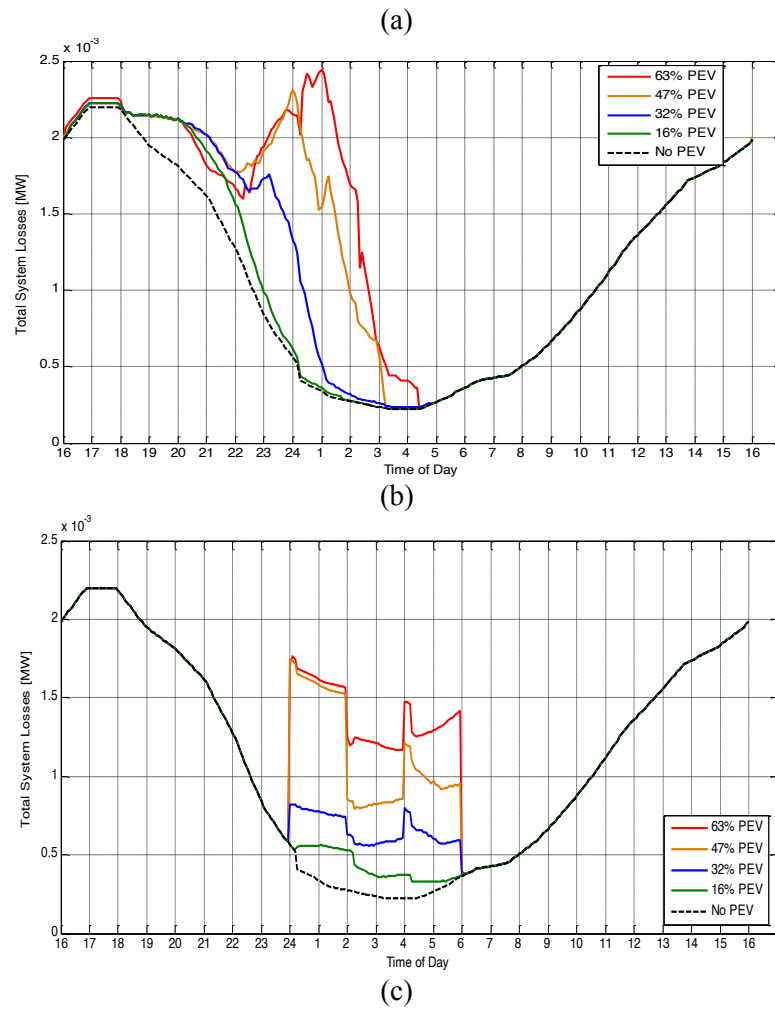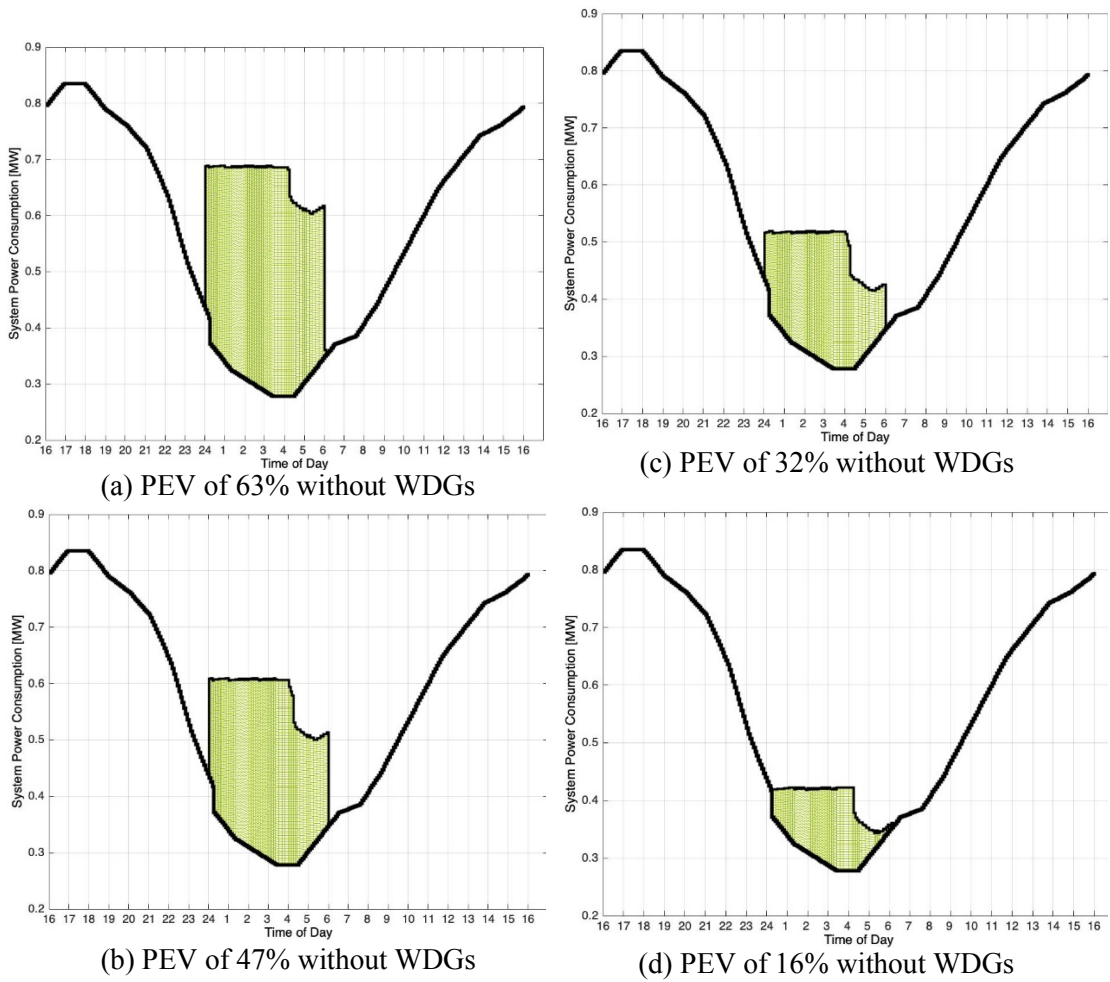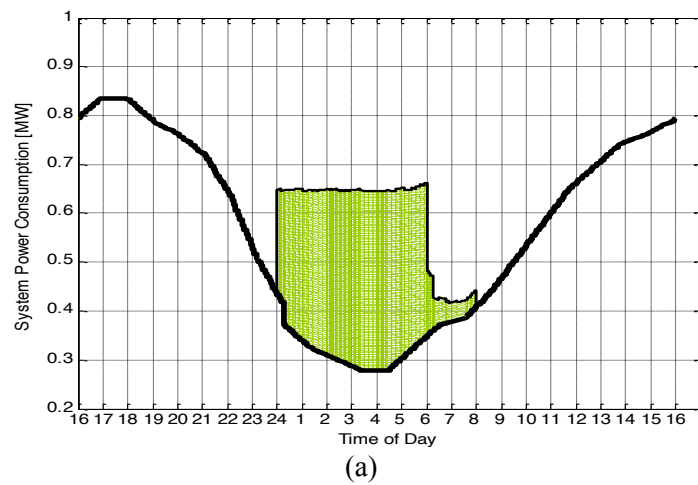
Fig. 6.7(a)-(d). Power consumption of the 449-bus SG (Fig. 6.3) with the proposed DL-MSSCC strategy for PEV injections of 32% and 16% without the WDGs.
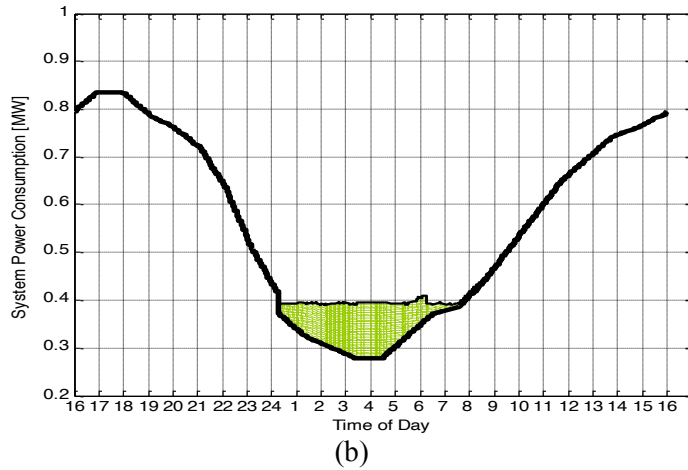

(a)

(b)

Fig. 6.8. Power consumption for the SG of Fig. 6.3 with the proposed delayed (DL-MSSCC) coordinated PEV battery charging with inaccurate estimates of $D_{t,max}$ resulting in some vehicles not being fully charged by 0600h with PEV injections of; (a) 63%, (b)16%.

6.5. Analyses of Proposed Delayed PEV Coordinated battery charging Strategy

The philosophy and coordination results of the proposed DL-MSSCC algorithm of this chapter are different than the OL-MSSCC of Chapter 4 and the OL-FCC of Chapter 5. To analyze and compare the performances of uncoordinated/random and coordinated (OL-MSSCC, OL-FCC and DL-MSSCC) EV battery charging, Table 6.4 is generated from the information of Tables 4.6, 5.2 and 6.3.

Main Advantages of Proposed DL-MSSCC:

✓ Unlike the OL-MSSCC which is designed to charge PEVs as soon as possible, the DL-MSSCC strictly avoids costly vehicle charging during the evening peak load hours. This is done to reduce cost and perform peak demand shaving.

✓ Comparison of rows 17-21 and 2-6 of Table 6.4 indicates that DL-MSSCC algorithm can overcome issues associated with random PEV battery charging such as high generation, high total costs, unacceptable voltage regulation and transformer overloading.

✓ Comparison of rows 17-21 and 7-11 of Table 6.4 indicates the DL-MSSCC algorithm

155

has better performance than the OL-MSSCC algorithm. It provides less losses and lower total cost without any voltage deviations and/or system overloading.

✓ Comparison of rows 17-21 and 12-16 of Table 6.4 indicates the DL-MSSCC algorithm also has better performance than the OL-FCC algorithm. It results in lower losses and cost with similar voltage deviations and system power consumptions.

Main Limitations of Proposed DL-MSSCC:

✓ With the proposed DL-MSSCC we may end up with less customer satisfaction since it does not allow different charging options. In order words, DL-MSSCC sacrifices consumer priorities to force inexpensive early morning PEV battery charging to reduce the overall network cost. Therefore, DL-MSSCC is not recommended for networks with many consumers who would like to have very quick high-priority or fast medium-priority PEV battery charging.

✓ Some vehicle batteries may not be fully charged by the selected end time ($T_{end}=$ 0600h) since the predicted maximum network demand level ($D_{t,max}$) of Eq. 6.1 is based on the number of PEVs in the PEV-Queue Table 6.1 at time $t = t_{delay} = 2400$h whilst some vehicles could be unpredictably plugged (arrive) after t_{delay}. For instance, two such unlikely scenarios are shown in Fig. 6.8(a) for a PEV injection of 63% and 6.8(b) for a PEV injection of 16%. A possible solution (not investigated in this Ph.D.) is to consider a dynamic $D_{t,max}$ with its level being continuously updated based on Eq. 6.1 and the updated value N_{PEV} in the PEV-Queue Table.

Table 6.4. Comparison of performances and PEV coordination results of online MSS-based OL-MSSCC algorithm of Chapter 4 (Table 4.6), the online fuzzy-based OL-FCC algorithm of Chapter 5 (Table 5.2) and the delayed MSS-based DL-MSSCC algorithm of this Chapter (Table 6.3). For nominal operation without any PEVs or WDGs, the values for "$|\Delta V|$", "Imax", "Generation Cost" and "Total Cost" are 7.646%, 0.147%, 770.3 \$/day and 786.2 \$/day, respectively.

PEV (%)	$\|\Delta V\|$ (%)	Imax (%)	Cost of Generation (\$/day) / (%)*	Total Network Cost (see Eq. 4.16) (\$/day) / (%)*
Uncoordinated (Random) PEV battery charging Case A of Chapters 4-6: Table 6.3; Rows 2-6				
63	17.60	0.307	958/24.4	1,250/59.0
47	16.20	0.263	916/18.9	1,180/50.0
32	9.050	0.218	871/13.07	1,090/38.6
16	7.690	0.179	829/7.62	1,030/31.0
Online MSS-Based Coordinated battery charging of PEVs (OL-MSSCC)** Case B of Chapter 4 (Table 4.6; Rows 7-11)				
63	10.00	0.171	875/13.59	895/13.84
47	10.00	0.160	858/11.38	878/11.67
32	7.65	0.159	838/8.79	855/8.75
16	7.65	0.159	808/4.89	825/4.93
Online Fuzzy-Based Coordinated battery charging of PEVs (OL-FCC)** Case C of Chapter 5 (Table 5.2; Rows 12-16)				
63	9.72	0.159	866/15.02	886/12.70
47	10.32	0.160	842/9.30	861/9.51
32	7.65	0.158	828/7.49	845/7.48
16	7.65	0.159	805/4.50	821/4.42
Delayed MSS-Based Coordinated battery charging of PEVs (DL-MSSCC)*** Case C of this Chapter (Table 6.3; Rows 12-16)*				
63	9.45	0.147	843.67/9.52	863.33/9.81
47	9.35	0.147	825.53/7.17	844.28/7.39
32	7.65	0.147	806.94/4.75	823.97/4.80
16	7.65	0.147	788.21/2.32	804.4/2.31

*) Increase or decrease in daily cost (excluding renewable energy cost) in percentage of the nominal cost without any PEVs or WDGs.
**) Considering high-, medium- and low-priority PEV battery charging options.
**) Considering only low-priority PEV battery charging option.

6.6. Conclusion

A delayed MSS-based coordinated battery charging (DL-MSSCC) algorithm is implemented in this chapter for the overnight/delayed battery charging of PEVs in smart power grids. The proposed strategy is practical, inexpensive, and relatively easy to implement. Therefore, it is suitable for realistic applications where usually PEV users want low PEV battery charging options. However, DL-MSSCC many cause customer dissatisfactions for consumers who would like to have very quick high-priority or fast medium-priority PEV battery charging.

CHAPTER SEVEN: COMBINED ONLINE FUZZY AND DELAYED MSS COORDINATED BATTERY CHARGING OF PEVS IN SMART POWER GRIDS WITH WIND AND SOLAR DISTRIBUTED GENERATIONS

The fourth and final contribution of this Ph.D. thesis is a new centralized online combined/hybrid fuzzy and delayed MSS-based coordinated battery charging (OL-F/DL-MSSCC) strategy for PEVs in smart power grid networks considering wind and solar (rooftop) distributed generations which was published by the author during his Ph.D. studies in Reference [58]. The proposed strategy aims to improve PEV owners' satisfaction by providing consumer priority options for i) expensive fact online charging during early evening hours, ii) inexpensive online daytime charging utilizing rooftop PV generations and, iii) cheap overnight service that guarantees full charge by 0600h. In addition, the proposed strategy attempts to reduce generation costs by charging the vehicle batteries during high wind and solar energy generation periods. This chapter introduces the concepts and formulations of the recommended OL-F/DL-MSSCC strategy and implements it on the 449 bus SG network considering both wind and solar (rooftop) distributed generations. This chapter is organized as follows:

- Section 7.1 introduces the concepts of proposed OL-F/DL-MSSCC algorithm.

- Section 7.2 presents problem formulation with the inclusion of wind and solar (rooftop) distributed generations.

- Section 7.3 presents the flow chart of OL-F/DL-MSSCC algorithm.

- Section 7.4 investigates the performance of OL-F/DL-MSSCC algorithm by implementing it on the 449-bus SG network without and with renewable DGs.

- This chapter ends with the conclusions in Section 7.5.

7.1. Concepts of Online Combined/Hybrid Fuzzy and Delayed MSS Coordinated battery charging OL-F/DL-MSSCC Strategy for PEVs

The concepts of proposed OL-F/DL-MSSCC strategy are aimed to improve the customer satisfaction by providing a variety of charging options and to reduce the generation cost by directly utilizing available renewable energy to charge the PEVs [58].

7.1.1. Consumer Priority Groups for Proposed OL-F/DL-MSSCC Strategy

Three consumer priority groups are defined to improve customer (PEV owners) satisfaction. These options are different than those defined in Chapters 4 and 5.

a) **The High-Priority Consumer Group-** This luxury group is intended for the PEV owners who request fast service and are happy to pay the high tariff to have their vehicles charged as soon as arriving home during early evening peak-load hours. The recommended OL-F/DL-MSSCC strategy will first attend these customers and try to charge their vehicles quickly as they are being randomly plugged-in. However, if the charging action causes any constraint violations, their service will be delayed to the next time interval until the violation is resolved. The online fuzzy-based PEV coordination charging strategy of Chapter 5 (OL-FCC) will be used to provide quick service to these high-priority customers.

b) **The Low-Priority Consumer Group-** This group is intended for the PEV owners who are requesting inexpensive service. They are not in hurry but need their vehicles fully charged by 0600h for their next day trips. Therefore, their vehicle charging is delayed and done overnight. The delayed MSS-based PEV coordination charging strategy of Chapter 6 (DL-MSSCC) will be used to provide overnight service to these low-priority customers while taking advantage of the available wind power generations.

c) The Medium-Priority Consumer Group- This group is intended for the PEV owners who park their vehicles at homes, public parking lots (e.g., park and ride bus/train stations) or offices to be charged during daytime for their afternoon trips. They don't immediately need their vehicles but require enough charging to get back home during the afternoon hours. The online OL-FCC algorithm of Chapter 5 with modified fuzzy membership functions tailored for daytime PEV battery charging will be used here while taking advantage of the available solar (rooftop) generations at residences, industrial and commercial buildings, public parks and parking lots.

7.1.2. Battery Charging Time Zones for OL-F/DL-MSSCC Strategy

Three time zones as shown in Fig. 7.1 are defined to decrease the grid cost related to purchasing the required energy for PEV battery charging [58].

a) Red Time Zone for Fast Battery Charging During Early-Evening Hours Considering Renewable DGs- This time zone is during the residential peak-load hours (1800h to 2200h). It is intended for the high priority PEV consumers seeking fast and expensive charging quickly after plugging their vehicles. As mentioned in the previous section, the fast OL-FCC strategy of Chapter 5 will be used in this charging time zone. The OL-FCC algorithm will rely on the fuzzy objective functions of Fig. 5.5 to accommodate the high-priory vehicles quickly after being plugged-in with the consideration of the grid cost objective function and the associated constraints of Eqs. 4.16-4.18. The online part of the recommended OL-F/DL-MSSCC aims to charge as many number of vehicles as possible using any the available renewable energy resources.

b) Green Time Zone for Delayed Battery Charging During Early-Morning Hours Considering Renewable DGs- This time zone is during the early-morning hours (2400h to 0600h) and is intended for the low-priority consumers seeking cheap

charging services. These consumers request their vehicles to be fully charged for the next day trip (e.g., by 0600h). As mentioned in the previous section, the delayed DL-MSSCC algorithm of Chapter 6 will be used to charge the low-priority PEVs.

c) **Blue Time Zone for Daytime PEV Battery Charging Considering Renewable DGs-** This time zone is from 0800h to1600h. It is intended for medium-priority consumers who plugged-in their vehicles at homes and publicly locations (e.g., industrial buildings and parking stations) and request daylight service. As mentioned in the previous section, the fast OL-FC algorithm of Chapter 5 will be used here. However, the fuzzy membership functions are modified for daytime charging utilizing solar energy.

7.1.3. PEV-Queue Table for Proposed OL-F/DL-MSSCC Strategy

The PEV-Queue Table of the proposed OL-F/DL-MSSCC is shown in Table 7.1. It is very similar to the queue tables for the online and delayed PEV coordination strategies of Chapters 4-7 (Table 4.1 and Table 6.1) with the following differences:

- There are three types of PEV battery charging coordination; i) fuzzy-based evening charging, ii) MSS-based overnight charging and, iii) fuzzy-based daytime charging.

- Both wind and solar DGs are considered.

- Each charging scheme is dedicated to only one type of consumers. Evening and daytime charging are allowed for the high-priority and the medium-priority consumers, respectively. Overnight charging is only allowed for the low-priority consumers.

- The membership functions for online evening fuzzy charging (Fig. 5.5) are slightly modified for online fuzzy daytime charging (Fig. 7.2).
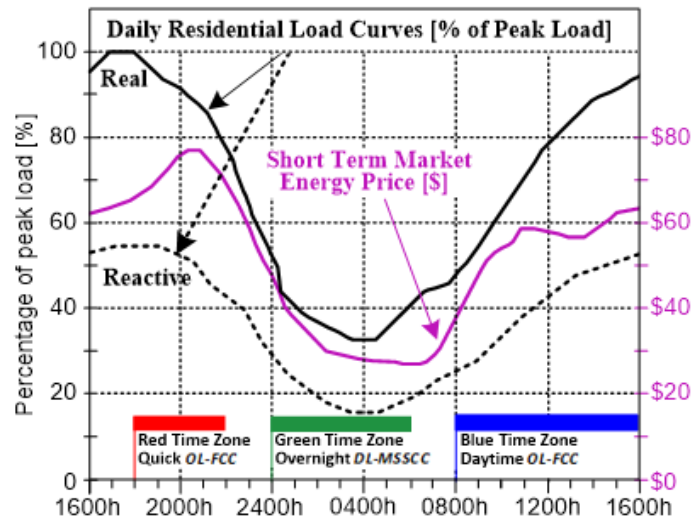
Fig. 7.1. Charging time zones (red, green and blue), service options (fast online fuzzy OL-FCC, delayed overnight DL-MSSCC and fast daytime fuzzy OL-FCC), price of energy, typical residential daily active power and reactive power curves [58].

Table 7.1. An example of the PEV-Queue Table for the proposed OL-F/DL-MSSCC strategy. Within each priority, some PEVs are already charged, some are in charge and others are waiting to be scheduled for (evening, overnight or daytime) charging by the ISO.

PEV-Queue Table for Proposed Combined Online Fuzzy and Delayed MSS Coordinated battery charging (OL-F/DL-MSSCC) of PEVs			
Charging Scheme	**PEV Type**	**PEV Number in the Queue**	**PEV Status**
Online Fuzzy-Based Coordinated battery charging (OL-FCC of Chapter 5)	**High Priority** to be Charged Early **Evening Hours** (**Red Zone**; Fig. 7.1)	R_1	Charged
		…..	…..
		$R_{charged,max}$	Charged
		$R_{charging,1}$	Charging
		…..	…..
		$R_{charging,max}$	Charging
		$R_{waiting,1}$	Waiting to be scheduled for evening charging
		…..	…..
		$R_{red,\,max}$	Waiting to be scheduled for evening charging
Delayed MSS-Based Coordinated battery charging (DL-MCCCC of Chapter 6)	**Low Priority** to be Charged Late **Overnight** (**Green Zone**; Fig. 7.1)	G_1	Charged
		…..	…..
		$G_{charged,max}$	Charged
		$G_{charging,1}$	Charging
		…..	…..
		$G_{charging,max}$	Charging
		$G_{waiting,1}$	Waiting to be scheduled for overnight charging
		…..	…..
		$G_{blue,max}$	Waiting to be scheduled for overnight charging
Online Fuzzy-Based Coordinated battery charging (OL-FCC of Chapter 5)	**Medium Priority** to be Charged **Daytime** (**Blue Zone**; Fig. 7.1)	B_1	Charged
		…..	…..
		$B_{charged,max}$	Charged
		$B_{charging,1}$	Charging
		…..	…..
		$B_{charging,max}$	Charging
		$B_{waiting,1}$	Waiting to be scheduled for daytime charging
		…..	…..
		$B_{green,max}$	Waiting to be scheduled for daytime charging

7.2. Formulation of Proposed OL-F/DL-MSSCC Strategy

The formulation of proposed OL-F/DL-MSSCC strategy for PEVs is the same as the MSS-based formulation of Chapter 4 (Eqs. 4.16-4.18) and the fuzzy-based formulation of Chapter 5 (Eqs. 5.2-5.6 and Fig. 5.5). The only difference is that the fuzzified membership characteristics of Fig. 5.5 are slightly modified for the daytime PEV battery charging employing solar energy resources as shown in Fig. 7.2.
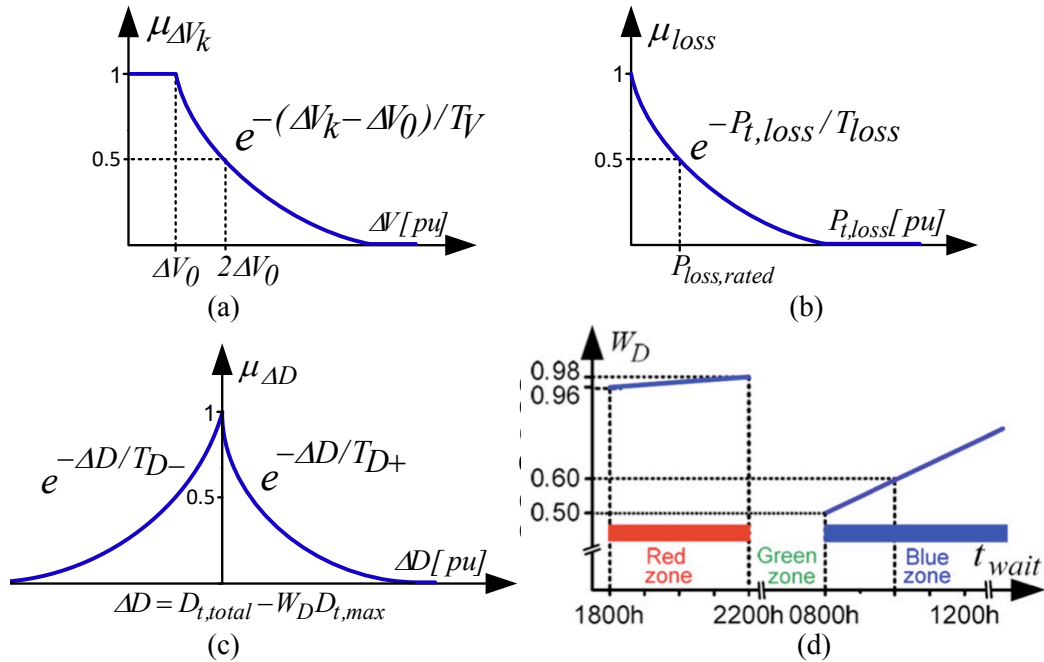
Fig. 7.2. Fuzzy membership functions of the proposed OL-F/MSSCC algorithm (Section 7.3, Stage 2) for; (a) voltage deviations (Eq. 4.17 and Eq. 5.2), (b) total system losses (Eq. 4.16 and Eq. 5.3), (c) maximum demand level (Eq. 4.18 and Eq. 5.3), (d) weighting factors for maximum network demand (Eq. 5.3 and Fig. 5.5(c)) [58]. Note that the membership functions of (a)-(c) are the same as the ones in Fig. 5.5(a)-(c).

7.2.3. Inclusion of Wind and Solar (Rooftop) Distribution Generations

The proposed OL-F/DL-MSSCC algorithm utilizes the available wind and solar energy for both online and delayed PEV battery charging. The scenarios of Section 7.4 are simulated for the SG network of Fig. 7.4 with the following number and locations of renewable energy resources:

✓ Three wind DGs are connected to high voltage 23 kV buses number 4, 7, and 12.

✓ Four solar DGs (rooftop PVs) are connected to each of the 22 residential feeders aet low voltage 415 V buses number a, i, l and n.

For the load flow calculations of Eqs. 4.1-4.14 (Fig. 4.3), the solar and wind energy resources are considered as PQ buses (loads) injecting negative active power to the network. In addition, the maximum network demand level $D_{t,max}$ (Eq. 4.18) is dynamically adjusted according to the available renewable energy. Therefore, the proposed OL-F/DL-MSSCC algorithm activates more PEVs during the peak wind/solar generation periods.

7.3. Flow Chart of Proposed OL-F/DL-MSSCC Algorithm

Flow chart of the proposed OL-F/DL-MSSCC algorithm is shown in Fig. 7.3. For each randomly plugged-in PEV depending on its consumer priority group (Section 7.1.1), the OL-F/DL-MSSCC algorithm will perform either quick online fuzzy-based evening charging, delayed MSS-based overnight charging or fast online fuzzy-based daytime charging. All charging options accommodate renewable (wind, solar) energy resources [58]. The algorithm minimizes the cost of purchasing/generating energy for PEV battery charging by directly utilizing the available renewable energy whilst maintaining maximum network demand and voltage deviation constraints (Eqs. 4.16-4.18).

There are five stages associated with each time interval $t = \Delta t = 5$ minutes of the proposed OL-F/DL-MSSCC algorithm (Fig. 7.3). Stages 1, 4-5 are the same as the ones used in Chapters 4-6. Stage 2 is like Stage 2 of the OL-FCC algorithm of Chapter 5 (Fig. 5.6) and Stage 3 is like Stage 2 of the DL-MSSCC algorithm of Chapter 6 (Fig. 6.2).

Stage 1 (Updating PEV, Wind and Solar DGs Statuses (Fig. 7.3):

▪ Step 1.1- Update PEV-Queue Table 7.1 according random PEV plug-in and plug-out.

▪ Step 1.2- Update $D_{t,max}$ (Eq. 4.18) based on wind and solar DGs output power.

▪ Step 1.3- Update market energy price based on real-time pricing of Fig. 7.1.

▪ Step 1.4- Run Newton-Raphson load flow (Fig. 4.3), calculate cost objective function with constraints (Eqs. 4.16-18), extract MSS vector from Jacobian matrix (Eqs. 4.13 and 4.19) and sort the order of EVs in the queue table according to the MSS values.

▪ Step 1.5- If $t_{delay} \geq t \geq t_{end}$ go to Stage 2 (online); otherwise, go to Step 3 (delayed).

Stage 2 (Online Fuzzy-Based Evening or Daytime PEV Scheduling (Fig. 7.3):

▪ Step 2.1 (Fuzzification of Losses and Constraints)

➤ Step 2.1.1- If $t_{delay} \geq t \geq 1600h$ (e.g., evening PEV battery charging) then Fuzzify losses and constraints using the memberships of Figs. 5.5 for online Fuzzy evening PEV coordination.

➤ Step 2.1.2- If $1600h > t > t_{end}$ (e.g., daytime PEV battery charging) then Fuzzify losses and constraints using the memberships of Figs. 7.2 for online Fuzzy daytime PEV coordination.

▪ Step 2.2 (T-Norm & α-Cut Defuzzification to Choose Most Suitable EVs to Charge)

➤ Step 2.2.1- Temporary charge the PEV at top of queue in Table 7.1.

➤ Step 2.2.2- Run Newton-Raphson load flow (Fig. 4.3).

➤ Step 2.2.3- Calculate membership function values (Eqs. 5.2-5.4).

➤ Step 2.2.4- Combine the membership function values using the additive t-norm approach (Eq. 5.5).

➤ Step 2.2.5- Defuzzify the combine membership function value using α-cut to calculate its crisp value S_{PEV} (Eq. 5.6).

Step 2.3 (Check Suitability of PEV for Charging)- For each vehicle, check the crisp value of $S_{PEV,j}$ to decide on whether to permanently charge it or defer its charging to next Δt.

Step 2.4- Repeat Steps 2.2 to 2.3 for all high-priority PEVs (seeking online evening charging) and all medium-priority PEVs (seeking online daytime charging).

Stage 3- Delayed Overnight MSS-Based PEV Coordination Scheduling (Fig. 7.3):

- Step 3.1- Estimate the maximum demand level for delayed overnight PEV battery charging ($D_{t,max}$ in Eq. 4.18) using Eq. 6.1 ($D_{t,max} = D_{t,max,overnight}$).

- Step 3.2- Run Newton-Raphson load flow of Fig. 4.3.

- Step 3.3- Excerpt MSS vector (Eq. 4.19) from the Jacobian matrix (Eq. 4.13).

- Step 3.4- Sort the order of EVs in the queue Table 7.1 in accordance to the MSS values of Eq. 4.19.

- Step 3.5 (Scheduling of Eligible PEVs):

  ➢ Step 3.5.1- Temporary charge the PEV at top of PEV-Queue Table 7.1.

  ➢ Step 3.5.2- If $\sum demands \ll D_{t,max}$, go to Step 3.6 (postpone charging this PEV until next Δt since it causes a damned constraint violation according to Eq. 4.18).

  ➢ Step 3.5.3- Run Newton-Raphson load flow of Fig. 4.3.

  ➢ Step 3.5.4- If $|\Delta V| \ll \Delta V_{max}$, go to Step 3.6 (postpone charging this PEV until next time interval since it causes a voltage constraint violation based on Eq. 4.17).

  ➢ Step 3.5.5- Permanently schedule the PEV for charging and remove it from the PEV-Queue Table 7.1.

- Step 3.6- Repeat Steps 3.2 to 3.5 for all low-priority PEVs.

Stage 4 (Updating Daily Load Curve):

- Step 4.1- Update the daily load curve by including the scheduled PEVs.

Stage 5 (Go to Next Time Interval Δt and Repeat):

- Step 5.1- If $t = 24$ hours stop; otherwise, repeat Stages 1-4 for the next time interval Δt.
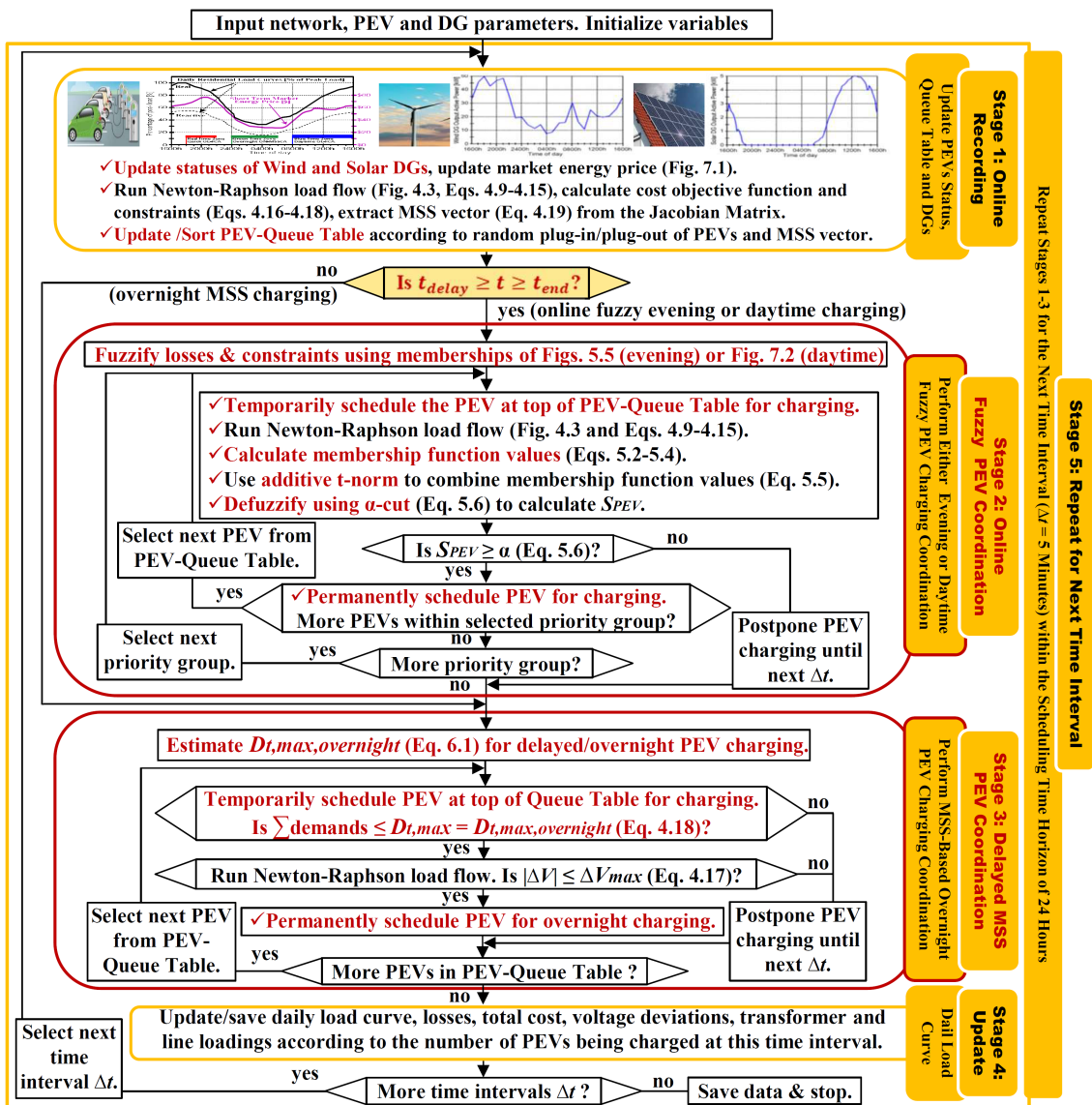
Fig. 7.3. Flow chart of the proposed OL-F/DL-MSSCC algorithm for combined online, delayed/overnight, and offline/daytime PEV battery charging considering wind and solar DGs.

7.4. Simulation Results Supporting Performance of OL-F/DL-MSSCC Algorithm

For the simulations and analyses of the proposed combined online and delayed PEV coordination charging OL-F/DL-MSSCC algorithm, the 449-bus SG topology of Chapters 4-6 (Fig. 7.4) is used. However, in addition to the three wind DGs at buses 4, 7 and 12, four rooftop PVs are also included in each of the 22 residential feeders at buses a, i, l and n. System and PEV parameters are provided in Tables 4.2-4.4 and Sections 4.5.2-4.5.4. Four PEV injections of 16%, 32%, 47% and 63% are considered that correspond to 3, 6, 9 and 12 houses with electric vehicles in each of the 22 low voltage residential feeders. For example, for the PEV injection of 63%, there are a total of 264 vehicles with 132, 88 and 44 vehicles in the blue, green, and red battery charging time zones of Fig. 7.1, respectively. The chosen output power characteristics of the wind and solar (rooftop) DGs are shown in Fig. 7.5(a) and 7.5(b), respectively.
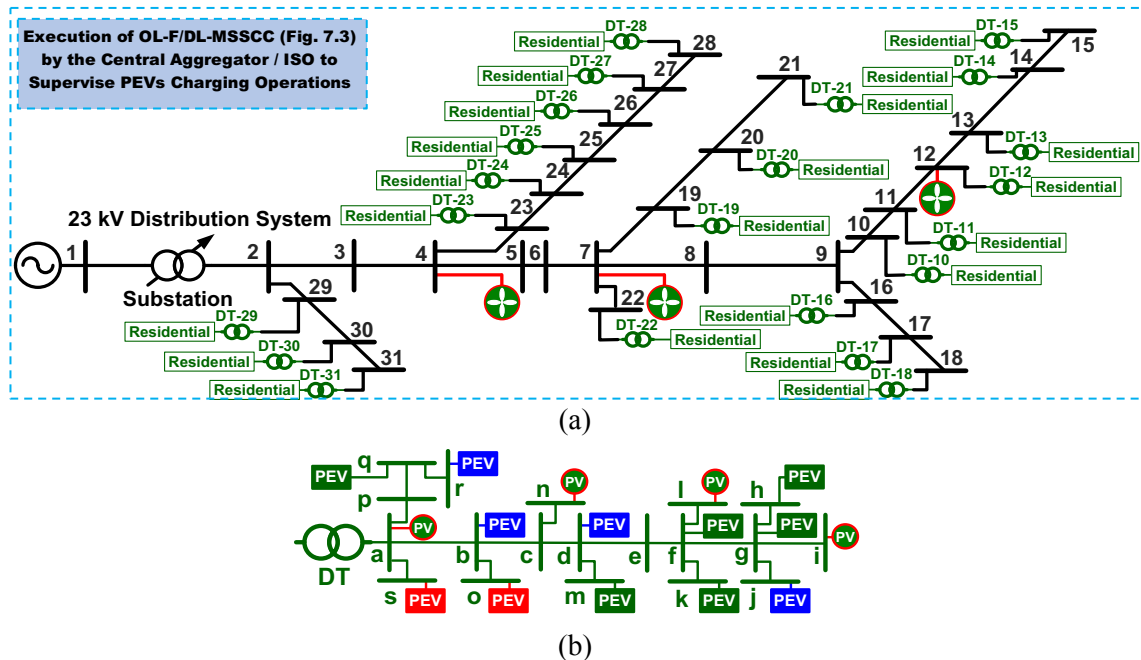

(a)

(b)

Fig. 7.4. The 449-bus smart power grid comprising of the IEEE 31-bus high-voltage 23 kV distribution network [129] joint with three WDGs (at buses 4, 7 and 12) and twenty two low-voltage 19-bus 415 V residential feeders with rooftop PVs at buses a, i, l and n; (a) system one-line diagram, (b) One of the residential feeders with PEV injections of 12/19≈63% (corresponding

to the total of 264 vehicles) highlighting the high (red color), medium (blue color) and low (green color) priority consumers/PEVs [58].

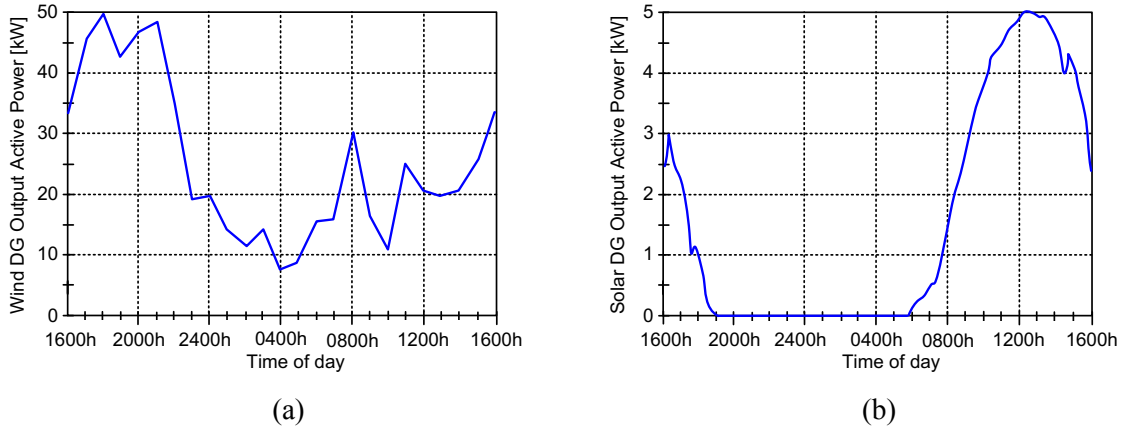(a)   (b)

Fig. 7.5. The active output power characteristics of the renewable DGs in Fig. 7.4; (a) for the three wind DGs at buses 4, 7 and 12 which is based on the scaled down actual recordings from the Walkway wind farm in Western Australia on July 7, 2012 with the peak output power period shifted to early evening hours1800h-2100h ([58]), (b) for the 4(22)=88 rooftop PVs (based on actual recordings of rooftop PV generation in WA, Australia ([58]).

combined online, delayed/overnight, and offline/daytime

The recommended combined/hybrid online, delayed/overnight, and offline/daytime OL-FC/DL-MSSCC strategy is used to simulate the following four PEV battery charging scenarios (Table 7.2):

✓ Case A- Uncoordinated (random) PEV battery charging with no wind and solar DGs.

✓ Case B- Uncoordinated (random) PEV battery charging with the three wind DGs and the 4(22)= 88 rooftop PVs.

✓ Case C- Coordinated PEV battery charging (using the proposed OL-FC/DL-MSSCC scheme) with no wind and solar DGs.

✓ Case D- Coordinated PEV battery charging (using the proposed OL-FC/DL-MSSCC algorithm) with the three wind DGs and the 88 rooftop PVs.

Detailed simulation results are presented in Figs. 7.6-7.7 and summarized in Table 7.3.

171

Table 7.2. The simulated uncoordinated and coordinated PEV battery charging case studies without/with wind and solar DGs for the 449-bus smart power grid of Fig. 7.4 with the characteristics of Fig. 7.1.

Case	Battery Charging Coordination Method	Simulation Results (Table 7.3)
A	PEV battery charging without coordination, without DGs	Figs. 7.6(a, c, e, g)
B	PEV battery charging without coordination, with wind/solar DGs	Figs. 7.6(b, d, f, h)
C	PEV battery charging with OL-F/DL-MSSCC coordination (Fig. 7.3) without wind/solar DGs	Figs. 7.7(a, c, e, g)
D	PEV battery charging with OL-F/DL-MSSCC coordination (Fig. 7.3) without wind and solar DGs	Figs. 7.7(b, d, f, h)

Table 7.3. Detailed simulation results for the four scenarios (case studies) of Table 7.2 [58]. For comparison, the same Gaussian function is used to generate random PEV distributions and random PEV plug-in times in all residential feeders. For nominal operation without any PEVs or WDGs, the values for "$|\Delta V|$", "Imax", "Generation Cost" and "Total Cost" are 7.646%, 0.147%, 770.3 \$/day and 786.2 \$/day, respectively.

PEV (%)	$|\Delta V|$ (%)	Imax (%)	Cost of Generation (\$/day) / (%)*	Total Network Cost (see Eq. 4.16) (\$/day) / (%)*
Case A: Uncoordinated PEV Battery Charging without DGs; Figs. 7.6(a, c, e, g)				
63	17.600	0.307	958.0/24.36	1,250/59.00
47	16.200	0.265	915.0/18.78	1,182/50.30
32	9.080	0.219	871.0/13.07	1,093/39.00
16	7.730	0.181	828.0/7.49	1,028/30.80
Case B: Uncoordinated PEV Battery Charging with DGs; Figs. 7.6(b, d, f, h)				
63	17.600	0.306	639.0/-17.04	876.0/11.40
47	16.200	0.263	595.0/-22.75	808.0/2.77
32	8.960	0.216	551.0/-28.47	719.0/-8.50
16	7.420	0.177	508.0/-34.05	654.0/-16.80
Case C: Proposed Coordinated (OL-F/DL-MSSCC) PEV Battery Charging without Wind and Solar DGs; Figs. 7.7(a, c, e, g)				
63	12.240	0.159	869.0/12.81	889.0/13.10
47	12.350	0.160	841.0/9.17	860.0/9.40
32	7.650	0.158	828.0/7.50	835.0/6.20
16	7.640	0.159	797.0/3.47	814.0/3.50
Case D: Proposed Coordinated (OL-F/DL-MSSCC) PEV Battery Charging with Wind and Solar DGs; Figs. 7.7(b, d, f, h)				
63	9.510	0.164	553.0/-28.21	568.0/-27.80
47	9.510	0.152	525.0/-31.84	539.0/-31.40
32	7.370	0.152	502.0/-34.83	515.0/-34.40
16	7.400	0.152	482.0/-37.42	494.0/-37.20

*) Increase or decrease in daily cost (excluding renewable energy cost) in percentage of the nominal cost without any PEVs or WDGs.

7.4.1. PEV Battery Charging without Coordination and Renewable DGs (Case A)

The first simulated scenario is the same as Case A in Chapters 4, 5 and 6. The outcomes are repeated in Table 7.3 (row numbers 4-8) to compare them with the results of Cases B, C and D. For Cases A-B, all vehicles charging activities start as they are randomly plugged-in from 1800h to 2200h without considering their detrimental impacts on the SG network. As most people usually get home during early evening hours, this uncoordinated PEV battery charging situation (Case A) results in enormous power demand (Fig. 7.6(a)), transformer overloading (Fig. 7.6(c)), power losses (Fig. 7.6(e)) and voltage deviations ((Fig. 7.6(g)).

7.4.2. Random PEV Battery Charging with Renewable DGs (Case B)

This case study is the same as Case A except for the inclusions of the three WDGs and the 88 rooftop PVs. Simulation results are plotted in Figs. 7.6(b), (d), (f) and (h) and summarized in Table 7.3 (rows 9-13). As anticipated, the introductions of wind and solar DGs have not considerably reduce power consumption, transformer loading and voltage deviations but resulted in significantly cost reductions.

- Comparison of Figs. 7.6(a) and 7.6(b) indicates that the addition of renewable DGs will not have significant impacts on the daily load curve (system power consumption) even for the high PEV injection of 63%.

- Figs. 7.6(c)-(d) and Table 7.3 (column 3, rows 4-8 and 9-13) confirm that the addition of renewable DGs will not have significant impacts on substation transformer loading for PEV injections of 16%, 32%, 47% and 63%.

- Comparison of Figs. 7.6(e) and 7.6(f) indicates that the accommodation of renewable DGs will not have significant impacts on system losses. This is true for all PEV injections of 16%, 32%, 47% and 63%.

173

- Figs. 7.6(g)-(h) present the voltage profiles at worst buses for PEV injections of 16%, 32%, 47% and 63% without and with DGs, respectively. Comparison of these figures and rows 4-8 and 9-13 of Table 7.3 (second column) reveals that the inclusion of renewable DGs will have slight impacts on voltage regulations at all PEV injections.

- However, the addition of wind and solar DGs will significantly reduce the generation cost and the total cost as confirmed by rows 4-8 and 9-13 of Table 7.3 (columns 4-6). For instance, for situation with 63% of PEV injection, the generation cost has dropped from 958 $/day (without renewable DGs) to 639 $/day (with renewable DGs) while the total cost has reduced from 1,250 $/day to 876 $/day. As a result, the percentage of increase in total cost (compared with the nominal cost) has decreased from +59% to 11.4% (Table 7.3, last column, rows 8 and 13). Similar improvements are noted for the PEV injections of 47%, 32% and 16%.

7.4.3. PEV Battery Charging with OL-FC/DL-MSSCC Coordination without Renewable Wind and Solar DGs (Case C)

The proposed OL-FC/DL-MSSC algorithm of this chapter is executed on the smart power grid of Fig. 7.4 (without the wind and solar DGs) and results are presented in Table 7.3 (rows 14-23) and Figs. 7.7 (a), (c), (e) and (g). As expected, there are considerable enhancements in the network operation in comparison to the uncoordinated PEV battery charging scenarios of Cases A-B.

## 7.4.4. PEV Battery Charging with OL-FC/DL-MSSCC Coordination with Renewable Wind and Solar DGs (Case D)

Case C is repeated with the addition of the three WDGs and the 88 rooftop PVs. As expected, the introduction of renewable DGs has further improved the system performance in all categories:

- According to Table 7.3 (last column, row numbers 8, 13, 18 and 23), there are considerable improvements in the increased amount of total network cost with 63% PEV injection from the unacceptable figure of 59% (without coordination without DGs) to the an satisfactory figure of 13.1% (coordinated battery charging without DGs) and from the large figure of 11.4% (without coordination with DGs) to the striking figure of -27.8% (coordinated battery charging with DGs) while all bus voltages and maximum network demand levels are kept within their permitted limits. Similar cost reductions are noticed for PEV injections of 47%, 32% and 16%.

- According to Table 7.3 (column 5, rows 8, 13, 18 and 23), there are considerable reductions in the generation cost for 63% PEV injection from 958 $/day (uncoordinated battery charging without DGs) to 869 $/day (coordinated battery charging without DGs) and from 639 $/day (uncoordinated battery charging with DGs) to only 553 $/day (coordinated battery charging with DGs). Similar reductions in generation costs are observed for PEV injections of 47%, 32% and 16%.

- Unlike the MSS-based delayed overnight coordination strategy (DL-MSSCC) of Chapter 6, the fuzzy-based online (evening and/or daytime) coordination algorithm of this chapter will allow for small violations of maximum network demand (see Fig. 7.7(a); $t \approx 21:30h$) and small deviations of bus voltages (see Fig. 7.7(g); $t \approx 11:30h-14:00h$). These are attained in accordance with the chosen membership functions that aim to limit losses and reduce the cost of generating energy.
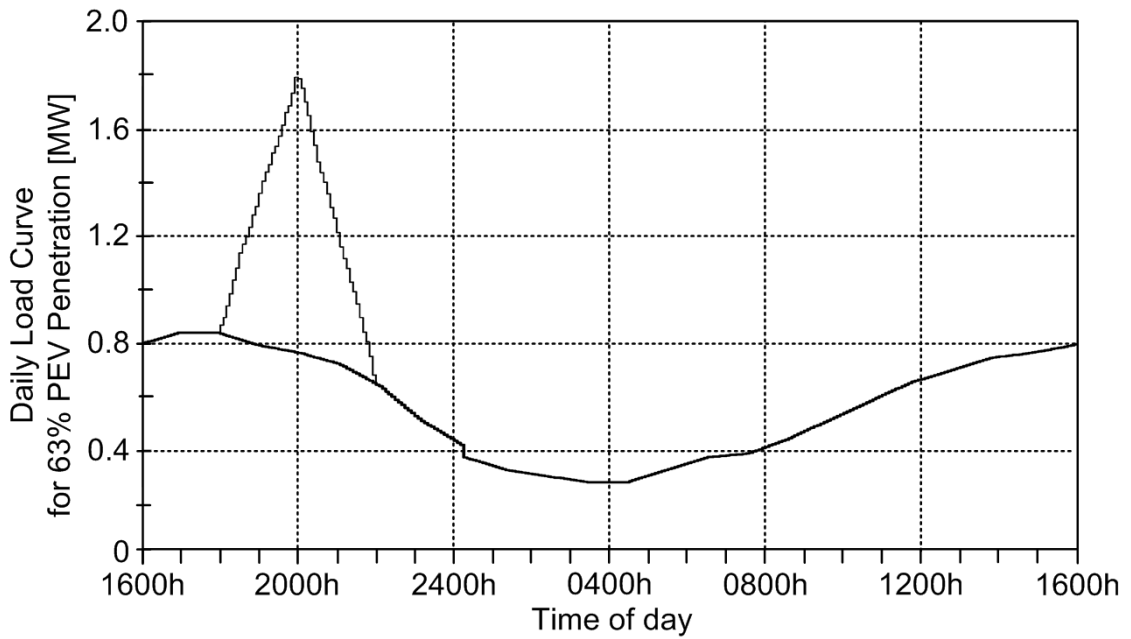
(a) PEV battery charging without coordination, without DGs
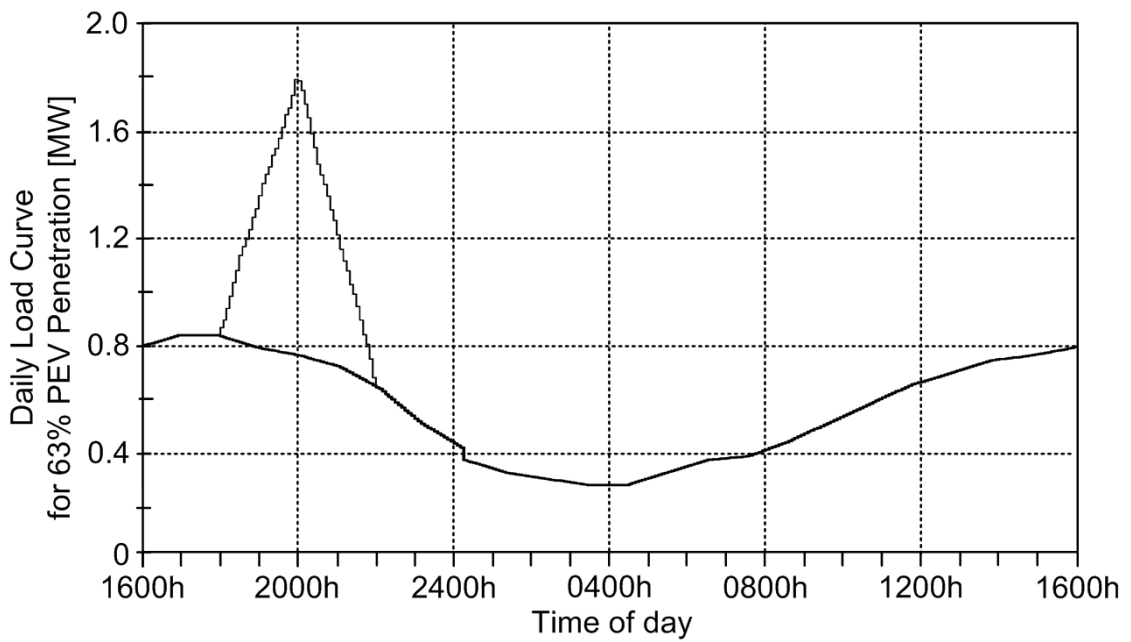
(b) PEV battery charging without coordination, with DGs

Fig. 7.6(a-b). Cases A-B (Uncoordinated PEV battery charging)- Daily load curves (system power consumption) for PEV injection of 63% without and with DGs.
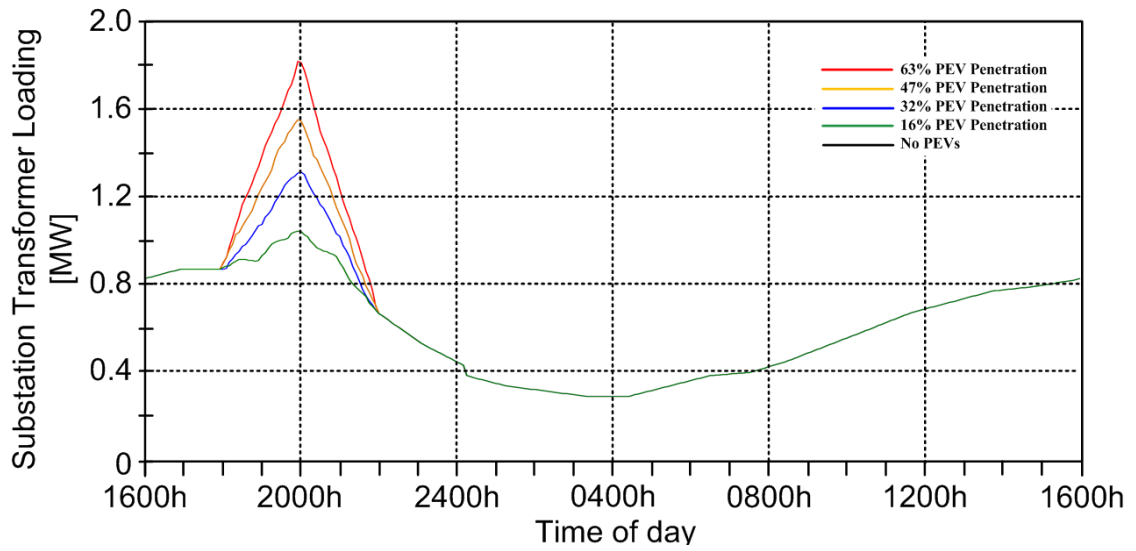
(c) PEV battery charging without coordination, without DGs
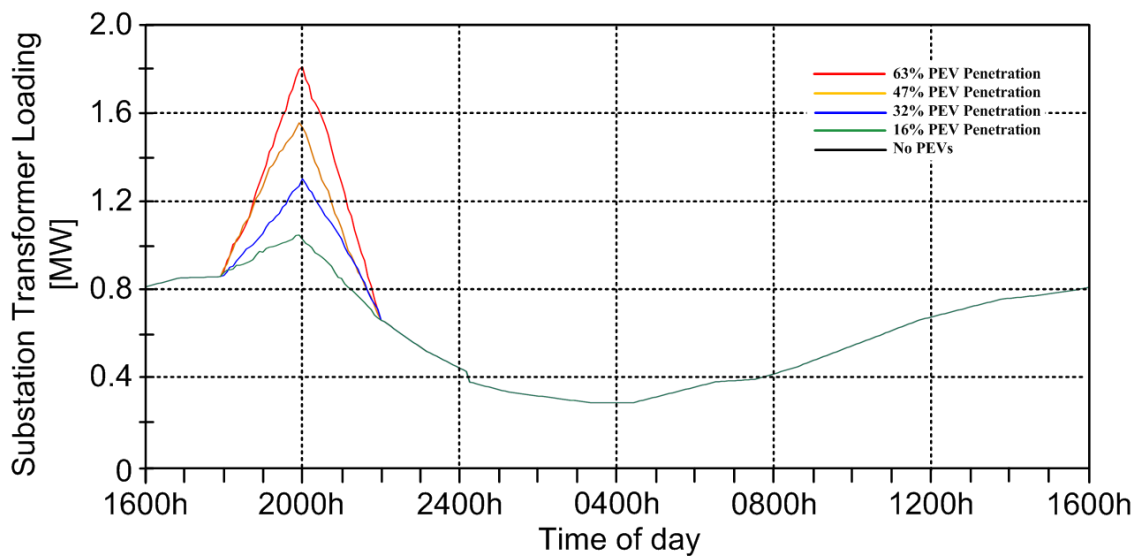
(d) PEV battery charging without coordination, with DGs

Fig. 7.6(c-d). Cases A-B (Uncoordinated PEV battery charging)- Substation Transformer loadings for PEV injections of 63%, 47%, 32% and 16% without and with DGs.
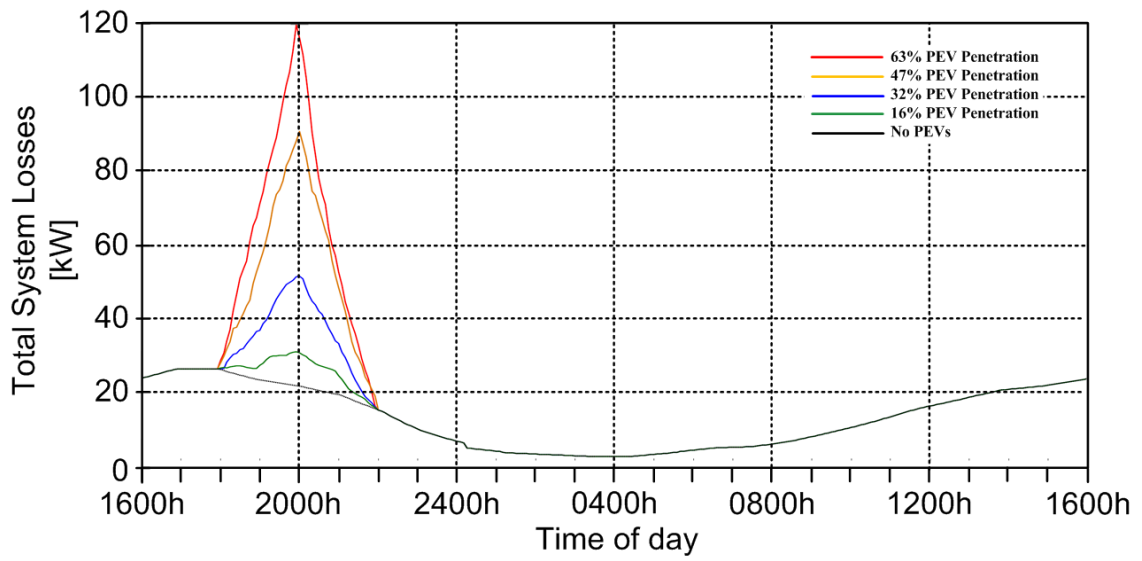
(e) PEV battery charging without coordination, without DGs
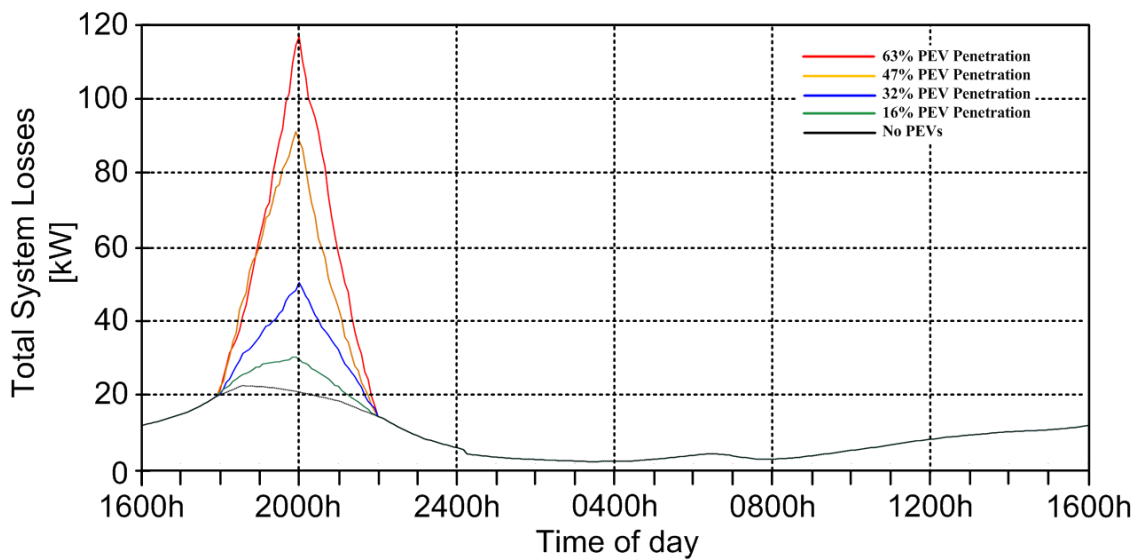
(f) PEV battery charging without coordination, with DGs

Fig. 7.6(e-f). Cases A-B (Uncoordinated PEV battery charging)- System losses for PEV injections of 63%, 47%, 32% and 16% without and with DGs.
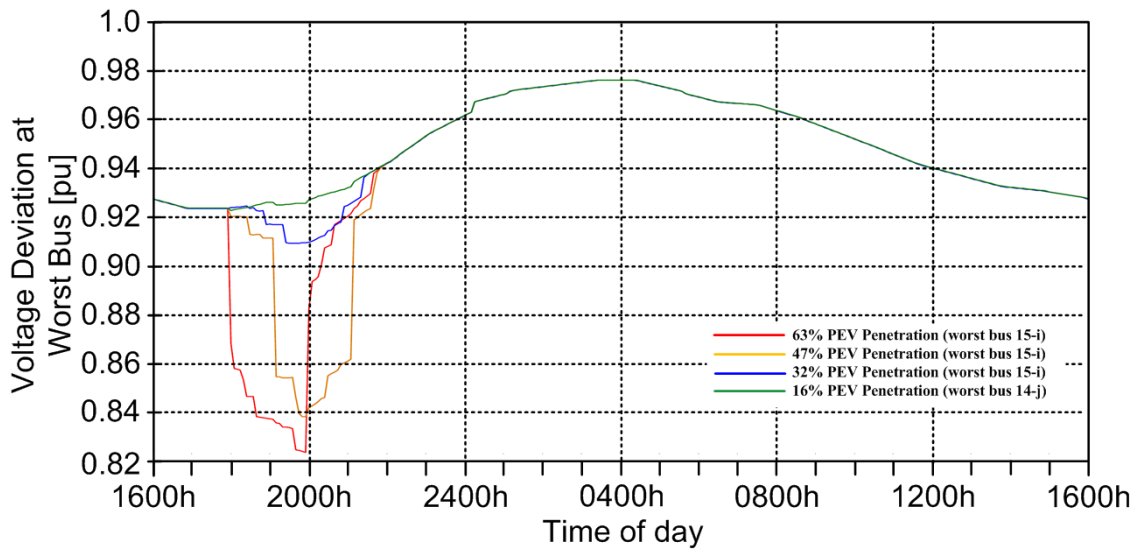
(g) PEV battery charging without coordination, without DGs
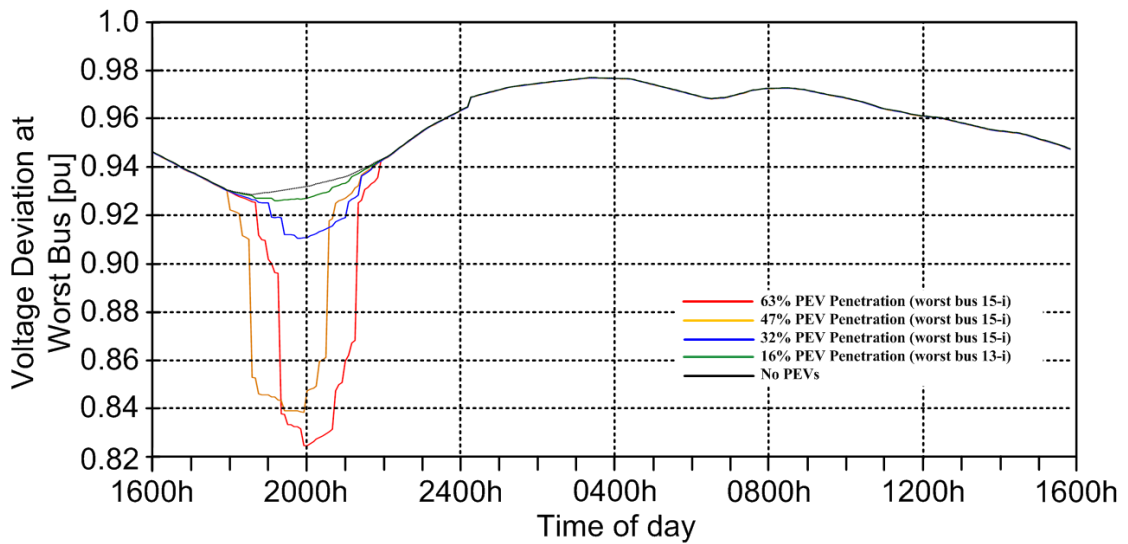
(h) PEV battery charging without coordination, with DGs

Fig. 7.6(g-h). Cases A-B (Uncoordinated PEV battery charging)- Voltage profiles at worst bus for PEV injections of 63%, 47%, 32% and 16% without DGs and with DGs.
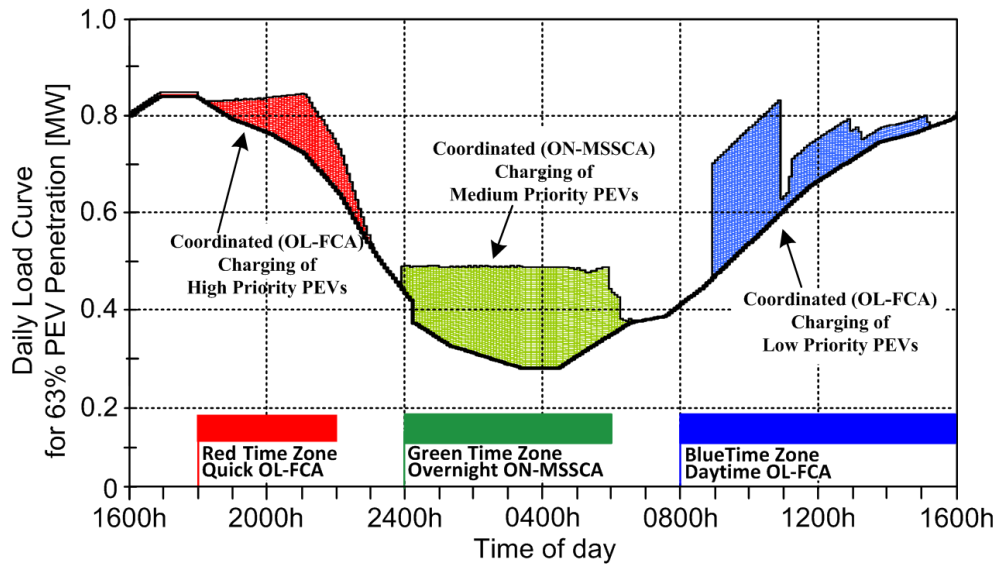
(a) Coordinated PEV battery charging without DGs
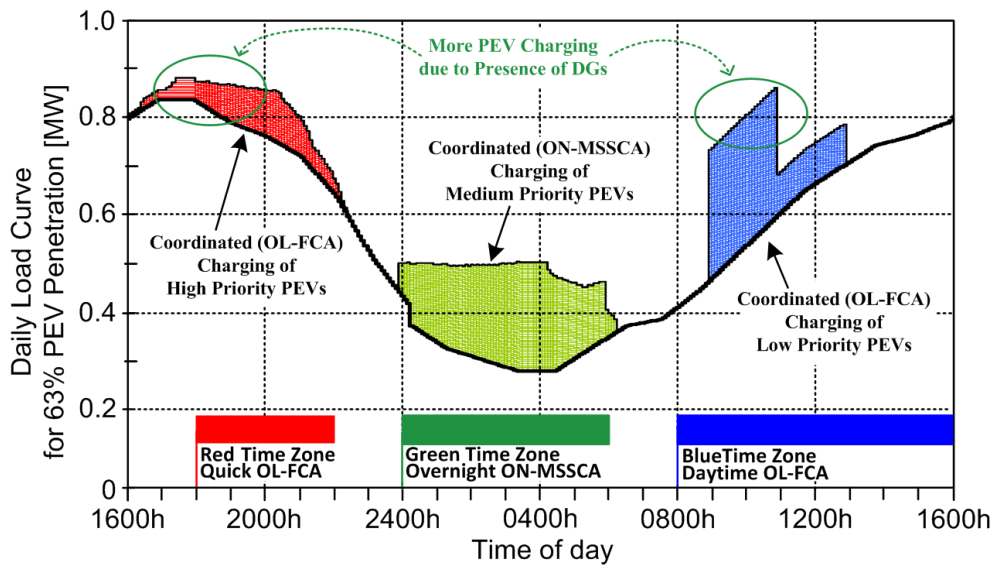
(b) Coordinated PEV battery charging with DGs

Fig. 7.7(a-b). Cases C-D (Coordinated PEV battery charging with proposed OL-F/DL-MSSCC)- Daily load curves (system power consumption) for 63% PEV injection without/with DGs.

(c) Coordinated PEV battery charging without DGs
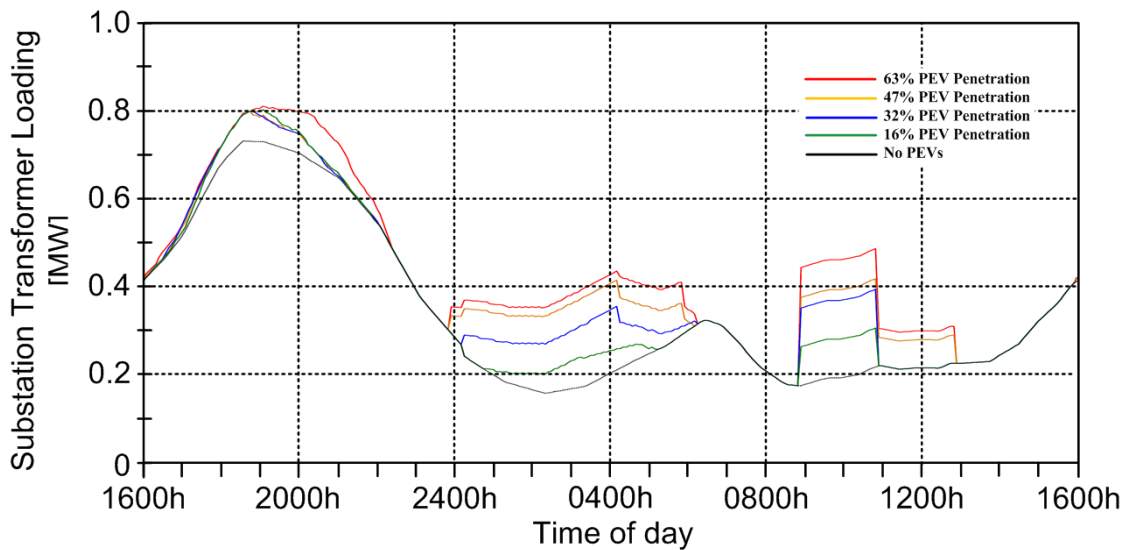
(d) Coordinated PEV battery charging with DGs

Fig. 7.7 (c-d). Cases C-D (Coordinated PEV battery charging with proposed OL-F/DL-MSSCC)-Substation Transformer loadings for PEV injections of 63%, 47%, 32% and 16% without/with DGs.
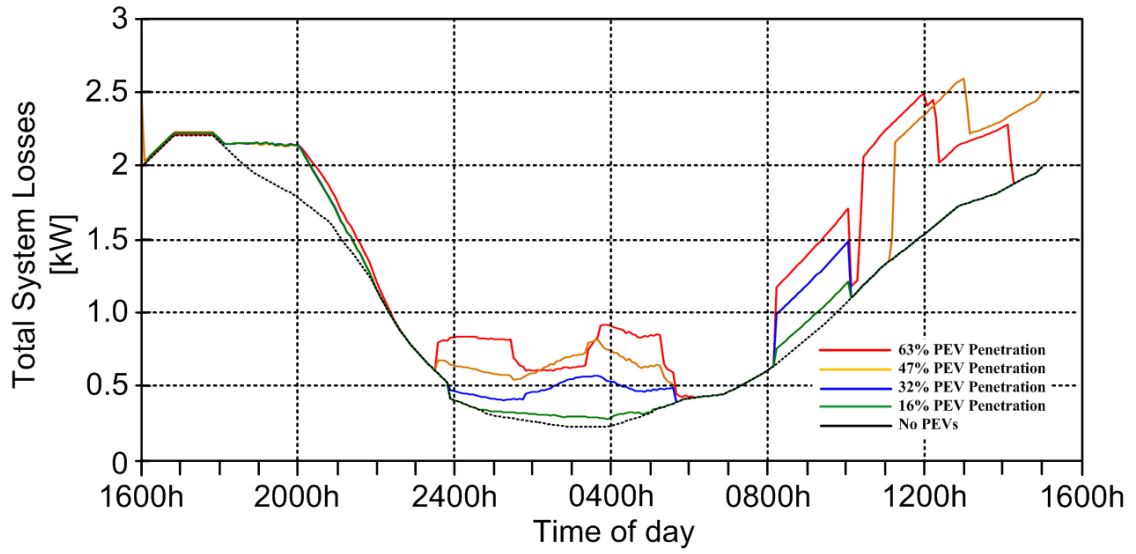
(e) Coordinated PEV battery charging without DGs
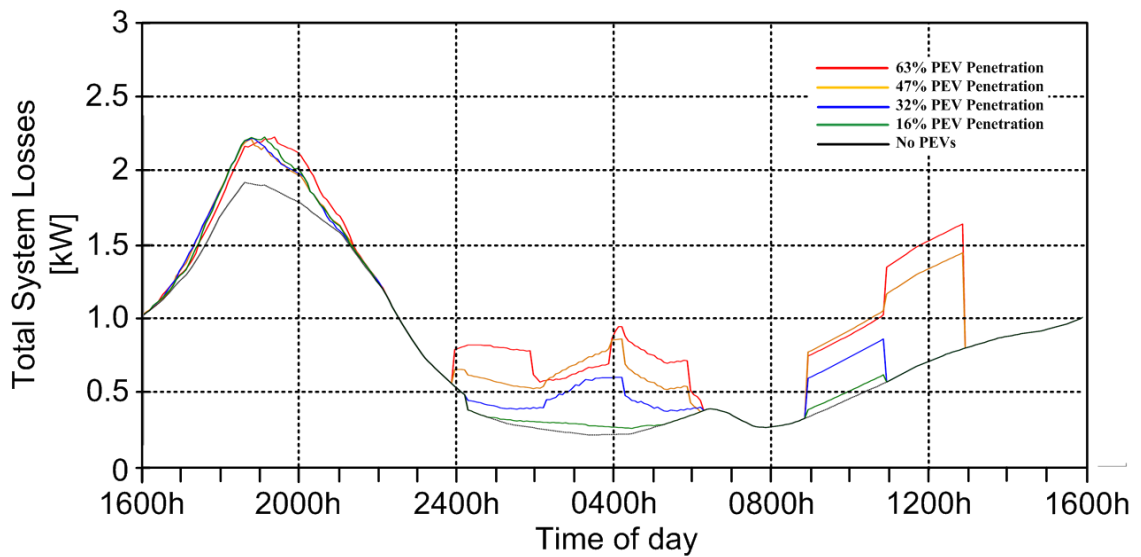
(f) Coordinated PEV battery charging with DGs

Fig. 7.7 (e-f). Cases C-D (Coordinated PEV battery charging with proposed OL-F/DL-MSSCC)- System losses for PEV injections of 63%, 47%, 32% and 16% without/with DGs.
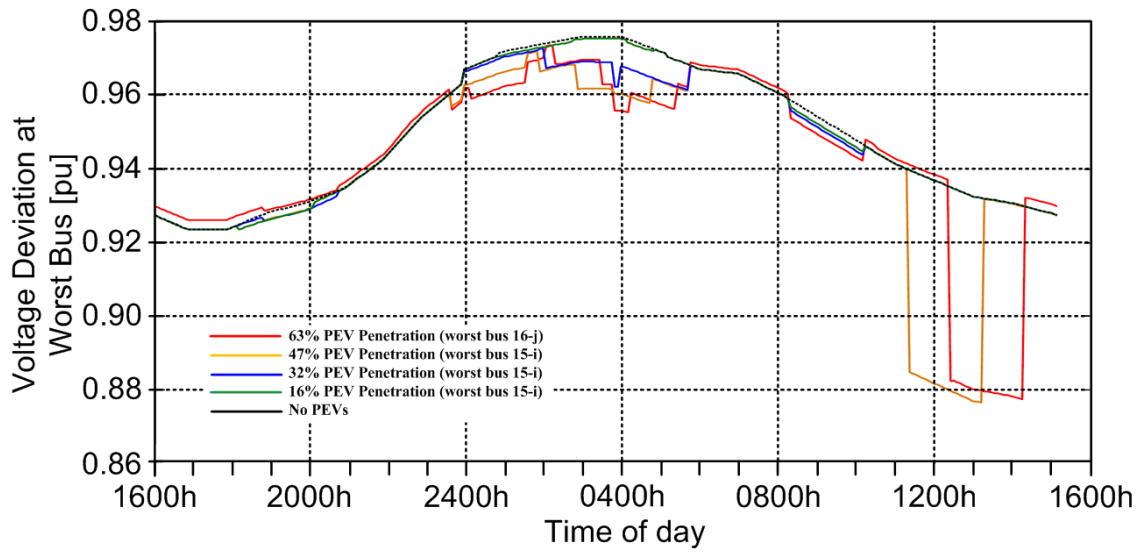
(g) Coordinated PEV battery charging without DGs
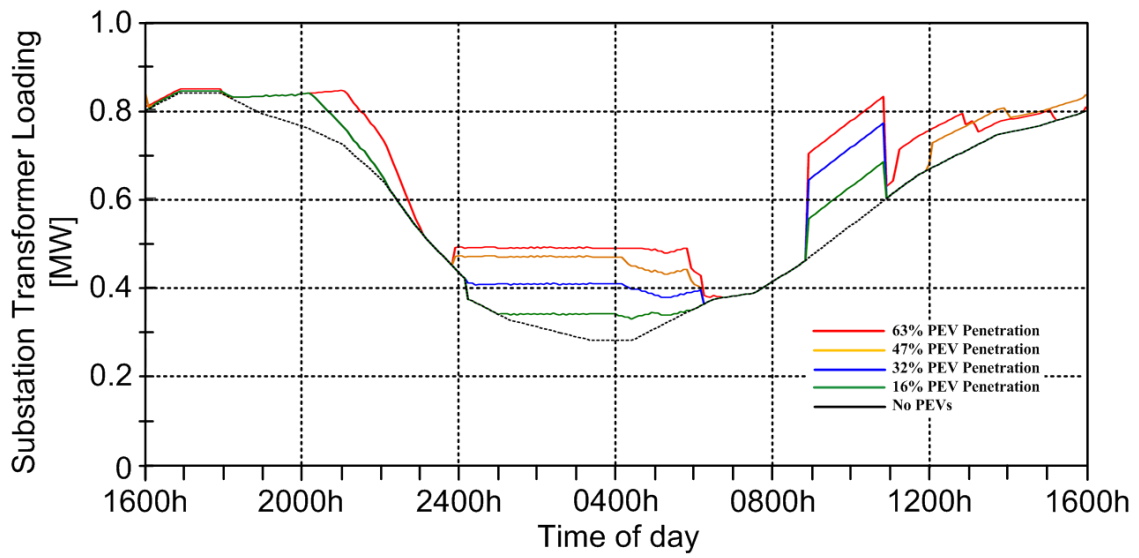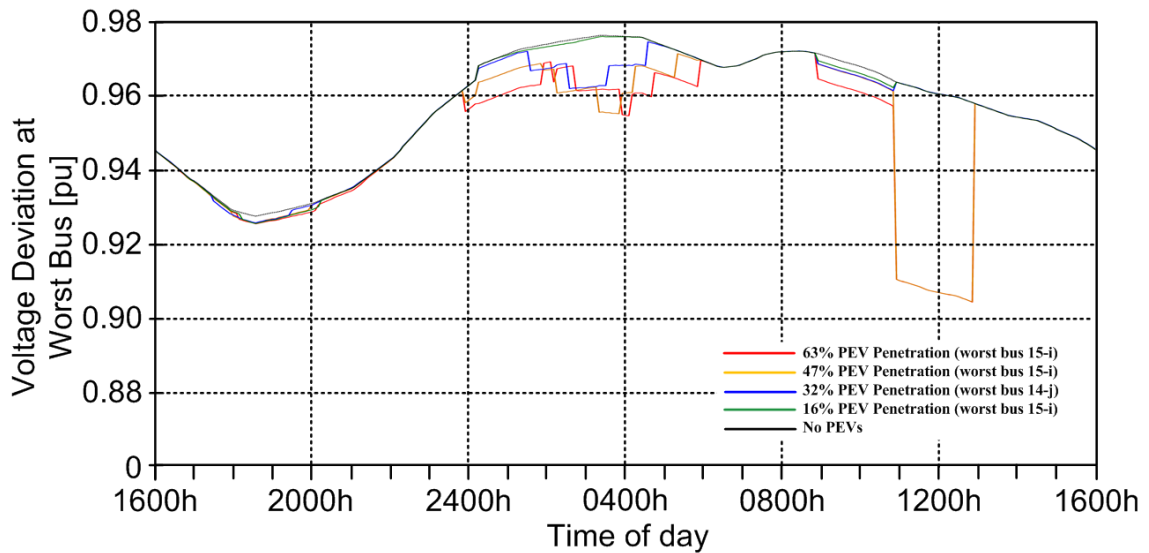

(h) Coordinated PEV battery charging with DGs

Fig. 7.7 (g-h). Cases C-D (Coordinated PEV battery charging with proposed OL-F/DL-MSSCC)-Voltage profiles at worst bus for PEV injections of 63%, 47%, 32% and 16% without/with DGs.

7.5. CONCLUSION

This chapter proposed a new combined/hybrid online fuzzy and delayed sensitivity-based coordinated battery charging (OL-FC/DL-MSSCC) strategy for PEVs in SGs. The proposed algorithm is implemented and verified on the 449-bus smart power grid network that includes the IEEE 22 kV distribution system plus 22 low voltage 415 V residential feeders with PEVs. Based on the comprehensive simulations and detailed analyses, the main contributions and advantages of the proposed OL-FC/DL-MSSCC algorithm are:

✓ It improves customer satisfaction by providing options for consumer priority (e.g., high- medium- and low-priority groups), PEV battery charging types (e.g., expensive fast online evening, inexpensive online daytime and cheap delayed overnight PEV battery charging) and charging time zones (e.g., red, blue and green time zones).

✓ It reduces the generation cost and the total network cost by considering short term market energy prices and directly utilizing distributed renewable (wind and solar) energy for vehicle charging.

✓ It keeps the bus voltages and maximum demand constraints within the permissible limits by using maximum sensitivity selections and fuzzy reasoning.

✓ The online part of the algorithm performs: i) fast expensive fuzzy-based evening PEV battery charging intended for high-priority consumers who are willing to pay high tariff rates for quick vehicle charging in the red charging time zone (1800h-2200h) and, ii) quick inexpensive fuzzy-based daytime PEVs charging intended for medium-priority consumers who are willing to pay moderate tariff rates for fast vehicle charging in the blue charging time zone (0800h-1600h).

✓ The delayed part of the algorithm performs cheap overnight MSS-based PEV battery charging that assurances full charge of all vehicles by 0600h and is intended for low-

priority consumers who are seeking low tariff rates but would like to have their vehicles fully charged for the next day trip.

✓ It decreases the burden on the (distribution/substation) transformers to reduce the possibility and cost of equipment failures and outages.

✓ It offers substantial improvements in terms of loss saving, voltage regulation, cost reduction, line and transformer loadings compared to the uncoordinated, online MSS-based coordinated, online fuzzy-based coordinated and delayed MSS-based coordinated PEV battery charging strategies of Chapters 4-6.

CHAPTER EIGHT: THESIS SUMMARY AND CONTRIBUTIONS

This Ph.D. dissertation investigates the effects PEV battery charging on the performance and operation cost of smart power grids. In addition to the conventional uncoordinated (random) battery charging of vehicles, four new PEV coordinated battery charging strategies based on maximum sensitivities selections (MSS) and Fuzzy reasoning are proposed, analyses, simulated and tested. To enhance the coordination outcomes, online, delayed and combined online-delayed charging strategies are considered. The proposed algorithms are implemented on an assembled 449-bus SG network that consist of the IEEE 31-bus high-voltage 23 kV distribution network [94] and several residential feeders with PEVs, wind DGs and rooftop PVs. Simulations are done for random plugged-in times and random distributed locations of PEVs with injection levels of 16%, 32%, 47% and 63% that correspond to 3, 6, 9, and 12 vehicles in each of the 22 residential networks, respectively. The total number of PEVs are 3x22=66 (for 16% injection), 6x22=132 (for 16% injection), 9x22=198 (for 16% injection), and 12x22=264 (for 16% injection).

To improve customer satisfaction and reduce the cost, real-time variable energy pricing, three consumer priority groups, three battery charging time zones and three charging options (expensive fast online evening, inexpensive online daytime and cheap delayed overnight) are considered. Comprehensive simulations and detailed analyses indicate that the four proposed PEV coordination algorithms mange to charge all vehicles and reduce the costs associated with energy generation and network losses while controlling the bus voltage deviations/regulations and maximum network demands within selected limits.

8.1. Ph.D. Thesis Summary

Chapters 2-3 present literature reviews on the innovating subjects of SG and coordinated PEV battery charging. Chapters 4-7 implement four new PEV coordinated battery

charging strategies and evaluate their performances with random battery charging, and with each other:

- In Chapter 4, a centralized online MSS-based coordinated battery charging (OL-MSSCC) algorithm for PEVs in SGs [55] is proposed and implemented which is an enhancement to the real-time smart load management (RT-SLM) algorithm of [63] with the inclusion of WDGs. The proposed OL-MSSCC algorithm is intended to be centrally executed by the independent system operator (ISO), operates on online bases with time intervals of $\Delta t = 5$ minutes, and relies on the grid, PEVs and WDGs information transmitted by the smart meters. Chapter 4 starts with a quick review of the load flow solution. Sections 4.3 to 4.6 present the concepts, formulation, flow chart, implementation, and simulations (including six case studies) of the OL-MSSCC algorithm and investigate the impacts of WDGs on its performance. The main advantage of the proposed OL-MSSCC over the RT-SLM method is the direct utilization of WDGs energy for PEV battery charging to reduce the possibility of overloading the lines and distribution transforms particularly during peak-load hours.

- In Chapter 5, a new centralized online fuzzy coordinated battery charging (OL-FCC) algorithm for PEVs in smart power grid networks with WDGs [56] is proposed, implemented and tested to achieve further reductions in the total grid cost while monitoring consumers priorities and controlling (voltage regulations and network demand) constraints. Chapter 5 starts with a quick review of fuzzification and defuzzification techniques. Sections 5.2 to 5.4 present the concepts, formulation, flow chart, implementation, and simulations (including ten case studies) of the proposed OL-FCC algorithm and compare its performance with uncoordinated/random and OL-MSSCC coordinated PEV battery charging strategies. The key benefits of OL-FCC

compared with OL-MSSCC of Chapter 4 are further savings in total cost under various operating conditions.

- In Chapter 6, a new and inexpensive PEV coordinated strategy is proposed and implemented that records the network and vehicle information online but postpones the PEV battery charging to early morning hours to reduce the total cost. A new centralized delayed sensitivity-based coordinated PEV battery charging (DL-MSSCC) tactic [57] is proposed, implemented, and tested. Unlike the OL-MSSCC and ON-FCC schemes of Chapters 4-5, the DL-MSSCC algorithm does not offer any priority group options to the PEV owners. Sections 6.2 to 6.5 present the concept, formulation, flow chart, implementation, and simulations (including four case studies) of the proposed DL-MSSCC strategy and compare its performance with the OL-MSSCC and OL-FCC algorithms. The main advantage of DL-MSSCC over OL-MSSCC and OL-FCC of Chapter 4-5 is an additional reduction in the total grid cost; however, it does not offer any consumer priority options and may end up with some customer dissatisfactions.

- In Chapter 7, the online and delayed coordination ideas of Chapters 4-6 are merged. A new centralized online combined fuzzy and delayed sensitivity-based coordinated battery charging (OL-F/DL-MSSCC) strategy [58] for PEVs in SG networks is proposed, implemented and tested that directly utilizes the WDGs and rooftop PVs energies for PEV battery charging. Sections 7.1 to 7.4 present the concept, formulation, flow chart, implementation and simulations (including four case studies) of the proposed OL-F/DL-MSSCC strategy and compare its performance with the OL-MSSCC, OL-FCC and DL-MSSCC algorithms. The main advantage of the proposed OL-F/DL-MSSCC strategy over the OL-MSSCC, OL-FCC and DL-MSSCC

algorithms of Chapter 4-6 is further reductions in the total cost while also improving customer satisfaction by offering three (high, medium and low) priority groups, three battery charging time zones and three (online evening, overnight and online daytime) charging options. It also considers the impacts and contributions of solar DGs (rooftop PVs) that are not included in Chapter 4-6.

The proposed PEV coordinated strategies are implemented in MATLAB and executed on the 449-bus SG network without/with PEVs, rooftop PVs and wind DGs.

8.2. Contributions of the Ph.D. Thesis

The key contributions of this research are:

✓ A centralized online sensitivity-based coordinated battery charging (OL-MSSCC) strategy for the management of PEVs in smart power grids with WDGs [55].

✓ A new centralized online fuzzy-based coordinated battery charging (OL-FCC) strategy for PEVs in SG networks with the consideration of WDGs [56].

✓ A new centralized delayed (overnight) MSS-based coordinated battery charging (DL-MSSCC) strategy for managing PEVs in SG networks with WDGs [57].

✓ A new centralized combined online fuzzy and delayed sensitivity-based coordinated battery charging (OL-F/DL-MSSCC) strategy for PEVs in SG networks with the consideration of wind and solar (rooftop) DGs [58].

The algorithms for the proposed strategies are implemented in MATLAB and executed on the 449-bus SG network. In addition, their performances are compared without and with wind and/or solar DGs.

8.3. Conclusions of the Ph.D. Thesis

This thesis starts with literature reviews on smart power grid and PEV technologies. The reviews highlight the detrimental impacts of uncoordinated PEV battery charging and the

need for practical and fast coordinated battery charging strategies that concurrently consider customer satisfaction, network constraints and cost. Therefore, four new centralized PEV coordinated battery charging strategies are proposed and implemented: 1) an online MSS-based (OL-MSSCC) algorithm [55] which is an enhancement to the RT-SLM algorithm of [63], 2) an online fuzzy-based (OL-FCC) algorithm [56], 3) a delayed MSS-based (DL-MSSCC) algorithm [57] and 4) an online combined fuzzy and delayed sensitivity-based (OL-F/DL-MSSCC) algorithm [58].

All proposed strategies leverage the available renewable solar/wind resources by directly charging the vehicles' batteries from the available wind and/or solar DGs. All proposed strategies are coded/implemented in MATLAB and tested/executed on an assembled 449-bus SG network that consists of the IEEE 31-bus distribution system [94], 22 residential feeders, rooftop residential PVs, PEVs, and residential/distribution wind DGs.

The following are the main conclusions of this thesis:

- Uncoordinated EV battery charging can have detrimental impacts on the distribution network. It can result in substantial increases in electricity demand, power generation requirement and network losses, as well as bus voltage regulation and maximum demand violations especially during peak hours of residential loads hosting large numbers of PEVs.

- All recommended algorithms rely on the SG communication resources. Their online nature eliminates the necessity of forecasting information related to the PEV and DGs statuses.

- All proposed strategies leverage the available renewable wind/solar resources by directly charging the vehicles' batteries from the available wind and/or solar DGs. This is done to lower transformer loadings and reduce the costs associated with

equipment failures and outages.

- All proposed algorithms can effectively schedule vehicle battery charging without and with renewable DGs and reduce the costs associate with generation and losses while retaining bus voltage deviations and maximum network demands within the designated permissible boundaries.

- The OL-MSSCC algorithm effectively schedules vehicle battery charging without and with WDGs at all PEV injection levels by considering three consumer (high, medium and low) priorities, three battery charging time (red, blue and green) zones, dynamic energy prices and grid operation constraints within its formulation.

- The OL-FCC algorithm relies on fuzzy membership functions to: i) provide quick service to the high-priority consumers during early evening hours, ii) intentionally postpone the services to medium-priority and low-priority consumers to reduce the total cost by dynamically adjusting the tolerance of maximum demand using time-dependent weighting factors and, iii) allow minor violations in voltage deviation and maximum demand constraints to accommodate more PEVs.

- The chief privilege of OL-FCC compared with OL-MSSCC is the applications of fuzzy reasoning to augment the probability of arriving at a better PEV coordination plan with less cost. However, it requires the knowledge of experienced engineers to design and develop suitable fuzzy membership functions.

- The DL-MSSCC algorithm is more practical compared to the OL-MSSCC and OL-FCC strategies as it is simple, inexpensive, and relatively easy to implement. Therefore, DL-MSSCC is a good candidate for real-life applications where most PEV drivers/owners are requesting cheap PEV battery charging options. However, it may cause customer dissatisfaction for consumers who require high-priority quick PEV

battery charging during peak load hours.

- The OL-F/DL-MSSCC algorithm offers the advantages of OL-MSSCC, OL-FCC and DL-MSSCC while resolving most of their limitations. It is a potential candidate for online coordination of PEVs in large smart power grid networks since it is relatively simple, fast, practical, and easy to implement. It improves customer satisfaction by offering: i) three consumer (high, medium and low) priority options, ii) three charging types (fast online evening, online daytime and cheap overnight) options, iii) three battery charging time (red, blue and green) zones and, iv) the ability to charge at high, medium or low tariff rates. It reduces the total network cost by considering short term market energy prices and directly using the accessible renewable (wind and solar) energy for battery charging while keeping bus voltages and maximum network demand constraints within the allowable bounds based on maximum sensitivity selections and/or fuzzy reasoning.

- The online part of the OL-F/DL-MSSCC algorithm performs: i) fast expensive fuzzy-based evening PEV battery charging intended for high-priority consumers who are willing to pay high tariff rates for quick vehicle charging in the red battery charging time zone (1800h-2200h) and, ii) quick inexpensive fuzzy-based daytime PEVs charging intended for medium-priority consumers who are willing to pay moderate tariff rates for fast vehicle charging in the blue charging time zone (0800h-1600h).

- The delayed part of the OL-F/DL-MSSCC algorithm performs cheap overnight MSS-based PEV battery charging that guarantees full level of battery charge of all vehicles by 0600h and is intended for low-priority consumers who are seeking low tariff rates but would like to have their vehicles fully charged for the next day trips.

- Renewable energy resources substantially enhance the performance of all proposed

strategies by reducing system losses, the cost of generation and the loading of transformers. The most appropriate areas for the installation of wind generation units are near the residential feeders with high injections of PEVs, the end of the high voltage feeders and close to the charging stations. For the smart power grid network of Fig. 4.7, the best buses for the placement of WDGs in the order of preference are: i) buses 10-15, ii) buses 6-8, iii) buses 16-18, iv) buses 20-21, and v) buses 24-28. The complete system performance will be enhanced if the peak WDG generation times are during early evening hours or if they overlaps with the peak PEV battery charging demands.

8.4. Future Recommendations

This thesis has considered and addressed several issues related to battery charging of electric vehicles and their possible impacts on the power networks. However, there are still several scopes and research directions for further studies:

- The proposed scheduling algorithms do not consider vehicle battery discharging scenarios which is still an open area for further research. The proposed MSS-based and the fuzzy-based PEV battery charging coordination solutions can be extended to also include battery discharging to inject active and/or reactive power into the grid.

- The proposed scheduling algorithms do not consider the impacts of driving paths and the traffic flows. Future research can be on the impacts of rush hour traffic and the high PEV demands at the charging stations on the power network.

- Finding the optimal locations and the optimal sizes of the public charging stations is another interesting research area. Then, the proposed centralized online fuzzy charging algorithm of chapter 5 can be extended to supervise the drivers and encourage them to charge their vehicles at the charging stations with shorter queues.

- The proposed PEV battery charging management tactics may be enhanced to also optimize customer's/driver's satisfaction.

- The implemented PEV coordinated battery charging algorithms can be improved by considering the impacts of traffic on trip patterns, times, and durations.

- Investigating the impacts of communication failure and/or communication interruptions on the performance and resilience of the EV battery charging coordination algorithms.

REFERENCES

Every reasonable effort has been made to acknowledge the owners of copyright material. I would be pleased to hear from any copyright owner who has been omitted or incorrectly acknowledged.

[1]. K. Zhangi, Y. Maoi, S. Leng, S. Maharjan, Y. Zhang, A. Vinel, M. Jonsson, "Incentive-Driven Energy Trading in the Smart Grid, IEEE Access, vol. 4. pp.1243-1255, 2016.

[2]. R. Deng, Z. Yang, M. Y. Chow, J. Chen, "A Survey on Demand Response in Smart Grids: Mathematical Models and Approaches", IEEE Trans. on Industrial Informatics, vol.11, no.3, pp.570-582, 2015.

[3]. H. Liang, A. K. Tamang, W. Zhuang, X. Shen, "Stochastic Information Management in Smart Grid", IEEE Communications Survey & Tutorials, vol.16, no.3, Third Quarter, pp.1746-1770, 2014.

[4]. X. Fang, S. Misra, G. Xue, D. Yang, "Smart Grid- The New and Improved Power Grid: A Survey," IEEE Communications Survey & Tutorials, vol.14, no.4, Fourth Quarter, pp.944-980, 2012.

[5]. S. P. Rosado, S. K. Khadem, "Development of Community Grid: Review of Technical Issues and Challenges", IEEE Trans. on Industry Applications, vol.55, no.2, pp.1171-1179, 2019.

[6]. D. Manz, R. Walling, N. Miller, B. LaRose, R. D'Aquila, B. Daryanian, "The Grid of the Future: Ten Trends that will Shape the Grid Over the Next Decade," IEEE Power and Energy Magazine, vol.12, no.3, pp.26-36, 2014.

[7]. H. Zou, S. Mao, Y. Wang, F. Zhang, X. Chen, L. Chang, "A Survey of Energy Management in Interconnected Multi-Microgrids", IEEE Access, vol.7, pp.72158-72169, 2019.

[8]. M. N. Alam, S. Chakrabarti, A. Ghosh, "Networked Microgrids: State-of-the-Art and Future Perspectives", IEEE Trans. on Industrial Informatics, vol.15, no.3, pp.1238-1250, 2019.

[9]. Y. Han, K. Zhang, H. Li, E. A. A. Coelho, J. M. Guerrero, "MAS-Based Distributed Coordinated Control and Optimization in Microgrid and Microgrid Clusters: A

Comprehensive Overview", IEEE Trans. On Power Electronics, vol.33, no.8, pp.6488-6508, 2018.

[10]. M. Faisal, M. Hannan, P. J. Ker, A. Hussain, M. B. Mansor, F. Blaabjerg, "Review of Energy Storage System Technologies in Microgrid Applications: Issues and Challenges", IEEE Access, vol.6, pp.35143-35164, 2018.

[11]. X. Li, S. Wang, "A Review of Energy Management, Operation Control and Application Methods for Grid Battery Storage Systems", Chinese Society for Electrical Engineering (CSEE) Journal of Power and Energy Systems, Early Access Article, 2020.

[12]. A. H. Mohsenian-Rad and A. Leon-Garcia, "Optimal Residential Load Control with Price Prediction in Real-Time Electricity Pricing Environments", IEEE Trans. Smart Grid, vol.1, no.2, pp.120-133, 2010.

[13]. P. Samadi, H. Mohsenian-Rad, R. Schober, V. W. Wong, "Advanced Demand Side Management for the Future Smart Grid using Mechanism Design," IEEE Trans. Smart Grid, vol. 3, no. 3, pp. 1170–1180, 2012.

[14]. A. Mohsenian-Rad, V. W. Wong, J. Jatskevich, R. Schober, A. Leon-Garcia, "Autonomous Demand Side Management based on Game-Theoretic Energy Consumption Scheduling for the Future Smart Grid," IEEE Trans. Smart Grid, vol. 1, no. 3, pp. 320–331, 2010.

[15]. P. Du, N. Lu, "Appliance Commitment for Household Load Scheduling," IEEE Trans. Smart Grid, vol. 2, no. 2, pp. 411–419, 2011.

[16]. H. Kanchev, D. Lu, F. Colas, V. Lazarov, B. Francois, "Energy Management and Operational Planning of a Microgrid with a PV-based Active Generator for Smart Grid Applications," IEEE Trans. Ind. Electron., vol. 58, no. 10, pp. 4583–4592, 2011.

[17]. A. Molderink, V. Bakker, M. G. C. Bosman, J. L. Hurink, G. J. M. Smit, "Management and Control of Domestic Smart Grid Technology", IEEE Trans. Smart Grid, vol.1, no.2, pp.109-119, 2010.

[18]. M. Parvania, M. Fotuhi-Firuzabad, "Demand Response Scheduling by Stochastic SCUC," IEEE Trans. Smart Grid, vol. 1, no. 1, pp. 89–98, Jun. 2010.

[19]. J. Zhang, J. D. Fuller, S. Elhedhli, "A Stochastic Programming Model for a Day-Ahead Electricity Market with Real-Time Reserve Shortage Pricing," IEEE Trans. Power Systems, vol. 25, no. 2, pp. 703–713, 2010.

[20]. J. Sun, V. Palade, X.-J. Wu, W. Fang, Z. Wang, "Solving the Power Economic Dispatch Problem with Generator Constraints by Random Drift Particle Swarm Optimization," IEEE Trans. Ind. Informat., vol. 10, no. 1, pp. 222–232, 2014.

[21]. M. A. A. Pedrasa, T. D. Spooner, I. F. MacGill, "Coordinated Scheduling of Residential Distributed Energy Resources to Optimize Smart Home Energy Services," IEEE Trans. Smart Grid, vol. 1, no. 2, pp. 134–143, 2010.

[22]. M. Pedrasa, T. D. Spooner, I. F. MacGill, "Scheduling of Demand Side Resources using Binary Particle Swarm Optimization," IEEE Trans. Power Systems, vol. 24, no. 3, pp. 1173–1181, 2009.

[23]. A. S. Bahaj, P. A. B. James, "Electrical Minigrids for Development: Lessons from the Field", Proceedings of the IEEE, vol. 107, no. 9, pp. 1967-1980, 2019.

[24]. S. P. Rosado, S. K. Khadem, "Development of Community Grid: Review of Technical Issues and Challenges," IEEE Trans. Industry Applications, vol. 55, no. 2, pp. 1171–1179, 2019.

[25]. C. C. Chu, H. H. C. Iu, "Complex Networks Theory For Modern Smart Grid Applications: A Survey," Journal on Emerging and Selected Topics in Circuits and System, vol. 7, no. 2, pp. 177-191, 2017.

[26]. J. Rodriguez-Molina, D. M. Kammen, "Middleware Architectures for the Smart Grid: A Survey on the State-of-the-Art, Taxonomy and Main Open Issues," IEEE Communications Surveys & Tutorials, vol. 20, no. 4, pp. 2992-3033, 2018.

[27]. W. Zhong, K. Xie, Y. Liu, C. Yang, S. Xie, Y. Zhang, "Online Control and Near-Optimal Algorithm for Distributed Energy Storage Sharing in Smart Grid," IEEE Trans. Smart Grid, Early Access Article, 2019.

[28]. D. Kodaira, W. Jung, S. Han, "Optimal Energy Storage System Operation for Peak Reduction in a Distribution Network Using a Prediction Interval," IEEE Trans. Smart Grid, Early Access Article, 2019.

[29]. F. Mancilla–David, A. Angulo, A. Street, "Power Management in Active Distribution Systems Penetrated by Photovoltaic Inverters: A Data–Driven Robust Approach," IEEE Trans. Smart Grid, Early Access Article, 2019.

[30]. Y. Xu, Z. Yang, W. Gu, M. Li, Z. Deng, "Robust Real-Time Distributed Optimal Control Based Energy Management in a Smart Grid," IEEE Trans. Smart Grid, vol. 8, no. 4, pp. 1568-1579, 2017.

[31]. X. Li, S. Wang, "A Review on Energy Management, Operation Control and Application Methods for Grid Battery Energy Storage Systems," CSEE Journal of Power and Energy Systems, Early Access Article, 2019.

[32]. P. Siano, G. D. Marco, A. Rolan, V. Loia, "A Survey and Evaluation of the Potentials of Distributed Ledger Technology for Peer-to-Peer Transactive Energy Exchanges in Local Energy Markets," IEEE System Journal, vol. 13, no. 3, pp. 3454-3466, 2019.

[33]. M. Erol-Kantarci, H. T. Mouftah, "Energy-Efficient Information and Communication Infrastructures in the Smart Grid: A Survey on Interactions and Open Issues," IEEE Communications Surveys & Tutorials, vol. 17, no. 1, pp. 179-197, 2015.

[34]. P. Kumar, Y. Li, G. Bai, A. Paverd, J. S. Dong, A. Martin, "Smart Grid Metering Networks: A Survey on Security, Privacy and Open Research Issues," IEEE Communications Surveys & Tutorials, vol. 21, no. 3, pp. 2886-2927, 2019.

[35]. A. Ghosal, M. Conti, "Key Management Systems for Smart Grid Advanced Metering Infrastructure: A Survey," IEEE Communications Surveys & Tutorials, vol. 21, no. 3, pp. 2831-2848, 2019.

[36]. K. Dehghanpour, Z. Wang, J. Wang, Y. Yuan, F. Bu, "A Survey on State Estimation Techniques and Challenges in Smart Distribution Systems," IEEE Trans. Smart Grid, vol. 10, no. 2, pp. 2312-2322, 2019.

[37]. P. Eder-Neuhauser, T. Zseby, J. Fabini, "Resilience and Security: A Qualitative Survey of Urban Smart Grid Architectures," IEEE Access, vol. 4, pp. 839-848, 2016.

[38]. [2017-1B]. K. E. Antoniadou-Plytaria, I. N. Kouveliotis-Lysikatos, P..S. Georgilakis, N. D. Hatziargyriou, "Distributed and Decentralized Voltage Control of Smart Distribution Networks: Models, Methods, and Future Research," IEEE Trans. Smart Grid, vol. 8, no. 6, pp. 2999-3008, 2017.

[39]. F. Nejabatkhah, Y. W. Li, H. Tian, "Power Quality Control of Smart Hybrid AC/DC Microgrids: An Overview," IEEE Access, vol. 7, pp. 52295-52318, 2019.

[40]. M. Ghorbanian, S. H. Dolatabadi, P. Siano, "Big Data Issues in Smart Grids: A Survey," IEEE System Journal, vol. 13, no. 4, pp. 4158-4168, 2019.

[41]. H. Sun, Q. Guo, J. Qi, V. Ajjarapu, R. Bravo, J. Chow, Z. Li, E. Nasr-Azadani, U. Tamrakar, G. N. Taranto, R. Tonkoski, G. Valverde, Q. Wu, G. Yang, "Review of Challenges and Research Opportunities for Voltage Control in Smart Grids," IEEE Trans. Power Systems, vol. 34, no. 4, pp. 2790-2801, 2019.

[42]. X. Liu, C. Qian, W. G. Hatcher, H. Xu, W. Liao, W. Yu, "Secure Internet of Things (IoT)-Based Smart-World Critical Infrastructures: Survey, Case Study and Research Opportunities," IEEE Access, vol. 7, pp. 79523-79544, 2019.

[43]. Global EV Outlook 2017, International Energy Agency (IEA); https://webstore.iea.org/global-ev-outlook-2017.

[44]. Global EV Outlook 2019, International Energy Agency (IEA); https://webstore.iea.org/global-ev-outlook-2019.

[45]. P.K. Konk, G.K. Karagiannidis, "Charging Schemes for Plug-In Hybrid Electric Vehicles in Smart Grid: A Survey", IEEE Access, vol. 4. pp.6846-6875, 2016.

[46]. J. C. Mukherjee and A. Gupta, "A Review of Charge Scheduling of Electric Vehicles in Smart Grid," IEEE System Journal, vol. 9, no. 4, pp. 1541-1553, 2015.

[47]. N. I. Nimalsiri, C. P. Mediwaththe, E. L. Ratnam, M. Shaw, D. B. Smith and S. K. Halgamuge, "A Survey of Algorithms for Distributed Charging Control of Electric Vehicles in Smart Grid," IEEE Trans. Intelligent Transportation Systems, Early Access Article, 2019.

[48]. K. Clement-Nyns, E. Haesen, and J. Driesen, "The impact of charging plug-in hybrid electric vehicles on a residential distribution grid," IEEE Trans. Power Syst., vol. 25, no. 1, pp. 371–380, Feb. 2010.

[49]. S. Alshahrani, M. Khalid and M. Almuhaini "Electric Vehicles Beyond Energy Storage and Modern Power Networks: Challenges and Applications", IEEE Access, vol. 7. pp.99031-99064, 2019.

[50]. D. Meyer and J. Wang, "Integrating Ultra-Fast Charging Stations within the Power Grids of Smart cities: a Review" IET Proceedings on Smart Grid, vol.1, no.1, pp.3-10, 2018.

[51]. S. Deilami, "Optimal Dispatch of Shunt Capacitors and Load Tap Changers in Distorted Distribution Systems using Ant Colony Algorithms," Master of Philosophy in Electrical and Computer Engineering, Curtin University, November 2010.

[52]. Amir S. Masoum, "Impact of Coordinated and Uncoordinated battery charging of Plug-in Electric Vehicle on Smart Grids," Master of Engineering Science in Electrical Utility Engineering, Curtin University, November 2010.

[53]. Amir S. Masoum, A. Abu-Siada, S. Islam, "Impact of Uncoordinated and Coordinated battery charging of Plug-in Electric Vehicle on Substation Transformer", IEEE ISGT Asia 2011 (Innovative Smart Grid Technologies Europe) Conference, Perth, WA, pp.1-7, Nov 13-16, 2011, and Elixir, Electrical Engineering International Journal, vol. 41, pp. 5779-5784, 2011.

[54]. Amir S. Masoum, S. Deilami, M.A.S. Masoum and A. Abu-Siada, "A heuristic approach for coordination of plug-in electric vehicles charging in smart grid", CSCanada, International Canadian Journal, Energy Science and Technology, vol.5, no.2, pp.16-24, 2013.

[55]. Amir S. Masoum, S. Deilami, M.A.S. Masoum, A. Abu-Siada, S. Islam, "Online Coordination of Plug-in Electric Vehicle Charging in Smart Grid with Distributed Wind power Generation Systems", 2014 IEEE PES General Meeting, pp.1-6, July 27-31, 2014, Washington, USA.

[56]. Amir S. Masoum, S. Deilami, M.A.S. Masoum, A. Abu-Siada, "Fuzzy Approach for Online Coordination of Plug-in Electric Vehicle Charging in Smart Grids," IEEE Trans. Sustainable Energy, vol.6, no.3, pp.1112-1121, 2015.

[57]. Amir S. Masoum, S. Deilami, M.A.S. Masoum, A. Abu-Siada, S. Islam, "Overnight Coordinated battery charging of Plug-in Electric Vehicle based on Maximum Sensitivities Selections", 2014 International Conference on Applied Engineering Sciences (ICAES 2014), Los Angeles, USA, July 23-24, 2014.

[58]. Amir S. Masoum, A. Abu-Siada, S. Islam, "Combined Online and Delayed Coordinated battery charging of Plug-in Electric Vehicles Considering Distributed Wind and Rooftop PV Generations", Technology and Economics of Smart Grids and Sustainable Energy 2016 Journal, Springer, Journal e-ISSN: 2199-4706 (Online), DOI: 10.1007/s40866-016-0012-3, pp.1-12, 2016.

[59]. https://en.wikipedia.org/wiki/Electric_car_use_by_country

[60]. Shareef, M. M. Islam and A. Mohamed, "A Review of the Stage-of-the-art Charging Technologies, Placement Methodologies, and Impacts of Electric Vehicles" Journal of Renewable and Sustainable Energy Reviews, Elsevier, vol. 64, pp.403-420, 2016.

[61]. A. Ahmadi, A. tavakoli, P. Jamborsalamati, N. Rezaei, M. R. Miveh, F. H. Gandoman, A. Heidari and A. E. Nezhad, "Power Quality Improvement in Smart Grids using Electric Vehicles: A Review" IET Proceedings on Electrical Systems in Transportation, vol.9, no.2, pp.53-64, 2019.

[62]. Amir S. Masoum, S. Deilami, P.S. Moses, M.A.S. Masoum, A. Abu-Siada, "Smart Load Management of Plug-in Electric Vehicle in Distribution and Residential Networks with Charging Stations for Peak Shaving and Loss Minimization Considering Voltage Regulation", IET Proceedings on Generation, Transmission and Distribution, vol.5, no.8, pp.877-888, 2011.

[63]. S. Deilami, Amir S. Masoum, P.S. Moses, M.A.S. Masoum, "Real-Time Coordination of Plug-in Electric Vehicle Charging in Smart Grids to Minimize Power Losses and Improve Voltage Profile", IEEE Trans. on Smart Grid, vol.2, no.3, pp.456-467, 2011.

[64]. E. Sortomme, M.M. Hindi, S.D.J. MacPherson and S.S. Venkata, "Coordinated battery charging of Plug-in Hybrid Electric Vehicles to Minimize Distribution System Losses", IEEE Trans. Smart Grid, vol.2, no.1, pp.198-205, 2011.

[65]. E. Sortomme and M.A. El-Sharkawi, "Optimal Scheduling of Vehicle-to-Grid Energy and Ancillary Services," IEEE Trans. Smart Grid, vol.3, no.1, pp.351-359, 2012.

[66]. S. Han, S. Han, and K. Sezaki, "Development of an optimal vehicle-to- grid aggregator for frequency regulation", IEEE Trans. Smart Grid, vol.1, no.1, pp.65-72, 2010.

[67]. D. Wu, D.C. Aliprantis and L. Ying, "Load scheduling and dispatch for aggregators of plug-in electric vehicles", IEEE Trans. on Smart Grid, vol.3, no.1, pp.368-376, 2012.

[68]. P. Richardson, D. Flynn and A. Keane, "Optimal charging of electric vehicles in low-voltage distribution systems," IEEE Trans. on Power Systems, vol.27, no.1, pp.268-279, 2012.

[69]. Y. Xu, "Optimal distributed charging rate control of plug-in electric vehicles for demand management," IEEE Trans. Power Syst., vol. 30, no. 3, pp. 1536–1545, May 2015.

[70]. T. Zhao and Z. Ding, "Distributed initialization-free cost-optimal charging control of plug-in electric vehicles for demand management," IEEE Trans. Ind. Informat., vol. 13, no. 6, pp. 2791–2801, Dec. 2017.

[71]. A. Ghavami, K. Kar, and A. Gupta, "Decentralized charging of plug-in electric vehicles with distribution feeder overload control," IEEE Trans. Autom. Control, vol. 61, no. 11, pp. 3527–3532, Nov. 2016.

[72]. J. Tan and L. Wang, "Enabling reliability-differentiated service in residential distribution networks with PHEVs: A hierarchical game approach," IEEE Trans. Smart Grid, vol. 7, no. 2, pp. 684–694, Mar. 2016.

[73]. K. Zhou and L. Cai, "Randomized PHEV charging under distribution grid constraints," IEEE Trans. Smart Grid, vol. 5, no. 2, pp. 879–887, Mar. 2014.

[74]. M. C. Kisacikoglu, F. Erden, and N. Erdogan, "Distributed control of PEV charging based on energy demand forecast," IEEE Trans. Ind. Informat., vol. 14, no. 1, pp. 332–341, Jan. 2018.

[75]. Y. Mou, H. Xing, Z. Lin, and M. Fu, "Decentralized optimal demand-side management for PHEV charging in a smart grid," IEEE Trans. Smart Grid, vol. 6, no. 2, pp. 726–736, Mar. 2015.

[76]. H. Xing, M. Fu, Z. Lin, and Y. Mou, "Decentralized optimal scheduling for charging and discharging of plug-in electric vehicles in smart grids," IEEE Trans. Power Syst., vol. 31, no. 5, pp. 4118–4127, Sep. 2016.

[77]. H. Liu, Z. Hu, Y. Song, and J. Lin, "Decentralized vehicle-to-grid control for primary frequency regulation considering charging demands," IEEE Trans. Power Syst., vol. 28, no. 3, pp. 3480–3489, Aug. 2013.

[78]. Z. Liu, Q. Wu, S. Huang, L. Wang, M. Shahidehpour, and Y. Xue, "Optimal day-ahead charging scheduling of electric vehicles through an aggregative game model," IEEE Trans. Smart Grid, vol. 9, no. 5, pp. 5173–5184, Sep. 2018.

[79]. M. Moghbel, "Decentralized Coordinated battery charging of Plug-in Electric Vehicles in Unbalanced Residential Networks to Control Distribution Transformer

Loading, Voltage Profile and Current Unbalance" Master of Philosophy in Electrical and Computer Engineering, Curtin University, March 2013.

[80]. Z. Xu, Z. Hu, Y. Song, W. Zhao, and Y. Zhang, "Coordination of PEVs charging across multiple aggregators," Appl. Energy, vol. 136, pp. 582–589, Dec. 2014.

[81]. Z. Peng and L. Hao, "Decentralized coordination of electric vehicle charging stations for active power compensation," in Proc. 86th IEEE Conf. Veh. Technol., Toronto, ON, Canada, Sep. 2017, pp. 1–5.

[82]. W. Yao, J. Zhao, F. Wen, Y. Xue, and G. Ledwich, "A hierarchical decomposition approach for coordinated dispatch of plug-in electric vehicles," IEEE Trans. Power Syst., vol. 28, no. 3, pp. 2768–2778, Aug. 2013.

[83]. W. Tushar, W. Saad, H. V. Poor, and D. B. Smith, "Economics of electric vehicle charging: A game theoretic approach," IEEE Trans. Smart Grid, vol. 3, no. 4, pp. 1767–1778, Dec. 2012.

[84]. W. Qi, Z. Xu, Z.-J. M. Shen, Z. Hu, and Y. Song, "Hierarchical coordinated control of plug-in electric vehicles charging in multifamily dwellings," IEEE Trans. Smart Grid, vol. 5, no. 3, pp. 1465–1474, May 2014.

[85]. J. Hu, S. You, M. Lind, and J. Ostergaard, "Coordinated battery charging of electric vehicles for congestion prevention in the distribution grid," IEEE Trans. Smart Grid, vol. 5, no. 2, pp. 703–711, Mar. 2014.

[86]. Y. Liu, R. Deng, and H. Liang, "A stochastic game approach for PEV charging station operation in smart grid," IEEE Trans. Ind. Informat., vol. 14, no. 3, pp. 969–979, Mar. 2018.

[87]. S. Vandael, B. Claessens, M. Hommelberg and T. Holvoet, G. Deconinck, "A scalable three-step approach for demand side management of plug-in hybrid vehicles," IEEE Trans. on Smart Grid, vol.4, no.2, pp.720-728, 2013.

[88]. C. Shao, X. Wang, X. Wang, C. Du, and B. Wang, "Hierarchical charge control of large populations of EVs," IEEE Trans. Smart Grid, vol. 7, no. 2, pp. 1147–1155, Mar. 2016.

[89]. C.-K. Wen, J.-C. Chen, J.-H. Teng, and P. Ting, "Decentralized plug-in electric vehicle charging selection algorithm in power systems," IEEE Trans. Smart Grid, vol. 3, no. 4, pp. 1779–1789, Dec. 2012.

[90]. C. P. Mediwaththe and D. B. Smith, "Game-theoretic electric vehicle charging management resilient to non-ideal user behavior," IEEE Trans. Intell. Transp. Syst., vol. 19, no. 11, pp. 3486–3495, Nov. 2018.

[91]. A. Malhotra, G. Binetti, A. Davoudi, and I. D. Schizas, "Distributed power profile tracking for heterogeneous charging of electric vehicles," IEEE Trans. Smart Grid, vol. 8, no. 5, pp. 2090–2099, Sep. 2017.

[92]. J. C. Mukherjee and A. Gupta, "Distributed charge scheduling of plug-in electric vehicles using inter-aggregator collaboration," IEEE Trans. Smart Grid, vol. 8, no. 1, pp. 331–341, Jan. 2017.

[93]. M. Zhongjing, D.S. Callaway and I.A. Hiskens, "Decentralized charging control of large populations of plug-in electric vehicles," IEEE Trans. on Control Systems Technology, vol.21, no.1, pp.67-78, 2013.

[94]. Y. He, B. Venkatesh, and L. Guan, "Optimal scheduling for charging and discharging of electric vehicles," IEEE Trans. Smart Grid,vol.3, no. 3, pp. 1095–1105, Sep. 2012.

[95]. L. Gan, U. Topcu, and S. H. Low, "Optimal decentralized protocol for electric vehicle charging," IEEE Trans. Power Syst., vol. 28, no. 2, pp. 940–951, May 2013.

[96]. G. Binetti, A. Davoudi, D. Naso, B. Turchiano, and F. L. Lewis, "Scal-able real-time electric vehicles charging with discrete charging rates," IEEE Trans. Smart Grid, vol. 6, no. 5, pp. 2211–2220, Sep. 2015.

[97]. D. M. Anand, R. T. de Salis, Y. Cheng, J. Moyne, and D. M. Tilbury, "A hierarchical incentive arbitration scheme for coordinated PEV charging stations," IEEE Trans. Smart Grid, vol. 6, no. 4, pp. 1775–1784, Jul. 2015.

[98]. J. Tan and L. Wang, "Real-time charging navigation of electric vehicles to fast charging stations: A hierarchical game approach," IEEE Trans. Smart Grid, vol. 8, no. 2, pp. 846–856, Mar. 2017.

[99]. M. Liu, P. K. Phanivong, and D. S. Callaway, "Electric vehicle charging control in residential distribution network: A decentralized event-driven realization," in Proc. 56th IEEE Annu. Conf. Decis. Control, Melbourne, VIC, Australia,, pp. 214–219, Dec. 2017.

[100]. L. Zhang, V. Kekatos, and G. B. Giannakis, "Scalable electric vehi-cle charging protocols," IEEE Trans. Power Syst., vol. 32, no. 2, pp. 1451–1462, Mar. 2017.

[101]. M. H. K. Tushar, A. W. Zeineddine, and C. Assi, "Demand-side management by regulating charging and discharging of the EV, ESS, and utilizing renewable energy," IEEE Trans. Ind. Informat., vol. 14, no. 1, pp. 117–126, Jan. 2018.

[102]. N. Rotering and M. Ilic, "Optimal charge control of plug-in hybrid electric vehicles in deregulated electricity markets," IEEE Trans. on Power Systems, vol.26, no.3, pp.1021-1029, 2011.

[103]. D. Dallinger, D. Krampe and M. Wietschel, "Vehicle-to-grid regulation reserves based on a dynamic simulation of mobility behavior," IEEE Trans. Smart Grid, vol. 2, no.2, pp.302-313, 2011.

[104]. Y. Ota, H. Taniguchi, T. Nakajima, K. M. Liyanage, J. Baba, and A. Yokoyama, "Autonomous distributed V2G (vehicle-to-grid) satisfying scheduled charging," IEEE Trans. Smart Grid, vol. 3, no. 1, pp. 559–564, Mar. 2012.

[105]. H. Yang, C. Y. Chung, and J. Zhao, "Application of plug-in electric vehicles to frequency regulation based on distributed signal acquisition via limited communication," IEEE Trans. Power Syst., vol. 28, no. 2, pp. 1017–1026, May 2013.

[106]. N. Rahbari-Asr and M.-Y. Chow, "Cooperative distributed demand management for community charging of PHEV/PEVs based on KKT conditions and consensus networks," IEEE Trans. Ind. Informat., vol. 10, no. 3, pp. 1907–1916, Aug. 2014.

[107]. X. Xi and R. Sioshansi, "Using price-based signals to control plug-in electric vehicle fleet charging," IEEE Trans. Smart Grid, vol. 5, no. 3, pp. 1451–1464, May 2014.

[108]. L.-R. Chen, S.-L. Wu, D.-T. Shieh, and T.-R. Chen, "Sinusoidal-ripple-current charging strategy and optimal charging frequency study for li-ion batteries," IEEE Trans. Ind. Electron., vol. 60, no. 1, pp. 88–97, Jan. 2013.

[109]. R. Wang, G. Xiao, and P. Wang, "Hybrid centralized-decentralized (HCD) charging control of electric vehicles," IEEE Trans. Veh. Tech-nol., vol. 66, no. 8, pp. 6728–6741, Aug. 2017.

[110]. R. Li, Q. Wu, and S. S. Oren, "Distribution locational marginal pricing for optimal electric vehicle charging management," IEEE Trans. Power Syst., vol. 29, no. 1, pp. 203–211, Jan. 2014.

[111]. W. Lee, L. Xiang, R. Schober, and V. W. S. Wong, "Electric vehicle charging stations with renewable power generators: A game theoretical analysis," IEEE Trans. Smart Grid, vol. 6, no. 2, pp. 608–617, Mar. 2015.

[112]. C. Jin, J. Tang and P. Ghosh, "Optimizing electric vehicle charging: A customer's perspective," IEEE Trans. on Vehicular Technology, vol.62, no.7, pp.2919-2927, 2013.

[113]. C. Wu, H. Mohsenian-Rad, and J. Huang, "Vehicle-to-aggregator interaction game," IEEE Trans. Smart Grid, vol. 3, no. 1, pp. 434–442, Mar. 2012.

[114]. M. E. Khodayar, L. Wu, and M. Shahidehpour, "Hourly coordination of electric vehicle operation and volatile wind power generation in SCUC," IEEE Trans. Smart Grid, vol. 3, no. 3, pp. 1271–1279, Sep. 2012.

[115]. A. Saber and G. Venayagamoorthy, "Resource scheduling under uncertainty in a smart grid with renewables and plug-in vehicles," IEEE Syst. J., vol. 6, no. 1, pp. 103–109, Mar. 2012.

[116]. C. Jin, J. Tang, and P. Ghosh, "Optimizing electric vehicle charging with energy storage in the electricity market," IEEE Trans. Smart Grid, vol.4, no. 1, pp. 311–320, Mar. 2013.

[117]. P. Richardson, D. Flynn, and A. Keane, "Local versus centralized charging strategies for electric vehicles in low voltage distribution systems," IEEE Trans. Smart Grid, vol. 3, no. 2, pp. 1020–1028, Jun. 2012.

[118]. Y. Lu, K. W. E. Cheng, and S. W. Zhao, "Power battery charger for electric vehicles," IET Power Electron., vol. 4, no. 5, pp. 580–586, May 2011.

[119]. O. Sundstr¨om and C. Binding, "Flexible charging optimization for electric vehicles considering distribution grid constraints," IEEE Trans. Smart Grid, vol.3, no.1, pp.26-37, 2012.

[120]. E. Sortomme and M. El-Sharkawi, "Optimal combined bidding of vehicle-to-grid ancillary services," IEEE Trans. Smart Grid, vol. 3, no. 1, pp. 70–79, Mar. 2012.

[121]. A.T. Al-Awami and E. Sortomme, "Coordinating vehicle-to-grid services with energy trading," IEEE Trans. Smart Grid, vol.3, no.1, pp.453-462, 2012.

[122]. W. Su and M.-Y. Chow, "Performance evaluation of an EDA-based large-scale plug-in hybrid electric vehicle charging algorithm," IEEE Trans. Smart Grid, vol. 3, no. 1, pp. 308–315, Mar. 2012.

[123]. X. Zhang, "Optimal scheduling of critical peak pricing considering wind commitment", IEEE Trans. on Sustainable Energy, vol.5, no.4, pp.637-645, 2014.

[124]. S. Deilami, "Online Coordination of Plug-in Electric Vehicles Charging, LTC and Switched Shunt Capacitors in Smart Grid to Minimize Cost of Generating Energy and Improve Power Quality" Doctor of Philosophy in Electrical and Computer Engineering, Curtin University, 2014.

[125]. A. Keyhani, Design of Smart Power Grid Renewable Energy Systems, Third Edition, Wiley, 2011.

[126]. M.A.S. Masoum, M. Ladjevardi, E.F. Fuchs and W. Grady, "Application of local variations and maximum sensitivities selections for optimal placement of shunt capacitor banks under nonsinusoidal operating conditions", International Journal of Electrical Power and Energy Systems, UK, vol.26, no.10, pp.761-769, 2004.

[127]. M.A.S. Masoum, M. Ladjevardi, E.F. Fuchs and W. Grady, "Optimal sizing and placement of fixed and switched capacitor banks under nonsinusoidal operating conditions", IEEE PES-2002 Summer Meeting, Chicago, USA, pp.807-813, July 2002.

[128]. M.A.S. Masoum, M. Ladjevardi, A. Jafarian and E.F. Fuchs, "Optimal placement, replacement and sizing of capacitor banks in distorted distribution networks by genetic algorithms", IEEE Trans. Power Delivery, vol.19, no.4, pp.1794-1801, Oct. 2004.

[129]. S. Civanlar and J. J. Grainger, "Volt/var control on distribution systems with lateral branches using shunt capacitors and voltage regulators part III: the numerical results," IEEE Trans. Power Apparatus and Systems, vol.PAS-104, pp.3291-3297, 1985.

[130]. M. Duvall, E. Knipping and M. Alexander, "Environmental assessment of plug-in hybrid electric vehicles", EPRI, vol.1: Nationwide Greenhouse Gas Emissions, 2007.

[131]. H. Hamrawi, S. Coupland, and R John, "Type-2 Fuzzy Alpha-Cuts," IEEE Trans. Fuzzy Systems, vol.27, no.3, pp.682-692, 2017.

[132]. L. A. Zadeh, "The concept of a linguistic variable and its application to approximate reasoning 1-2," Information Sciences, vol. 8, pp. 199–249, 301–357 1975.

[133]. L. A. Zadeh, "A Summary and Update of "Fuzzy Logic"," IEEE International Conference on Granular Computing, San Jose, California, USA, 14-16 August 2010.

[134]. T. J. Ross, "Fuzzy Logic with Engineering Applications", John Wiley & Sons, Ltd, Chapter 4, Second Edition, 2004.

[135]. https://en.wikipedia.org/wiki/Construction_of_t-norms

[136]. G. Deschrijver, "Additive and multiplicative generators in interval-valued fuzzy set theory", IEEE Trans. Fuzzy Systems, vol.15, no.2, pp.222-237, 2007.

APPENDIX A – PUBLICATIONS EXTRACTED FROM THIS THESIS

1. [58]. **Amir S. Masoum**, A. Abu-Siada and S. Islam, "Combined online and delayed coordinated battery charging of plug-in electric vehicles considering distributed wind and rooftop PV generations", Technology and Economics of Smart Grids and Sustainable Energy 2016 Journal, Springer, Journal e-ISSN: 2199-4706 (Online), DOI: 10.1007/s40866-016-0012-3, pp.1-12, 2016.

2. [56]. **Amir S. Masoum**, S. Deilami, M.A.S. Masoum, A. Abu-Siada, "Fuzzy Logic Approach for Online Coordination of Charging Plug-In Electric Vehicles in Smart Grids," IEEE Transactions on Sustainable Energy, vol.6, no.3, pp.1112-1121, 2015.

3. [54]. **Amir S. Masoum**, S. Deilami, M.A.S. Masoum and A. Abu-Siada, "A heuristic approach for coordination of plug-in electric vehicles charging in smart grid", CSCanada, International Canadian Journal, Energy Science and Technology, vol.5, no.2, pp.16-24, 2013.

4. [57]. **Amir S. Masoum**, S. Deilami, M.A.S. Masoum, A. Abu-Siada, S. Islam, "Overnight Coordinated battery charging of Plug-In Electric Vehicles Based on Maximum Sensitivities Selections", 2014 International Conference on Applied Engineering Sciences (ICAES 2014), LA, USA, July 23-24, 2014.

5. [55]. **Amir S. Masoum**, S. Deilami, M.A.S. Masoum, A. Abu-Siada, S. Islam, "Online Coordination of Plug-In Electric Vehicle Charging in Smart Grid with Distributed Wind Power Generation Systems", 2014 IEEE PES General Meeting, pp.1-6, July 27-31, Washington, USA, 2014.

6. [53]. **Amir S. Masoum, A. Abu-Siada,** S. Islam "Impact of uncoordinated and coordinated battery charging of plug-in electric vehicles on substation transformer", IEEE ISGT Asia 2011 (Innovative Smart Grid Technologies Europe) Conference, Perth, WA, pp.1-7, Nov 13-16, 2011, and Elixir, Electrical Engineering International Journal, vol. 41, pp. 5779-5784, 2011.

7. [54]. **Amir S. Masoum**, S. Deilami, M.A.S. Masoum and A. Abu-Siada, "A heuristic approach for coordination of plug-in electric vehicles charging in smart grid", CSCanada, International Canadian Journal, Energy Science and Technology, vol.5, no.2, pp.16-24, 2013.

APPENDIX B – STATEMENTS OF CONTRIBUTION FOR PAPER PUBLICATIONS

Statement of contribution for:

Amir S. Masoum, S. Deilami, M.A.S. Masoum, A. Abu-Siada, "Fuzzy Logic Approach for Online Coordination of Charging Plug-In Electric Vehicles in Smart Grids," IEEE Transactions on Sustainable Energy, vol.6, no.3, pp.1112-1121, 2015.

Contributors:

Amir Sherkat Masoum

I, Amir Sherkat Masoum, am the principle author of the above manuscript and was accountable for generating the concept and design, acquiring the data and inputs, data manipulation and statistical analysis, modelling and generating of results, interpretation and discussion, manuscript preparation and the final approval of the manuscript.

Signature: Date:

Sara Deilami

I, Sara Deilami, am a co-author of the above manuscript and contributed to the review and approval of the manuscript.

Signature: Date:

Professor Mohammad Ali Sherkat Masoum

I, Professor Mohammad Ali Sherkat Masoum, am a co-author of the above manuscript and contributed to the review and approval of the manuscript.

Signature: Date:

A/Professor Ahmed Abu-Siada

I, A/Professor Ahmed Abu-Siada, am a co-author of the above manuscript and contributed to the supervision of the research, review of the results and discussions and the review and approval of the manuscript.

Signature: Date:

Contributors:
Amir Sherkat Masoum
Amir Sherkat Masoum
I, Amir Sherkat Masoum, am the principle author of the above manuscript and was accountable for generating the concept and design, acquiring the data and inputs, data manipulation and statistical analysis, modelling and generating of results, interpretation and discussions, manuscript preparation and the final approval of the manuscript.

Signature: Date:

A/Professor Ahmed Abu-Siada
I, A/Professor Ahmed Abu-Siada, am a co-author of the above manuscript and contributed to the supervision of the research, review of the results and discussions and the review and approval of the manuscript.

Signature: Date:

Professor Syed Islam
I, Professor Syed Islam, am a co-author of the above manuscript and contributed to the review of the results and discussion and the review and approval of the manuscript.

Signature: Date:

214

Contributors:

Amir Sherkat Masoum

I, Amir Sherkat Masoum, am the principle author of the above manuscript and was accountable for generating the concept and design, acquiring the data and inputs, data manipulation and statistical analysis, modelling and generating of results, interpretation and discussion, manuscript preparation and the final approval of the manuscript.

Signature: Date:

A/Professor Ahmed Abu-Siada

I, A/Professor Ahmed Abu-Siada, am a co-author of the above manuscript and contributed to the supervision of the research, review of the results and discussions and the review and approval of the manuscript.

Signature: Date:

Professor Syed Islam

I, Professor Syed Islam, am a co-author of the above manuscript and contributed to the review of the results and discussion and the review and approval of the manuscript.

Signature: Date:

Contributors:

Amir Sherkat Masoum

I, Amir Sherkat Masoum, am the principle author of the above manuscript and was accountable for generating the concept and design, acquiring the data and inputs, data manipulation and statistical analysis, modelling and generating of results, interpretation and discussions, manuscript preparation and the final approval of the manuscript.

Signature: Date:

Sara Deilami

I, Sara Deilami, am a co-author of the above manuscript and contributed to the review and approval of the manuscript.

Signature: Date:

Professor Mohammad Ali Sherkat Masoum

I, Professor Mohammad Ali Sherkat Masoum, am a co-author of the above manuscript and contributed to the review and approval of the manuscript.

Signature: Date:

A/Professor Ahmed Abu-Siada

I, A/Professor Ahmed Abu-Siada, am a co-author of the above manuscript and contributed to the supervision of the research, review of the results and discussions and the review and approval of the manuscript.

Signature: Date:

Professor Syed Islam

I, Professor Syed Islam, am a co-author of the above manuscript and contributed to the review of the results and discussion and the review and approval of the manuscript.

Signature: Date:

Contributors:

Amir Sherkat Masoum

I, Amir Sherkat Masoum, am the principle author of the above manuscript and was accountable for generating the concept and design, acquiring the data and inputs, data manipulation and statistical analysis, modelling and generating of results, interpretation and discussions, manuscript preparation and the final approval of the manuscript.

Signature: Date:

Sara Deilami

I, Sara Deilami, am a co-author of the above manuscript and contributed to the review and approval of the manuscript.

Signature: Date:

Professor Mohammad Ali Sherkat Masoum

I, Professor Mohammad Ali Sherkat Masoum, am a co-author of the above manuscript and contributed to the review and approval of the manuscript.

Signature: Date:

A/Professor Ahmed Abu-Siada

I, A/Professor Ahmed Abu-Siada, am a co-author of the above manuscript and contributed to the supervision of the research, review of the results and discussions and the review and approval of the manuscript.

Signature: Date:

Professor Syed Islam

I, Professor Syed Islam, am a co-author of the above manuscript and contributed to the review of the results and discussion and the review and approval of the manuscript.

Signature: Date: